The role of metalloproteinases and their tissue inhibitors in adipose tissue remodelling and metabolic risk

Matthew Fenech
Norwich Medical School
University of East Anglia

A thesis submitted for the degree of
Doctor of Philosophy
December 2017

This copy of the thesis has been supplied on condition that anyone who consults it is understood to recognize that its copyright rests with the author and that use of any information derived there from must be in accordance with current UK Copyright Law. In addition, any quotation or extract must include full attribution.

Declaration

This thesis is the result of my own work. Experiments were carried out at the BioMedical Research Centre, University of East Anglia, Norwich. This work was funded by the British Heart Foundation (FS/12/27/29405), the Diabetes Research and Wellness Foundation (SCA/OF/12/11) and the Elsie Bertram Diabetes Centre, Norfolk and Norwich University Hospital.

Abstract

Metabolically unhealthy obesity (MUO) is associated with insulin resistance. In MUO, adipose tissue (AT) demonstrates features suggestive of dysfunctional remodelling, including adipocyte hypertrophy, ectopic lipid deposition and AT inflammation. Metalloproteinases (MPs) and their tissue inhibitors (TIMPs) have been implicated in AT remodelling, but their functions therein remain unclear. My investigations have identified an association between subcutaneous adipose tissue (SAT) *Timp3* expression and adipocyte size. In order to address potential roles for TIMP-3 in MUO I have investigated its role in regulating shedding of the adipogenic regulator Dlk-1 and cytokine receptors in cultured human preadipocytes.

39 female subjects of a wide range of Body Mass Index (BMI) were recruited to a clinical study. SAT *Timp3* expression correlated with SAT adipocyte area ($r = 0.429$, $p = 0.041$). In vitro, induction of preadipocyte differentiation significantly reduced *Timp3* mRNA levels by 75%, while Tumour Necrosis Factor (TNF)-α reduced Timp3 mRNA levels by 66% (both $n=3$, $p<0.0001$). Increased shedding of both Dlk-1 and soluble TNF receptor (sTNFR) -1 by preadipocytes was observed in response to TNF-α treatment or by overexpression of adenovirally-delivered TIMP-3.

MPs and TIMPs regulate adipose tissue remodelling. TIMP-3 emerges as a novel node integrating inflammatory signals with networks controlling adipose remodelling. I hypothesise that dynamic modulation of TIMP-3 expression is essential for healthy adipose tissue expansion, but in MUO, excess TIMP-3 expression/activity may increase basal Dlk-1 shedding and reduce matrix turnover in adipogenesis, restricting preadipocyte differentiation and shifting AT growth towards adipocyte hypertrophy.

Acknowledgements

First and foremost I would like to thank my supervisors Professor Jeremy J.O. Turner, Dr. Jelena Gavrilovic and, for a brief period, Professor David Crossman. Jeremy and Jelena have been exemplary supervisors throughout my time as a PhD student. Their patience, knowledge and inexhaustible enthusiasm for this project and my own personal development are gratefully acknowledged. Dr Gavrilovic's group at the BioMedical Research Centre, University of East Anglia (Damon Bevan, Irene Pla Navarro, Matthew Mayhew, Matt Yates) provided much needed guidance and moral support.

I would also like to thank Dr. Frankie Swords and the Directorate of Diabetes and Endocrinology at the Norfolk and Norwich University Hospital for funding the PhD fees requested by the University of East Anglia. Dr. Paul Thomas from the Wellcome Laboratory for Cell Imaging was invaluable in helping develop a pathway for the analysis of human adipose tissue sections. Ms. Miriam Mansha, UEA medical student, also helped by using this protocol to determine mean adipocyte areas for a large cohort of samples.

Furthermore, I would like to thank Prof. Andy Baker, now at the University of Edinburgh, and his team for providing me with the TIMP-3-overexpressing adenovirus, as well as guidance on optimization of its use in primary human mesenchymal stromal cells. The surgical and gynaecological teams at the Norfolk and Norwich University Hospital, including the surgeons (Miss Rozina Ali, Mr Andrea Figus, Mr Richard Haywood, Mr Martin Heaton, Mr Mike Lewis, Mr Eddie Morris and Miss Elaine Sassoon) and the administrators (Sue Smith and Karen Turner), were incredibly helpful in identifying potential participants for these studies, and once these provided their consent, collecting the adipose tissue for cell culture or analysis. The Comprehensive Local Research Network (CLRN) research nurses (Georgie Glister, David Tomlinson, Kirsti Whittington Powell) were invaluable in recruiting study participants. The radiology team at the Norfolk and Norwich University Hospital (Professor Andoni Toms, Dr. Paul Malcolm, Mr. Richard Greenwood) expertly conducted the MRI scans required for the clinical arm of this study, while the Histopathology department (Professor Richard Ball, Mr. Iain Sheriffs and colleagues) undertook the histopathological handling of adipose tissue samples from the clinical study. Similarly, the Biochemistry departments at the Norfolk and Norwich University Hospital and the Bob Champion Research and Education Centre, University of East Anglia (Mrs. Sue Kerry, Dr Jonathan Tang and Mr. Christopher Washbourne) performed the analysis of plasma/serum samples collected for these studies.

Most importantly, I would like to thank Sarah for her immense support and patience throughout this long journey.

Contents

List of Figures

List of Tables

List of Abbreviations

Abbreviation	Full phrase
Ad0	Control adenovirus RAd35
ADAM	A disintegrin and metalloproteinase
ADAMTS	A disintegrin and metalloproteinase with thrombospondin repeats
AdT3	TIMP-3-overexpressing experimental adenovirus
AP-1	Activator protein-1
APMA	Aminophenylmercuric acetate
ASAT	Abdominal subcutaneous adipose tissue
ATP	Adenosine triphosphate
BHF	British Heart Foundation
BMI	Body mass index
CCL2	Chemokine (C-C motif) ligand 2
CD	Cluster differentiation
cDNA	Complementary DNA
CMIA	Chemiluminescent microparticle immunoassay
CRP	C-reactive protein
CT	Computed tomography
DAB	Dimethlyamino-benzaldehyde
Dlk-1	Delta-like protein-1
DNA	Deoxyribonucleic acid
dsDNA	Double-stranded DNA
DXA	Dual energy X-ray absorptiometry
ECM	Extracellular matrix
EGF	Epidermal growth factor factor (KGF)
EGFR	Epidermal growth factor receptor
ELISA	Enzyme-linked immunosorbent assay
ETS	E26 transformation-specific
FAK	Focal adhesion kinase
FCS	Fetal calf serum
FFA	Free fatty acids
FGF	Fibroblast growth factor
GK	Glycerol kinase
GPCR	G-protein coupled receptor
HA	Hyaluronic acid
HFD	High-fat diet
HGF	Hepatocyte growth factor
HOMA-IR	Homeostatic model assessment of insulin resistance
IGF-I	Insulin-like growth factor-I
IL	Interleukin
Insr	Insulin receptor
IR	Insulin resistance
KGF	Keratinocyte growth factor
m-XXX	membrane bound-XXX
MCK	Muscle creatine kinase

MCP-1	Monocyte chemoattractant protein-1
MEF	Mouse embryonic fibroblast
MMP	Matrix metalloproteinase
MP	Metalloproteinase
MRI	Magnetic resonance imaging
MSC	Mesenchymal stromal cell
MT-MMP	Membrane-type matrix metalloproteinase
MUO	Metabolically unhealthy obese
NAFLD	Non-alcoholic fatty liver disease
NGF	Nerve growth factor
PAGE	Polyacrylamide gel electrophoresis
PAI-1	Plasminogen activator inhibitor-1
PCR	Polymerase chain reaction
PDGF	Platelet-derived growth factor
PDGFRα+	Platelet-derived growth factor receptor-alpha-positive
PPARγ	Peroxisome proliferator-activated receptor-gamma
Pref-1	Preadipocyte factor-1
PVDF	Polyvinylidene diflouride
qRT-PCR	Quantitative reverse transcription polymerase chain reaction
RECK	Reversion-inducing cysteine-rich protein with Kazal motifs
RIP	Regulated intramembrane proteolysis
RNA	Ribonucleic acid
RPLP0	Large ribosomal protein P0
S-V	Stromo-vascular
s-XXX	soluble-XXX
SAA	Serum amyloid A
SAT	Subcutaneous adipose tissue
SBGS	Simpson-Behmel-Golabi syndrome
SD	Standard deviation
SDS	Sodium dodecyl sulphate
SFD	Standard-fat diet
SNP	Single nucleotide polymorphisms
T2DM	Type 2 diabetes mellitus
TACE	TNF-alpha converting enzyme
TGF-β	Transforming growth factor-beta
THBS-1	Thrombospondin-1
TIMP	Tissue inhibitor of metalloproteinases
TLDA	Taqman® Low Density Array
TLR-4	Toll-like receptor-4
TNF-α	Tumour necrosis factor-alpha
TNFR	Tumour necrosis factor-alpha receptor
VAT	Visceral adipose tissue
VEGF	Vascular endothelial growth factor
VLDL	Very low density lipoprotein
WAT	White adipose tissue
WC	Waist circumference

WHO	World Health Organisation
WHR	Waist-to-hip ratio
WT	Wild type

Chapter 1: Introduction

1.1: Obesity, adipose tissue and metabolic disease

Overweight and obesity, defined as a body mass index (BMI) of 25-29.9 and ≥30 kg/m^2 respectively, are associated with many adverse health outcomes, and ultimately increased mortality [1]. The inexorable rise in their prevalence is a major factor contributing to the increasing prevalence of metabolic disease, particularly insulin resistance (IR) and type 2 diabetes (T2DM). T2DM accounts for 85-95% of all cases of diabetes, of which there are an estimated 285 million cases worldwide; this latter figure is expected to rise by over 50% by 2030 [2]. Current strategies for preventing and treating T2DM are limited in their range and effectiveness. Furthermore, not everyone who is obese develops IR [3]. For these reasons, increased understanding of the roles of the molecular players responsible for development of IR/T2DM in obesity is required. This knowledge may identify new therapeutic targets for potential pharmacological manipulation.

1.1.1 White adipose tissue

Triglycerides are the main energy storage molecules in humans - in an average Caucasian male, approximately 100,000 kcal of energy is stored as triacylglycerol in adipose tissue, compared to only 600 kcal as glycogen [4]. Adipocytes, which are capable of accumulating triglycerides as one large cytoplasmic droplet, are the major cell type in white adipose tissue (WAT) – a 2003 study found that in adult women, adipocytes outnumbered stromal cells 5-to-1 in each gram of adipose tissue [5, 6]. The remainder of adipose tissue has been collectively referred to as the stromal-vascular (S-V) fraction, and is composed of macrophages and other immune cells, adipocyte precursors, fibroblasts, smooth muscle cells and endothelial cells [7]. Far from being a passive energy repository, adipocytes and the various other cells within adipose tissue interact with each other and other organs such as the hypothalamus and liver to actively regulate energy homeostasis, via the secretion of various adipocytokines, including leptin, adiponectin, resistin, and interleukins (IL)-6, 8 & 1β [8].

WAT can be broadly divided into two major depots – subcutaneous (SAT) and visceral (VAT) – that are thought to perform different functional roles and may thus make different contributions to the development of metabolic disease. For example, visceral fat is characterised by smaller adipocytes than subcutaneous adipose, and is more lipolytic and less sensitive to the anti-lipolytic effects of insulin [9]. The secretion of free fatty acids (FFAs) into the portal circulation by visceral adipose, and subsequent uptake by the liver, can reduce hepatic insulin sensitivity leading to increased hepatic gluconeogenesis [10]. Centrally-distributed obesity, characterized by a high waist circumference (WC) and/or waist-

to-hip ratio (WHR), is associated with a greater risk of developing clinical outcomes of insulin resistance such as the metabolic syndrome [11]. The specific influence of visceral adipose tissue as opposed to abdominal subcutaneous adipose tissue (ASAT) has been controversial, given the difficulty in quantifying the contribution of increased VAT volume or increased ASAT volume to increased WHR/WCs in study subjects [12, 13]. Increased use of imaging techniques such as dual energy X-ray absorptiometry (DXA), computed tomography (CT) and magnetic resonance imaging (MRI) in such studies has served to highlight the critical role of VAT expansion in metabolic dysfunction in obesity [14, 15].

1.1.2 Adipose tissue inflammation, restricted adipose expansion and whole-body lipid distribution – linking obesity to insulin resistance and type 2 diabetes

When mammals gain weight, adipose tissue depots increase in volume. As this happens the adipose tissue takes on a pro-inflammatory phenotype, which in turn is thought to lead to the development of IR and T2DM [8, 16-20]. This low grade, chronic, systemic inflammatory response is characterised by elevated circulating markers of inflammation including C-reactive protein (CRP), IL-6, serum amyloid A (SAA), plasminogen activator inhibitor (PAI)-1 and fibrinogen [21-23]. There is an accumulation of immune cells (predominantly macrophages) in adipose tissue depots [24-26], and these cells, in conjunction with the adipocytes, display increased secretion of canonical cytokines such as IL-6, IL-8, tumour necrosis factor (TNF)-α, and monocyte chemoattractant protein (MCP)-1 [27, 28]. Population studies have repeatedly shown a direct correlation between levels of these inflammatory mediators and states of metabolic dysfunction such as obesity and T2DM, and modulation of the TNF-α system and its downstream pathways were shown to directly affect insulin sensitivity [29-31].

It has been suggested that as adipose tissue reaches a ‘maximum storage capacity’, there is an inability of the more insulin-sensitive subcutaneous adipose tissue to expand sufficiently to accommodate excess ingested energy. According to the ‘lipid overflow’ hypothesis [10], this leads to triglycerides being diverted to visceral adipose tissue, and also being deposited in ectopic sites such as the liver, skeletal muscle and pancreas [32]. Lipodystrophy, a congenial or acquired condition in which there is complete or partial failure of adipose tissue development, represents the clinically-extreme phenotype of this process of ‘lipid overflow’, with little or no triglycerides stored in adipocytes, and large amounts of extra-adipose fat in liver, pancreas and muscles [33]. Excess fat in non-adipose tissue is metabolised by alternative pathways leading to the phenomenon of lipotoxicity [34-36]. In the pancreas, for example, the products of lipid peroxidation can accelerate the progression from insulin resistance to T2DM by causing beta-cell dysfunction [9], whereas hepatic lipotoxicity

underpins non-alcoholic fatty liver disease (NAFLD), the most prevalent form of chronic liver disease worldwide and a significant cause of hepatic failure and hepatocellular carcinoma [37]. At a cellular level, it is thought that when the ability of preadipocytes to differentiate into lipid-storing adipocytes is impaired, adipose tissue expansion occurs by hypertrophy, generating fewer, larger adipocytes. Larger adipocytes are more insulin-resistant with increased secretion of TNF-α and resistin, decreased release of adiponectin, and increased secretion of free FFAs to the circulation [32].

1.1.3 Adipose tissue extracellular matrix

Although adipose tissue inflammation has been extensively studied and is the subject of much ongoing research, comparatively little is known about adipose tissue extracellular matrix (ECM), but there is emerging evidence that it is an important regulator of adipocyte function. In common with other cells of mesodermal origin, such as osteoblasts and chondrocytes, adipocytes are surrounded by a basal lamina rich in collagen IV, laminin and nidogen [38, 39]. In adipose tissue, this basal lamina also has significant quantities of collagen VI [39, 40]. Thus, preadipocyte differentiation necessitates a process of matrix remodelling from a fibrillar, fibronectin/collagen I-rich stromal matrix to the basal lamina composed of IV & VI, laminin and nidogen [41, 42]; this process has been observed in the original electron microscopy descriptions of murine preadipocyte differentiation [43]. Fibronectin expression in fact decreases during differentiation of both preadipocytic cell lines and primary human preadipocytes, and mature subcutaneous adipocytes express little fibronectin [42]. Another matrix component with an emerging role in preadipocyte differentiation is collagen XVIII, a widely-expressed basement membrane constituent with structural features of both collagens and proteoglycans [44]. Collagen XVIII exists as three alternatively processed variants: short, medium and long forms, which differ according to the presence or otherwise of three N-terminal noncollagenous domains. Aikio and colleagues demonstrated that the medium/long variants of collagen XVIII are upregulated during 3T3-L1 differentiation, whereas the short variant is downregulated – reciprocal changes are observed when 3T3-L1 adipocytes are induced to dedifferentiate using Wnt3a-conditioned medium. Furthermore, the specific absence of medium/long collagen XVIII reduces mouse embryonic fibroblast (MEF) adipogenic differentiation, while short variant absence does not have this effect. *Col18a1*$^{P2/P2}$ mice lacking medium/long collagen XVIII demonstrate a phenotype reminiscent of lipodystrophy, with reduced adiposity, increased liver fat, hypertriglyceridaemia and high very low density lipoprotein (VLDL) levels [44].

Adipose ECM also undergoes significant changes in obesity. Microarray analysis of epididymal WAT collagen expression in metabolically unhealthy obese *db/db* mice revealed

upregulation of various collagens, including collagens I, IV, V and VI, as compared to obese, metabolically healthy, adipoTG mice whose hyperplastic WAT is composed of adipocytes that constitutively overexpress adiponectin [45]. A role for adipose ECM in determining whole-body metabolic outcomes is suggested by the obese *col6KOob/ob* mouse strain, which is both collagen VI and leptin-deficient [45]. The lack of collagen VI in the adipocyte basal lamina allows seemingly unlimited adipocyte hypertrophy, and although adipocyte hypertrophy is normally associated with 'metabolically unhealthy' obesity and an increased risk of development of insulin resistance [46], the *col6KOob/ob* mouse strain displays a metabolically-favorable obese state [45]. Adipose tissue from these mice demonstrates an 'anti-fibrotic' expression programme, with increased decorin, and decreased lumican and transforming growth factor (TGF)-β expression. Similar changes are seen in metabolically favourable states such as PPARγ agonist administration [45].

Glycosaminoglycans constitute another class of structural ECM components implicated in obesity, with hyaluronan or hyaluronic acid (HA) being particularly well-studied in this class. HA is enriched in WAT of *ob/ob* and *db/db* mice, and this has been hypothesized to contribute to increased WAT inflammation by facilitating monocyte attachment and migration [47].

Apart from changes in the expression of structural ECM proteins, matricellular protein expression is also regulated in WAT. Thrombospondin (THBS)-1, a large adhesive ECM glycoprotein expressed predominantly in visceral adipose tissue, is downregulated during human adipogenesis [42]. Mice lacking *Thbs1* are protected from adipose tissue inflammation and insulin resistance; conversely, this gene is upregulated in murine WAT inflammation [47].

In human subjects, metabolic dysfunction in obesity is associated with increased adipose tissue fibrosis, suggesting that adipose tissue dysfunction is associated with disordered ECM turnover [23]. Fibrosis causes pathology in a number of different organs, including in the liver and lung, and is defined as a pathological condition characterized by excessive production and accumulation of collagen, loss of tissue architecture, and organ failure in response to chronic inflammation [48-50]. The primary form in which collagen is found in animal tissues is as very long fibrils with a characteristic axial periodic structure, which provide a key scaffold for cell attachment and anchorage of macromolecules, allowing the shape and form of tissues to be defined and maintained [51]. Increased collagen deposition in fibrosis is thought to increase adipose tissue rigidity, limiting the ability of individual adipocytes to respond dynamically to changes in nutritional status – that is, preventing

adipocyte expansion in positive energy balance and preventing adipocyte shrinkage in negative energy balance [52]. Thus, adipose tissue fibrosis, via its effect on tissue rigidity, may be of metabolic importance. Indeed, the degree of subcutaneous WAT fibrosis correlates with markers of adipose tissue inflammation, while the degree of visceral WAT fibrosis is inversely associated with metabolic parameters such as circulating triglyceride levels [53]. Furthermore, following a 56-day period of overfeeding, expression of *Col1a1*, *Col3a1*, *Sparc* and *Tgfβ* in whole subcutaneous adipose samples from male subjects is increased, and there is a trend towards an increase in fibronectin expression [54]. Mice deficient in SPARC, a profibrotic protein that is upregulated in processes requiring ECM restructuring such as wound healing, demonstrate less WAT fibrosis and larger epididymal fat pads with more numerous adipocytes than wild-type mice [55], while in obese human subjects, SPARC expression by both visceral and subcutaneous WAT correlates with measures of insulin resistance [56]. Recent work by Marcelin and colleagues has begun to address the question of which cells are responsible for the development of adipose tissue fibrosis in obesity. This group has identified a subset of platelet-derived growth factor receptor-α-positive (PDGFRα^{+}), CD9^{high} adipose-derived mesenchymal stromal cells that are enriched in omental adipose tissue of metabolically unhealthy obese (MUO) subjects. Furthermore, activation of the PDGFRα pathway in these cells in mice results in the development of a pro-fibrotic adipose phenotype, implicating this pathway in WAT fibrosis [57].

Members of different proteinase families have been implicated in adipose tissue ECM remodelling, including zinc metalloproteinases.

1.1.4 The role of metalloproteinases in the development of obesity-associated metabolic dysfunction

Metalloproteinases are recognised effectors and modulators of the innate immune system in other chronic inflammatory conditions [58], so it is not unreasonable to hypothesise that they also play a role in the chronic inflammation and dysfunctional adipose ECM remodelling that characterises metabolic dysfunction associated with obesity. Intriguingly, various members of this family also appear to play a role in regulating the differentiation of adipocyte precursors into mature adipocytes. Since failure of differentiation may lead to reduced adipocyte numbers and thus decreased adipose tissue storage capacity, metalloproteinases may function at the interface between the two aforementioned processes (inflammation and restricted adipose expansion) that appear to be two of the main drivers of the development of IR in obesity. Consequently, this system is an attractive subject for study in the search for new therapeutic targets for these conditions.

1.2: Zinc metalloproteinases and their inhibitors

The zinc metalloproteinases are evolutionarily ubiquitous proteins that rely on the presence of a zinc ion for their catalytic activity, and are thus characterised by a minimal zinc-binding motif (with amino acid sequence HGXXH), wherein the zinc ion is co-ordinated by the two histidine residues [59]. Metzincins represent one subgroup, or clan, of this protease superfamily, in which the zinc-binding motif is extended to include three histidines (HEXXHXXGXXH...M) (Figure 1.1). *M*atrix *m*etallo*p*roteinases (matrixins, MMPs) and metalloproteinases of the ADAM (*a d*isintegrin *a*nd *m*etalloproteinase) family, in turn, belong to this clan. Both families are characterised by an N-terminal combination of a pro-domain, which has chaperoning and regulatory functions, and the catalytic metalloproteinase (MP) domain. ADAM and membrane type- (MT-) metalloproteinases have a transmembrane region and a cytoplasmic tail, which is highly variable in length and sequence (Figure 1.2). The MMPs and ADAMs have been reviewed in [60] and [61].

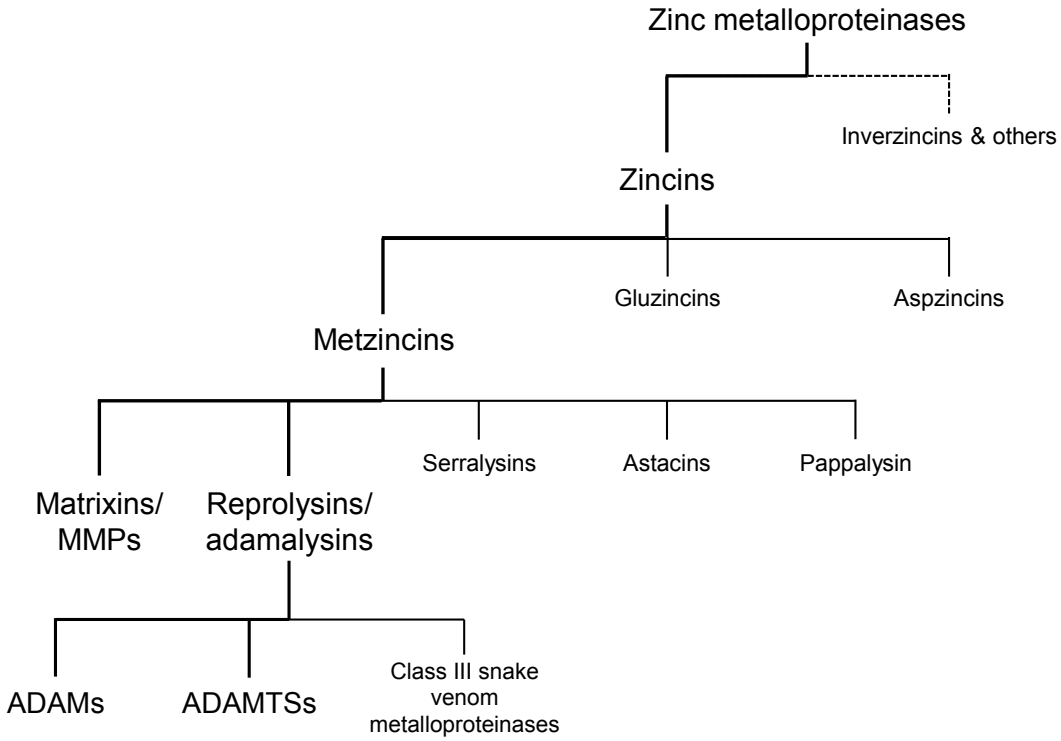

Figure 1.1: A schematic diagram showing the relationship between different clans and families that all belong to the zinc metalloproteinase superfamily. ADAMs and ADAMTS proteinases belong to the reprolysin or adamlysin family. Adapted from [62], [63] and [64].

1.2.1 Matrix metalloproteinases

24 mammalian MMPs have been identified, of which 23 are expressed in humans [60]. They share a typical tertiary structure, with a five-stranded β-sheet and 3 α-helices organised in a distinctive sequence [65]. They can be either secreted or membrane-bound, restricting their activity to the juxtamembrane and extracellular spaces. Most are not usually expressed in healthy tissues, but become detectable when repair & remodelling processes are set off, for example with infection or inflammation. Most tissues are capable of expressing MMPs, but the degree and range of MMPs expressed varies widely.

The purported roles of MMPs have expanded beyond simple extracellular matrix degradation, as was initially thought when the first MMPs were identified in the 1960s. Proteomic approaches, and investigations involving both loss-of-function and gain-of-function mutants have indicated that MMPs perform a variety of tasks during the inflammatory response, including potential direct and indirect bactericidal activity (the latter by activating α-defensins) [66], altering matrix to allow cell migration in wound healing [67], and modulating chemokine activity by establishing concentration gradients [68] or by converting them to antagonists of chemotaxis [69].

1.2.2 ADAMs and ADAMTSs

In ADAM proteins, the catalytic domain is followed by a disintegrin domain and a cysteine-rich domain, and in the ADAMTS subgroup, a variable number of thrombospondin-like repeats are found interposed with spacer regions. There are 21 secreted and transmembrane human ADAM proteins, of which 8 have no protease activity. All 19 human ADAMTS proteins are secreted, and their major role is to interact with and degrade ECM components including procollagens and proteoglycans such as hyalectans and aggrecan [70].

The activities of the 13 catalytically-active ADAMs proteins can be summarised into ectodomain shedding and modulation of *r*egulated *i*ntramembrane *p*roteolysis (RIPping) [61]. In the former, ADAMs cleave ectodomains of membrane-bound proteins, including pro-ligands, receptors and cell adhesion molecules, providing a powerful way of regulating cell signalling and adhesion. For example, TNF-α activity is regulated in this way, with *T*NF-*α* *c*onverting *e*nzyme (TACE, now known as ADAM-17) releasing soluble TNF-α from its membrane-bound form allowing it to act in a paracrine manner. The release of ligand-binding regions of transmembrane receptors, on the other hand, can attenuate signalling by 'mopping up' soluble ligands. RIPping, in contrast, refers to the cleavage of membrane-bound proteins through the transmembrane domain, releasing a cytoplasmic region into the

cytosol, where it may have signalling activity or be proteolytically degraded. Given their pivotal role at the crucial interface between cells and their immediate microenvironment, it is unsurprising that the ADAMs proteases have been implicated in many fundamental homeostatic and developmental processes, from inflammation to reproduction [62].

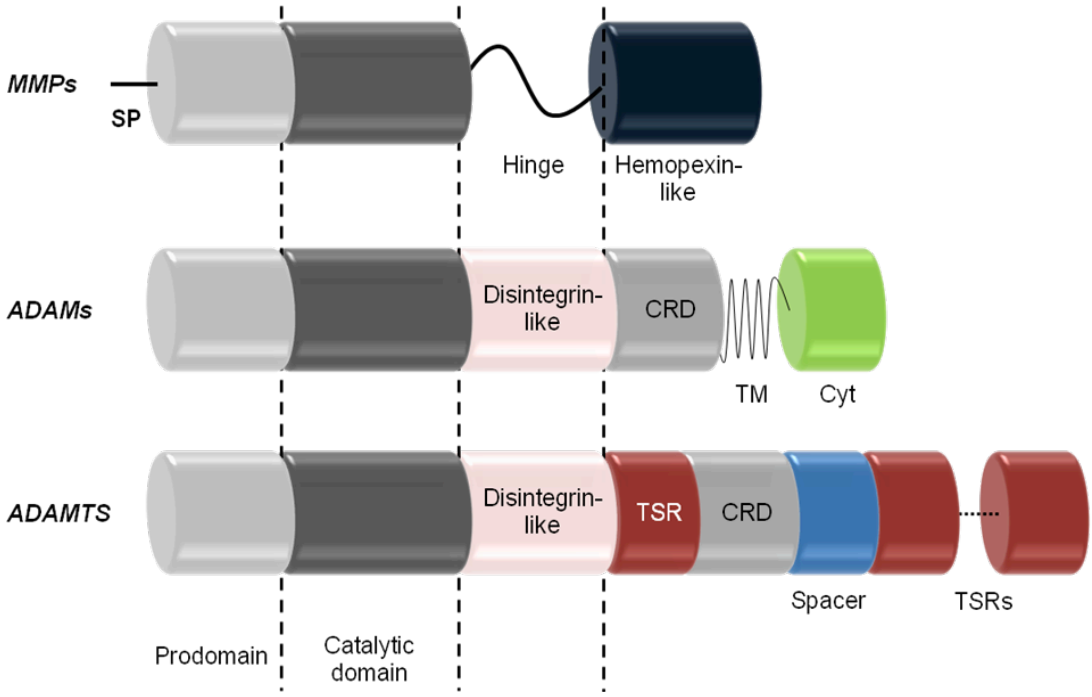

Figure 1.2: Domain architecture of MMPs, ADAMs and ADAMTS proteases. All three groups of proteins share a minimal structure of a regulatory N-terminal prodomain and a zinc-coordinating catalytic domain. In the basic MMP structure shown, this minimal domain combination is preceded by a signal peptide (SP). C-terminal to the catalytic domain, a hinge region and hemopexin-like domain are found in most members of the matrixin family. Exceptions include MMP23, which is a type II membrane MMP that has a signal anchor at the N-terminal end, and in which the hinge and hemopexin-like domains are replaced by a cysteine array domain and an immunoglobulin-like domain respectively (not shown). Further C-terminal to the hemopexin-like domain, other membrane-type (MT) MMPs have a transmembrane (TM) and cytoplasmic (Cyt) domain (e.g. MMPs 14-16), or a glycosylphosphatidylinositol anchor (MMPs 17 and -25). ADAMs and ADAMTS proteases are similar in that both groups are characterised by a disintegrin-like domain and a cysteine-rich domain (CRD); in ADAMTS proteases, these are separated by a thrombospondin repeat (TSR) and a spacer region. A variable number of TSRs constitute the C-terminal end of the ADAMTS proteins. ADAMs are all membrane-associated and thus have a TM and Cyt domain at the C-terminus. Adapted from [60], [62] and [58].

1.2.3 Regulation of metalloproteinase expression

As with other proteins, expression of MPs occurs in two phases: transcription of DNA to messenger (m)RNA, and translation of RNA to proteins (Figure 1.3).

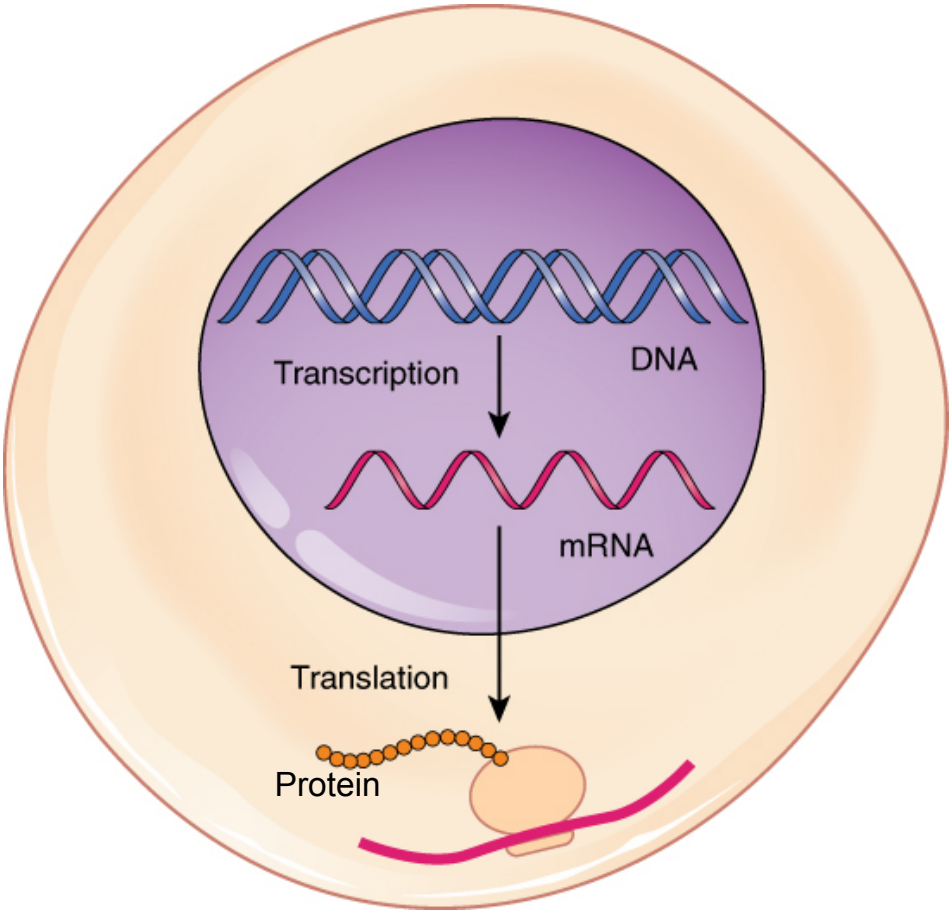

Figure 1.3: Protein expression may be simplistically viewed as the result of two steps: transcription of DNA to messenger RNA, and translation of mRNA to an amino acid sequence, that then goes on to adopt secondary and tertiary structure to become a protein. Image adapted from 'OpenStax Anatomy and Physiology Textbook' version 8.25, and reproduced here under the Creative Commons Attribution 4.0 International license.

Metalloproteinase promoters harbour several *cis*-elements, allowing for regulation of MP gene expression at the transcriptional level by a diverse set of *trans*-activators including activator protein (AP)-1, PEA3 (a subfamily of the ETS [E26 transformation-specific] family of transcription factors, Sp-1, β-catenin/Tcf-4, and nuclear factor kappa-light-chain-enhancer of activated B cells (NF-κB). A large variety of cytokines or growth factors, including interleukins, interferons, epidermal growth factor (EGF), nerve growth factor (NGF), hepatocyte growth factor (HGF), fibroblast growth factor (FGF), vascular endothelial growth factor (VEGF), platelet-derived growth factor (PDGF), keratinocyte growth factor (KGF), tumour necrosis factor (TNF)-α, and transforming growth factor (TGF)-β activate signalling

pathways leading to the *trans*-activation of MP promoters at the AP-1 and/or PEA3 elements [71]. Similarly, the AP-1 and PEA3 *cis*-elements mediate the induction of MP expression by ECM proteins; interaction of cell-surface integrins with ECM components activates focal adhesion kinase (FAK), which transmits signals intersecting with the MAPK pathway, thereby increasing the transcriptional activity of AP-1 and PEA3 [72].

The adipokine chemerin, circulating levels of which correlate with body weight, appears to be an adipose tissue-specific regulator of MP expression [73]. Chemerin signalling appears to inhibit NF-κB signalling in mature adipocytes, leading to reduced MP expression. Indeed, inhibition of chemerin signalling increased MP activity and the recruitment of macrophages towards adipocyte-conditioned media [73]. This effect was not replicated by synthetic chemerin added in culture, indicating that the secretion of this adipokine specifically by adipocytes is somehow important in determining its function.

1.2.4 Regulation of metalloproteinase activity

Like most proteases, regulation of MP activity can occur at several levels. Gene and protein expression is induced by mediators such as cytokines and growth factors via cognate pathways in situations of tissue injury and repair [74]. Once expressed as proteins, their pericellular location determines their spectrum of activity, by separating them from or bringing them closer to their substrates. MMPs are kept close to the cell membrane, for example, by binding to integrins, CD44 and surface proteoglycans [58]. MMP proteins are initially expressed as inactive proMMPs, in which the catalytic zinc ion is coordinated by a cysteine residue from the pro-domain. Interference with this interaction, for example by cleavage of the pro-domain by proteins of the furin family, plasmin and other activated MMPs, allows proMMP activation [58, 60].

ADAM surface expression is regulated by trafficking. Signalling within the cell can also modulate ADAM activity at the cell surface. In ‘triple-membrane passing signalling’, G-protein coupled receptor (GPCR) ligands activate signalling pathways relying on phosphoinositide-3-kinase (PI-3K) and Src, which stimulate ADAM activity presumably by phosphorylation of the intracellular region, modulating ADAM-mediated epidermal growth factor receptor (EGFR) ligand release [75].

Various proteins also serve as natural inhibitors of MPs. In adipose tissue, one group is of particular relevance: *t*issue *i*nhibitors of *m*etallo*p*roteinases (TIMPs). TIMPs 1 to 4 are two-domain proteins, with an inhibitory N-terminal domain thought to fit into the MP catalytic cleft, and a C-terminal domain that determines specificity. They selectively inhibit MMPs in a 1:1

stoichiometric manner. The inhibition of ADAMs proteases is thought to be more complex, with multiple protein-protein interactions. Not all TIMPs inhibit all MPs; TIMP-3 inhibits all MMPs and several ADAMs, for example, and is the main inhibitor for TACE/ADAM17 [61]. Furthermore, not all MP-TIMP interactions are inhibitory – binding of both TIMP-2 and active MMP-14 is required for MMP-2 activation [76, 77], [78].

Another natural inhibitor of MPs is *re*version-inducing *c*ysteine-rich protein with *K*azal motifs (RECK), a membrane-bound glycoprotein known to inhibit MMPs -2, -9 and -14 and ADAM-10 [58, 60]. Furthermore, circulating α2-macroglobulin, α1-proteinase inhibitor and α1-chymotrypsin bind several enzyme types, including MPs, allowing uptake by scavenger receptors [58, 60].

1.3: Roles for metalloproteinases and tissue inhibitors of metalloproteinases in obesity and metabolic disease

1.3.1 Introduction

The expression and function of MPs and TIMPs has been investigated extensively in various model systems, ranging from cell lines to human clinical studies. In this section, I outline and discuss the various sources of evidence that indicate potential roles for MPs and TIMPs in adipose tissue function and dysfunction. I focus on their expression, roles in adipogenic differentiation, and the conclusions that can be drawn from study of knockout mice phenotypes and analysis of clinical studies.

1.3.2 Expression of MP/TIMP mRNA/proteins from cultured cells and whole adipose tissue – cell lines, murine, and human

1.3.2.1 Cell lines

3T3-L1 adipocytes [79] express *Mmp2*, *Mmp9* and *Mmp14* mRNA [80]; gelatinase activity suggestive of MMP-2 (gelatinase A) and MMP-9 (gelatinase B) secretion was identified in 3T3-L1 [80] and 3T3F442A [81] conditioned media, and MMP-14 protein presence was confirmed on immunoblot [80]. TIMP-1 expression has also been reported in 3T3-L1 cultures, and both mRNA and protein levels are increased by stimulation with the beta-adrenergic agonist isoproterenol [82].

When the expression profiles of cultured Simpson-Golabi-Behmel syndrome (SGBS) human adipocytes [83] were investigated using microarrays, 1088 transcripts were found to be differentially regulated, depending on whether the cells were exposed to control adipocyte feeding medium (CON), control macrophage culture medium (UC), or U937 macrophage-conditioned (MC) medium, a model of adipose inflammation in obesity. With the latter treatment, the expression of various MMPs, particularly 1, 3, and 10, and interleukins 1β, 6, 7, 8 and 11 was markedly increased [84]. The increased expression of *Mmp1* and *Mmp3* could also be appreciated when SBGS adipocyte cultures were stimulated with TNF-α, and upregulation of MMP-1 and MMP-3 protein was confirmed by ELISA [84]. Similarly, undifferentiated SGBS preadipocytes exposed to U937 MC medium upregulate MMP-3, MMP-9 and MMP-12 expression [85].

1.3.2.2 Primary cell culture

Primary rat adipocytes cultured on Matrigel® secrete 72kDa and 62kDa gelatinase activity, likely corresponding to MMP-2. This appears to be required for adipocyte migration through, and turnover of, the Matrigel® extracellular matrix, as both these activities were inhibited by the MMP inhibitor 1,10-phenanthroline, taking into account the cytotoxic effect of 1,10-phenanthroline [86]. Similarly, human *in vitro*-differentiated primary adipocyte cultures express MMP-2 and MMP-9, and gelatinase activity is detected in media conditioned for 24 hours by human subcutaneous adipose tissue explants [81], [87]. Both human primary preadipocytes and *in vitro*-differentiated adipocytes stimulated by MC medium upregulate MMP-1 and MMP-3 expression, an effect that appears to be mediated by IL-1β and TNF-α [88].

1.3.2.3 Murine adipose tissue

Rodent models of genetic obesity and diet-induced obesity also display consistently altered MMP and TIMP expression patterns, when compared to wild type or lean mice. MMP-2 expression is higher in the epididymal and subcutaneous white adipose tissue (WAT) of (i) wild-type mice on a high-fat diet (HFD) and (ii) genetically obese db/db mice, as compared to wild-type mice on a standard-fat diet (SFD) [89]. Likewise, epididymal WAT obtained from *ob*/*ob* or *db*/*db* mice, or from AKR mice (an inbred strain in which the *AK*V *r*etrovirus genome is integrated in the mouse genome, such that the mice are viraemic from birth [90]) fed a HFD [91], showed increased expression of MMPs-2, -3, -12, -14, -19 and TIMP-1, and reduced expression of MMP-7 and TIMP-3, as compared to lean C57BL/6 controls [7]. In wild type mice fed a HFD for 15 weeks, WAT expression levels of 11 MMPs and TIMPs as assessed by semiquantitative RT-PCR were different from littermates fed a standard fat diet (SFD), with particularly large increases seen in MMP-3 and TIMP-1 expression [92]. Whole

WAT TIMP-1 messenger RNA and protein overexpression with HFD feeding in wild-type mice and in *ob*/*ob* mice has also been described more recently, along with increased circulating TIMP-1 levels in these obese mouse models [93]. A role for MMP-2 and MMP-9 in adipose tissue remodelling is suggested by the finding that their expression and activity vary with weight loss as well as with weight gain. Following HFD feeding for 50 weeks, obese C57BL/6 mice were subjected to caloric restriction (27 kJ/day) for 6 weeks, during which they lost ~40-50% of their body weight. As compared to obese controls maintained on a HFD, *Mmp2* mRNA and gelatinase activity were higher in subcutaneous and gonadal fat pads from mice in the experimental group, whereas MMP-9 levels in tissue as assessed by ELISA were reduced with weight loss [94]. A summary of MMP and TIMP expression by whole WAT from various obese mouse models is provided in Table 1.1 (a discussion of MP/TIMP expression in whole human adipose tissue is found in section 1.3.5, page 25).

	Increased expression	***Decreased expression***
ob/ob, db/db mice	MMP-2, 3, 12, 14, 19	MMP-7
	TIMP-1	TIMP-3
AKR mice fed HFD	MMP-2, 12, 19	MMP-7
	TIMP-1	TIMP-3
Wild type mice fed HFD	MMP-2, 3, 11, 12, 13, 14	MMP-7, 9, 16, 24
	TIMP-1	TIMP-4
Calorie-restricted obese wild type mice	MMP-2	MMP-9

Sources: [7, 89, 92-94]

Table 1.1: Differential expression of MMPs/TIMPs by WAT from obese mice. Despite the differing aetiologies for obesity, the expression patterns are similar and consistent.

On separation of *ob/ob* adipose tissue into adipocyte and non-adipocyte (or S-V) fractions, analysis of MMP/TIMP mRNA levels revealed that the greatest differences between obese mice and lean controls occurred in the S-V fraction (Table 1.2), leading to the suggestion that, in obesity, the S-V fraction of adipose tissue changes its expression of MPs and TIMPs to a greater degree than adipocytes [7].

	Adipocyte fraction (change vs. lean control)	***S-V fraction*** (change vs. lean control)
MMP-12	4.4x ↑	17.8x ↑
MMP-7	1.9x ↓	4.6x ↓
MMP-2	2.2x ↑	3x ↑
TIMP-1	2.6x ↑	4.4x ↑
TIMP-3	3.6x ↓	8.2x ↓

Source: [7]

Table 1.2: Changes in expression levels of various MMPs/TIMPs as assessed by Northern blot and quantitative reverse transcription PCR, when murine adipose tissue is separated into adipocyte & non-adipocyte fractions

1.3.3 MMPs, ADAMs and TIMPs are involved in preadipocyte differentiation via extracellular matrix remodelling and effects on signalling

The process by which preadipocytes differentiate into adipocytes is complex, involving a highly regulated sequence of transcriptional events [95]. *In vitro*, the spindle-shaped preadipocytes appear to detach from their surrounding matrix and take on a more rounded appearance, while beginning to accumulate triglycerides as cytoplasmic lipid droplets surrounded by a phospholipid monolayer [95]. Simultaneously, the surrounding ECM is remodelled from a stromal matrix to one more closely resembling a basal lamina, as described earlier. MPs and TIMPs may be involved in this process of ECM detachment and remodelling, and may modulate the availability and activity of extracellular cues for preadipocyte differentiation.

1.3.3.1 Differentiating preadipocytes modulate expression of MPs and TIMPs

All four TIMPs are downregulated at the induction of 3T3-L1 differentiation, but this effect is most dramatic in the case of TIMP-3 [96], which is also significantly downregulated in mouse embryonic fibroblasts, human subcutaneous preadipocytes and human visceral preadipocytes after two days of treatment with differentiation induction medium [96]. Taken as a whole, MMP expression changes over the course of differentiation are more complex, with a number being upregulated (e.g. MMPs-2, -7 and -11), and others demonstrating biphasic expression in 3T3-F442A and 3T3-L1 preadipocytes (e.g. TIMP-1, MMPs-9 and -14; see Table 1.3) [80, 92, 97]. The regulation of MMP-2, MMP-9, TIMP-1 and TIMP-4 expression during differentiation has been corroborated by zymography and reverse zymography of conditioned media from both these cell lines [80, 92]. Biphasic *Timp1*

expression changes are also seen in 3T3-L1 preadipocytes, with an initial downregulation followed by upregulation one week after differentiation induction, as determined by Northern blot [7] and quantitative RT-PCR [93]. MMP-1 and MMP-3 appear to be significantly downregulated at the induction of differentiation of human preadipocytes in culture [88]. MMP-3 downregulation is also seen in differentiating 3T3-L1 preadipocytes [98], where it appears to be regulated by the transcription factor retinoid-related orphan receptor (ROR)-γ [99]. It should be noted, however, that differentiation induction medium typically contains dexamethasone, and a direct effect of glucocorticoids, including dexamethasone, in reducing MMP-1 and MMP-3 expression in a variety of cell types, including bovine [100] and equine [101] primary articular chondrocytes, a human synovial sarcoma cell line [102], and a gingival fibroblast cell line [103], has been noted previously. Therefore, further investigation is needed to determine whether the downregulation of collagenase-1 and stromelysin-1 expression in differentiating human preadipocytes is due to the initiation of differentiation or due to the direct effect of dexamethasone in the differentiation induction medium.

Expression change	***MP or TIMP***
Upregulated	MMP-2, MMP-3*, MMP -7, MMP -11, MMP -12, MMP-13
Downregulated	MMP-3*, proMMP-14, MMP-17, TIMP-2, TIMP3, TIMP-4
Upregulated then downregulated	MMP-9**, Active MMP-14, MMP-19, ADAM-12
Downregulated then upregulated	MMP-9**, MMP-10, MMP-16, MMP -24, TIMP-1

*: MMP-3 has been reported as being upregulated in 3T3-F442A differentiation, while it is downregulated in 3T3-L1 differentiation
**: MMP-9 has been reported as showing opposite biphasic expression patterns in 3T3-F442A differentiation

Sources: [80, 92, 96-99, 104]

Table 1.3: Expression of different MPs and TIMPs over the course of differentiation of 3T3-F442A and 3T3-L1 preadipocytes, as assessed using semi-quantitative RT-PCR, gelatin zymography, reverse zymography or Western blotting.

1.3.3.2 MPs and TIMPs have roles in ECM remodelling in adipogenesis

The regulation of MP and TIMP expression over the course of preadipocyte differentiation implies a functional role for these proteins. In fact, MMPs may remodel the ECM surrounding preadipocytes into a more permissive environment for differentiation. Fibronectin (Fn) is thought to be a major component of adipose ECM with which preadipocytes interact [42, 105, 106]. MMP-2 upregulation in the initial stages of differentiation may be required to degrade this fibronectin network; inhibition of MMP-2 action with both broad-spectrum and

specific inhibitors results in maintenance of a Fn-rich ECM and reduced adipogenesis [80] (see also 'Effects of MP inhibition', below).

Another MP that may be involved in Fn remodelling during adipogenesis is ADAM-12. Overexpression of ADAM-12 at the cell surface in 3T3-L1 preadipocytes causes reorganisation of extracellular Fn from a fibrillar network to a dense, basement membrane-like pericellular configuration. In parallel, the cells spontaneously become rounder and there is cortical relocalisation of the actin cytoskeleton – changes that are all typical of preadipocyte differentiation [104]. The interaction with actin filaments is particularly intriguing; ADAM-12 appears to reduce β1 integrin activation at the onset of differentiation in a protease-independent manner, suggesting a role for ADAM-12 in modulating signalling between the extracellular matrix and the cytoskeleton [104]. A pro-adipogenic effect of ADAM-12 has also been indicated by the phenotypes of transgenic mice overexpressing soluble ADAM-12 in their skeletal muscle [107], and ADAM-12 deficient mice [108] (see 'Mutant rodent strains' section below).

Chun and colleagues have also implicated MT1-MMP or MMP-14, a membrane-bound matrixin, in adipocyte differentiation. They discovered that adipocytes from *Mmp14* null mice were smaller than in WT, and that WAT from *Mmp14-/-* mice had a higher collagen content than that in WT controls. Intriguingly, preadipocytes from these knockout mice differentiated normally when cultured on flat surfaces, but could not do so when cultured in a three-dimensional collagen I gel, but their adipogenic potential in 3D could be restored by reduction of the collagen density of the 3D collagen I matrix [109]. MMP-14-mediated collagen turnover may also be required during HFD-induced adipose tissue turnover, as *Mmp14* haploinsufficient mice on a HFD demonstrated increased collagen accumulation, decreased collagen cleavage, and reduced adipose depot size [110] (see 'Mutant rodent strains' section below). These data have led to the suggestion that MMP-14 is required to remodel the 3D matrix into a permissive environment for WAT expansion, particularly via its effect on pericellular collagen fibrils.

Aggrecan and versican are also remodelled in adipogenic differentiation. ADAMTS-4 and ADAMTS-5 are well-described aggrecanases in many human tissues such as cartilage and tendons [111], but Gorski *et al* found that deletion of *Adamts5* from murine adipose-derived stromal cells did not affect aggrecan or versican degradation, suggesting that other members of the ADAMTS family may be involved in this aspect of ECM turnover in adipose tissue [112]. However, the finding of increased proteoglycan synthesis in cells carrying this

deletion indicates that ADAMTS-5 still plays a role in regulating adipose ECM structure and function [112].

1.3.3.3 MPs and TIMPs modulate adipogenic signalling

Given the well-described role of TACE/ADAM-17 in the shedding of many cell surface proteins, including adhesion molecules, cytokine and growth factor receptors and many ligands of the EGF receptor (reviewed in [113, 114]), ADAM-17's effects on adipogenesis may shed light on the signalling factors regulating preadipocyte differentiation.

One such factor is preadipocyte factor (Pref)-1, the mouse homolog of human Delta-like protein (Dlk)-1. It is an EGF-like repeat containing protein that is present in preadipocytes but absent in adipocytes, thus serving as a marker for the former [115]. Unlike other proteins containing EGF-like repeats, such as Jagged, Pref-1 lacks a Notch interaction domain so it does not activate Notch signaling [116] Originally cloned from a cDNA library from 3T3-L1 preadipocytes [117], it is expressed in many embryonic tissues, but in adulthood it is found only in preadipocytes, pancreatic beta cells, pituitary somatotrophs, adrenal tissue, skeletal muscle and thymic stroma. Pref-1 is subject to genomic imprinting with expression only from the paternally inherited allele [116]. It is known to be involved in other mesenchymal differentiation processes apart from adipogenesis, such as osteoblastogenesis and chondrogenesis, as well as having roles in haematopoeisis and lymphocyte B-cell differentiation. In general, Pref-1 seems to function to maintain proliferating progenitor cells in an undifferentiated state during development [118].

Pref-1 undergoes considerable post-transcriptional and post-translational modification. There are four splice variants, A-D, each of which can undergo post-translational modifications with sialic acids and N-linked oligosaccharides being tagged to the extracellular domain. Membrane-bound Pref-1 (mPref-1) can also be proteolytically cleaved at two sites to generate two forms of soluble Pref-1, or sPref-1 – a 25 kDa and a 50 kDa form. Only Pref-1A and B display the cleavage site necessary to create the circulating 50 kDa sPref-1, and this lytic step is catalysed by ADAM-17 [119]. Stimulation of ADAM-17 activity by phorbol 12-myristate 13-acetate (PMA) increases Pref-1 shedding, an effect that is nullified by the addition of ADAM-17 inhibitors such as TIMP-3, TAPI-0 and GM6001 (a broad MMP/ADAM inhibitor). The full-length, membrane bound mPref-1 and the shed sPref-1 appear to have divergent roles in adipose tissue remodelling. It is the long, 50 kDa form of sPref-1 that is thought to be biologically active in inhibiting preadipocyte differentiation, as 25 kDa sPref-1 and mPref-1 do not exhibit this activity [120]. mPref-1, however, appears to strongly inhibit preadipocyte proliferation – an effect not shared by sPref-1 [121]. Thus, Pref-

1 may constitute a major regulator of adipose tissue expansion, and given ADAM-17's role in TNF-alpha shedding, the ADAM-17/sPref-1 axis provides another link between adipose tissue inflammation and regulation of preadipocyte differentiation.

Manipulation of ADAM-17/Pref-1 activity *in vitro* and *in vivo* has appreciable effects on both adipocyte differentiation and markers of metabolic function. Both treatment with GM6001 and transfection with ADAM-17-directed siRNA (inhibiting sPref-1 shedding) lead to increased lipid droplet accumulation in preadipocyte model cell lines, whereas transfection with a Lenti-TACE virus to bring about ADAM-17 overexpression decreases this [119]. Wild-type mice fed a HFD show increased soluble Pref-1 (sPref-1) levels but decreased Pref-1 mRNA when compared to *Adam17+/-* mice [122]. Transgenic mice expressing an sPref-1/hFc fusion protein under the control of the adipocyte fatty acid binding protein (aP2) promoter display decreased adipose tissue mass, decreased adipocyte marker expression (such as leptin, fatty acid synthase [FAS] and C/EBPα), and hypertriglyceridaemia, hyperglycaemia and insulin resistance – a lipodystrophic –like phenotype [123]. Interestingly, adipose tissue mass is also reduced when mice are engineered to overexpress sPref-1 in their liver (under the control of the albumin promoter), suggesting a possible endocrine role for this molecule [123]. Furthermore, WAT from ADAM-17 haploinsufficient and functional ADAM-17 knockout mice has smaller adipocytes packed together at increased density than that in WT mice [122, 124], suggesting that reduced ADAM-17 activity may decrease sPref-1 shedding and allow increased hyperplastic adipose tissue expansion (see 'Mutant rodent strains' section below).

A number of different constitutive and conditional Pref-1-null mouse strains have been generated. *Dlk1*^{tmHsul} mice [125], for example, show significant neonatal lethality – those that survive the neonatal period initially weigh significantly less than their wild-type littermates, but after weaning onto a high fat diet go on to gain weight faster than wild-type mice, due to larger white adipose tissue depots with larger adipocytes. They also display increased serum triglycerides, cholesterol and free fatty acids [125]. *Dlk1*^{cons} mice, which demonstrate a significantly larger deletion than that in *Dlk1*^{tmHsul} mice, are also smaller than controls in the neonatal period [116]. Female *Dlk1*^{cons} mice on a normal diet had lower retroperitoneal, inguinal and parametrial fat pad weights, and in both males and females mean adipocyte size was smaller than in controls at 6 weeks, but not different from controls at 16 weeks [116] (Table 1.4).

	Cell lines (3T3 L1, MEFs)	*Mouse models*
Pref-1/Dlk-1 overexpression	Reduced differentiation into adipocytes	Decreased adipose tissue mass, hyperlipidaemia, insulin resistance
Pref-1/Dlk-1 knockout/knockdown	Increased lipid droplet accumulation	Larger fat depots, larger adipocytes, hyperlipidaemia

Sources: [116, 121, 123]

Table 1.4: A summary of the effects of Pref-1/Dlk-1 overexpression or knockout/knockdown in experiments involving cell lines or mouse models.

The signalling pathways mediating the inhibition of preadipocyte differentiation by sPref-1 are incompletely understood, but fibronectin-stimulated integrin signalling appears to be required [126]. Fibronectin-integrin binding is known to activate ERK/MAPK pathways via Rho-like GTPases, which corresponds with work identifying this canonical signalling pathway as necessary for Pref-1's inhibition of adipocyte differentiation [127]. The activation of ERK/MAPK signalling upregulates & maintains the expression of Sox9, a transcription factor that suppresses the expression of CCAAT enhancer binding proteins (C/EBP)-β and -δ. These in turn serve to induce C/EBP-α and peroxisome-proliferator activated receptor (PPAR)-γ, transcription factors needed for adipocyte differentiation (Figure 1.3) [128]. In this regard, MMP-2-mediated fibronectin degradation at the onset of differentiation may be an additional mechanism by which the anti-adipogenic effect of sPref-1 is abrogated.

Another ADAM that has Pref-1 as a substrate is ADAM-12. *Adam12*-null and *Adam12*-overexpressing mouse strains exhibit phenotypes that are incongruous with those of mice with ADAM-17 deficiency or overexpression, indicating that ADAM-17 and ADAM-12 are unlikely to perform redundant roles (see 'Mutant rodent strains' section below). Furthermore, ADAM-12 is involved in fibronectin remodelling and integrin signalling as described above, suggesting that ADAM-12 plays a complex role in this process.

ADAM-17 may also affect preadipocyte differentiation through its release of soluble TNF-α. Higher BMI and higher WHR are both associated with increased MAP4K4 expression in preadipocytes. MAP4K4 activity can be induced by TNF-α, and leads to inhibition of PPARγ activation and thus inhibition of adipogenesis. Addition of TNF-α to human preadipocytes inhibits differentiation into adipocytes; this effect is reversed by its removal from the medium [129].

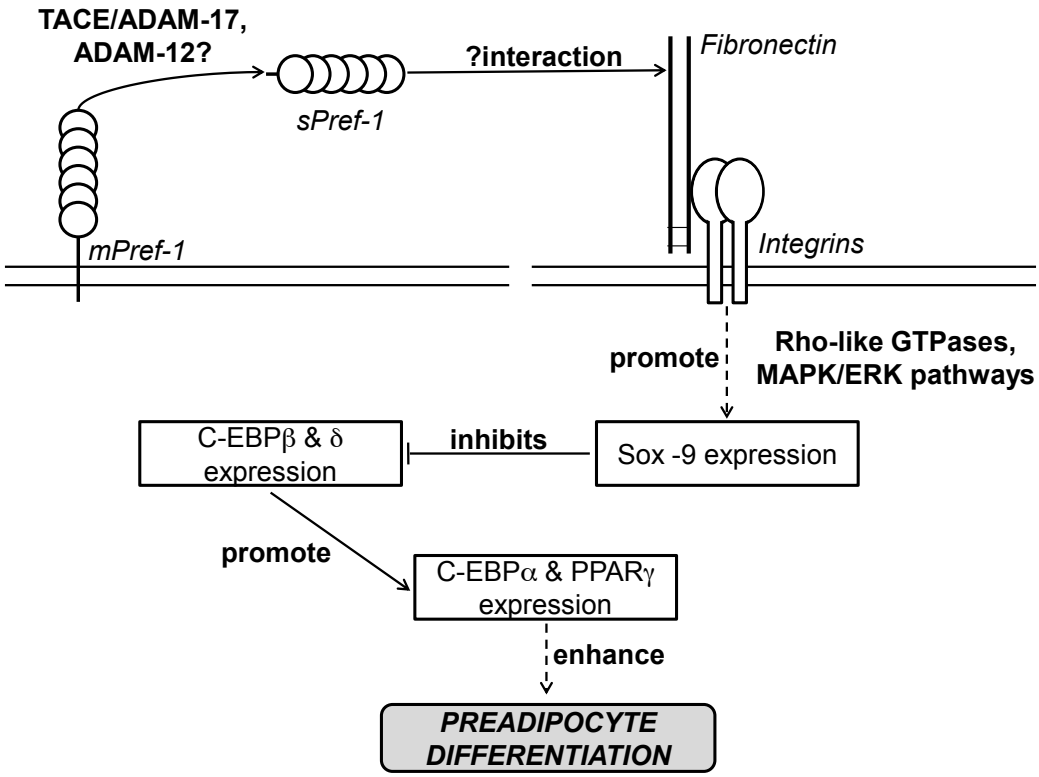

Figure 1.4: Proposed mechanism by which sPref-1 inhibits differentiation of preadipocytes. Interaction of sPref-1 with fibronectin may trigger integrin signalling, which enhances Sox-9 expression. This in turn reduces the expression of transcription factors that promote differentiation, including C-EBPs and PPARγ.

1.3.3.4 Effects of MP inhibition

Given the complex regulation of MP expression in adipogenesis, and the varied roles proposed for this superfamily, it is unsurprising that MP inhibition can have both pro- and anti-adipogenic effects. Various strategies to inhibit or reduce MP activity have been utilised, including pharmacological inhibitors, TIMP overexpression, anti-MP antibodies and MP knockdown using RNAi technology, and the differential effects on preadipocyte differentiation may be due to the different spectra of inhibition of these approaches. The effects of modulation of MP function on preadipocyte differentiation are summarised in Table 1, Appendix A.

1.3.4 Mutant rodent strains demonstrate metabolic consequences of MP/TIMP manipulation

1.3.4.1 MMPs

Gelatinases are regulated during preadipocyte differentiation, and their inhibition has varying effects on adipogenesis. *Mmp2-/-* mice fed a HFD for 15 weeks gained less weight, and had smaller adipose depots with larger adipocytes than WT counterparts – a similar phenotype to that shown by WT mice fed a HFD and treated with the gelatinase inhibitor tolylsam (see Table 1, Appendix A) [130]. *Mmp9* null mice fed a HFD, on the other hand, do not differ from their WT littermates in terms of their body weights, fat mass, or adipose tissue architecture in either subcutaneous or perigonadal depots [131]. This is in keeping with the finding that shRNA-mediated knockdown of *Mmp9* does not appear to affect *in vitro* differentiation of 3T3-F442A preadipocytes [97], but does not explain the association between circulating MMP-9 levels and obesity in human females [131] (see 'Human studies' section below).

Disruption of either stromelysin-1 (*Mmp3*) or stromelysin-3 (*Mmp11*) genes, on the other hand, invariably produces a metabolic phenotype. *Mmp3-/-* mice are hyperphagic, and after a 15-week period of HFD feeding have larger adipose depots than WT controls. In *Mmp3* null mice, perigonadal adipose tissue demonstrates larger adipocytes and a higher vessel density, but circulating triglycerides are lower. Interestingly, adipogenesis is also accelerated during mammary gland involution in these mice, with mammary tissue from *Mmp3-/-* mice showing an increased number of larger adipocytes after weaning than controls [98]. This is consistent with increased differentiation of 3T3-L1 preadipocytes when these are treated with a specific MMP-3 inhibitor or are subjected to siRNA-mediated *Mmp3* knockdown [99] (see Table 1, Appendix A), and with the finding, in the same study, that ROR-γ is a regulator of MMP-3 expression and that *Rorγ* deficient mice show enhanced adipogenesis [99] (see 'Expression of MPs and TIMPs during differentiation' section above). HFD feeding in *Mmp11-/-* mice similarly caused increased weight gain as compared to WT counterparts, with larger adipose depots and hypertrophic adipocytes, but there was no difference in fasting glucose, triglyceride or total cholesterol levels [132].

Conversely, MMP-14 activity appears to be important in adipogenesis. *Mmp14-/-* preadipocytes do not differentiate in three-dimensional collagen I gels (see 'Roles in ECM remodelling' section above), and *Mmp14* null mice have undetectable serum leptin and increased hepatic triglyceride [109]. On a HFD, *Mmp14* haploinsufficient mice gain less weight than controls, and have smaller inguinal and perigonadal adipose tissue depots, with no differences in food intake or metabolic rates [110].

MMP-19 may also play a role in adipose remodelling, as *Mmp19-/-* on a HFD gain more weight than WT littermates, and display adipocyte hypertrophy in both main adipose depots, with no detectable difference in expression of adipogenesis-related genes [133]. Mice deficient in macrophage elastase (MMP-12), however, gain weight at the same rate as WT controls on a HFD, and their metabolic phenotype is very subtle, with a trend towards higher plasma glucose and smaller subcutaneous adipocytes. There was no difference in macrophage infiltration between *Mmp12-/-* and *Mmp12+/+* mice, but null mice had a lower number of crown-like structures (CLS; the microscopic appearance of multiple macrophages which fuse and surround a dying adipocyte, phagocytosing it), which suggests that this metalloproteinase plays a role in the formation of these multinucleated syncytiae thought to be involved in the clearing of dead adipocytes [134].

1.3.4.2 ADAM-12

The putative roles of ADAM-12/meltrin α in adipogenesis have been alluded to above, with evidence suggesting functions in Fn remodelling and regulation of Fn-integrin interaction in preadipocyte differentiation, as well as possibly serving as a Pref-1 sheddase (see 'ECM remodelling' and 'Adipogenic signalling' sections above). About 30% of ADAM-12 deficient pups die within 1 week of birth; those that survive display a mild phenotype on a standard diet, with about a third of them having smaller interscapular brown adipose tissue depots in early life [108]. On a HFD, *meltrin α-/-* mice gained less weight than WT controls, had lower circulating leptin levels, and had smaller BAT, WAT and livers. The difference in WAT depot size was found to be due to a smaller number of adipocytes in the knockout strain – the mean adipocyte size did not differ from that in WT mice – corroborating the findings of *in vitro* studies suggesting a role for ADAM-12 in differentiation [135]. Interestingly, on a standard diet the ADAM-12 deficient mice were more insulin sensitive on an insulin tolerance test (ITT), and had lower circulating triglycerides and NEFA levels than their controls, but these differences were absent when both groups were fed a HFD [135].

Transgenic mice overexpressing the soluble form of ADAM-12 (ADAM-12-S) under the control of the muscle creatine kinase (MCK) promoter also demonstrate an interesting phenotype suggesting a role for ADAM-12 in adipogenesis. In this strain, ADAM-12 is overexpressed by skeletal and, to a lesser extent, cardiac muscle, and is found circulating at high levels in the serum. The transgenic mice have larger adipose tissue depots with a greater number of similarly-sized adipocytes as compared to controls, and also display large numbers of adipocytes within their skeletal muscle, in close proximity to myocytes (there is no intramyocellular lipid, indicating that this phenotype is not due to ectopic lipid deposition). Despite the greater fat mass, these mice do not differ from controls in terms of fasting

glucose, insulin, triglyceride and cholesterol levels. The ADAM-12 protease domain appears to be essential for the development of this phenotype, as transgenic mice overexpressing a form of ADAM-12-S lacking the metalloproteinase domain are no heavier than littermate controls [107].

1.3.4.3 TIMP-3 and TACE/ADAM-17

TIMP-3 is downregulated in *ob/ob*, *db/db* and AKR mice fed a HFD [7]. To investigate its effects in obesity, mouse strains deficient in TIMP-3 were generated. When compared to wild-type (WT) mice, *Timp3* null mice have similar fasting/fed glucose and insulin levels, leptin and adiponectin levels, and glucose tolerance. When the offspring generated by crossing these mice with *Insr* haploinsufficient mice (a model for insulin resistance) are fed a HFD, these *Insr+/-Timp3-/-* mice demonstrate worse hyperglycaemia and hyperinsulinaemia than wild-type, *Timp3-/-* or *Insr+/-* controls fed a HFD, indicating that the effects of TIMP-3 deficiency are additive. Analysis of their adipose tissue indicates increased expression of inflammatory mediators such as MCP-1, CCR2 and IL-6. Liver transaminases are also significantly raised, and histological analysis of liver tissue from HFD-fed *Insr+/-Timp3-/-* mice reveals changes indicative of ectopic fat deposition. These changes are absent or much more subtle in wild-type, *Timp3-/-* and *Insr+/-* mice fed a HFD [136]. These histological appearances are similar to those seen in grade 3 non-alcoholic fatty liver disease (NAFLD), a condition associated with obesity and insulin resistance in humans [137], suggesting a role for TIMP-3 in the processes of inflammation and ectopic lipid deposition that have been implicated in the progression from obesity to insulin resistance and T2DM.

Further experiments on *Insr* haploinsufficient mice have identified a role for TIMP-3 and one of the major MPs it inhibits, *T*NF-*α c*onverting *e*nzyme (TACE, now known as ADAM-17), in this process. Researchers stratified *Insr*+/- mice into normoglycaemic (*Insr*+/-N) and diabetic (*Insr*+/-D) groups. In the diabetic cohort, there is significantly reduced skeletal muscle expression and activity of TIMP-3, as compared to both *Insr*+/-N and WT littermates [138]. Furthermore, *Insr*+/-D mice show higher circulating and skeletal muscle TNF-α levels. It is hypothesised, therefore, that TIMP-3 deficiency allows unchecked TACE activity, releasing more soluble TNF-α and driving inflammation and metabolic dysfunction. The hyperglycaemic phenotype, in fact, can be reversed by administration of anti-TNF-α antibody or a TACE/MMP-2/-9 inhibitor, TAPI-1, to Insr+/-D mice. *T*NF-α *p*rotease *i*nhibitor (TAPI)-1 treatment, in particular, reduced glucose, insulin and TNF-α levels to those of WT mice [138]. Complete *Tace*/*Adam17* deficiency is lethal in the perinatal period [139], but offspring of *Insr+/-* mice crossed with *Tace*/*Adam17* haploinsufficient mice (*Tace*/*Adam17+/-*) do not become hyperinsulinaemic when fed a HFD, suggesting that partial ADAM-17 deficiency

may be metabolically protective [136]. *Tace*/*Adam17+/-* mice fed a HFD gain less weight, show lower fed glucose, fasting/fed insulin and non-esterified fatty acid levels, and decreased insulin resistance as compared to WT mice fed the same diet. WAT from WT mice shows higher levels of free TNF-α, and increased phosphorylation of insulin receptor substrate (IRS)-1 at S307, which is characteristic of TNF-α-induced insulin resistance [122]. Similarly, TaceMx1 mice, in which a systemic temporal deletion of *Tace*/*Adam17* can be induced by intraperitoneal administration of polyinosinicpolycytidylic acid (pIpC), have smaller adipocytes, improved insulin sensitivity on both ITT and glucose tolerance tests, and reduced hepatic lipid as compared to control littermates on a HFD [140].

The creation of mice lacking functional TACE has shed further insights into its role in adipocyte function [124]. $Tace^{\Delta Zn/\Delta Zn}$ mice have a deletion in exon 11 of the *Tace*/*Adam17* gene, affecting the MP domain and therefore its catalytic activity. Although significant numbers of these mice die before reaching adulthood, those that do survive are smaller and lighter than both wild-type and $Tace^{\Delta Zn/\Delta Zn}$ mice, with reductions in both total fat and lean mass. The reduction in fat mass is significantly different when this is normalised for total body weight. As expected, $Tace^{\Delta Zn/\Delta Zn}$ mice also have lower serum leptin levels than both wild-type and heterozygotes, but interestingly this is also lower than leptin levels in wild-type mice that are calorie-restricted to achieve the same percentage fat mass as the $Tace^{\Delta Zn/\Delta Zn}$ mice. Food intake is also the same as in wild-type mice, meaning that in spite of reduced serum leptin levels there is no compensatory hyperphagia. The mice show increased mitochondrial UCP-1 expression, increased oxygen consumption, decreased ambulation and a normal respiratory exchange ratio. They also have lower glucose levels and better glucose tolerance than wild-type mice [124].

1.3.4.4 TIMP-1

It is unclear whether addition of recombinant TIMP-1 to 3T3-L1 cultures enhances [98] or inhibits [93] preadipocyte differentiation (see Table 1, Appendix A). In a *Timp1*-overexpressing transgenic mouse strain [98], mammary gland involution and replacement with adipose tissue is accelerated, while *Timp1-/-* mice gain less weight on a HFD than controls in spite of similar food intake, and have improved metabolic parameters such as fasting glucose and total cholesterol [141]. These mice have smaller adipocytes packed at higher density in both subcutaneous and perigonadal depots. These findings suggest that TIMP-1 has a proadipogenic effect *in vivo*.

A summary of the phenotypes of mutant murine strains wherein MP/TIMP genes are manipulated is provided in Table 2, Appendix A.

1.3.5 Evidence from human studies

MMPs-2 and -9 have been the subject of much investigation with respect to their roles in adipose tissue remodelling. As outlined in the sections above, their expression is regulated in adipogenesis, and their inhibition affects preadipocyte differentiation. Increased *Mmp2* mRNA expression has been identified in adipose tissue of subjects with T2DM compared to BMI-matched controls without diabetes [142] and higher circulating MMP-2 levels are found in obese individuals as compared to lean controls [143]. In T2DM patients with increased MMP-2 expression, a larger average adipocyte size and decreased expression of markers of adipogenic differentiation such as aP2 have been described [143]. Mononuclear cells from obese adults display higher *Mmp9* expression [144]. Obese children and adolescents also have higher circulating MMP-9 levels, which correlate with BMI and fasting insulin [145, 146], and in obese adults, these increased serum MMP-9 levels decrease after weight loss [131]. Expression of *Mmp9* is greater in both omental and subcutaneous adipose tissue from metabolically healthy obese subjects as compared to lean controls. Furthermore, mRNA expression of *Mmp15* in subcutaneous and omental adipose tissue is negatively correlated with HOMA-IR in obese subjects [147].

It should be noted, however, that increased circulating MMP-2 and MMP-9 levels, as well as increased MMP-2 expression by mononuclear cells, have been described in healthy subjects who ingest a 75g oral glucose load [148]. Likewise, obese subjects ingesting a high-fat, high carbohydrate meal have higher circulating MMP-9 levels than lean controls [149]. It is therefore unclear whether increased circulating gelatinase levels are reflective of increased gelatinase expression or activity in adipose tissue, or whether there are derived from another source, such as mononuclear cells. Similarly, it is unknown whether gelatinases are definitively involved in the pathogenesis of obesity-related insulin resistance and T2DM, or whether increased expression is a result of hyperglycaemia and impaired carbohydrate/energy handling in established diabetes.

Investigations in Pima Indians have revealed a role for adipose expression of MMP-3 in development of type 2 diabetes mellitus [150]. In this study, Traurig and colleagues found a negative correlation between MMP-3 expression levels in the stromovascular fraction of subcutaneous adipose, and BMI. They went on to examine several sequence variants in the MMP-3 gene in over 1,000 subjects and found two that were associated with BMI and T2DM and a further two that were associated exclusively with T2DM, although none of these variants were associated with MMP-3 expression [150]. More recently, however, *Rorγ* expression in subcutaneous adipose stromovascular fraction has been found to correlate

with both BMI and *Mmp3* expression [99], a finding that is inconsistent with the results of Traurig *et al* [80]. MMP-3 mRNA expression also correlated positively with adipocyte size [99]. Genotyping of *Mmp3* in over 16,000 European children has revealed a variant of a single nucleotide polymorphism (SNP) (rs646910) and a diplotype (H3/H3) that are both associated with higher BMI, waist circumference (WC) and hip circumference (HC) [151].

Another intensively studied MMP with a potentially crucial role in adipose remodeling is MMP-14. Assessment of *Mmp14* haplotypes in over 3000 healthy Japanese subjects identified one (haplotype 122) that was associated with both BMI and WHR. Regression analysis was then used to discover that genotype at a SNP (rs2236302) associates with BMI and WHR, with the minor allele being associated with a 0.42 kg/m^2 increase in BMI [110].

Investigations in humans on the role of ADAM-17/TACE and TIMP-3 have focused on their role in skeletal muscle, one of the major insulin-responsive tissues. Human subjects with T2DM exhibit reduced TIMP-3 levels and increased TACE activity in their skeletal muscle, along with increased circulating TNF-α, TNF-α receptor (TNFR)-1 and IL-6 receptor (IL-6R) levels [152]. Administration of pioglitazone reduces skeletal muscle ADAM-17/TACE activity in tandem with improvements in insulin sensitivity, with no changes in TACE or TIMP-3 expression [153]. ADAM-17/TACE is the main sheddase for Pref-1, and TIMP-3 is the major ADAM-17 inhibitor (see 'Adipogenic signalling' section above). In metabolically unhealthy obese subjects, Pref-1/Dlk-1 levels in subcutaneous and omental adipose tissues are higher than in age- and BMI-matched metabolically healthy counterparts. Furthermore, omental Pref-1/Dlk-1 expression is significantly associated with adipocyte hypertrophy, hepatic fat, and increased fasting insulin, glucose and triglycerides [154].

Genomic analysis has also implicated the ADAMTS subset of MPs in the development of T2DM, as a meta-analysis of three genome-wide association studies (GWAS) identified a cluster of single nucleotide polymorphisms (SNPs) 38kb upstream of the ADAMTS9 gene on chromosome 3 as a susceptibility locus for T2DM [155].

1.4: Conclusion

Adipocytes and their precursors express MPs and TIMPs. Their expression can be altered by exposing adipocytes to inflammatory milieus, and is also related to the genetic background and nutritional exposure of mice, with obese mice displaying a characteristic pattern of MP/TIMP expression. Experimental manipulation of MP/TIMP expression, through

the use of knockout mice, siRNA and lentivirus transfection experiments, for example, leads to altered metabolic parameters that mirror those seen in obese humans developing T2DM. For instance, TIMP-3 deficient mice challenged with either a genetic background predisposing to insulin resistance or a HFD display worse dysglycaemia, in an additive fashion. Symmetrically, mice deficient in TACE, one of the major MPs inhibited by TIMP-3, are relatively protected from the metabolic effects of a HFD insult. These metabolic outcomes maybe in part mediated by the effects of these MPs/TIMPs on adipogenesis – WAT deficient in TACE shows increased cellularity. In turn, effects on differentiation are likely to be influenced by both MP/TIMP effects on Pref-1 and TNF-α release, and on the regulation of the ECM remodelling that accompanies the transition from a preadipocyte to an adipocyte. The effects of individual MPs and TIMPs are likely to be subtle and additive, and some redundancy is undoubtedly a feature of these systems, as many mouse strains with MP/TIMP manipulations only display a metabolic phenotype when exposed to the metabolic stress posed by a HFD. A synthesis of the evidence for MP and TIMP involvement in obesity-related metabolic disease is provided in Table 3, Appendix A.

Although results from different experiments may appear inconsistent, certain commonalities may be drawn from the above description of the roles of MPs and TIMPs in adipose tissue function. MMP-2, and to a lesser extent MMP-9, appear to play roles in adipogenic differentiation. As gelatinases, their substrates include collagens I, III and fibronectin. The decrease in fibronectin content of surrounding ECM during preadipocyte differentiation may therefore be, at least in part, dependent on gelatinase activity. Likewise, ADAM-12's capacity to degrade fibronectin may play an important role in its pro-adipogenic activity. MMP-14 may have a dual function – it is a true collagenase, therefore likely degrading collagen I surrounding preadipocytes in differentiation, and it is also required for MMP-2 activation. MMP-3, on the other hand, appears to have an anti-adipogenic role, which may be related to its capacity to degrade collagens IV and VI, which are components of the ECM surrounding adipocytes. Generally speaking, TIMP3 deficiency has adverse metabolic consequences, whereas ADAM-17/TACE deficiency is metabolically protective – this dyad's role in the shedding of important mediators such as TNF-α and Dlk-1 in human adipose tissue remains to be fully elucidated.

Much of the evidence in this field currently comes from *in vitro* studies, including experiments with (pre)adipocyte cell line models and rodents. Translation of results from other organisms into better health outcomes for humans is fraught with difficulty, as the field of MP/TIMP biology knows only too well. Initial *in vitro* positive results that were observed when MMP inhibitors were being investigated as potential anticancer treatments, for

example, were not replicated when these agents were tested in long-term clinical trials. Certain cases actually caused unexpected adverse outcomes, probably as a result of their broad spectrum of activity [62]. A greater understanding of MP roles in human biology must be the foundation on which future clinical trials looking at pharmacological manipulation of these systems are designed. In the area of human obesity and metabolic disease, however, evidence of MP/TIMP involvement is limited to small observational studies and GWAS, which provide associative evidence rather than verification of cause-and-effect relationships.

In summary, the adverse metabolic consequences of obesity may rest on the development of an inflammatory state in which there is (a) the induction of insulin resistance through well-characterised modulation of downstream signalling pathways, along with (b) impaired ability of WAT to recruit new adipocytes, leading to hypertrophy of the tissue by enlargement of existing adipocytes, and deposition of fat in ectopic sites (Figure 1.4). By playing potentially central roles in integrating the inflammatory signal with adipose remodelling in obesity, MPs and TIMPs are attractive subjects for further study and may constitute targets for therapeutic pharmacological manipulation.

1.5 Research questions

I developed the following research questions, based on the literature review above:

1. Which are the key MPs and TIMPs expressed by human adipocytes and preadipocytes, and how is this expression modulated by inflammatory or pro-adipogenic stimuli?
2. In human adipose tissue, does altered MP/TIMP expression contribute to maladaptive adipose tissue remodelling, whole-body lipid maldistribution and metabolic dysfunction?
3. In human adipose tissue, what role does TIMP-3 play in regulating i) ECM turnover and ii) expression and shedding of the anti-adipogenic mediator Dlk-1, and ultimately adipogenic differentiation and hyperplastic adipose expansion?

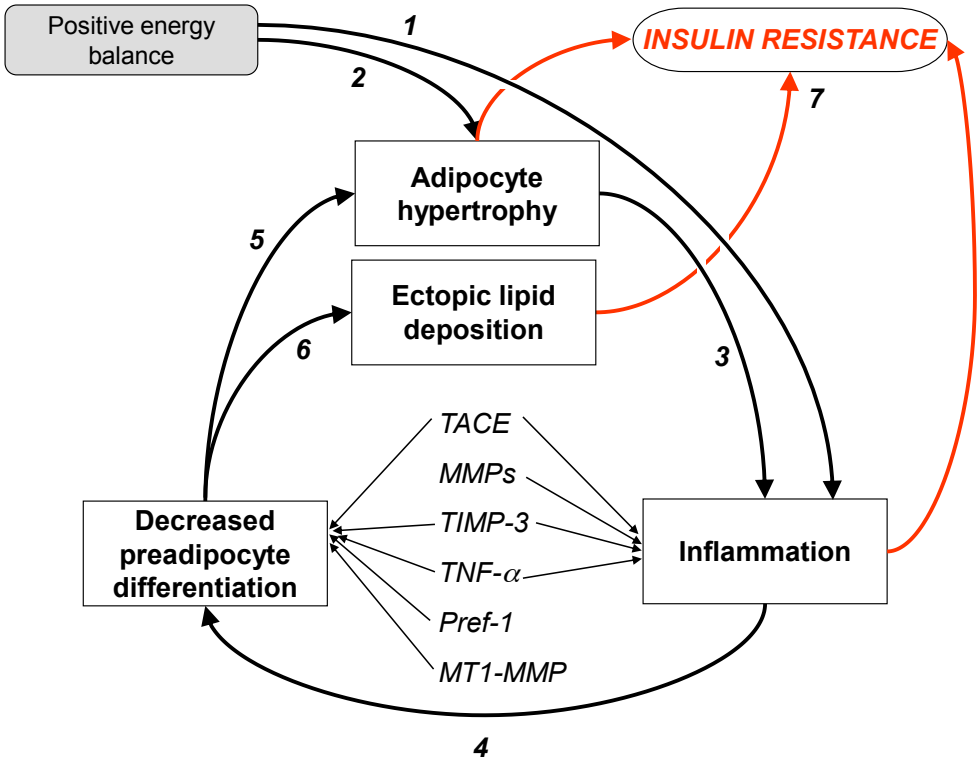

Figure 1.5: A schematic representation of the possible interrelationship between adipocyte differentiation, inflammation and insulin resistance, with the potential points at which ADAMs, MMPs and TIMPs may play a role. Eating too much and exercising too little leads to positive energy balance, weight gain and increased white adipose tissue (WAT) mass. This results in adipose inflammation (1), with immune cell infiltration of the WAT and the adipocytes taking on a more inflammatory phenotype. The individual adipocytes begin to increase in size by a process of hypertrophy (2), with increased secretion of free fatty acids (FFAs) and inflammatory mediators (3). Inflammation results in modulation of the MP/TIMP balance, which is also linked to altered preadipocyte differentiation (4). Reduced capacity to differentiation induces further growth by hypertrophy (5) and eventually lipid overspill to non-adipose sites (6). Inflammation, ectopic lipids and hypertrophied adipocytes are each independently linked with insulin resistance (7).

Chapter 2: Materials & Methods

2.1: Introduction

As outlined in the Introduction, these studies were designed to address whether (1) human preadipocytes and adipocytes express metalloproteinases (MPs) and their tissue inhibitors (TIMPs), (2) whether this expression is regulated by inflammatory stimuli and by the process of preadipocyte differentiation into mature adipocytes, and (3) whether expression of MPs and TIMPs in human subcutaneous and intra-abdominal adipose tissue is related to established metrics of metabolic function, such as adipocyte size and the homeostatic model assessment of insulin resistance (HOMA-IR) [156, 157], and with whole-body lipid distribution. The techniques used to address these questions have therefore been performed in a model of human preadipocytes and adipocytes and in *ex vivo* samples of human adipose tissue.

2.2: Human adipose-derived mesenchymal stromal cell and *in vitro*-differentiated adipocyte culture

2.2.1 Introduction

This model is well-established in the primary supervisor's laboratory [158-160], and within the adipose research community as a validated model with which to study human adipose function [161-163]. An existing collaboration with the Department of Plastic Surgery at the Norfolk and Norwich University Hospital allows access to a supply of human abdominal subcutaneous adipose tissue for isolation of primary cells, as described below. Cell line models of preadipocytes that accumulate lipids *in vitro* exist, such as the 3T3-L1 [79] and 3T3-F442A [164] preadipocyte lines, and Simpson-Behmel-Golabi syndrome (SBGS) human preadipocytes [83], and work with cell lines has a number of advantages such as easy availability, widespread use and consequent acceptance of research performed using these lines by the scientific community. Nevertheless, they are imperfect models of human adipose physiology; 3T3-L1 and 3T3-F442A cells are of murine origin, for example, while the SBGS cell line is unresponsive to some inflammatory stimuli including the Toll-like receptor (TLR)-4 ligand lipopolysaccharide (LPS) (unpublished data, personal communication Dr D Morganstein, Imperial College London), which is of relevance given the research questions this project is designed to address.

The term adipose-derived mesenchymal stromal cell (MSC) refers to the various cell populations within the heterogeneous population making up the stromal vascular fraction (SVF) of adipose tissue. These cells are readily available, and are very well studied due to

their ability to differentiate into the range of mesodermally-derived tissue types, such as bone, cartilage, muscle, and adipose [165]. However, the difficulties in identifying the adipose-committed subpopulation within this heterogeneous population are well-documented. These difficulties are consequent to the facts that (i) there is a lack of distinct markers of the preadipocyte population and (ii) the difficulty defining precisely where in the commitment and differentiation process a given cell lies [166-168]. Nevertheless, as indicated previously, the protocols for directing this population towards adipogenic differentiation *in vitro* are long-standing and universally adopted by the adipose community. Thus, although it is accurate to refer to the cells used to establish primary *in vitro*-differentiated adipocyte cultures as adipose-derived MSCs, in the interests of brevity cells of this type will be referred to as 'preadipocytes' throughout this thesis.

As outlined in subsection 2.2.2 below, differentiation of primary preadipocytes *in vitro* into adipocytes was preferred to the use of primary human adipocytes. This is primarily for technical reasons: the high lipid content of primary mature adipocytes makes them impossible to pellet by centrifugation, and they also do not adhere to the bottom of tissue culture flasks or wells.

2.2.2 Method

With research ethics committee approval (NRES Committee London – Fulham 12/LO/1232), and with the generous help of Miss Rozina Ali, Mr Andrea Figus, Mr Richard Haywood, Mr Martin Heaton and Miss Elaine Sassoon, healthy, non-obese female subjects undergoing breast reconstruction surgery (deep inferior epigastric perforators [DIEP] flap) or abdominoplasty were recruited, and written informed consent to acquire samples of subcutaneous abdominal adipose intraoperatively was secured. As part of the normal DIEP flap operative procedure, blood vessels called deep inferior epigastric perforators, as well as the skin and subcutaneous abdominal adipose connected to them, are removed from the lower abdomen and transferred to the chest to reconstruct a breast after mastectomy without the sacrifice of any of the abdominal muscles [169]. Any excess subcutaneous abdominal adipose tissue left over following the completion of breast reconstruction, which would in the normal course of events be discarded, was donated to this study. Similarly, the operative process in abdominoplasty involves the removal of large amounts of skin and subcutaneous abdominal adipose tissue following the patient's weight loss. Whereas this tissue would normally be discarded, study participants gave their informed consent for the tissue to be collected and used in this study. Exclusion criteria included active infection or autoimmune disease, active malignancy, use of strong anti-inflammatory drugs such as corticosteroids or disease-modifying anti-rheumatic drugs (DMARDs), and diabetes. Primary human

preadipocytes were isolated ex vivo from these samples by collagenase digestion according to established techniques [162]. Fresh subcutaneous adipose tissue was transported immediately from the operating theatre to be processed under sterile conditions in a laminar flow hood. The tissue was dissected to remove blood vessels, skin and connective tissue, then minced and incubated for 30 minutes with agitation in serum-free Dulbecco's Modified Eagle's Medium (DMEM; PAA, Pasching, Austria) containing 0.5 mg/ml *Clostridium histolyticum* collagenase type 1A (Sigma, Poole, UK), and 0.1 mg/ml DNAse type I from bovine pancreas (Roche, Mannheim, Germany). The digestate was filtered through a 70 μm sterile nylon mesh (BD Biosciences, Oxford, UK), and the filtrate was topped up with DMEM containing 10% fetal calf serum (FCS; Gibco, a subsidiary of Life Technologies, Paisley, UK), and centrifuged at 400 x *g* for 5 minutes. The pellet containing the adipose stromo-vascular fraction was resuspended in 1ml of red cell lysis buffer (Sigma) for 1 minute with agitation, and the suspension was then washed and re-centrifuged at 400 x *g* for 5 minutes. The pellet was resuspended in basal medium containing high-glucose (4.5 g/l) DMEM, 10% FCS and 1% antibiotic/antimycotic solution (10,000 units of penicillin, 10,000 μg of streptomycin, and 25 μg of Amphotericin B per mL) (PAA) and plated. Cells were grown to subconfluence, with media changed every 72 hours, and passaged for a maximum of 2 passages with 1x trypsin-EDTA (0.05%/0.02% in PBS; PAA) with a maximum ratio of 1:2. For most experiments, cells were used at P1.

For *in vitro* differentiation, cells were passaged into the required experimental format, grown to confluence, and medium was changed to adipogenic medium 48 hours after confluence was achieved. Adipogenic medium consisted of basal medium supplemented with 100 nM human insulin, 1 μM dexamethasone, 0.2 mM indomethacin, and 0.5 mM 3-isobutyl-1-methylxanthine (IBMX; all from Sigma). Adipogenic medium was changed every 72-96 hours for 14 days, during which the quality of differentiation was assessed by phase-contrast light microscopy. Oil Red O staining (see below) was used in some cases to estimate final differentiation efficiency.

For experiments in which cells were challenged by the inflammatory stimulus tumour necrosis factor (TNF)-α, media were changed to low glucose (1g/l) DMEM/10% FCS/1% PSA for 72 hours, to allow habituation to control media and for the anti-inflammatory effect of dexamethasone to remit. TNF-α was used for 24 or 48 hours at 50 ng/ml as per our group's established protocols [159, 160]. TNF is a potent pro-inflammatory cytokine, and human adipocytes and adipocyte precursors express the TNF receptor and exhibit biological responses to TNF [20, 170, other references].

Depending on the downstream analysis planned, cell culture supernatants were collected, and cells were lysed in Triton lysis buffer (25 mM HEPES [4-(2-hydroxyethyl)-1-piperazineethanesulfonic acid], 100 mM sodium chloride, 1 mM EDTA [ethylenediaminetetraacetic acid], 10% (v/v) glycerol, 1% (v/v) Triton X-100) for subsequent immunoblot of lysates or in RNA stabilization buffer (Buffer RLT (proprietary product); Qiagen, Crawley, UK) for RNA extraction.

2.2.3 Choice of fetal calf serum

Cell culture media are a combination of both standard, invariant simple components, such as glucose, and complex, variable ones. The latter category includes fetal calf serum (FCS). It is well known that serum-specific components such as bovine serum albumin (BSA) and insulin-like growth factor (IGF)-I may vary between different batches, and that these components play a crucial role not only in the activation but also differentiation of various cell types. Thus, in the interests of consistency and replicability of the investigations in this study, I tested the influence of four different batches and brands of serum on preadipocyte differentiation (Table 2.1). Preadipocytes from three unique donors at P1 passage were plated in 12-well plates and differentiated as described above. Following the standard 14-day differentiation period, a process of quantitative Oil Red O staining (see section 2.3) was used to assess how differentiation efficiency varied between the different batches and brands of FCS.

Abbreviated Name	Brand	Batch number
Gibco I	Gibco/Life Technologies	07G5331K
Gibco II	Gibco/Life Technologies	07G7531K
Gibco III	Gibco/Life Technologies	07F7134K
Sigma	Sigma	0331M3395

Table 2.1: The brands and batch numbers of the four different types of FCS used in the batch testing exercise. The term 'abbreviated name' refers to the label given to each FCS type during the experiment, as shown in Figure 2.1.

As seen in Figure 2.1, use of serum Gibco II (batch number 07G7531K) resulted in optimal differentiation efficiency within the group of FCS brands/batches tested. As a result, this brand and batch of serum was used in all subsequent experiments described in this thesis.

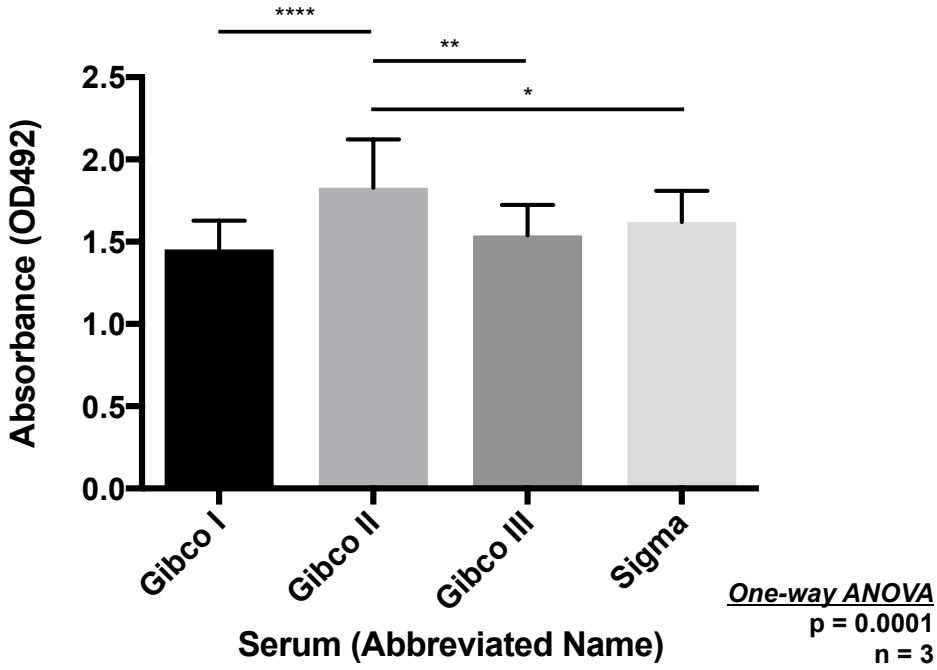

Figure 2.1: Use of Gibco® II fetal calf serum (batch number 07G7531K) leads to greater differentiation efficiency of primary preadipocytes into *in vitro*-differentiated adipocytes as compared to three other serum batches/brands (see Table M.1). Data is from 3 biological replicates from each of 3 different donors (each bar represents the mean absorbance + SD for these 9 samples). Data for each experimental condition was compared to Gibco II using an unpaired Student's *t* test (*, $p < 0.05$; **, $p < 0.01$; ****, $p < 0.0001$).

2.3: Quantitating adipogenic differentiation

2.3.1 Introduction

Adipogenic differentiation is central to the process of hyperplastic adipose tissue expansion, which is thought to be a feature of metabolically healthy obesity [171]. Therefore, I sought to gain expertise in reliable, replicable methods of quantitating the degree of adipogenic differentiation by primary human adipose-derived mesenchymal stromal cells in different conditions. These included using Oil Red O dye and a proprietary fluorescent dye, QBT®.

2.3.2 Quantitative Oil Red O staining

Oil Red O (also known as Sudan Red 5B) is a lipophilic dye that is used to stain accumulated triglycerides in cultured cells, as well as in sectioned tissue samples [172]. Lipid accumulation following 14 days in adipogenic media was visualized and quantified by Oil Red O staining for cells from certain donors. Briefly, stock solution was made up by dissolving Oil Red O (Sigma) at a concentration of 3mg/ml in 99% isopropanol. This was mixed at a ratio of 3:2 with deionised water to make Oil Red O working solution. Cell culture

medium was removed, and cells were washed with 1x phosphate buffered saline (PBS), fixed with 4% paraformaldehyde for 5 min at room temperature, washed with water and incubated for 5 minutes with 60% isopropanol, followed by a 5 min staining with Oil Red O. The excess dye was removed by repeated washes with water, and photomicrographs of the cells were taken at this stage (Figure 2.2). Cells were then incubated in 100% isopropanol for 15 minutes with gentle shaking, to extract Oil Red O from intracellular lipids. The isopropanol was loaded onto a 96-well plate, and the absorbance at 492nm was read spectrophotometrically using an ELISA plate reader (FLUOstar Omega, BMG Labtech, Ortenberg, Germany).

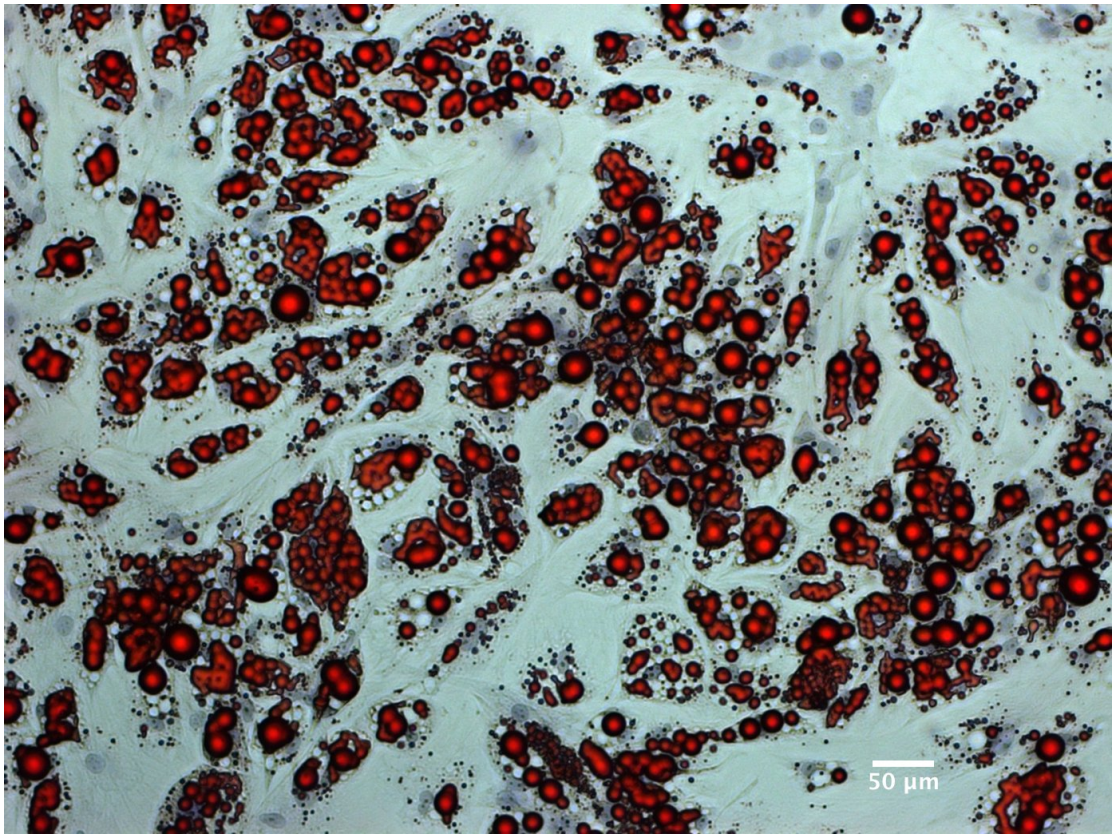

Figure 2.2: Photomicrograph taken of *in* vitro-differentiated adipocytes 14 days after the initiation of differentiation, following staining with Oil Red O dye, at 10x magnification. Image acquired using the Zeiss Axiovert 40 CFL inverted microscope using the AxioVision LE software V4.8 (Carl Zeiss Microscopy, Cambridge, UK).

2.3.3 QBT® Fatty Acid Uptake Assay Kit

An alternative assay to Oil Red O staining used to quantitate differentiation efficiency was the QBT® Fatty Acid Uptake Assay (Molecular Devices, Sunnyvale, CA, US). This is a proprietary assay that uses a BODIPY®-dodecanoic acid fluorescent fatty acid analog, and

employs a patented quenching dye to reduce background fluorescence and to improve the signal-to-noise ratio. The BODIPY®-fluorescent fatty acid analog is a known substrate for fatty acid transporters and behaves much like natural fatty acids, becoming activated by acyl-CoA attachment and being incorporated into di-and triglycerides. Thus, cells containing intracellular lipid droplets, such as *in vitro*-differentiated primary adipocytes, accumulate the analog; there is a linear relationship between the intensity of fluorescence and the amount of intracellular lipid, which itself is used as a surrogate marker for degree of differentiation.

The dye was used according to the manufacturer's instructions. Briefly, primary preadipocytes were plated in 96-well plates and differentiated *in vitro* as described above. On the day of the assay, they were incubated for 4-5 hours in basal medium, then serum-deprived for one hour. 1X Hank's Balanced Salt Solution (HBSS)/20 mM Hepes/0.2% fatty acid-free BSA was then prepared. 10 ml of this solution were added to Component A of the QBT® Fatty Acid Uptake Assay Kit, and 100 µl of this Loading Buffer were added to each assay well. Loading Buffer was also added to a set of cell-free wells for background controls. Following a one-hour incubation with Loading Buffer, cells were washed with serum-free medium, and plates were read in the FLUOstar Omega plate reader (BMG Labtech) using Omega software V1.02, at 485nm excitation/515nm emission with bottom read. Figure 2.3 shows photomicrographs of differentiated and undifferentiated cells, both treated and untreated with QBT® Fatty Acid Uptake Assay, to provide a visual demonstration of the specificity of this assay.

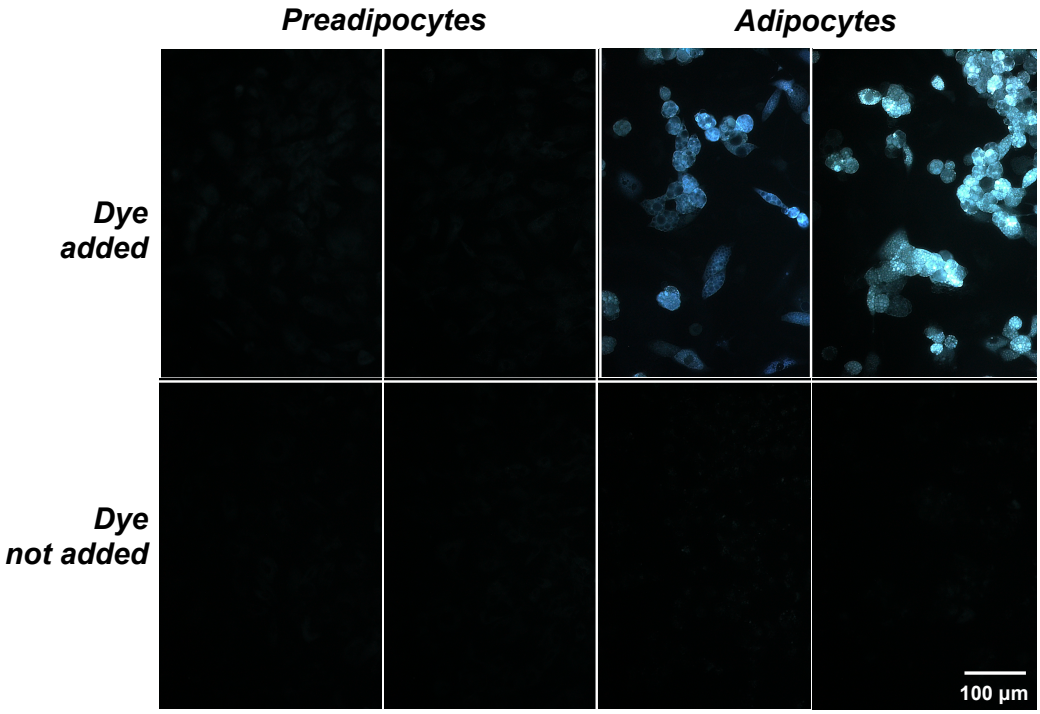

Figure 2.3: Photomicrographs taken of preadipocytes and *in* vitro-differentiated adipocytes following incubation with QBT® Fatty Acid Uptake Assay, at 5x magnification. Image acquired using the Zeiss Axioplan 2ie widefield upright microscope using the AxioVision LE software V4.8 (Carl Zeiss Microscopy, Cambridge, UK).

2.4: RNA isolation, reverse transcription and quantitative RT-PCR

RNA was isolated using a commercially available kit (Qiagen, Crawley, UK) according to the manufacturer's instructions. Briefly, following experimentation, cells in culture were lysed, and cell lysates were homogenized by centrifugation through a proprietary 'shredder' column. The homogenate was collected, and 70% ethanol was added to cause nucleic acid precipitation. Centrifugation of this suspension through another proprietary spin column allowed selective RNA binding to a silica-based membrane. A series of washes then removed contaminants such as cell culture media components, proteins and genomic DNA, and total RNA was eluted in 30 µl of nuclease-free water and stored at -80°C.

Quantitative reverse transcription polymerase chain reaction (qRT-PCR) allows quantification of mRNA (see below), which in turn allows an assessment of the transcription, and hence expression, of a particular gene to be made. Classical PCR techniques can only be applied to DNA, due to the reliance on thermostable Taq polymerase, but total RNA can be reverse transcribed to complementary DNA (cDNA) that can then be used in qRT-PCR reactions. Reverse transcription was carried out according to standard methodology [173] - following incubation with random hexamers (Life Technologies) for 10 minutes at 70°C, the

RNA was incubated with Superscript II reverse transcriptase (an engineered version of M-MLV reverse transcriptase to reduce RNase H activity; Life Technologies), deoxyribonucleotide triphosphates (dNTPs; Bioline, London, UK) and RNasin® ribonuclease inhibitor (Promega, Southampton, UK) for 1 hour at 42°C. Enzyme activity was then terminated at 70°C for 10 minutes, and cDNA samples were stored at -20°C.

In qRT-PCR, specific cDNA sequences are amplified by a polymerase chain reaction – specificity is provided by well-designed complementary forward and reverse primers, while the quantitation of PCR products occurs on a real-time basis by generation and detection of a fluorescent signal. For this project, TaqMan® qRT-PCR chemistry (Applied Biosystems, Foster City, CA, USA) was used, which relies on the 5'-3' exonuclease activity of Taq polymerase. TaqMan probes are dual-labelled oligonucleotides that consist of a fluorophore covalently attached to the 5'-end and a quencher at the 3'- end. In the unhybridised state, the quencher prevents the detection of the fluorescent signal from the fluorophore. When hybridized to the complementary target sequence on a PCR product, the 5'-nuclease activity of the polymerase cleaves the probe. This separates the fluorophore from the quencher, allowing fluorescence to be detected. Fluorescence therefore increases proportionately to the amount of probe cleavage and thus the amount of the PCR product. A greater starting amount of target sequences means that a particular fluorescence threshold (or cycling threshold, C_T) is reached sooner than if the starting amount of sequences was lower – this allows an assessment of gene expression to be made.

For the analysis of mRNA expression of all human MPs and TIMPs in primary *in vitro*-differentiated human adipocytes (see Chapter 3: Expression of metalloproteinases and their inhibitors), microfluidic Taqman® Low Density Array (TLDA) cards were used, custom designed to include all 66 human MMP, ADAM, ADAMTS and TIMP genes as well as 3 positive control genes (IL-6, IL-8, chemokine (C-C motif) ligand 2 [CCL2]), and two housekeeping genes (large ribosomal protein P0 [RPLP0] and 18S). The TLDAs were used as described previously [174], and relative quantification of genes on the cards was performed using the ABI Prism® 7900 HT (Applied Biosystems) sequence detection system. Basal expression was assessed in low glucose media cultures and compared to expression in high glucose media, and in low glucose media supplemented with 50 ng/ml TNF-α or 10 ng/ml LPS, using the $2^{-\Delta\Delta Ct}$ method [175], with RPLP0 as the comparator. Each sample was analysed in triplicate and mean C_T values of samples from 3 individual donors with the highest RNA yield were calculated.

2.5: Enzyme-linked immunosorbent assay

The concentration of proteins secreted by preadipocytes and *in vitro*-differentiated adipocytes was assayed by sandwich enzyme-linked immunosorbent assay (ELISA). This is an established technique that relies on two specific antibodies: a capture, or primary, antibody and a detection, or secondary, antibody, that recognize non-overlapping epitopes on the protein of interest. The detect antibody is biotinylated, allowing binding of streptavidin, which is conjugated to horseradish peroxidase (HRP; streptavidin-HRP conjugate obtained from R&D Systems, Abingdon, UK). This enzyme catalyzes the oxidation of 3,3',5,5'-tetramethylbenzidine (TMB; KPL, Gaithersburg, MD, USA) forming a blue product. On cessation of this reaction by addition of diluted H_2SO_4, a deep yellow product is formed. This can be quantified spectrophotometrically using the absorbance at 450nm. Therefore, there is a resolvable relationship between the amount of detected protein and the absorbance at 450nm; the use of a standard curve allows the calculation of the protein of interest in the sample.

The concentration of IL-8, MMP-1 and Dlk-1 in culture media was determined by proprietary ELISA kits (R&D Systems), following the manufacturers' instructions. Absorbance was read and analyzed at 450nm on the FLUOstar Omega spectrophotometric ELISA plate reader (BMG Labtech) using Omega software V1.02.

2.6: Western blotting and protein concentration by trichloroacetic acid precipitation

Western blotting is a long-established technique used for the detection of proteins in a sample. A protein-containing sample, such as a cellular lysate or a concentrated sample of conditioned media, is separated using polyacrylamide gel electrophoresis (PAGE). The use of sodium dodecyl sulphate (SDS) allows electrophoretic separation of denatured proteins based on their molecular mass, as SDS confers a negative charge in proportion to their length. The separated proteins are then transferred to a polyvinylidene diflouride (PVDF) membrane by a process of electroblotting, arranging the proteins on a thin surface to aid detection by a primary antibody. Following washing of excess unbound primary antibody, any primary antibody that is bound to membrane-bound protein is detected by a secondary antibody that targets a species-specific epitope on the primary. The secondary antibody is conjugated to HRP, which catalyzes a chemiluminescent reaction. Thus, the degree of

luminescence, which can be detected using X-ray film placed over the membrane in a dark room, is related to the amount of membrane-bound target protein.

In this study, all SDS-PAGE was performed in denatured, reducing conditions on 10% gels, and all primary antibodies were from Abcam (Cambridge, UK), and secondary antibodies were from DAKO (Ely, UK), unless stated otherwise.

No quantification of Western blot results was performed in this study. This is due to concerns regarding the lack of linearity in the relationship between target protein abundance on the membrane and the intensity of chemiluminescence. Thus, Western blotting was used as a semi-quantitative assay in this study. It is understood that this approach limits the ability to draw conclusions regarding the expression/presence of proteins in different experimental conditions, given that quantitative estimates of protein abundance could not be obtained and thus statistical techniques such as calculation of measures of central tendency (e.g. mean, median), calculation of confidence intervals/error bars, and hypothesis testing could not be carried out. Future work that aims to replicate the study's results, and to build upon its findings, could undertake a process of systematic quantification of chemiluminescence for known concentrations of target protein, in order to determine the nature of the relationship between the two variables and thus be better able to quantify target protein accurately using Western blotting [176].

2.6.1 Modifications of Western blot analysis for assessment of TIMP-3 expression

TIMP-3 is differs from other human TIMPs in that it has the broadest inhibitory spectrum for MPs and is tightly bound to the extracellular matrix [177]. It is the main inhibitor for ADAM-17/TACE [178], and exists in glycosylated (29kDa) and unglycosylated (24kDa) forms [179]. The post-translational regulation of TIMP-3 expression is complex, with secretion into the extracellular space being followed by rapid endocytic uptake in a lipoprotein receptor-related protein (LRP)-dependent mechanism – this re-uptake is blocked by heparin [180].

For experiments in which the objective was to assess TIMP-3 expression, *in vitro*-differentiated adipocytes were incubated with heparin at 100 µg/ml, TNF-α at 50 ng/ml, or both for 48 hours following habituation in serum-free low glucose control media. The medium was then removed after 48 hours, 6.1N trichloroacetic acid (TCA) was added to 5%, and incubated overnight at 4˚C. Following centrifugation at 10,000 x *g* for 10 minutes, the pellet was washed twice with ice-cold acetone, then resuspended in SDS sample buffer, electrophoretically separated and transferred to a PVDF membrane using standard techniques. TCA-precipitated conditioned media from HEK293 cells transfected with a

pCEP4 expression plasmid encoding C-terminally FLAG-tagged human TIMP-3 (a generous gift from Dr Linda Troeberg, Kennedy Institute of Rheumatology, University of Oxford) was included on the gel as a positive control. Blots were probed with TIMP-3 antibody (ab39184; Abcam), and developed using an HRP-conjugated anti-rabbit/anti-mouse secondary antibody (Dako, Ely, UK) and enhanced chemiluminescence (ECL) detection reagents (GE Healthcare Life Sciences, Little Chalfont, UK).

2.7: Gelatin zymography

This polyacrylamide gel electrophoretic method allows the detection of proteases with gelatinolytic activity from various sources. The major targets are MMP-2 (gelatinase A) and MMP-9 (gelatinase B), which can be detected in cell culture media, tissue explants and biological fluids [181]. The technique relies on the ability of these enzymes to catalyse the hydrolysis of denatured collagen I, which is the main constituent of gelatin. Thus, unreduced, native samples are run on polyacrylamide gels co-polymerised with gelatin. As the samples are unreduced, the proteins can be partially renatured by washing out of SDS using Triton X-100 and incubation in a divalent cation-containing buffer. The conformational changes brought about by these steps result in the exposure of the active site and thus the ability of the MMP to degrade gelatin contained within the gel. When the gel is then stained with Coomassie Blue, areas of gelatin degradation, and thus gelatinase activity, appear as a clear region on a blue background [182]. Latent/pro-forms of MMPs may also appear as catalytically active using this technique, as the steric hindrance provided by the N-terminal pro-domain may be removed by the tertiary structural unfolding brought about by SDS [181] (Figure 2.4).

In this study, gelatin zymography was carried out using 7% polyacrylamide gels impregnated with 0.5mg/ml gelatin from bovine skin (Sigma). Samples were run unreduced, and the gel was washed twice in 2.5% Triton X-100. The gel was then incubated overnight in Tris Assay Buffer, containing 50 mM Tris-HCl buffer pH 7.8, 150 mM NaCl and 5 mM CaCl2 at 37°C or at room temperature. The gel was then stained using a Coomassie Blue solution (50% methanol, 10% acetic acid and 0.05% Coomassie Brilliant Blue R250), and destained using a 30% methanol, 1% acetic acid solution to visualize areas of gelatin degradation. The gels were then scanned using the Odyssey Infrared Imager using the Image Studio software V3.1.4 (LI-COR Biosciences, Lincoln, NE, USA).

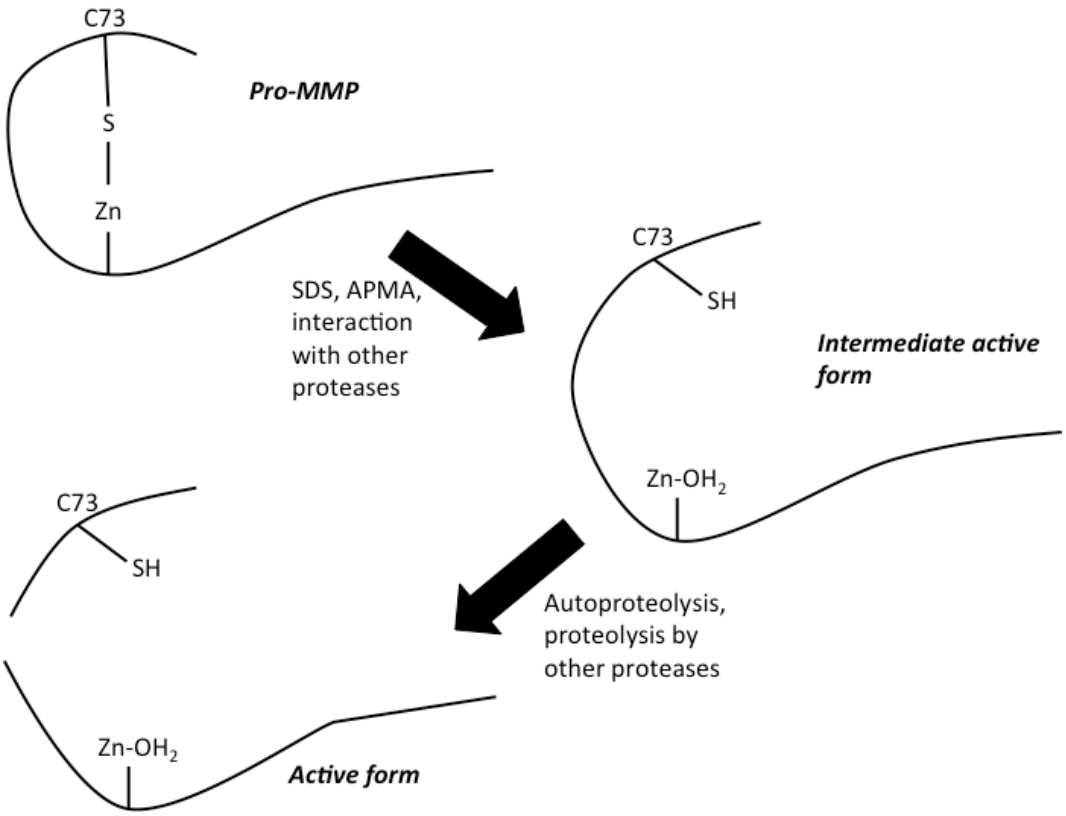

Figure 2.4: Steps in the activation of MMPs, showing involvement of 4-aminophenylmercuric acetate (APMA), other proteases, and the effect of SDS in gelatin zymography. The disruption of the interaction between the sulphydryl group in the cysteine residue at position 73 of the prodomain and the zinc ion co-ordinated within the active site is known as the 'cysteine switch'. Figure adapted from [182].

2.8: TIMP-3 overexpression by adenoviral transduction

2.8.1 Introduction

Replication-deficient recombinant adenoviruses are widely used to effectively deliver transgenes into primary cells. This technique is all the more important when working with primary cells, which tend to be resistant to common transfection reagents that are usually suitable for use in cell lines, such as lipofectamine [160]. There are 57 accepted human adenovirus types, and most adenoviral vectors are based on serotype 5 (Ad5). Ad5-based vectors use a combination of high-affinity binding to the Coxsackie-Adenovirus Receptor (CAR) and interaction with αV-integrins to effect internalization by endocytosis. Upon entry, adenoviral DNA does not integrate into the genome and is not replicated during cell division [183].

The adenovirus genome is a linear, 36-Kb double-stranded DNA (dsDNA) molecule containing multiple, heavily spliced transcripts. Genes are divided into early (E1-4) and late (L1-5) transcripts. Recombinant viruses have the E1 and E3 regions of the adenoviral genome deleted, preventing replication and removing the adenoviral genes known to subvert intracellular signalling. Deletion of these two components results in a transgene packaging capacity of >8 Kb.

The viruses used in this study were kindly donated by Professor Andrew H Baker's group at the BHF Centre of Regenerative Medicine for Cardiovascular Sciences, University of Edinburgh. The control virus was adenovirus RAd35 (referred to as Ad0 throughout this study), which expresses the bacterial *lacZ* gene (β-galactosidase) from the cytomegalovirus major immediate early promoter (CMV IEP; [184]). Thus, identification of cells transduced with this adenovirus can be performed by X-gal staining (see section 2.8.3 below).

The TIMP-3-overexpressing experimental virus (referred to as AdT3 throughout this study) was previously constructed by Professor Baker's group. Briefly, human TIMP-3 (hTIMP-3) sequences were cloned into the pAL119 plasmid to create pAL119TIMP-3. This was then cotransfected with pJM17 into low-passage 293 cells. pJM17 contains the entire Ad5 DNA molecule with an insert in the E1 region that exceeds the packaging constraints of the adenovirus capsid. Since the pAL119TIMP-3 plasmid contains E1 along with the hTIMP-3 sequence, cotransfection of 293 cells with both plasmids produces recombinant virions at high efficiencies [185].

2.8.2 Optimising transduction of human primary preadipocytes and transduction protocol

For this study, I had to adapt the transduction technique specifically to human primary preadipocytes. I therefore designed an experiment in which preadipocytes were exposed for 2, 4, 12, 24 and 48 hours to Ad0 adenovirus at multiplicities of infection (MOI) ranging from 5:1 to 500:1. Following the pre-specified incubation time, cells were subjected to X-gal staining as described below, and the number of blue cells (indicating β-galactosidase expression and thus viral transduction) was counted. As shown in Figure 2.5, optimal transduction efficiency was obtained when cells were exposed to Ad0 adenovirus at a MOI of 500:1 for 48 hours. Therefore, for experiments involving adenoviral transduction to bring about hTIMP-3 overexpression, cultures of preadipocytes were incubated with AdT3 adenovirus for 48 hours at MOI of 500:1 in serum free media, after which cells were returned to serum-containing media and were left to overexpress for 48 hours prior to commencing experimentation. Side-by-side transduction of cells from the same donor was performed with Ad0 control adenovirus, to ensure that conditions were suitable for successful infection and

over-expression. Similarly, Western blot for TIMP-3 (performed as described in section 2.6.1 above) served to indicate successful transduction (Figure 2.6). However, the limitation that successful transduction could not be easily assessed directly in cells exposed to AdT3 with this system (as would have been the case, for example, if a GFP co-expressing experimental adenovirus was used) is noted.

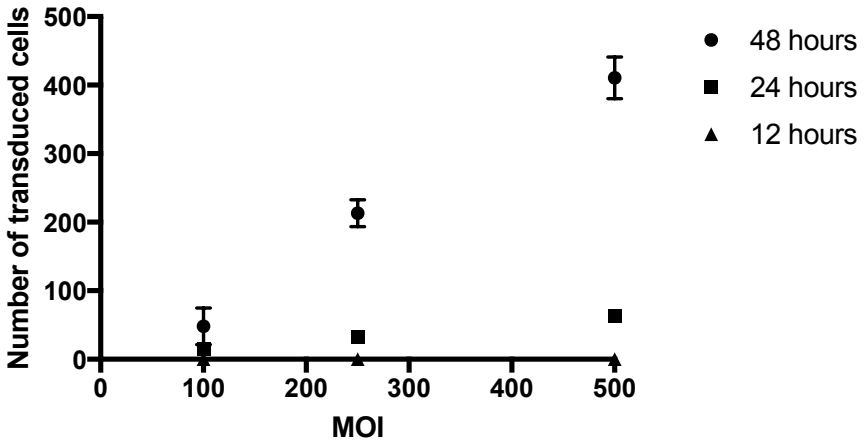

Figure 2.5: Optimal incubation time and multiplicity of infection (MOI) for transduction of human primary preadipocytes with adenovirus was assessed by exposing two biological replicates from a single donor to 35 conditions (MOIs of 5, 10, 25, 50, 100, 250 and 500:1, for 2, 4, 12, 24 and 48 hours) in a single 96-well plate. Each data point shows the mean number of transduced cells ± SD for these two biological replicates. Data for MOIs 5, 10, 25, and 50:1, and 2 and 4 hour timepoints is omitted from this figure as the number of transduced cells was 0 in each case.

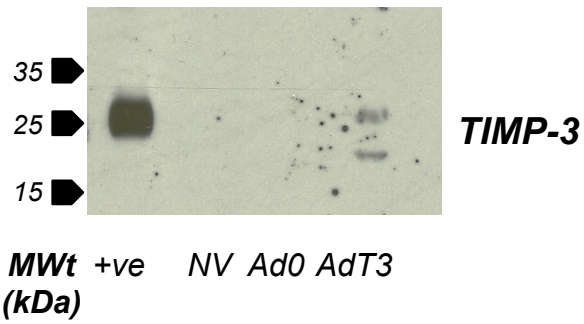

Figure 2.6: Immunoblot for hTIMP-3 from serum-free media conditioned by cells transduced with no virus (NV), control adenovirus (Ad0) or TIMP-3-overexpressing adenovirus (AdT3). It is important to note that no heparin (see section 2.6.1) was added to the media, which explains the lack of detection in the NV and Ad0 conditions, and highlights the degree of overexpression in the AdT3 condition. TCA-precipitated conditioned media from HEK293 cells transfected with a pCEP4 expression plasmid encoding C-terminally FLAG-tagged human TIMP-3 (a generous gift from Dr Linda Troeberg, Kennedy Institute of Rheumatology, University of Oxford) was included on the gel as a positive control.

2.8.3 Preparation of X-gal and associated buffers, and X-gal staining of primary cells

5-bromo-4-chloro-3-indolyl β-D-galactopyranoside (X-gal) is a widely used, colourless chromogenic substrate. Since it is a lactose analog, X-gal can be hydrolysed by the β-galactosidase enzyme, yielding galactose and 5-bromo-4-chloro-3-hydroxyindole. The latter spontaneously dimerizes and is oxidized into 5,5'-dibromo-4,4'-dichloro-indigo, an insoluble blue product.

To prepare the X-gal dilution buffer, 800 mg of potassium hexacyanoferrate III, 1050mg of potassium hexacyanoferrate II and 100 mg of magnesium chloride were dissolved in 500 ml of PBS. This was stored at 4°C protected from light, and warmed to 37°C prior to use. X-gal stock solution (8% in N,N-dimethylformamide [DMF]) was prepared by dissolving 1 g X-gal in 50 ml DMF, and stored at -20°C.

To stain cells, X-gal stock solution was diluted 1:40 in warmed dilution buffer. At the end of the experiment in question, medium was removed and cultured cells were fixed for 15 minutes in 0.5% gluteraldehyde. Cells were then washed with PBS and ddH_2O, and incubated in working solution for 1 hour at 37°C or overnight at 4°C. To stop the staining process, the working solution was removed and replaced with PBS. The cells were visualized with standard light microscopy, and quantified by counting.

2.9: TIMP-3 knockdown by RNA interference (RNAi)

2.9.1 Introduction

Long double-stranded (ds)RNAs (typically >200 nucleotides [nt]) are used to reduce the expression of (silence, or knockdown) target genes in a variety of cell types. Upon introduction, the long dsRNAs enter a cellular pathway known as the RNA interference (RNAi) pathway. First, the dsRNAs are processed into 21-23 nt small interfering RNAs (siRNAs) by an enzyme called Dicer [186]. Next, the siRNAs are recognised by the RNA-induced silencing complex (RISC) [187]. The siRNA strands then guide the RISCs to complementary mRNA molecules, where they cleave and degrade the target mRNA [188]. In practice, short synthetic siRNA can be directly introduced into the cell, therefore circumventing Dicer and decreasing the likelihood of an innate interferon response.

2.9.2 RNAi in preadipocytes

Transfection of RNAi oligonucleotides was used for knockdown of *Timp3* in human primary preadipocytes. Previous work in our laboratory has indicated that human primary

preadipocytes and adipocytes show low viability 24 hours after techniques such as DharmaFECT® or electroporation (Dr Corinne Brenner, personal communication). Therefore, a cationic lipid formulation (siIMPORTER™ siRNA transfection reagent; Upstate, Milton Keynes, UK) was used. For transfecting cells in a 12-well plate, cells were plated the day before transfection at a seeding density of ~10^4 cells/cm^2 to ensure ~60% confluence at the time of transfection. On the day of transfection, 35 µl of siRNA/siIMPORTER™ mixture was added to each well containing 465 µl of serum-free medium. The siRNA/siIMPORTER™ mixture was prepared by mixing 2.5 µl of transfection reagent (diluted 1:6 in serum-free medium) with 20 µl siRNA diluent containing the required amount of siRNA for a final concentration of 50nM. This mixture was first incubated for 10 min to allow formation of siRNA/lipid complexes and then added to each well. The specific oligonucleotide and the length of time of incubation of cells with siRNA were selected following a process of optimisation. Cells were incubated with two different RNAi oligonucleotides (Table 2.2) for for 24, 48 or 72 hours. Following this time period, cells were washed and incubated in serum-free medium with heparin (as per section 2.6.1) for a further 24 hours. At the end of this experiment, cells were lysed for RNA extraction and media were collected. RNA collected was used to assess steady-state *Timp3* mRNA levels using qRT-PCR (Figure 2.7A), whereas media were trichloroacetic acid (TCA) precipitated and probed for TIMP-3 protein (Figure 2.7B). Following this process, RNAi oligonucleotide A (siRNA ID s14147; Thermo-Fisher Scientific, Waltham, MA USA) was chosen for all subsequent RNAi experiments throughout the study.

Target Gene	siRNA ID	Source	Label in Figure 2.7
Negative control (scrambled)	AM4635	Thermo-Fisher Scientific	scr
Timp3	s14147	Thermo-Fisher Scientific	A
Timp3	s14148	Thermo-Fisher Scientific	B

Table 2.2: RNAi oligonucleotides used in this study.

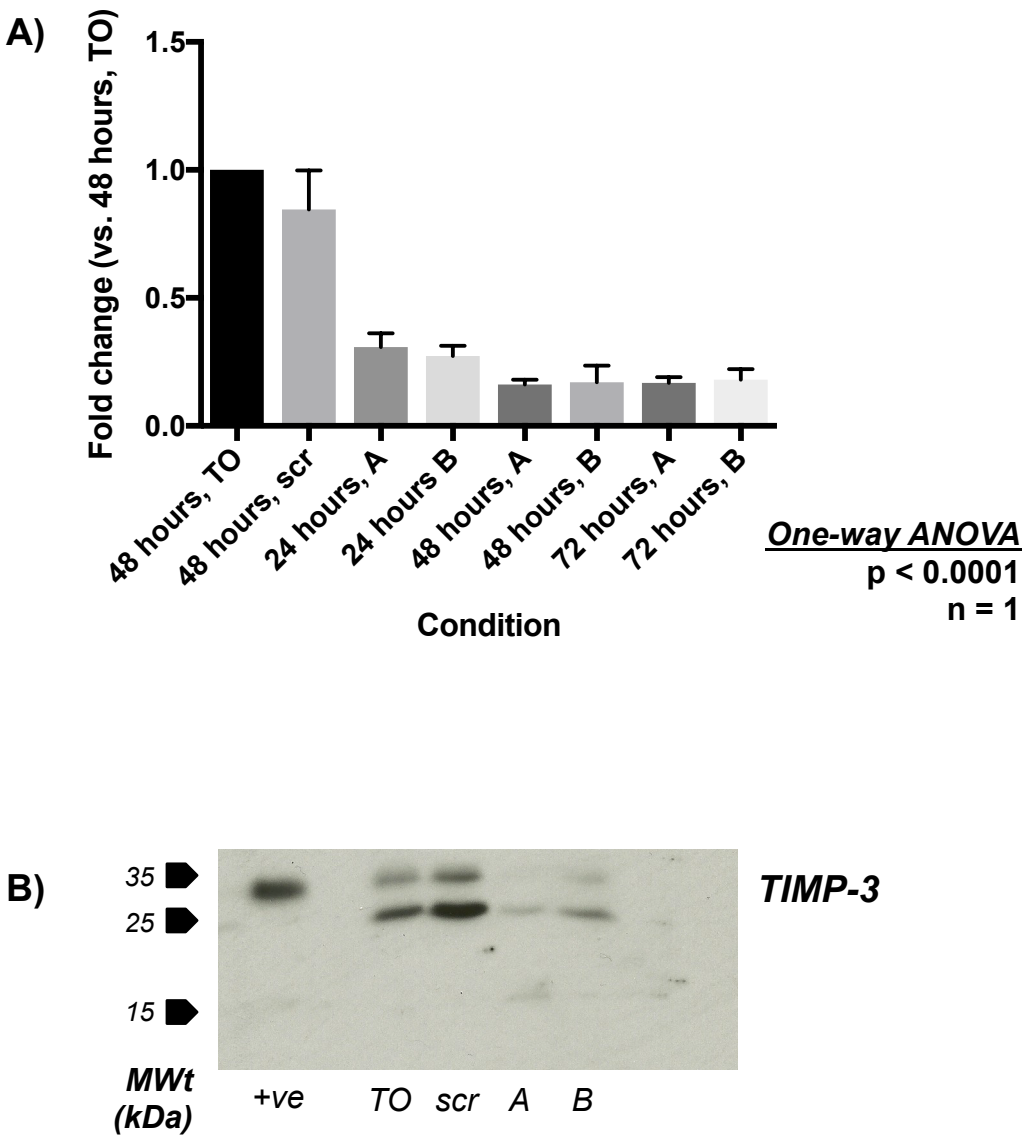

Figure 2.7: Assessment of RNAi efficacy in primary human preadipocyte cultures. A) qRT-PCR for steady-state *Timp3* mRNA levels following knockdown for 24, 48 and 72 hours with two different RNAi oligonucleotides (A and B, see Table 2.2). Two negative controls were used – a transfection agent only (TO) condition, and a scrambled (scr) oligonucleotide, for 48 hours. Data shown is mean fold change + SD for three biological replicates from one unique donor, normalised to expression in the 48 hour, TO condition (set at 1). Post hoc analysis by Tukey's multiple comparison showed that expression at all timepoints with both A and B oligonucleotides was significantly different from expression in the TO, 48 hour condition (all $p < 0.0001$). B) Immunoblot for hTIMP-3 from serum-free media conditioned by cells transfected with negative control scrambled (scr) siRNA, transfection agent only (TO), and two Timp3-directed oligonucleotides (A: s14147; B: s14148).

2.10: Collagen I coating of plates and hydroxyproline assay

2.10.1 Introduction

Type I Collagen is a major structural component of the ECM, and is thought to be one of the main matrix proteins that preadipocytes interact with *in vivo* [42, 43]. As a result, a necessary condition for adipogenic differentiation is that preadipocytes remodel the surrounding collagen I-rich ECM [109, 110]. Given that modulation of this process may affect adipogenic differentiation and consequently the capacity for adipose tissue to expand in a hyperplastic fashion, I sought to develop a quantitative assay of the degree of collagen I remodeling by human primary preadipocytes *in vitro*.

2.10.2 Coating of tissue culture plates with acid-extracted rat tail collagen I

In order to develop an assay of preadipocyte collagen I remodelling. I first attempted to optimise the seeding and incubation of these primary human cells on collagen I-coated tissue culture plates. I amended the protocols described by Artym and Matsumoto [189] and Itoh *et al* [190, 191]. Briefly, acid-extracted rat-tail collagen I (Corning, Corning, NY, US) is acidic, so it was neutralized by diluting in 10x minimum essential medium (MEM; Sigma, Poole, UK) and 10x reconstitution buffer (made by dissolving 2.2g sodium bicarbonate ($NaHCO_3$) and 4.8g HEPES in 100ml distilled water, and sterile filtering the resultant solution). To obtain a final pH of 7.2, small amounts of 2N sodium hydroxide and 37% hydrochloric acid were added. This neutralized collagen I was then diluted in 1x PBS to obtain a solution with a working concentration of 0.5 µg/µl. 200 µl of this solution (100 µg collagen I) was placed in wells of a 24-well plate, while 200 µl of 1x PBS were added to control wells. Plates were left in an incubator at 37°C for 2 hours, and then air-dried overnight at room temperature in a laminar flow hood. The next day, wells were washed with sterile distilled water to remove any crystalline salts.

Cells were seeded at a density of 4×10^4 cells/cm^2, and left for 24 hours to acclimatise to the coated or uncoated tissue culture surface prior to experimentation.

2.10.3 Hydroxyproline assay

Hydroxyproline is a major component of collagen and is essential for stability of the collagen triple helix tertiary structure [192]. It is formed by post-translational hydroxylation of proline residues by prolyl hydroxylase [193]. Given its enrichment in collagen sequences, the detection of hydroxyproline in culture media indicates collagenlysis. Therefore, an assay that quantitates the amount of hydroxyproline released into media can serve as a surrogate marker for the degree of collagen turnover by cells in culture. It is for this reason that the

hydroxyproline assay has been used for multiple mesenchymal cell types, such as fibroblasts [194] and tenocytes [195]. Similarly, I adapted established protocols for use with human primary preadipocyte cultures.

Briefly, preadipocytes seeded on collagen I-coated plates or control culture plates were exposed to experimental conditions such as proadipogenic medium or TNF-α at 50 ng/ml. Media collected over the course of the experiment was treated by boiling at 105°C in concentrated hydrochloric overnight, causing hydrolysis of the proteins and peptides present in the media, releasing the hydroxyproline residues. The hydrochloric acid was then evaporated using an acid-resistant vacuum concentrator, and the precipitate was suspended in double-distilled water.

The samples were treated with 7% chloramine T solution in an acetate-citrate buffer, which oxidises the hydroxyproline to a pyrrole intermediate. Addition of 4-dimethlyamino-benzaldehyde (DAB) causes the synthesis of a red product whose concentration is proportional to the initial amount of hydroxyproline present, allowing for the colorimetric assessment of hydroxyproline content by spectrophotometry at 530nm. A trans-4-hydroxy-L-proline (Sigma, Poole, UK) standard curve ranging from 0 to 30 μg/μl enabled inference of hydroxyproline concentrations in experimental media.

2.11 Clinical study protocols, methods and materials

2.11.1 Introduction

In order to understand the metabolic consequences of variation in expression of MPs and TIMPs in human adipose tissue, I designed an investigation with the following objectives:

1. To measure levels of key MPs and TIMPs identified during the *in vitro* arm of my study (MMPs-1, -2, -14 and TIMP-3, as well as the inhibitor of adipogenesis Dlk-1) in subcutaneous and visceral adipose tissue samples obtained from lean and obese subjects
2. To measure the subjects' homeostatic model assessment-insulin resistance (HOMA-IR) [157], which provides an assessment of their insulin sensitivity.
3. To analyse the subjects' adipose tissue for evidence of dysfunction, by measuring mean adipocyte size.

To fulfil these objectives, I undertook a clinical study of subcutaneous and visceral adipose tissue samples, blood samples and MRI scans from thirty-nine adult subjects. The sample size was discussed with Dr Allan Clark, Senior Lecturer in Medical Statistics, Norwich Medical School, University of East Anglia. This study was exploratory in nature, and there are no reliable estimates of between and within group variation (effect size and variance) in these variables (e.g. MP and TIMP levels) in human adipose tissue. Therefore, a formal power calculation was not performed for this pilot feasibility work. However, I was aware of one previous investigation of TIMP-3 in human metabolism, which looked at TIMP-3/ADAM-17 activity in skeletal muscle [138], and one investigation of Pref-1 in human adipose [154]. In the latter, recruitment and analysis of 29 obese patients (12 'metabolically healthy', 17 'metabolically unhealthy') identified significant differences in Pref-1 levels and markers of adipose function. Thus, a recruitment total of 39 subjects seemed reasonable. I only recruited female patients for donation of their subcutaneous and visceral adipose tissue, given that the initial *in vitro* work that informed this study's objectives was performed in cultures established from adipose tissue donated by female subjects. This provided a homogenous model environment for these initial investigations. Given the undoubted differences in risk of metabolic consequences of obesity between males and females, it is not unreasonable to suppose that there may be sex differences in the role/regulation of MPs and TIMPs in adipose tissue. Therefore, by using only females, I removed this source of potential variation between samples.

2.11.2 Participant recruitment and pathway through study

Ethical approval was obtained (12/EE/0498) to recruit female subjects who were scheduled to undergo elective surgical procedures in which access to subcutaneous and visceral adipose tissue is part of the procedure from surgical and gynaecological clinics. The subjects' involvement in the study is described below:

1. Research participants were recruited via Mr Michael Lewis' (consultant surgeon) and Mr Edward Morris' (consultant gynaecologist) surgical and gynaecological practice at the Norfolk and Norwich University Hospital respectively.
2. Body mass index (BMI) was measured at the surgical/gynaecological clinic appointment, and was used as a stratifying variable to allow stratified sampling. Stratified sampling is desirable in this instance as it ensured that a wide range of BMIs were represented in this exploratory study. Approximately equal numbers of patients were recruited in each of the following 5 groups:
    a. BMI 18.5-24.9 kg/m^2
    b. BMI 25-29.9 kg/m^2
    c. BMI 30-34.9 kg/m^2

d. BMI 35-39.9 kg/m^2
e. BMI ≥40 kg/m^2

3. Once identified as eligible using pre-determined eligibility criteria (see box 2.1), the initial approach was made to the patient at the time of booking of the procedure. The purpose of the study and their potential role in it were explained, and potential participants were provided with a study-specific participant information sheet.
4. At the time of routine pre-operative assessment, I, or members of the research nurse team, re-approached these potential participants and asked to provide full informed consent.
5. Once consented, volunteer demographic data were collected, including such as age and past medical history, and pseudonymised.
6. Participants had a chest, abdomen and pelvis MRI scan at the Department of Radiology, Norwich & Norwich University Hospital, performed by at team led by Professor Andoni Toms, Dr Paul Malcolm (consultant radiologists) and Mr Richard Greenwood (specialist MRI radiographer). During this MRI scan, participants were scanned using a 3T or 1.5T GE Healthcare® (Chalfont St Giles, UK) scanner (see section 2.11.4 below for scan protocol and analysis).
7. On the day of their operation, while fasted in advance of their general anaesthetic, 15 millilitres of blood were obtained by venepuncture performed by myself or a member of the research nurse team. The samples were pseudonymised, centrifugally separated to obtain serum and plasma, and stored at -80˚C in the Clinical Research and Trials Unit, Norfolk & Norwich University Hospital, for later analysis (see section 2.11.5 below for analysis).
8. At their planned surgery, small samples of fat tissue (2 cm^3) were taken from beneath the skin and from within the abdomen. Other than this, the participants underwent exactly the same operation as expected from their NHS care and if they had chosen not to take part in the study (see section 2.11.3 below for description of tissue handling following collection and analysis of this tissue).
9. The participant's involvement in this study ended here.

Given the risk of incidental findings on MRI or fasting glucose analysis uncovering undiagnosed diabetes, we developed a protocol for addressing these situations. Briefly, abnormal MRI scans and fasting glucose results were reported in full by the respective clinical expert, and participants were invited to discuss these results with me and my primary supervisor, Professor Jeremy Turner. We then made any onward referrals as necessary, and informed the subject's GP using a standardized letter.

Inclusion Criteria

1. Female patients
2. Aged over 18
3. BMI ≥18.5
4. Undergoing elective general or gynaecological surgery under the care of the General Surgical or Gynaecological Teams at the Norfolk & Norwich University Hospital

Exclusion Criteria:

1. Unable to consent to involvement in research
2. Appropriate samples not collected during surgery
3. Pregnancy
4. Infective, inflammatory or malignant pathology
5. Regular use of anti-inflammatory medications e.g. corticosteroids, non-steroidal anti-inflammatory drugs.
6. Any condition that precludes safe MRI (including permanent pacemakers, intracranial clips/coils, metallic prostheses, risk of metallic intra-ocular foreign body, claustrophobia, use of metallic intrauterine contraceptive device, and others as per MRI standard operating procedure [SOP])
7. Weight >227kg or width at widest point >70cm

Box 2.1: Eligibility criteria for the clinical study.

2.11.3 Tissue handling and analysis

During surgery, 2 cm^3 adipose samples were obtained from both subcutaneous and visceral compartments. Samples were immediately placed in cooled saline and transported on ice to the BioMedical Research Centre, University of East Anglia. Every effort was made to reduce the amount of time spent in transit; on average, this took about 20 minutes.

On arrival at the BioMedical Research Centre, the samples were immediately divided into two sections.

2.11.3.1 Histopathology and adipocyte size assessment

The protocol for preparing adipose tissue for histopathological analysis was adapted from Cinti *et al* [196]. Briefly, 1cm^3 was fixed in 4% paraformaldehyde at 4°C overnight, and

transferred to the Norfolk and Norwich University Hospital Histopathology laboratory. There, following a process of dehydration and paraffin-embedding, samples were sectioned, mounted on slides and stained with haematoxylin and eosin. Three discontinuous slides were obtained for each sample. These steps were kindly performed by the staff at the Histopathology Lab, led by Mr Iain Sheriffs.

Slides were then photographed using a Zeiss AxioPlan 2ie widefield upright microscope equipped with an AxioCam HRm CCD camera, and using the AxioVision LE software V4.8 (Carl Zeiss Microscopy, Cambridge, UK) (Figure 2.8). Three randomly selected views were photographed for each slide.

Photomicrographs were used to measure mean adipocyte cross-sectional area, using a method adapted from established automated object finding protocols, with the help of Dr Paul Thomas (Facility Manager, Henry Wellcome Laboratory for Cell Imaging, University of East Anglia). This process was performed by myself and by Ms Miriam Mansha, second year medical student, University of East Anglia, who joined our group for a self-selected study research module. Briefly, photomicrographs were loaded onto ImageJ (version 1.46r, National Insitutes of Health, US) [197] and scaled according to the magnification of the image. Following a process of background subtraction, contrast and brightness were adjusted and the image was converted to black and white. A threshold image was then created such that separate objects in the image (that is – individual adipocytes) could be identified and numbered by the automated ImageJ system (Figure 2.9). These individual ‘particles’, as referred to in the ImageJ literature, could then be analysed by the software to obtain cross-sectional area. This process was repeated for all three views of two non-consecutive slides prepared from each adipose tissue sample collected. These data were exported to a Microsoft Excel® spreadsheet and means/standard deviations for each sample were calculated.

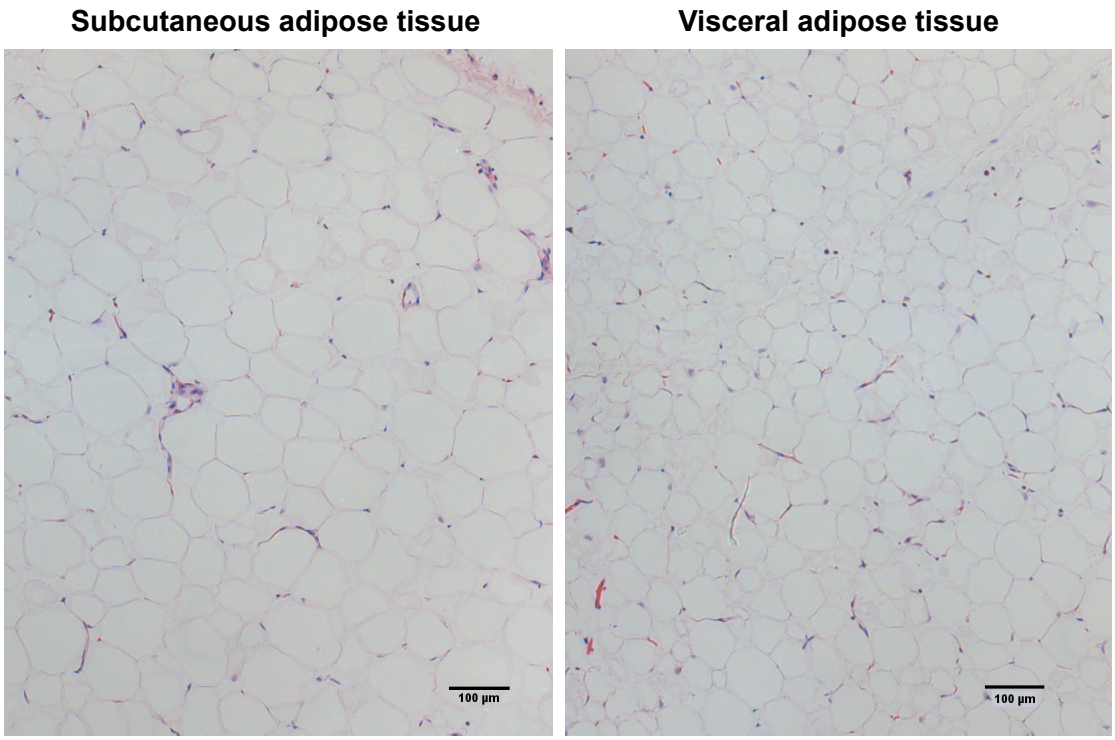

Figure 2.8: Photomicrographs of paired subcutaneous and visceral adipose tissue samples donated by donor A08-13TB0411. Photomicrographs were obtained with a Zeiss AxioPlan 2ie widefield upright microscope equipped with an AxioCam HRm CCD camera, and using the AxioVision LE software V4.8 (Carl Zeiss Microscopy, Cambridge, UK).

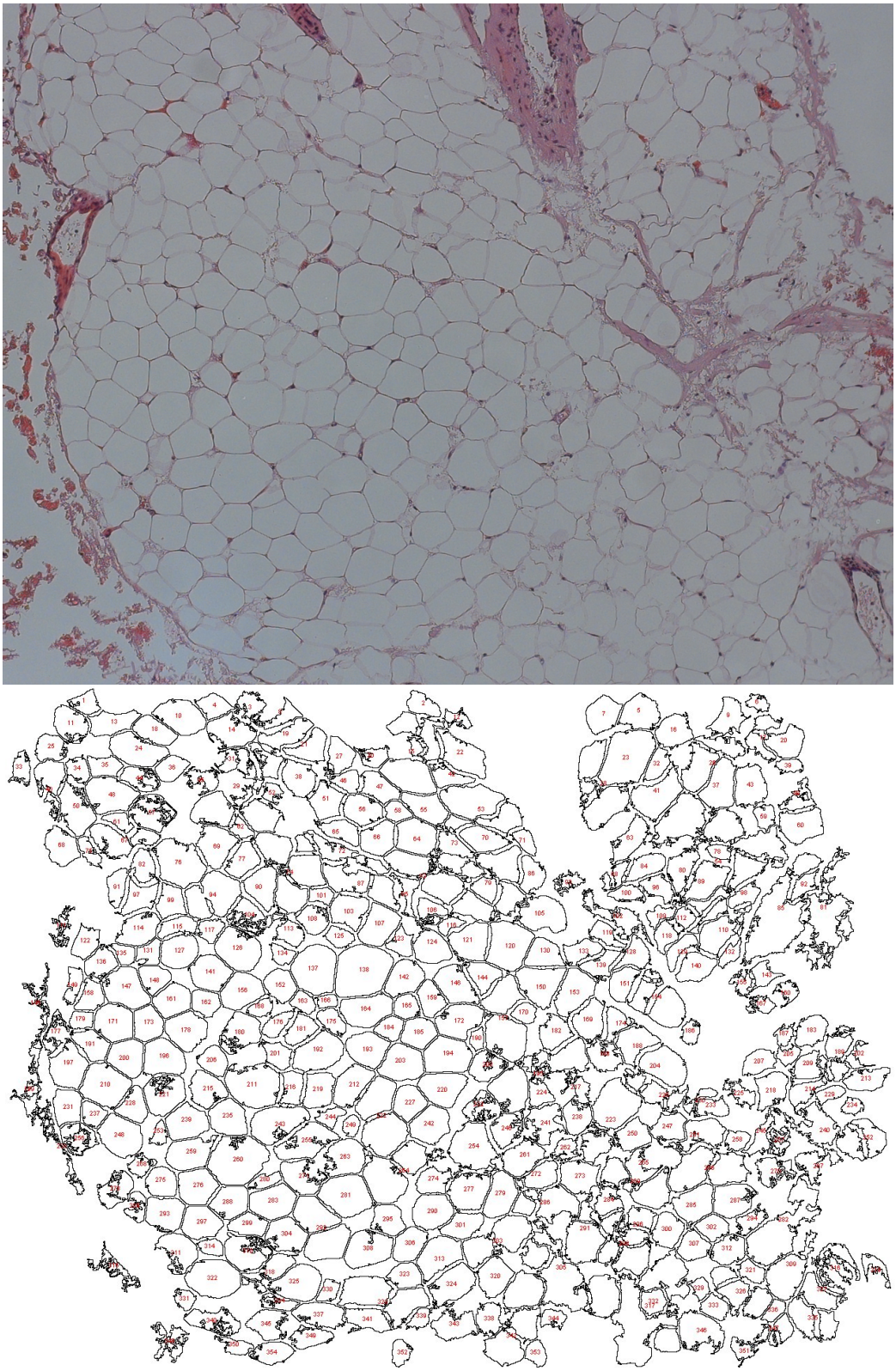

Figure 2.9: Process of automated object finding in ImageJ, allowing measurement of adipocyte cross-sectional area. The top panel is the raw photomicrograph that was analysed according to the protocol outlined in section 2.11.3.1. The bottom panel shows the 'particle image', wherein the image is resolved into numbered individual 'particles' corresponding to adipocytes, whose size can be measured.

2.11.3.2 RNA stabilisation and extraction, quantitative RT-PCR

The remaining 1 cm^3 of adipose tissue from each depot for each donor was placed in 2 ml of RNALater® (Qiagen, Crawley, UK), and left at 4°C overnight. The next day, the excess fluid was removed and the sample was frozen at -20°C for storage. RNA extraction was performed using the RNeasy® Lipid Tissue Mini Kit (Qiagen). Reverse transcription and quantitative reverse transcription PCR was then performed for targets of interest as outlined in section 2.4 above.

2.11.4 MRI scan protocol and analysis of images

MRI studies involved breathhold IDEAL scans of approximately 20s of chest, abdomen, pelvis and similar scans of the lower limbs for bulk fat measurement. A breathhold scan of the liver was also performed for percentage liver fat measurement.

Analysis of fat compartment volumes was performed using an automated tool for quantification of subcutaneous, visceral and non-visceral internal fat developed by AMRA™, a spin-off of the Centre for Medical Image Science and Visualization (CMIV), the Department of Biomedical Engineering (IMT), and the Department of Medicine and Health (IMH) at Linköping University, Sweden. Once MRI studies were obtained, they were transferred securely to Professor Magnus Borga and Dr Olof Dahlqvist Leinhard in Linköping, who kindly performed this analysis for me. Briefly, MR images acquired using the two-point Dixon technique in the abdominal region were subjected to a process of three-dimensional phase unwrapping to provide water and fat images, image intensity inhomogeneity correction, and morphon-based registration and segmentation of the tissue [198]. As a result, data for total adipose tissue (TAT), subcutaneous adipose tissue (ASAT), and visceral adipose tissue (VAT) volumes were obtained, as well as percentage liver fat.

2.11.5 Blood sample handling and analysis

Venepuncture was performed on all study subjects, to collect ~15ml of whole blood into a lithium heparin (Li hep) and a SST (serum separator tube) bottle. Once collected, the blood was put on ice and taken immediately to a centrifuge in the Clinical Research and Trials Unit, Norfolk and Norwich University Hospital, and spun as follows:

- Li hep: 4400 rpm for 6 mins – to obtain plasma
- SST: 3300 rpm for 5 mins – to obtain serum

The plasma and serum were then aliquoted into two cryotubes and immediately stored at in the -80°C.

Analysis of these samples was kindly performed by the Norfolk and Norwich University Hospital Biochemistry Laboratory, led by Susan Kerry. The glucose, follicle stimulating hormone (FSH) and triglyceride assays were performed on an Abbott ARCHITECT platform (Abbott, Sittingbourne, UK), whereas the insulin assay was performed on a Roche Elecsys platform (Roche, Mannheim, Germany), as follows:

2.11.5.1 Glucose

Glucose is phosphorylated by hexokinase (HK) in the presence of adenosine triphosphate (ATP) and magnesium ions to produce glucose-6-phosphate (G-6-P) and adenosine diphosphate (ADP). Glucose-6-phosphate dehydrogenase (G-6-PDH) specifically oxidizes G-6-P to 6-phosphogluconate with the concurrent reduction of nicotinamide adenine dinucleotide (NAD) to reduced nicotinamide adenine dinucleotide (NADH). One micromole of NADH is produced for each micromole of glucose consumed. The NADH produced absorbs light at 340 nm and can thus be detected spectrophotometrically as an increased absorbance.

2.11.5.2 FSH

A two-step chemiluminescent microparticle immunoassay (CMIA) is used to determine the presence of FSH in serum and plasma. In the first step, sample and anti-β-FSH-coated paramagnetic microparticles are combined, which bind the FSH present in the sample. After washing, anti-α-FSH-acridinium labelled conjugate is added. A direct relationship exists between the amount of FSH in the sample and the intensity of the resulting chemiluminescent reaction that is measured as relative light units (RLUs), detected by the ARCHITECT system.

2.11.5.3 Triglycerides

Triglycerides are enzymatically hydrolyzed by lipase to free fatty acids and glycerol. The glycerol is phosphorylated by adenosine triphosphate (ATP) with glycerol kinase (GK) to produce glycerol-3-phosphate and adenosine diphosphate (ADP). Glycerol-3-phosphate is oxidized to dihydroxyacetone phosphate (DAP) by glycerol phosphate oxidase (GPO) producing hydrogen peroxide (H_2O_2). In a colour reaction catalyzed by peroxidase, the H_2O_2 reacts with 4-aminoantipyrine (4-AAP) and 4-chlorophenol (4-CP) to produce a red coloured dye. The absorbance of this dye is proportional to the concentration of triglyceride present in the sample, and is measured at a wavelength of 500nm.

2.11.5.4 Insulin

The Elecsys Insulin assay employs two human insulin-specific monoclonal antibodies. First, insulin, a biotinylated monoclonal insulin-specific antibody, and a monoclonal insulin-specific antibody labeled with a ruthenium complex (Tris(2,2'-bipyridyl)ruthenium(II)-complex (Ru(bpy)) form a sandwich complex. The complex then is bound to streptavidin-coated microparticles, which are then magnetically captured onto the surface of an electrode. Application of a voltage to the electrode then induces chemiluminescent emission which is measured by a photomultiplier. The amount of light produced is directly proportional to the amount of insulin in the sample.

2.12: Statistical analysis

Comparative two-sample statistical analysis was by Mann Whitney U-test for non-parametric data and Student's *t* test for parametric (normally distributed) data. The ANOVA generalisation was used for comparisons involving more than two samples. Correlation analysis was performed in the clinical study to statistically analyse pairs of continuous variables: non-parametric data were analysed using Spearman analysis, whereas parametric (normally distributed) data were analysed using Pearson analysis. In all cases, a p value of <0.05 was accepted as demonstrating statistical significance. Analysis was performed using GraphPad Prism 7 (GraphPad Software, La Jolla, USA).

Chapter 3:

Expression of metalloproteinases and their inhibitors by primary human adipose-derived mesenchymal stromal cells and in vitro-differentiated adipocytes

3.1: Introduction

Metalloproteinases (MPs) and their tissue inhibitors (TIMPs) are key players in the remodelling of various tissues in response to diverse environmental cues, and expression is observed in human and murine preadipocyte and adipocyte models (see Chapter 1). Their expression and role in human adipose tissue remodelling is less well understood. Indeed, my review of the existing literature led me to identify the following unaddressed question in human adipose tissue research:

> *Which are the key MPs and TIMPs expressed by human adipocytes and preadipocytes, and how is this expression modulated by inflammatory or pro-adipogenic stimuli?*

To this end, I undertook expression analysis at both messenger RNA and protein level of MPs and TIMPs by primary human adipose-derived mesenchymal stromal cells (used as a model for human preadipocytes, see Chapter 2), and by primary human *in vitro*-differentiated adipocytes, in conditions were chosen to provide physiologically-relevant models of adipose tissue in obesity, metabolic syndrome and diabetes. High-glucose Dulbecco's Modified Eagle's medium, for example, contains 4.5g/l, or 25 mmol/l of glucose, which is a circulating level of glucose that can be associated with undiagnosed diabetes mellitus [199]. The presence of a pro-inflammatory environment in metabolically-unhealthy obese adipose tissue is well-recognised (see Chapter 1). Lastly, adipose tissue in weight gain expands by hyperplasia and hypertrophy, meaning that adipogenic differentiation is a feature of adipose tissue remodelling in obesity.

3.2: mRNA expression of MPs and TIMPs by human adipocytes

To determine which of the 66 human MPs and TIMPs are expressed by primary *in vitro*-differentiated human adipocytes, we used custom-designed Taqman Low Density Arrays (see Chapter 2: Methods). Following 72 hours of habituation in low glucose basal medium, *in vitro*-differentiated adipocytes from five independent donors were exposed to the following conditions for 24 hours – low glucose basal medium as a control, high glucose (4.5 g/l glucose DMEM) basal medium, low glucose basal medium with TNF-α at 50ng/ml, and low glucose basal medium with lipopolysaccharide (LPS) at 10ng/ml. These stimuli were chosen as TNF-α is a well-established mediator of adipose inflammation (see Chapter 1), while other work in our group has shown that LPS is an important regulator of insulin responses in

adipocytes [158, 160, 200] and other published work has linked the receptor for LPS, Toll-like receptor (TLR)-4, to adipose inflammation and diabetes in mouse [201].

Media were collected, and RNA extracted and reverse transcribed as described previously (see Chapter 2: Methods). Due to poor quality RNA (as indicated by low 260/280 absorbance ratios), the RNA from two donors was not reverse transcribed and used for further analysis, meaning that cDNA from three donors was used in the Taqman Low Density Arrays.

To ensure that cells demonstrated expected biological responses, culture media from 5 donors were assayed for IL-8 by ELISA following treatment with high glucose media, TNF-α or LPS. IL-8 was chosen for this purpose as it is a well-established adipocyte-secreted cytokine, or adipokine [202, 203]. IL-8 expression and secretion has been shown to be increased in human adipocytes exposed to an inflammatory stimulus [204], and obese subjects have higher circulating levels of IL-8 than lean controls [205]. In my cultures, IL-8 expression was increased 38- and 53-fold with TNF-α (mean ± SD: 18799 pg/ml ± 2207) and LPS (26176 pg/ml ± 12616) stimulation respectively (all $p < 0.0001$) as compared to control (492 pg/ml ± 822); it was not significantly changed by high glucose medium (Figure 3.1).

TLDA analysis revealed mRNA expression for 57 MP and TIMP genes, including 20 MMPs, 16 ADAM proteases, 17 ADAMTS proteases and the 4 TIMPs. Many of these genes were regulated by the chosen inflammatory stimuli, with some genes being upregulated while others were downregulated. More genes were regulated by inflammatory stimuli than by varying glucose concentration in the cell culture medium (Figure 3.2). The top quartile of MP and TIMP genes expressed by primary *in vitro*-differentiated adipocytes in low glucose medium is shown in Table 4, Appendix A.

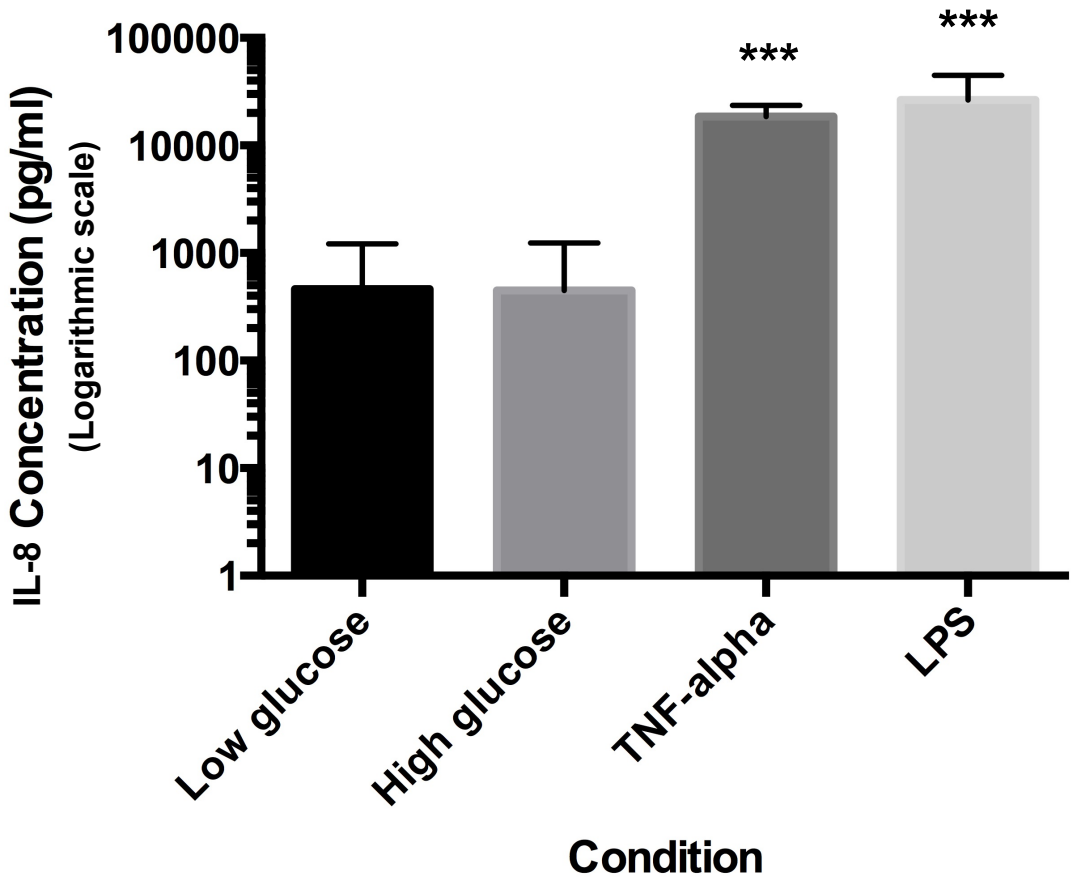

Figure 3.1: Stimulation of *in vitro*-differentiated adipocytes with TNF-α or LPS but not with high glucose media increases IL-8 expression. IL-8 concentration in cell culture supernatants following 24 hours of treatment in low glucose basal media, high glucose basal media, or low glucose media supplemented with TNF-alpha or LPS was quantified using ELISA. Data is from 3 biological replicates from each of 5 different donors (each bar represents the mean + SD for these 15 samples). Data for each experimental condition was compared to low glucose untreated control using an unpaired Student's *t* test (***, $p < 0.001$).

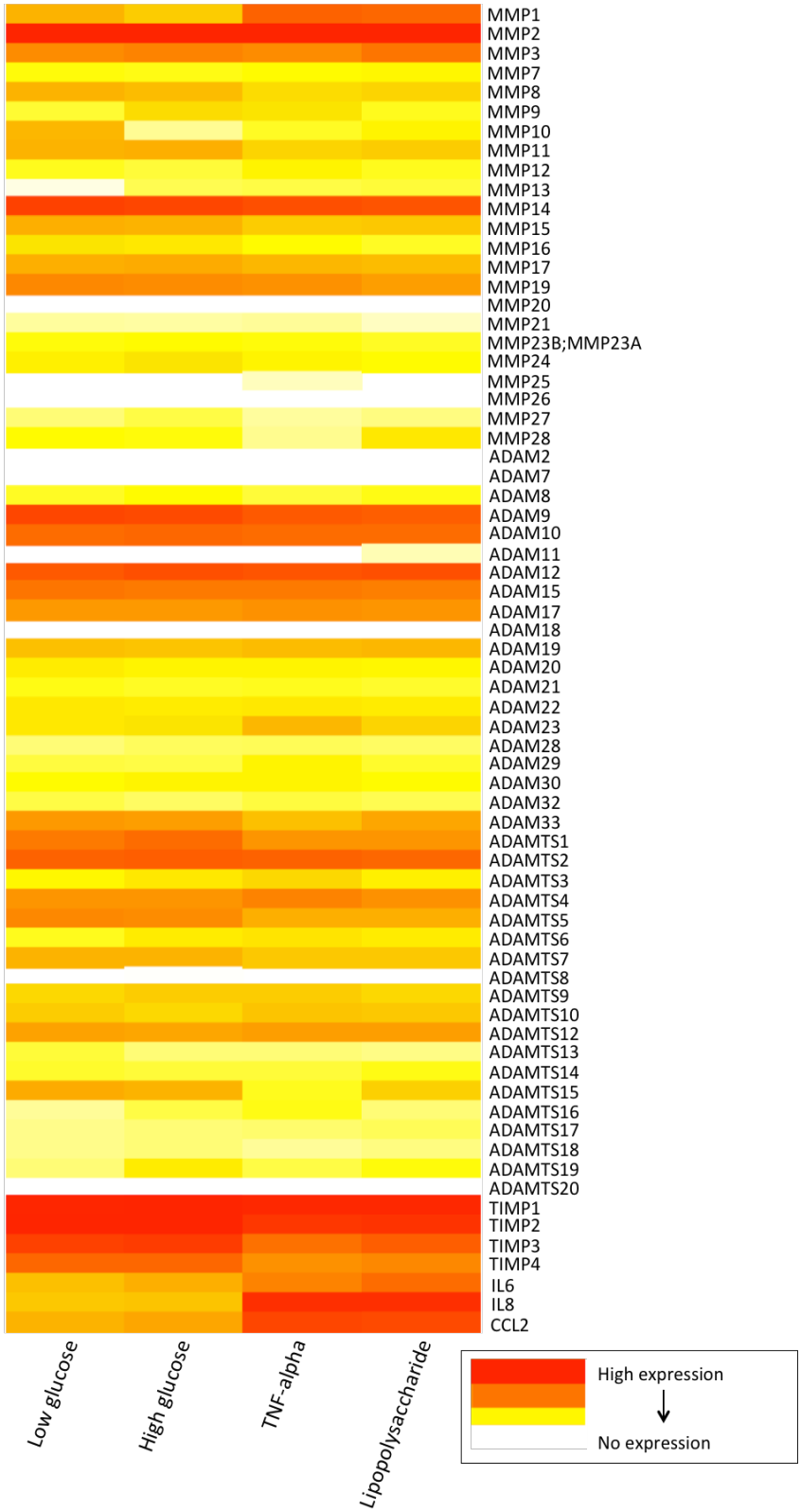

Figure 3.2: 'Heat map' showing expression of all 66 human MP and TIMP genes and 3 control genes (IL6, IL8, CCL2) in primary cultured adipocytes in four conditions: low glucose medium, high glucose medium, TNF-alpha at 50ng/ml, and lipopolysaccharide at 10ng/ml. $2^{-\Delta\Delta Ct}$ expression data was calculated using RPLP0 as the reference gene. Data is from 3 biological replicates from each of 3 independent donors. (Red, high expression; white, no expression)

On stimulation with high glucose medium, TNF-α or LPS, regulation of steady-state mRNA levels of multiple MP and TIMP genes was observed. Of the most readily-detectable MP/TIMP genes in control conditions, 6 genes (*Timp3*, *Timp4*, *Adamts1*, *Adamts5*, *Mmp3* and *Adamts4*) demonstrated a two-fold or greater change of mRNA expression. The greatest degree of upregulation was observed for MMP-1; mRNA expression increased 28.4-fold with TNF-α and 19.6-fold with LPS ($p < 0.001$) (Figure 3.3).

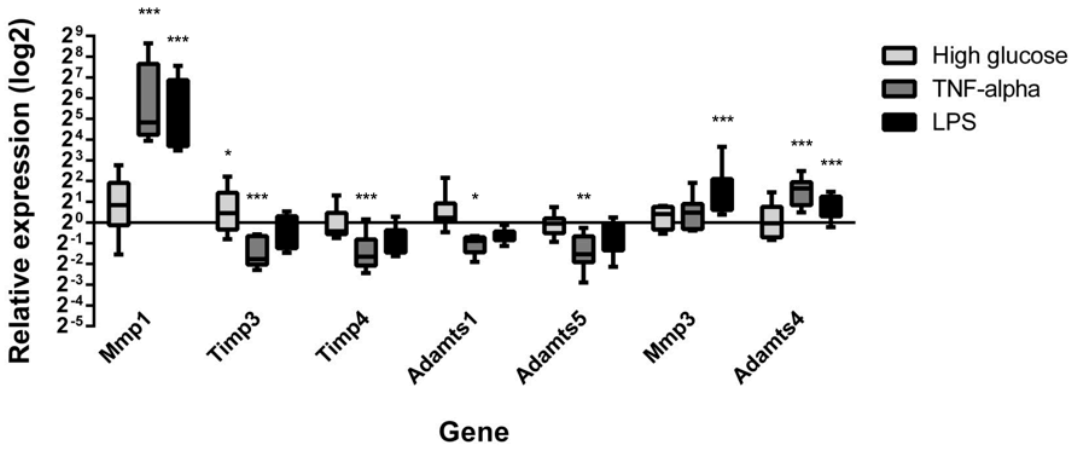

Figure 3.3: Steady-state mRNA levels for selected MPs and TIMPs varies in different experimental conditions. Fold change in expression was calculated by the $2^{-\Delta\Delta Ct}$ method for all 66 MPs and TIMPs, compared to expression in control (low glucose) medium. For each gene, expression in low glucose control medium is arbitrarily set at 1 (2^0). Log2 fold change is shown for those highly-expressed genes which demonstrate a two-fold increase or decrease in expression in any one of the three experimental conditions, compared to low glucose medium. Data for *Mmp1* is included as this gene demonstrated the greatest change in expression (28.4-fold increase in expression on exposure to TNF-alpha at 50ng/ml, and 19.6-fold increase in expression on exposure to lipopolysaccharide [LPS] at 10ng/ml). Data is from 3 biological replicates of each of 3 independent donors, and was analysed using the Mann-Whitney U test (*, $p < 0.05$; **, $p < 0.01$; ***, $p < 0.001$).

3.3: Protein expression of MPs and TIMPs by human adipocytes

As can be appreciated from the results above, MMPs -1, -2 and -14, and TIMP-3 were amongst the most readily-detectable and highly-regulated MMPs and TIMPs at mRNA level in primary human *in vitro*-differentiated adipocytes. This is in keeping with previous studies of the roles of MPs and TIMPs in adipose and other tissues. MMP-1 and MMP-14 are true collagenases, for example; the latter has been implicated in collagen I-rich extracellular matrix in adipogenesis, while the former is upregulated in inflammation. Various human studies have focused on associations between MMP-2 levels and obesity and diabetes,

while TIMP-3 is acknowledged to be the main inhibitor of ADAM-17/TACE in many tissues, and TNF-α is a major mediator of obesity-associated adipose tissue inflammation (see Chapter 1). For these reasons, I explored the expression of MMPs-1, -2 and -14 and TIMP-3 at protein level.

3.3.1 MMP-1

Since *Mmp1* mRNA was strongly upregulated, I sought to explore expression at the protein level by ELISA of culture media following 24 hours of stimulation with high glucose medium, TNF-α and LPS. Total MMP-1 protein secretion increased with TNF-α (19-fold increase) and LPS (12-fold increase) (both $p < 0.001$) but was unchanged by high glucose medium (Figure 1.4).

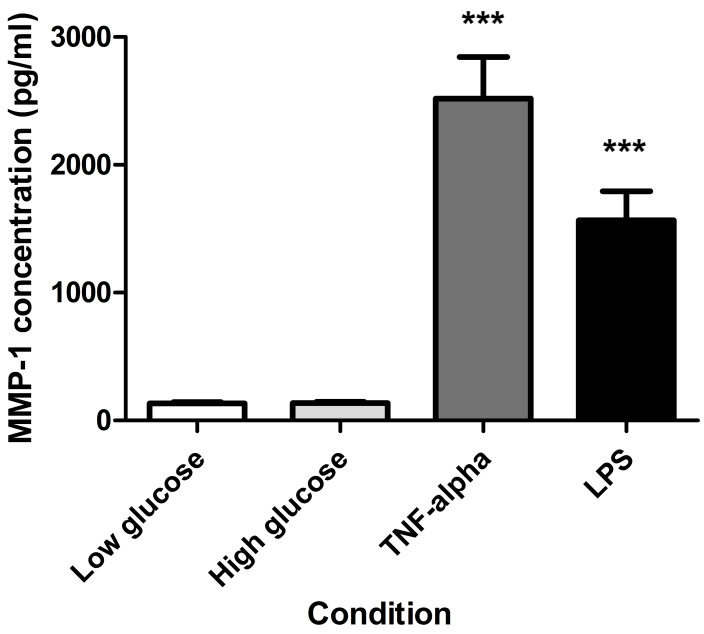

Figure 3.4: Stimulation of primary adipocytes with TNF-alpha and LPS, but not with high glucose medium, leads to increased expression of total MMP-1. In vitro-differentiated adipocytes were incubated for 24 hours in low glucose medium (untreated control), high glucose medium, low glucose medium containing 50 ng/ml TNFα, or in low glucose medium containing 10 ng/ml LPS. The expression of total MMP-1 in cell culture medium following stimulation was assessed using ELISA. Data is from 3 biological replicates from each of 5 independent donors (mean + SEM). Data for each experimental condition was compared to low glucose untreated control using a Mann-Whitney U test (***, $p < 0.001$). (TNF: tumour necrosis factor-alpha; LPS: lipopolysaccharide)

3.3.2 MMPs-2 and -14

MMP-2 (gelatinase A) was the most highly expressed MP on the TLDA array but did not appear to be regulated by high glucose, TNF-α or LPS. Gelatin zymography (see Chapter 2: Methods) was therefore used to determine whether 65 kDa gelatinase activity suggestive of MMP-2 secretion could be detected in cell culture media. Following habituation in low glucose basal media, cells were stimulated using 50ng/ml TNF-α in serum-free low glucose DMEM, or with 10 ng/ml LPS in 0.2%FCS-containing low glucose DMEM (serum is required as a source of LPS-binding protein [LBP], which is required for LPS to bind to CD14, TLR-4 and lymphocyte antigen 96, and thus stimulate a biological response). Conditioned media were recovered after 24 hours and gelatin zymography was performed. Gelatinase activity suggestive of MMP-2 was detected in all samples tested (Figure 3.5). This activity was inhibited when gels were incubated in 1,10-phenanthroline. This is a strong chelator of metal ions including zinc, so it functions as a metalloproteinase inhibitor – inhibition of gelatinolytic activity by 1,10-phenanthroline thus suggests that this activity is caused by a zinc metalloproteinase (Figure 3.5).

MMP-14 was also detected on TLDA analysis. Western blotting of cellular lysates treated as for the TLDA analysis revealed expressed of MMP-14 protein, which did not appear to be regulated by inflammatory stimuli, confirming the results at mRNA level (Figure 3.6).

A)

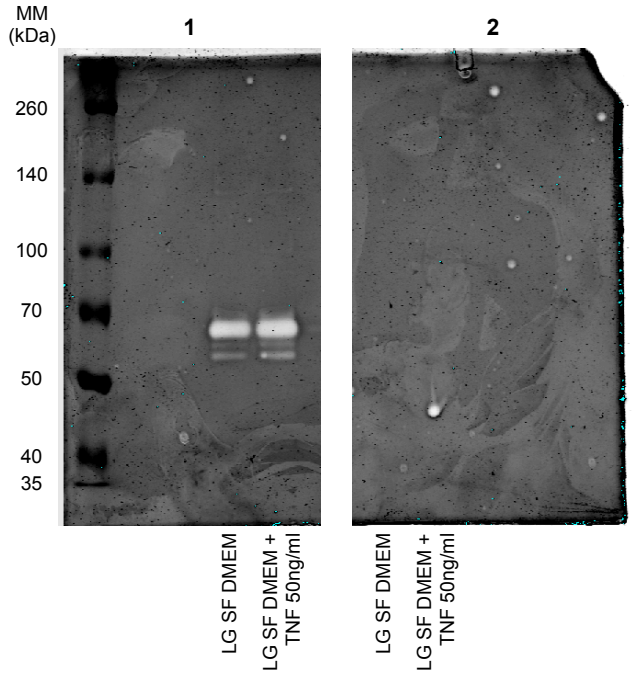

B)

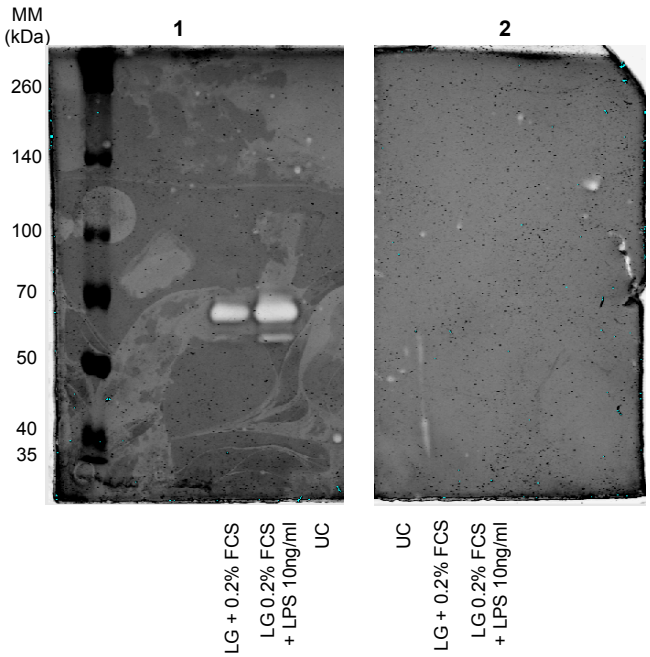

Figure 3.5: Gelatin zymography reveals the presence of gelatinase activity at 65 kDa which is inhibited by 1,10-phenanthroline. Panel A shows the results of zymography carried out when cells were treated with serum-free media ± TNF-alpha, whereas panel B shows a similar experiment with cells treated with 0.2% FCS-containing media ± LPS. No activity was noted when unconditioned low glucose media with 0.2% FCS was run on the gel. In both panels A and B, gels were split into two after PAGE, and gel 1 was incubated overnight at 37°C in Tris Assay Buffer, while gel 2 was incubated in Tris Assay Buffer supplemented with 2mM 1,10-phenanthroline. Zymography was repeated for samples from three independent donors (representative zymogram shown). (LG: low glucose; SF: serum-free; UC: unconditioned media with 0.2% FCS).

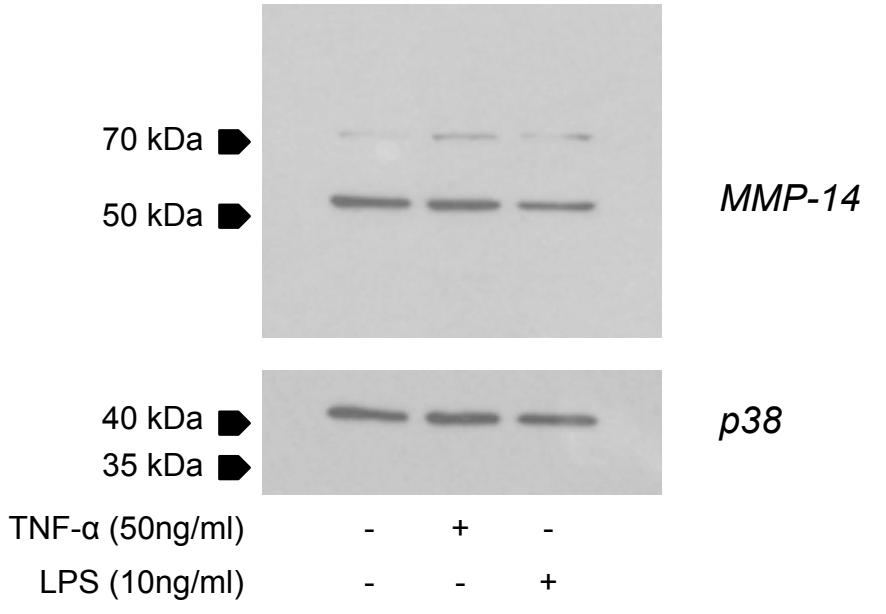

Figure 3.6: MMP-14 protein is expressed by primary human *in vitro*-differentiated adipocytes, and is not regulated by inflammatory stimuli. Adipocyte cultures were incubated for 24 hours in control media, TNF-alpha containing media or LPS-containing media, and cellular lysates were collected and subjected to immunoblotting. p38 (mitogen-associated protein kinase [MAPK]) was used as a loading control. Three independent donors analysed, representative blot shown. (TNF: tumour necrosis factor-alpha; LPS: lipopolysaccharide; MAPK: mitogen-activated protein kinase).

3.3.3 TIMP-3: regulation by inflammatory stimuli

TIMP-3 is downregulated in the adipose tissue of obese rodents [7, 136]. ADAM-17/TACE is inhibited by TIMP-3 and is responsible for the pericellular processing of various signalling molecules, including the inhibitor of adipose differentiation Pref-1 in murine models [206]. Furthermore, TIMP-3 has a broad spectrum of metalloproteinase inhibition, potentially inhibiting the MMP-mediated turnover of ECM during adipose remodelling. Thus, downregulation of TIMP-3 mRNA on stimulation with TNF-α on TLDA analysis would suggest a potential mechanism by which adipose remodelling can be regulated by inflammatory signals. I therefore sought to establish whether TIMP-3 protein expressed by *in vitro*-differentiated human adipocytes and adipose-derived mesenchymal stromal cells is regulated by stimulation with TNF-α. As described in Chapter 2, heparin can be added to culture medium to block TIMP-3 re-uptake, thus allowing its detection by Western blotting of TCA-precipitated culture media [180, 207, 208]. Adipocyte and mesenchymal stromal cell cultures from eight independent donors were incubated with heparin at 100 µg/ml, TNF-α at 50 ng/ml, or both for 48 hours following habituation in low glucose control media. Stimulation with TNF-α for 48 hours caused downregulation of TIMP-3 protein expression in five donors, no change in two donors, and upregulation of TIMP-3 protein expression in one donor (Figure 3.7). To identify whether the addition of heparin regulated TIMP-3 expression, *in*

vitro-differentiated adipocytes from three of these donors were exposed to the same conditions for 24 hours. RNA was collected from, reverse transcribed, and qRT-PCR analysis was performed for *Timp3* mRNA expression. Significant downregulation of *Timp3* mRNA was seen with TNF-α and with heparin and TNF-α in combination (Figure 3.8).

3.4: Regulation of TIMP-3 by adipogenic differentiation

TIMP-3 has been shown to be downregulated at the onset of adipogenic differentiation of 3T3-L1 cells [96]. As is the case with inflammatory stimulation, this downregulation may play a disinhibitory role on TIMP-3 regulation of adipogenic matrix turnover and shedding of adipogenic regulators. Therefore, to begin to explore a potential role for TIMP-3 in human adipose remodelling in obesity-associated inflammation, its expression by human preadipocytes at the onset of differentiation was assessed by qRT-PCR.

Human primary adipose-derived mesenchymal stromal cell cultures 48 hours post-confluence were induced to differentiate in adipogenic medium, with or without TNF-α at a concentration of 50ng/ml. Cellular lysates for RNA extraction were collected at 12 hours, 24 hours, 3 days and 6 days. Differentiation was confirmed by measurement of adiponectin mRNA expression (*Adipoq*); no *Adipoq* mRNA was detected at 0 and 12 hours, but was detected in cells exposed to differentiation medium only at 24 hours. qRT-PCR revealed downregulation of *Timp3* mRNA at differentiation induction (35.9 ± 9.4% (mean±SD) reduction in *Timp3* expression at 12 hours; 66.0 ± 11.1% reduction at 24 hours), and further downregulation by inflammatory stimulation (44.9 ± 9.5% reduction vs differentiation medium at 12 hours; 55.3 ± 3.2% reduction vs differentiation medium at 24 hours) (Figure 3.9).

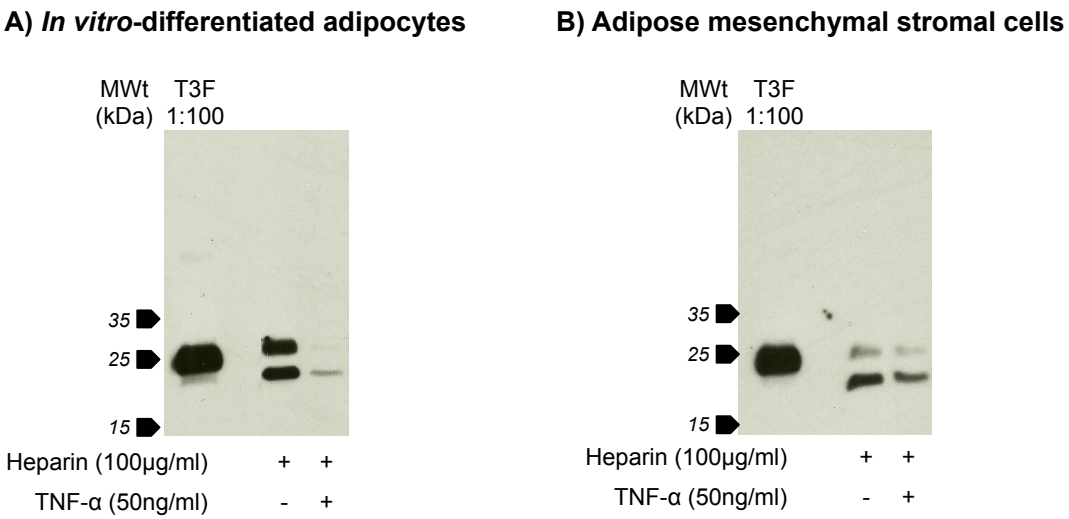

Figure 3.7: Stimulation of A) primary *in vitro*-differentiated adipocytes and B) primary adipose mesenchymal stromal cells with TNF-alpha leads to reduced expression of TIMP-3 protein. *In vitro*-differentiated adipocytes and adipose-derived mesenchymal stromal cells were incubated for 48 hours in low glucose serum-free medium with or without heparin (100 µg/ml) and TNF-α (50 ng/ml). The expression of TIMP-3 was assessed by immunoblot of TCA-precipitated conditioned media. Conditioned media from HEK293 cells overexpressing C-terminally FLAG-tagged human TIMP-3 (T3F) was included as a positive control (see Chapter 2: Methods). Cells from eight independent donors were used; a representative image is shown. (T3F: C-terminally FLAG-tagged human TIMP-3; TNF: tumour necrosis factor-alpha)

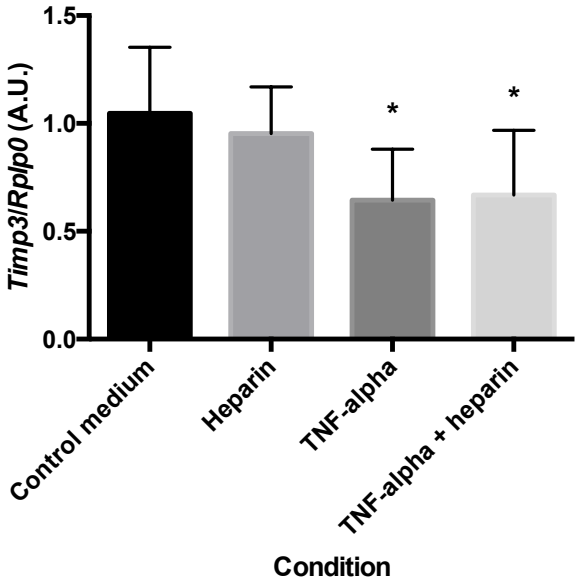

Figure 3.8: *Timp3* steady-state mRNA levels are downregulated by TNF-alpha but not by heparin. RNA was extracted and reverse transcribed from primary *in vitro*-differentiated adipocytes following stimulation for 24 hours with heparin (100 µg/ml), TNF-α (50 ng/ml) or both. cDNA was analysed by qRT-PCR for expression of *Timp3*, which was normalised to *Rplp0* expression. Data is from 3 biological replicates from each of 3 independent donors (mean + SD). Results were analysed by one-way ANOVA ($p = 0.01$), and Tukey's post-hoc multiple comparisons test, in which each condition was compared to the control condition (*: $p < 0.05$). (A.U. arbitrary units; TNF-alpha: tumour necrosis factor alpha).

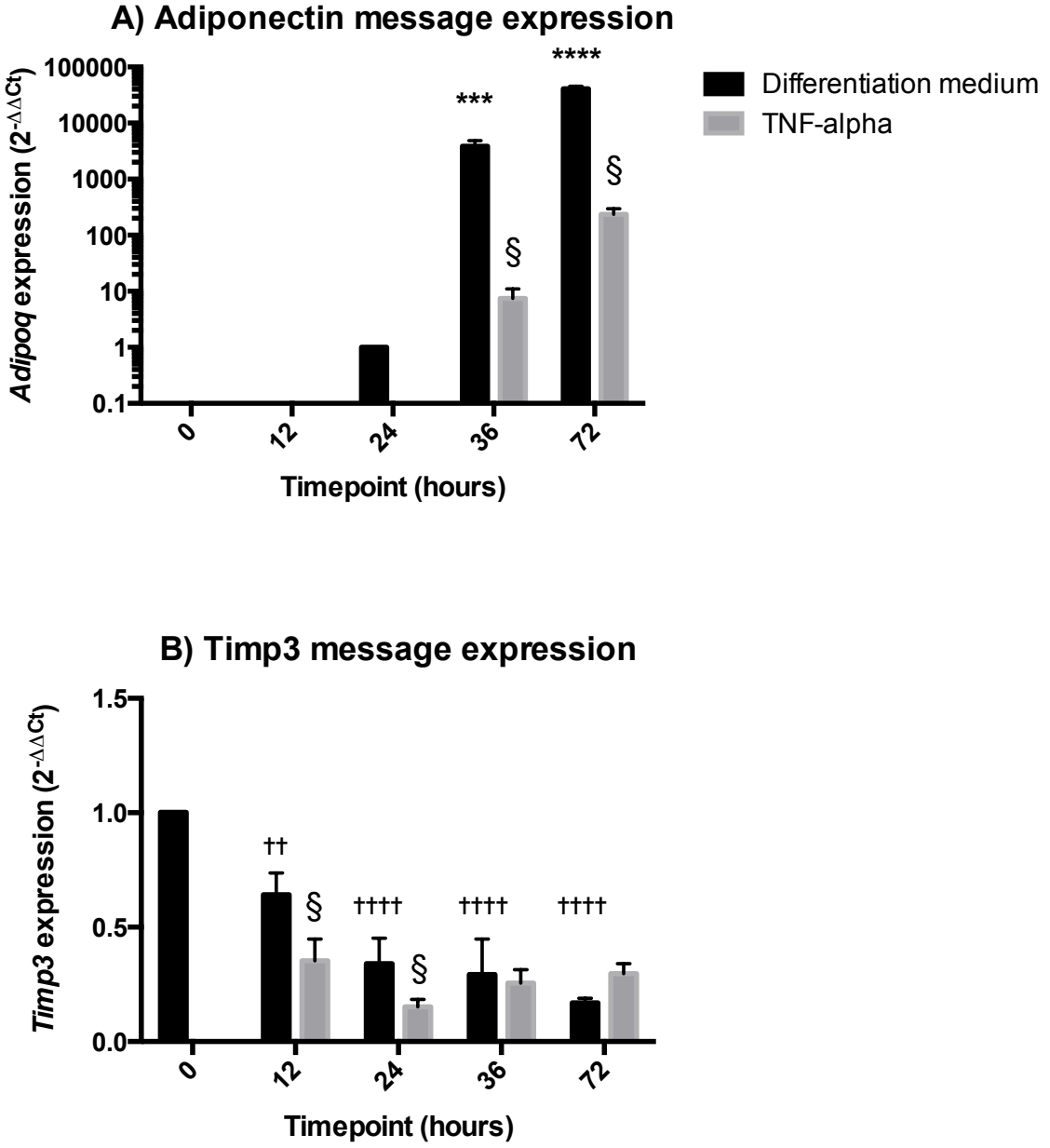

Figure 3.9: Expression of *Timp3* is regulated during preadipocyte differentiation. 48 hours after reaching confluence, preadipocyte cultures were induced to differentiate with adipogenic media, with or without TNF-alpha at 50 ng/ml added. Cellular lysates were collected at 12, 24, 36 and 72 hours. RNA was extracted and qRT-PCR was performed for (A) *Adipoq* and (B) *Timp3*. Results are expressed as $2^{-\Delta\Delta Ct}$, relative to expression at Day 0 (i.e. before the onset of differentiation) for *Timp3* and 24 hours for *Adipoq*, and with *Rplp0* as the comparator gene. Data are from four replicates from each of three independent donors, and were analysed using a two-way ANOVA with post-hoc Dunnett's multiple comparison (*Adipoq* expression vs 24 hours: ***: $p < 0.001$, ****: $p < 0.0001$; *Timp3* expression vs 0 hours: ††: $p < 0.01$, ††††: $p < 0.0001$; Expression TNF-alpha vs differentiation medium at each timepoint: §: $p < 0.0001$).

3.5: Discussion

In obesity associated with metabolic sequelae (metabolically 'unhealthy' obesity (MUO)), white adipose tissue (WAT) has two characteristics that are thought to contribute to the development of these adverse metabolic outcomes:

1. Chronic, low-grade inflammation, with elevated circulating markers of inflammation and infiltration by macrophages [19, 20, 23]
2. An inability of subcutaneous WAT to expand sufficiently to store surplus ingested energy, resulting in excess lipids diversion to ectopic sites (liver, skeletal muscle, pancreas and visceral adipose), leading to lipotoxicity and insulin resistance [32, 35]. While 'healthy' subcutaneous adipose expansion involves recruitment and differentiation of adipocyte precursors (preadipocytes) into mature adipocytes, limited expandability in MUO is thought to, at least partly, relate to failure of this process and a tendency for expansion to occur by adipocyte hypertrophy. Hypertrophied adipocytes contributed to elevated circulating free fatty acid levels, and are associated with increased adipose tissue TNF-α and IL-6, all of which are related to an increased risk of IR (see Chapter 1).

Preadipocyte differentiation and adipocyte hypertrophy are two central processes required for the adipose remodelling that occurs in weight gain. As in other tissues, remodelling in WAT is thought to involve extracellular matrix turnover, which in turn requires the regulated expression and activity of proteins capable of hydrolysing WAT ECM components such as collagens I, IV, VI, fibronectin and laminin, as well as modulating the availability and activity of cytokines and other signalling molecules, such as Pref-1 and TNF-α. Preadipocyte and adipocyte-expressed metalloproteinases (MPs) and their tissue inhibitors (TIMPs) are thought to be involved in these matrix turnover and shedding processes.

This chapter presents the first comprehensive description of the expression of all human metalloproteinase and TIMP genes by primary human *in vitro*-differentiated adipocytes in culture, in basal, hyperglycaemic, and inflammatory conditions. Furthermore, the expression of target candidates thought to be particularly important in WAT remodelling has been described in conditions of inflammatory stimulation and during preadipocyte differentiation. MMP-1, MMP-2, and MMP-14/MT1-MMP are major players in ECM remodelling, with collagen I, IV, gelatin, fibronectin and laminin amongst their many targets [209]. All four are expressed by human adipocytes in the culture system presented in this report; MMP-1 is upregulated by inflammatory conditions. Data have also been presented indicating that TIMP-3 mRNA and protein are downregulated by inflammatory stimulation of adipocytes and

at the onset of preadipocyte differentiation. With respect to TIMP-3 protein, donor-to-donor variability was observed, which is not unexpected in studies using primary human cells in culture. The experiment wherein primary human adipose-derived mesenchymal stromal cells and *in vitro*-differentiated adipocytes were stimulated with TNF-α in medium containing heparin was repeated with cells from eight independent donors. In five donors, there was clear downregulation of TIMP-3 protein. In two donors, there was no change, whereas with one donor, there was upregulation of TIMP-3 protein with inflammatory stimulation. Downregulation at protein level in 5/8 donors tested, along with downregulation at mRNA level in three of these donors (Figure 3.8) and in three separate donors in the TLDA experiment (Figure 3.2) is highly suggestive that TIMP-3 is indeed downregulated by inflammatory stimulation. Interestingly, this is in keeping with previous work by the Gavrilovic group showing that MCEC-1 endothelial cells also respond to TNF-α and IL-1 showing a reduction in steady state *Timp3* mRNA levels [210].

These results are consistent with previous investigations of MP/TIMP expression, carried out in murine adipose tissue and adipocyte cell lines. Upregulation of MMPs -1 and -3 was seen in SGBS adipocytes exposed to macrophage-conditioned medium, whereas downregulation of TIMP-3 was observed in white adipose tissue from genetically obese (*ob/ob*, *db/db*) mice and mice on high-fat diet (HFD), as well as at the onset of differentiation of 3T3-L1 preadipocytes (see Chapter 1).

TIMP-3 was one of the most readily-detectable MPs/TIMPs on the TLDA array, and also one of the most significantly regulated by inflammatory stimulation with TNF-α. Given its high expression, it may exert a 'tonic' inhibitory effect on MMP and ADAM activity in the pericellular milieu in the basal state. In inflammation or tissue remodelling, its downregulation may be disinhibitory on MP activity. Thus, TIMP-3 may be an important node in adipose remodelling, as it may integrate adipose inflammation, ECM remodelling and regulation of preadipocyte differentiation. Specifically, TIMP-3 downregulation may allow increased ADAM-17 activity, which would result in increased local adipose tissue inflammation due to increased shedding of active TNF-α, and would reduce preadipocyte differentiation as a result of increased solubilisation of Pref-1/Dlk-1. This in turn may lead to a metabolically maladaptive state in which preadipocyte recruitment is chronically impaired and adipocyte hypertrophy becomes the preferential, or even exclusive, mode of adipose tissue expansion. *In vivo* murine work provides some corroborative evidence for this hypothesis, as *Timp3* knockout aggravates metabolic dysfunction and increases the ectopic deposition of lipids in the liver of insulin resistant *Insr+/-* mice, while ADAM-17 inhibition/deficiency rescues the phenotype [136].

A number of pertinent questions remain to be addressed in order to fully elucidate the role of MPs and TIMPs in WAT remodelling, obesity and metabolic disease. Although it is reasonable to surmise that TIMP-3 downregulation in adipose inflammation and preadipocyte differentiation would allow increased MP activity leading to increased (i) ECM turnover and (ii) shedding of signalling molecules such as sDlk-1, this has not been ascertained in a physiologically relevant model of human adipose tissue. Furthermore, in humans, there have been few attempts to date to describe the relationship between adipose MP/TIMP expression and (i) markers of metabolic health such as whole body insulin sensitivity and (ii) whole body lipid distribution. Notable exceptions include the 2010 study by Madec and colleagues, which identified reduced expression of MMP-2 and TIMP-2 in adipocytes isolated from subcutaneous and visceral adipose tissue samples donated by lean hypertensive patients as opposed to normotensive controls (although this study did not look at obese subjects) [211], and the 2010 study by Unal and colleagues which reported a positive correlation between subcutaneous adipose tissue *Mmp9* mRNA expression and body mass index and negative correlation between subcutaneous adipose tissue *Mmp9* mRNA expression and insulin sensitivity [212].

Therefore, I designed a clinical cross-sectional study to investigate the relationship between MP/TIMP expression in human adipose tissue and metabolic parameters (Chapter 4), and *in vitro* experiments to investigate the role of TIMP-3 in adipose ECM remodelling and Dlk-1 shedding (Chapter 5). These investigations focused on a prioritised candidate list of most interesting 'hits' from the TLDA screen: MMPs -1, 2 and 14 and TIMP-3. I selected these candidate molecules because:

- TIMP-3, MMPs-2 and 14 had amongst the highest basal expression levels.
- MMP-1 and TIMP-3 were the most strongly regulated MPs/TIMPs by TNF-α and LPS.
- TIMP-3 is a broad-spectrum inhibitor of many MPs, and is the major inhibitor for ADAM-17 [177]. ADAM-17 has been implicated in adipose tissue biology via its effects on TNF-α and Pref-1 shedding [119, 124].

Although some regulation of MP and TIMP expression was seen in hyperglycaemic conditions (Figures 3.2 and 3.3), I decided to focus on an experimental model for adipose inflammation in obesity, as this is thought to exist in the 'pre-diabetic' state, rather than continuing to expose cells to conditions modelling glucose concentrations typical of established diabetes. Therefore, I used differentiation medium and/or TNF-α stimulation as the main experimental condition in subsequent experiments investigating the role of TIMP-3 in ECM remodelling and Dlk-1 shedding. Better understanding of the roles of TIMPs and

MPs in the process by which obesity increases the risk of developing type 2 diabetes may lead to better diagnostic and therapeutic modalities, helping to uncouple obesity from its metabolic sequelae.

Chapter 4:

Relationships between human adipose expression of metalloproteinases and their tissue inhibitors, whole-body lipid distribution and systemic insulin resistance

4.1: Introduction

As demonstrated in the previous chapter, metalloproteinases and their tissue inhibitors are expressed by human *in vitro*-differentiated adipocytes, and this expression is regulated by inflammatory stimuli. The other cellular constituents of adipose tissue, such as mesenchymal stromal cells, macrophages, endothelial cells and fibroblasts [23] have all been shown to express metalloproteinases and their inhibitors in adipose tissue and other tissues (see Chapter 1, section 1.3.2). Given their ubiquitous role in remodelling and inflammation in myriad other tissues, it is reasonable to hypothesise that adipose tissue remodelling in weight gain involves metalloproteinases and TIMPs expressed by various cells within the adipose tissue, with intercellular crosstalk regulating this expression. Nevertheless, relatively little is known about human adipose tissue remodelling in early obesity and whether these remodelling processes directly contribute to the development of insulin resistance, or whether maladaptive remodelling in a subset of obese subjects predisposes to insulin resistance and type 2 diabetes. A better understanding of the processes that occur in adipose tissue during weight gain in human obesity may aid the development of improved markers of early insulin resistance, potentially allowing the prevention of progression to type 2 diabetes through the targeted deployment of lifestyle interventions.

Studies of the roles of metalloproteinases and TIMPs in human obesity have to date predominantly focused on associations of (i) circulating levels of MMPs (such as MMPs-2 and -9) or (ii) certain SNPs and haplotypes with measures of adiposity and whole-body metabolic status (see Chapter 1, section 1.3.5). Although two studies have identified positive correlations between adipocyte size and MMP-2 [143] or MMP-3 expression [99], there has been relatively little focus on the relationship between these proteins/genes and adipose tissue remodeling in human subjects, and no studies at all on their role in whole-body lipid distribution. To this end, I carried out a cross-sectional investigation with the aim of testing the hypothesis that there is an association between expression of MMPs-1, -2, and -14, TIMP-3 and Dlk-1 in human subcutaneous and visceral adipose tissue, and parameters of whole body metabolic status (fasting plasma glucose, fasting serum insulin and HOMA-IR), systemic inflammation (serum C-reactive protein [CRP]), adipose tissue remodelling and inflammation (adipocyte size and CD68 immunoreactivity), and whole-body lipid distribution (magnetic resonance imaging measurements of adipose depot volume and hepatic fat fraction).

4.2: Baseline characteristics of study population

Thirty-nine female subjects undergoing elective NHS surgery at the Norfolk and Norwich University Hospital (NNUH) were recruited to participate in this study (see Chapter 2: Methods for details of recruitment pathways and eligibility criteria). Participants were recruited to five body mass index (BMI) bins (18.5-24.9, 25-29.9, 30-34.9, 35-39.9 and >40 kg/m^2), ensuring that a range of BMIs were represented in the study. Their baseline characteristics are detailed in Table 4.1. Given that the age range of study subjects (22-73 years) spanned the average menopausal age in the UK (51 years, [213]), serum samples donated by subjects were assayed for circulating levels of follicle stimulating hormone (FSH) using the two-step ARCHITECT FSH immunoassay (see Chapter 2). A serum FSH level >30 IU/l was considered to indicate established menopause; by this measure, 43.6% of the study cohort were post-menopausal at the time of participation.

Parameter (unit) [normal range]		**Mean (SD)** or **n (%)**
Age (years)		48.2 (12.1)
Post-menopausal (FSH ≥30 IU/l)		17 (43.6%)
Weight (kg)		78.9 (17.4)
Body mass index (kg/m^2)		29.0 (6.1)
BMI categories	BMI 18.5 – 24.9 kg/m^2	14 (35.9%)
	BMI 25.0 – 29.9 kg/m^2	9 (23.1%)
	BMI 30.0 – 34.9 kg/m^2	8 (20.5%)
	BMI 35.0 – 39.9 kg/m^2	6 (15.4%)
	BMI >40.0 kg/m^2	2 (5.12%)
Diagnosis of diabetes at recruitment		1 (2.56%)
Fasting glucose (mmol/l) [3.5-6.0]		5.35 (0.65)
Fasting insulin (pmol/l) [0-60]		67.3 (42.4)
Fasting triglycerides (mmol/l) [0.5-1.7]		1.23 (0.66)
HOMA-IR [<1]		1.28 (0.81)
Serum CRP (µg/ml) [<5]		3.02 (2.20)

Table 4.1: Baseline characteristics of the 39 study subjects, all of whom were female. Data is mean +/- SD or n (%), presented to 3 s.f. (CRP: C-reactive protein)

Due to the nature of the study pathway, it was not possible to collect all intended samples from each study participant. In some cases, for example, adipose tissue was not available at operation, and in other cases, participants were lost to follow-up before their magnetic resonance imaging (MRI) scan could be scheduled. Table 4.2 outlines the samples and data

	Study ID	Anthropometrics					Blood	Subcutaneous adipose tissue	Visceral adipose tissue	MRI
		Weight	*Height*	*BMI*	*WC*	*HC*				
1	A01-13TB0052							**	**	
2	A02-13TB0091									
3	A03-13TB0112									
4	A04-13TB0121							**	**	
5	A05-13TB0186									
6	A06-13TB0210							**	**	
7	A07-13TB0392									
8	A08-13TB0411									
9	A09-13TB0396									
10	A10-13TB0504									
11	A11-13TB0553									
12	A12-13TB0671									
13	A14-14TB0247									
14	A15-14TB0442									
15	B01-13TB0073						*			
16	B02-13TB0457							**	**	
17	B03-13TB0474						*	**	**	
18	B04-13TB0518							** / ***	** / ***	
19	B05-13TB0520									
20	B06-13TB0663									
21	B07-14TB0158							**		
22	B08-14TB0286									
23	B09-14TB0307									
24	C01-13TB0395									
25	C02-13TB0466									
26	C03-13TB0558							**	**	
27	C04-14TB0144									
28	C05-14TB0287									
29	C06-14TB0288									
30	C07-14TB0463						*			
31	C08-14TB0473									
32	D01-13TB0110									
33	D02-13TB0347									
34	D03-13TB0505									
35	D04-14TB0157									
36	D05-14TB0161									
37	D06-14TB0627									
38	E01-13TB0519							***	***	
39	E02-13TB0638									

Table 4.2: Samples and data collected from study participants. A green colour indicates that the sample or data in question was collected for the participant. When blood or adipose tissue samples were of insufficient volume or quality to allow all the different types of analysis to be applied, this is indicated in the respective columns (*: sample insufficient for CRP assay; **: sample inadequate for histological analysis; ***: sample inadequate for RNA extraction and qRT-PCR analysis). (BMI: body mass index; WC: waist circumference; HC: hip circumference; MRI: magnetic resonance imaging).

collected for each participant in the study. Waist circumference and hip circumference started being recorded for subjects at the end of the study following an amendment to the ethical approval for the study, explaining why so few participants had this data recorded.

Initial analysis of data collected from study participants focused on identifying expected correlations between anthropometric, metabolic, and adipose remodelling parameters, to determine whether the study cohort was broadly representative of the United Kingdom adult female population in metabolic terms. BMI correlated positively with systemic insulin resistance as quantified using HOMA-IR, fasting plasma glucose and serum C-reactive protein (Figure 4.1). This indicates that more obese subjects in our cohort were more insulin resistant, with one participant being diabetic (Figure 4.1b: subject 36, fasting plasma glucose 7.49 mmol/l). The positive relationship between serum CRP as a parameter of systemic inflammation and obesity has also been described previously [22, 214].

The methodology used to quantify adipose tissue depot volume is explained in Chapter 2, but briefly, the total adipose tissue depot (TAT) is defined as the total adipose volume from neck to femoral region of the study subject as determined by automated fat-water segmentation. The abdominal subcutaneous adipose tissue depot (ASAT) is defined as the non-intraabdominal component of the total adipose volume in the abdominal region, whereas the visceral adipose depot (VAT) equates to the intraabdominal component of the TAT in the abdominal region. Hepatic fat fraction is the percentage of representative hepatic voxels that demonstrates a lipid-characteristic signal on magnetic resonance imaging (as opposed to a water- or air-characteristic signal). Within our study population, more obese subjects had great depot volumes and an increased hepatic fat fraction on MRI (Figure 4.2), which is entirely as expected [198, 215].

Mean adipocyte cross-sectional areas were calculated from three field views of two non-consecutive haematoxylin and eosin (H&E)-stained sections of each depot, as detailed in Chapter 2. Mean visceral adipocyte size correlated positively with both body mass index and HOMA-IR, but surprisingly there was no correlation between mean subcutaneous adipocyte area and BMI or HOMA-IR (Figure 4.3). Positive associations between subcutaneous adipocyte size, BMI and insulin resistance have previously been identified [216, 217].

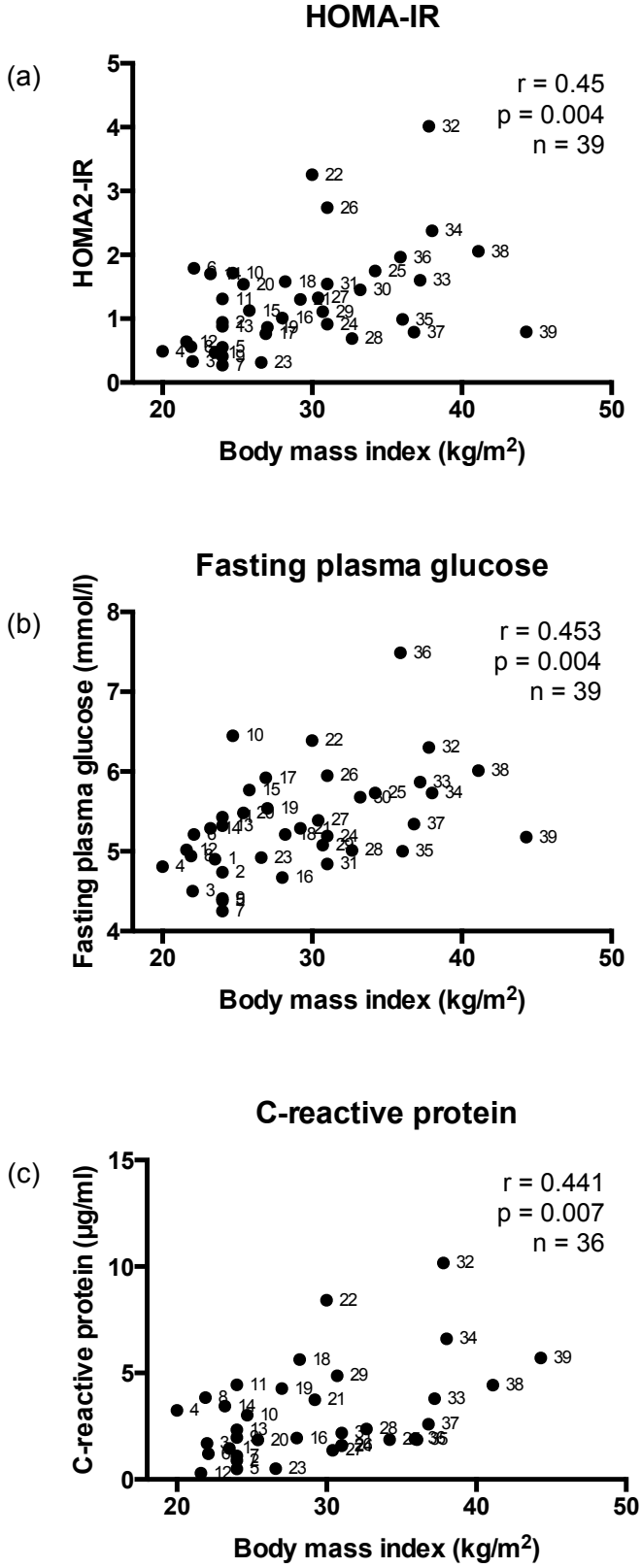

Figure 4.1: Body mass index correlates positively with (a) HOMA-IR, the homeostatic model assessment of insulin resistance, (b) fasting plasma glucose, and (c) serum C-reactive protein. The numbered label associated with each data point refers to the study subject in question, as laid out in Table 4.2.

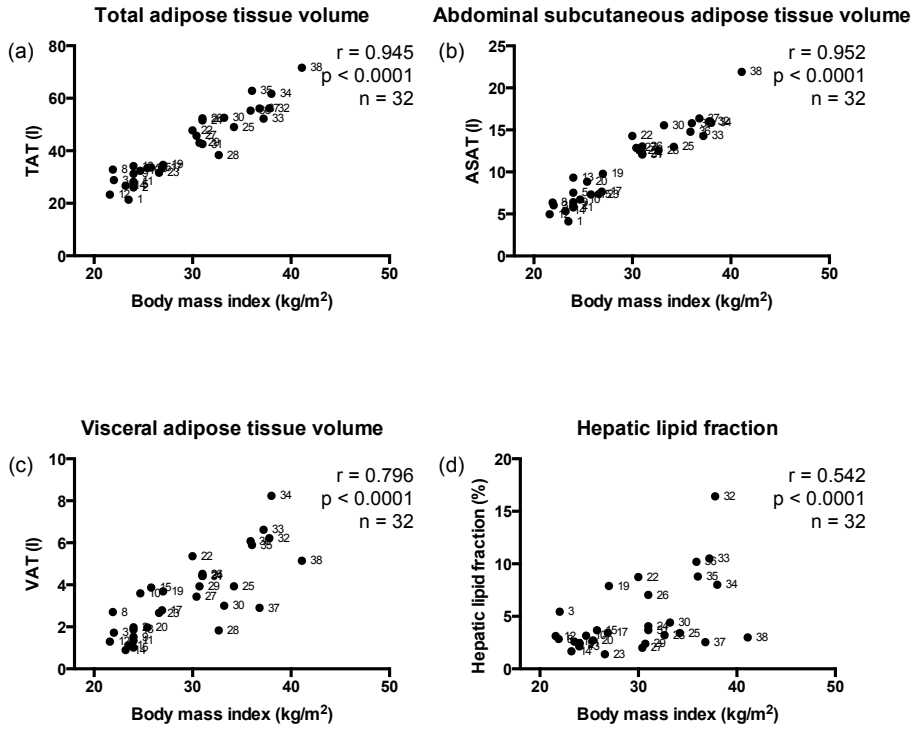

Figure 4.2: Body mass index correlates positively with magnetic resonance imaging parameters of adiposity, including (a) total adipose tissue volume (TAT), (b) abdominal subcutaneous adipose tissue volume (ASAT), (c) visceral adipose tissue volume (VAT), and (d) hepatic lipid fraction. Note that the scale on the y-axis of each scatter plot is different, reflecting the different ranges displayed by each adipose depot in terms of volume.

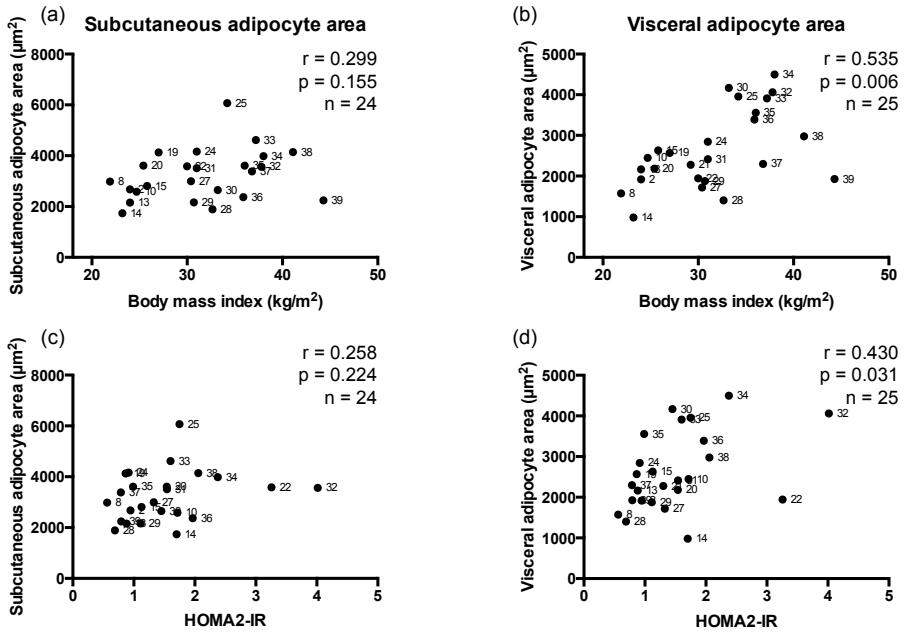

Figure 4.3: Body mass index does not vary with (a) mean subcutaneous adipocyte area, but is positively related to (b) mean visceral adipocyte area. Similarly, mean subcutaneous adipocyte area does not correlate with HOMA-IR (c), but visceral adipocyte area does (d). Mean adipocyte area was calculated from three fields of view from H&E stained-sections of paraffin-embedded adipose tissue donated by study subjects, using the methodology outlined in Chapter 2: Methods.

	Anthropometric variables										
	Age (years)	*BMI (kg/m^2)*	*Waist circumference (cm)*	*Waist-to-hip ratio*	*Waist-to-height ratio*	*Total adipose volume (l)*	*Abdominal subcutaneous adipose tissue (l)*	*Non-visceral adipose volume (TAT-VAT) (l)*	*Visceral adipose volume (l)*	*VAT/TAT (%)*	*Hepatic fat fraction (%)*
Correlation with HOMA-IR r, (n)	0.109 (39)	0.450** (39)	0.145 (9)	0.220 (9)	0.076 (9)	0.569** (32)	0.565** (32)	0.537** (32)	0.652**** (32)	0.500** (32)	0.681**** (32)

Table 4.3: Pearson correlation coefficients (r) of correlations between anthropometric and magnetic resonance imaging variables and HOMA-IR. (BMI: body mass index; VAT: visceral adipose tissue volume; TAT: total adipose tissue volume)
(**: $p < 0.01$; ****: $p < 0.0001$)

	Subcutaneous adipocyte area (μm^2)	*Visceral adipocyte area (μm^2)*	*Total adipose volume (l)*	*Abdominal subcutaneous adipose tissue (l)*	*Non-visceral adipose volume (TAT-VAT) (l)*	*Visceral adipose volume (l)*	*VAT/TAT (%)*	*Hepatic fat fraction (%)*
Correlation with subcutaneous adipocyte area r, (n)	1 (24)	0.592** (24)	0.462* (23)	0.392 (23)	0.435* (23)	0.487* (23)	0.373 (23)	0.286 (23)
Correlation with visceral adipocyte area r, (n)	0.592** (24)	1 (24)	0.680**** (23)	0.575** (23)	0.636** (23)	0.742**** (23)	0.516* (23)	0.617** (23)

Table 4.4: Pearson correlation coefficients (r) of correlations between mean adipocyte area in subcutaneous and visceral depots, and magnetic resonance imaging variables. (VAT: visceral adipose tissue volume; TAT: total adipose tissue volume)
(*: $p < 0.05$; **: $p < 0.01$; ****: $p < 0.0001$)

4.3: Relationships with metalloproteinase and TIMP mRNA expression

Given that metalloproteinases (MPs) and their tissue inhibitors (TIMPs) are expressed by human adipose-derived mesenchymal stromal cells (MSCs) and *in vitro*-differentiated adipocytes, I proceeded to quantify the mRNA expression of MPs and TIMPs of interest identified in Chapter 3 in subcutaneous and visceral adipose tissue samples donated by study subjects. I also quantified the expression of Dlk-1 given its purported role in adipogenesis and regulation by MP/TIMP activity. In all these experiments, RNA was extracted from whole adipose tissue samples. I then analysed how the expression of these genes in these whole tissue samples related to various parameters of systemic metabolic status, adipose tissue remodelling and whole-body lipid distribution.

4.3.1 Timp3

TIMP-3 is highly expressed by human MSCs and adipocytes, and is downregulated in inflammatory conditions and at the onset of differentiation (see Chapter 3). Its expression in the subcutaneous adipose depot is positively correlated with mean subcutaneous adipocyte cross-sectional area (Figure 4.4). Large subcutaneous adipocyte size is generally associated with adverse metabolic status, but this was not the case in this study's cohort (Figure 4.3). A disassociation between adipocyte size and metabolic impairment has been previously reported in terms of alterations in adipose tissue remodelling, as is the case in the *col6KOob/ob* mouse, in which absence of collagen VI may allow increased adipocyte expansion without attendant adverse metabolic outcomes [45]. In view of this, I performed partial correlation analysis to explore the relationship between subcutaneous *Timp3* mRNA expression and metabolic, remodelling and distribution parameters when controlling for TAT volume and subcutaneous adipocyte area (Table 4.5). As shown, the association between subcutaneous *Timp3* expression and mean subcutaneous adipocyte area becomes stronger when controlling for TAT, indicating that in a group of study subjects with the same TAT, those with the highest *Timp3* expression have the greatest subcutaneous adipocyte area. Furthermore, when controlling for subcutaneous *Timp3* expression, the expected positive correlation between systemic insulin resistance and mean subcutaneous adipocyte area is observed. When controlling for mean subcutaneous adipocyte area, negative correlations emerge between subcutaneous *Timp3* expression and HOMA-IR, and between subcutaneous *Timp3* expression and VAT volume. These results all indicate the

central role that *Timp3* may play in adipose tissue remodelling and the determination of adipocyte size.

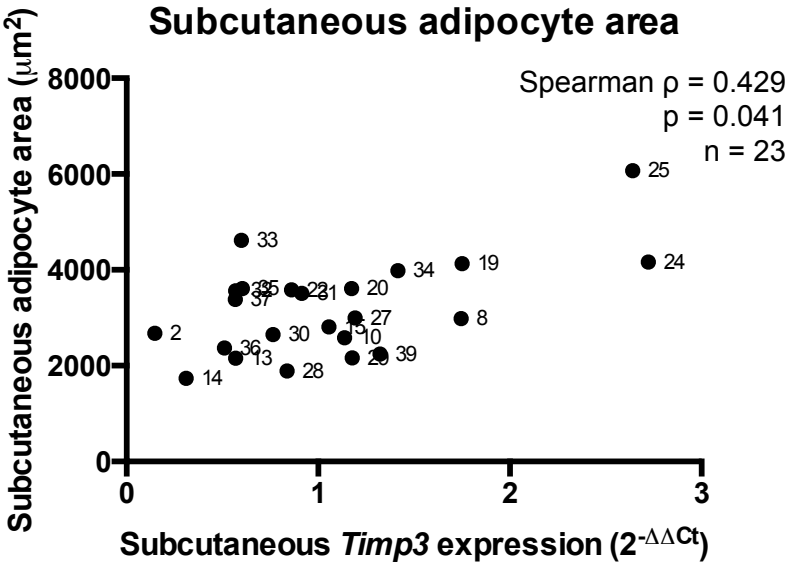

Figure 4.4: Subcutaneous *Timp3* expression correlates with adipose remodelling parameters. RNA was extracted from whole subcutaneous adipose tissue samples donated by study subjects and reverse transcribed. Real-time quantitative reverse transcription PCR (qRT-PCR) for *Timp3* steady state mRNA levels was performed. Results were normalized to expression of *Rplp0*, via the $2^{-\Delta\Delta Ct}$ method. Paired subcutaneous adipose samples were used to quantify subcutaneous adipocyte cross-sectional area.

Variable 1	Variable 2	Control variable	Spearman ρ	*p* value	n
Mean subcutaneous adipocyte area	Subcutaneous *Timp3* expression	None	0.429	0.041	23
Mean subcutaneous adipocyte area	Subcutaneous *Timp3* expression	Total adipose tissue volume	0.700	<0.0001	20
Subcutaneous *Timp3* expression	HOMA-IR	Mean subcutaneous adipocyte area	-0.505	0.017	20
Subcutaneous *Timp3* expression	Visceral adipose tissue volume	Mean subcutaneous adipocyte area	-0.445	0.038	20
Mean subcutaneous adipocyte area	HOMA-IR	Subcutaneous *Timp3* expression	0.502	0.017	20

Table 4.5: Partial correlations between subcutaneous adipose *Timp3* expression (expressed as $2^{-\Delta\Delta Ct}$) and an adipose remodelling variable (mean subcutaneous adipocyte area), an adipose distribution variable (visceral adipose tissue volume) and a metabolic variable (HOMA-IR), controlling for total adipose tissue volume or mean subcutaneous adipocyte area.

4.3.2 Dlk1

Dlk-1 is expressed by human MSCs (see Chapter 3), but not by adipocytes. I hypothesized that donors with a metabolically-favourable adipose distribution and characteristics (more SAT vs VAT, smaller mean adipocyte area) would have higher SAT *Dlk1* expression, as this would indicate more preadipocytes allowing a shift towards a hyperplastic mode of expansion. However, not all donors had detectable *Dlk1* expression in their adipose depots. Donors with no detectable subcutaneous *Dlk1* expression had higher mean percentage visceral adipose tissue (that is – visceral adipose tissue volume expressed as a percentage of total adipose tissue volume, VAT/TAT%), than donors where subcutaneous *Dlk1* mRNA was detected (Figure 4.5a). In overweight and obese donors (BMI ≥ 25kg/m^2) where subcutaneous *Dlk1* expression was detected, this correlated negatively with mean subcutaneous adipocyte area (Figure 4.5b).

Similarly, *Dlk1* mRNA expression in the visceral adipose depot was associated with adipose distribution and metabolic parameters (Figure 4.6). In subjects in whom visceral *Dlk1* mRNA expression was seen, there was a negative correlation between this variable and percentage visceral adipose tissue volume (Figure 4.6a). Mean fasting triglycerides were higher in donors with visceral *Dlk1* expression (n = 16) as compared to those in whom visceral *Dlk1* mRNA was undetectable (n = 9, Figure 4.6b). This is in keeping with previously published data detailing an association between adipose *Dlk1* expression and circulating triglycerides [154, 218].

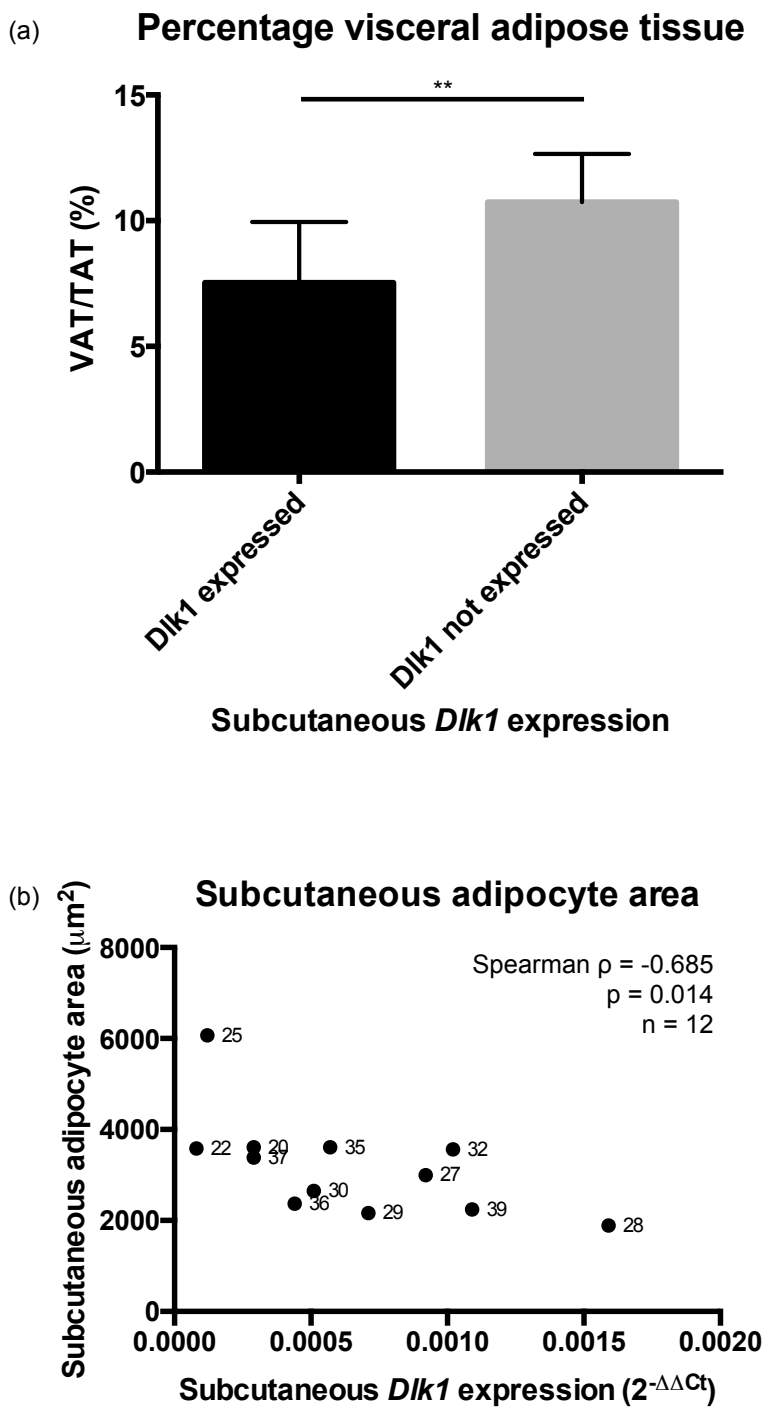

Figure 4.5: Subcutaneous *Dlk1* expression varies with adipose remodelling and distribution parameters. RNA extracted from whole subcutaneous adipose tissue samples was reverse transcribed and used for real-time quantitative reverse transcription PCR analysis (qRT-PCR) of *Dlk1* expression. Results were normalized to expression of Rplp0, via the $2^{-\Delta\Delta Ct}$ method. *Dlk1* cycling threshold (Ct) values of ≥40 were interpreted as indicating an absence of *Dlk1* expression. (a) Presence (n = 17) or absence (n = 8) of subcutaneous Dlk1 varies with percentage visceral adipose tissue volume, calculated as the ratio of visceral adipose tissue volume to total adipose tissue volume measured on magnetic resonance imaging. (Data shown are mean + SD, **: $p < 0.01$ by Student's t test). (b) In overweight/obese donors where Dlk1 mRNA expression was detected in the subcutaneous compartment, this is negatively correlated with mean subcutaneous adipocyte area. (VAT: visceral adipose tissue volume; TAT: total adipose tissue volume).

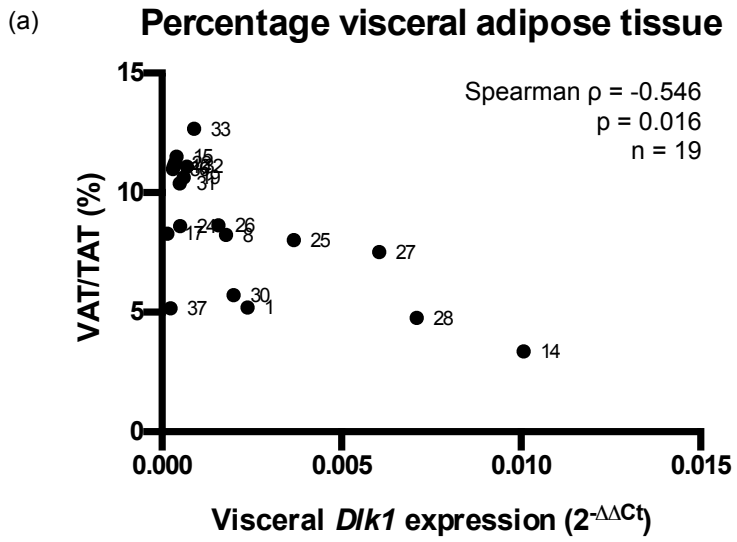

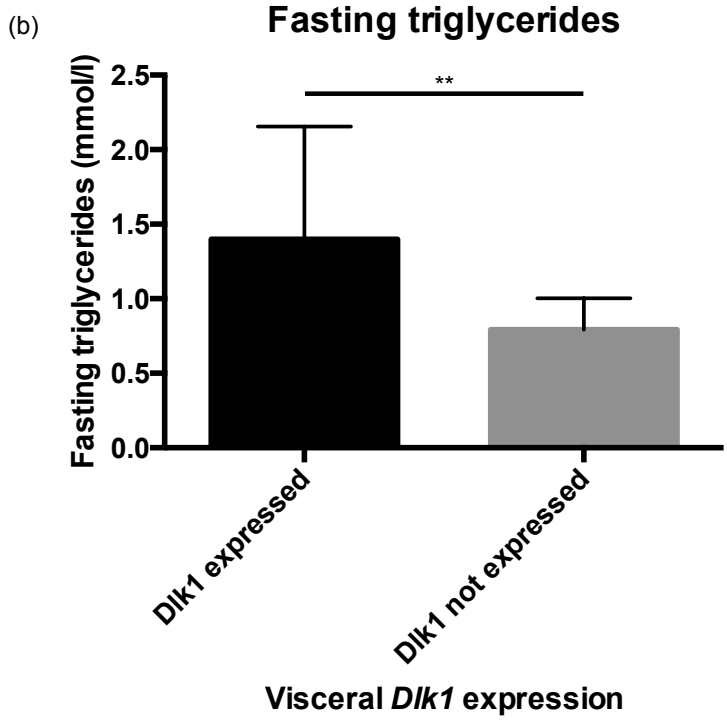

Figure 4.6: Visceral *Dlk1* expression varies with adipose distribution and metabolic parameters. RNA extracted from whole visceral adipose tissue samples was reverse transcribed and used for qRT-PCR analysis of Dlk1 expression. Results were normalized to expression of Rplp0, via the $2^{-\Delta\Delta Ct}$ method. *Dlk1* cycling threshold (Ct) values of ≥40 were interpreted as indicating an absence of Dlk1 expression. (a) In subjects where Dlk1 mRNA is expressed in visceral adipose, this correlates negatively with percentage visceral adipose tissue. (b) Overweight and obese subjects wherein visceral Dlk1 expression is detected (n = 16) have higher fasting triglycerides than those in whom visceral Dlk1 expression is not detected (n = 9) (VAT: visceral adipose tissue volume; TAT: total adipose tissue volume). (Data is mean + SD; *: $p < 0.05$ by Student's t test)

4.3.3 Mmp14 and *Mmp2*

MMP-14 activity has been implicated in collagen I remodelling by murine preadipocytes (see Chapter 1), and it is highly expressed by human primary *in vitro*-differentiated adipocytes (see Chapter 3). MMP-14 is also required for MMP-2 activation, in conjunction with TIMP-2 (see Chapter 1), and MMP-14 and MMP-2 expression were highly correlated in both subcutaneous and visceral adipose tissue depots in this study (Figure 4.7).

A role for MMP-14 in human adipose tissue remodelling is suggested by the findings that abdominal subcutaneous adipose tissue volume is positively correlated with visceral *Mmp14* expression (Figure 4.8a). Although no relationship between visceral adipose tissue volume and subcutaneous *Mmp14* expression was identified when the whole cohort was analysed, in the case of postmenopausal subjects these two parameters are negatively correlated (Figure 4.8b and c). This was an unexpected finding. The only previous description of a relationship between metalloproteinase levels and menopausal status comes from a 2012 study by Miksztowicz *et al*, wherein 39 female subjects (13 lean and 26 overweight/obese) had plasma MMP-2 levels, adiponectin, HOMA-IR, CRP and lipoprotein profile measured. Overweight/obese women had higher circulating MMP-2 levels than lean controls, but this difference was lost in postmenopausal women. On the other hand, MMP-2 levels were positively correlated with HOMA-IR in both pre- and post-menopausal women [219].

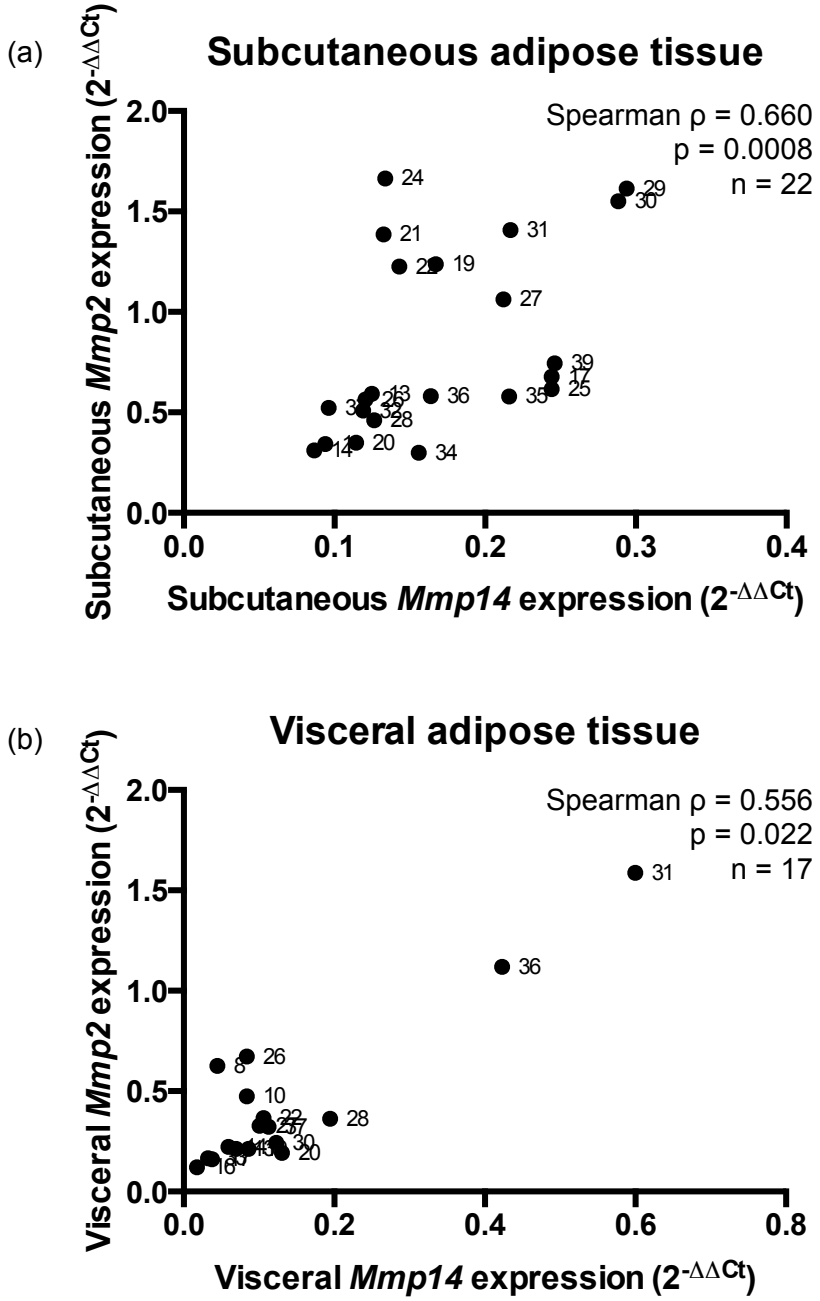

Figure 4.7: *Mmp2* and *Mmp14* expression are positively correlated in both subcutaneous and visceral adipose depots. RNA extracted from whole adipose tissue samples was reverse transcribed and used for qRT-PCR analysis of *Mmp2* and *Mmp14* mRNA expression. Results were normalized to expression of Rplp0, via the $2^{-\Delta\Delta Ct}$ method.

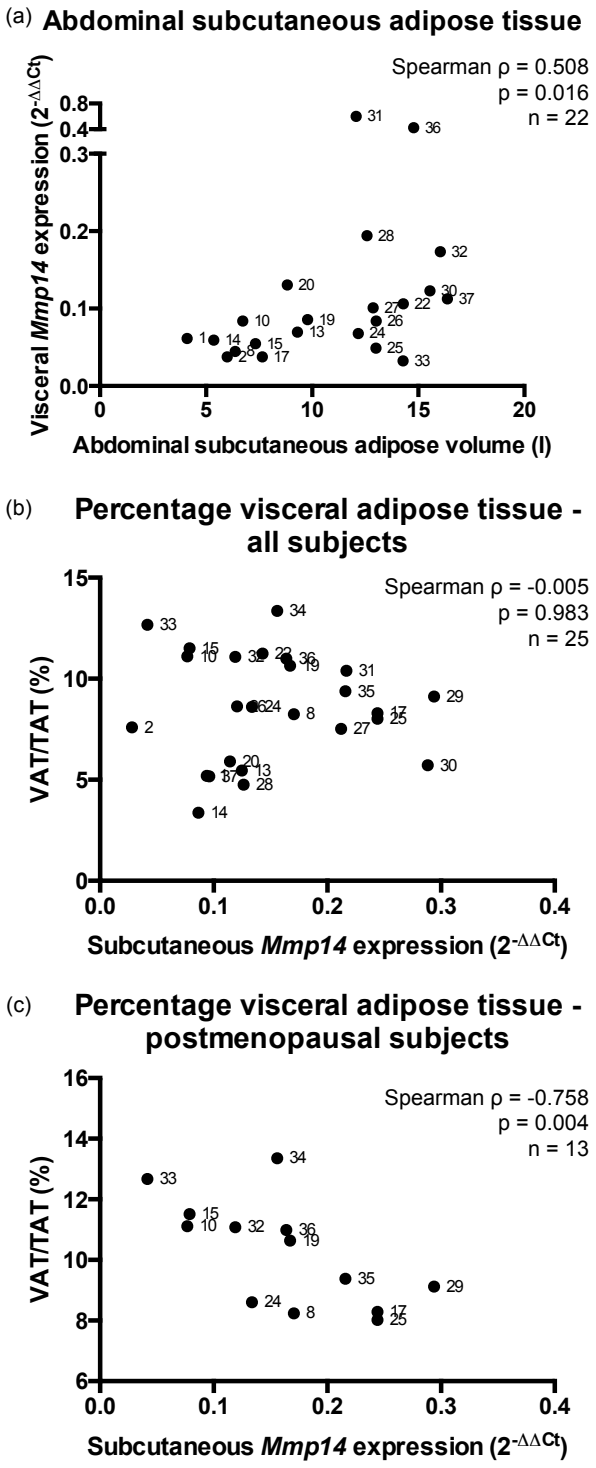

Figure 4.8: *Mmp14* expression varies with whole body adipose distribution parameters. *Mmp14* mRNA expression was assayed by qRT-PCR of cDNA samples reverse transcribed from RNA isolated from subcutaneous and visceral adipose tissue samples donated by study subjects. (a) In visceral samples, *Mmp14* mRNA expression correlated positively with abdominal subcutaneous adipose tissue volume, measured using magnetic resonance imaging. b) There is no correlation between subcutaneous *Mmp14* expression and visceral adipose tissue volume when all subjects are considered, but in postmenopausal subjects, subcutaneous *Mmp14* expression strongly correlates negatively with percentage visceral adipose tissue. (ASAT: abdominal subcutaneous adipose tissue volume; VAT: visceral adipose tissue volume; TAT: total adipose tissue volume)

4.3.4 Mmp1

MMP-1 steady state mRNA levels and protein levels are highly upregulated by inflammatory stimuli in human primary *in vitro*-differentiated adipocytes (see Chapter 3). In spite of this *in vitro* finding, there was no association between *Mmp1* mRNA expression in either adipose depot and circulating C-reactive protein level (Figure 4.9a). In subjects in whom *Mmp1* expression was detected in the subcutaneous compartment, mean fasting glucose was higher than in those in whom there was no detectable subcutaneous *Mmp1*. There was no similar relationship between *Mmp1* presence and fasting insulin or fasting triglyceride levels (Figure 4.9).

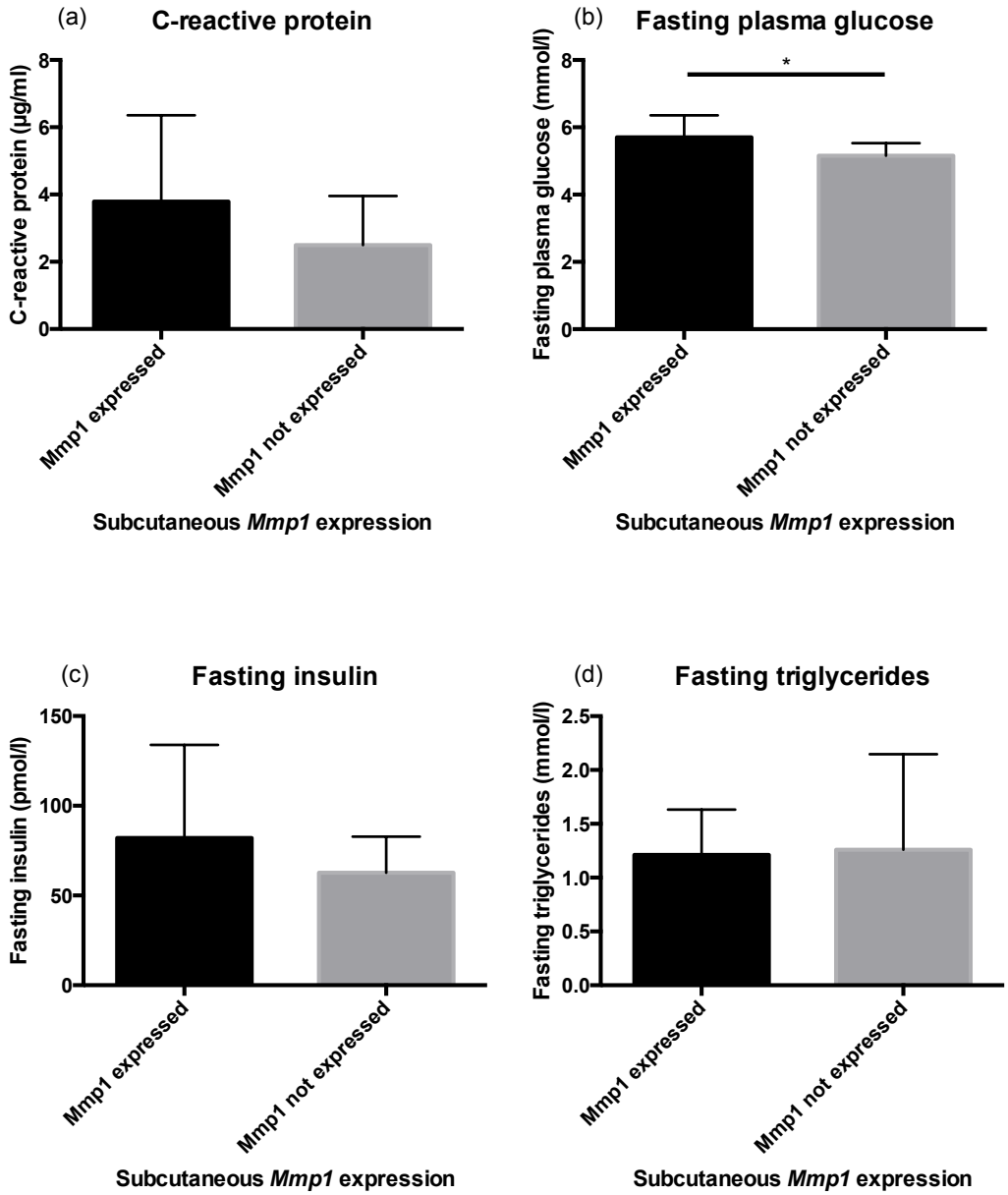

Figure 4.9: Subcutaneous *Mmp1* expression varies with fasting plasma glucose, but not with C-reactive protein, fasting insulin or fasting triglycerides. RNA extracted from whole subcutaneous adipose tissue samples was reverse transcribed and used for qRT-PCR analysis of *Mmp1* expression. Results were normalized to expression of *Rplp0*, via the $2^{-\Delta\Delta Ct}$ method. *Mmp1* cycling threshold (Ct) values of ≥40 were interpreted as indicating an absence of expression. (b) Mean fasting plasma glucose was higher in those donors in whom *Mmp1* mRNA expression was detected in subcutaneous adipose tissue (n = 18), as compared to those in whom *Mmp1* expression was undetectable (n = 12). (Data is mean + SD, *: $p < 0.05$ by Student's *t* test).

4.4 Discussion

This study is, to my knowledge, the first of its kind in attempting to study the relationship between MP and TIMP expression and whole-body lipid distribution. The use of female subjects only is justified by the use of adipose tissue from female donors to establish primary human cultures in the initial phases of this research (see Chapters 2 and 3). Future work will focus on using tissue from male subjects, and thus performing comparisons between males and females to see if relationships identified in female adipose tissue can be generalized to males. Furthermore, the term 'expression' in this study was taken to mean messenger RNA expression as detected by qRT-PCR. Given the complex post-transcriptional and post-translational regulation of MPs and TIMPs, this increased mRNA expression does not necessarily translate into increased MP/TIMP protein levels and indeed activity. Future studies will need to determine MP and TIMP protein levels in donated tissue biopsies, for example by immunohistochemistry for proteins of interest. Moreover, the use of only two non-consecutive slides for each depot is a limitation of the analyses of adipocyte cross-sectional area in relation to MP/TIMP expression and other metabolic markers, and of the generalisability of conclusions drawn from these analyses. A further section of each adipose sample has already been prepared and stained, and the fixed/embedded samples are stored in the Norfolk and Norwich University Hospital Tissue Bank, meaning that further sections can be cut, mounted and stained. Thus, future work will involve obtaining more photomicrographs of these samples, and quantifying mean adipocyte cross-sectional area for these additional samples, to increase the number of unique slides tested per donor.

The relationships identified between genes of interest and (i) parameters of adipose tissue remodelling/distribution and (ii) metabolic parameters will need to be revisited in larger studies to see if these findings can be replicated. Nevertheless, this study offers interesting insights into the potential roles of adipose-expressed MPs and TIMPs in regulating whole-body metabolic status. It is reassuring to observe that *Mmp14* and *Mmp2* expression are closely related in both subcutaneous and visceral compartments, for example, given their well-documented interaction in the activation of MMP-2. This gelatinase has been studied extensively in relation to human metabolic outcomes (as outlined in Chapter 1), but in this study, was not associated in a statistically significant manner with another of the metabolic or adipose distribution outcomes chosen. The associations between *Mmp14* expression and ASAT and VAT volumes may indicate an 'overspill' effect. As ASAT volume

increases, more lipid 'overspills' into the visceral adipose depot, leading to increased visceral adipogenesis and hence increased visceral *Mmp14* expression (Figure 4.13a). In those post-menopausal subjects where there is less subcutaneous *Mmp14* expression, there is reduced adipogenic capacity in this depot and thus more overspill into the visceral compartment, leading to an increased VAT% on MRI (4.13c). The directionality being suggested is of course speculative, and a longitudinal study or an interventional weight gain study will be required to clarify cause and effect in these cases.

Subcutaneous *Dlk1* expression is associated with less VAT% in participants in this study, and in those where it is expressed, smaller subcutaneous adipocytes (Figure 4.10). Although shed Dlk-1 is thought to be an inhibitor of adipogenesis, membrane-bound Dlk-1 may be a promoter of preadipocyte proliferation and survival [121]. Thus, with increased subcutaneous Dlk-1 expression, there may be a larger subcutaneous preadipocyte pool, allowing for increased subcutaneous expansion by hyperplasia (explaining the small mean adipocyte cross-sectional area) and reduced overspill into the visceral depot. The complex regulation of Dlk-1 activation by MPs and TIMPs, presumed to be predominantly by ADAM-17 and TIMP-3 in humans, may explain why visceral *Dlk1* expression is also associated with less VAT%.

The associations and partial correlations between *Timp3* expression and adipocyte size, VAT volume and HOMA-IR are interesting. The observed associations between *Timp3* and adipocyte size (positive correlation) and between *Timp3* and VAT volume & HOMA-IR (negative partial correlations) appear to be conflicting – hypertrophied subcutaneous adipocytes are usually associated with increased VAT volumes and insulin resistance. Indeed, once subcutaneous *Timp3* expression is used a control variable, a positive correlation emerges between mean subcutaneous adipocyte area and HOMA-IR. This is suggestive of a role for TIMP-3 in the regulation of adipocyte size. TIMP-3 is indeed a broad-spectrum inhibitor of MP activity, and is therefore expected to inhibit extracellular matrix turnover. Increased TIMP-3 expression may therefore result in reduced collagenolysis required for adipogenesis, leading to reduced preadipocyte differentiation and adipocyte hypertrophy. On the other hand, TIMP-3 is the primary inhibitor for ADAM-17, which is thought to be the primary sheddase responsible for shedding and activation of Dlk-1. Increased TIMP-3 expression may therefore be expected to reduce Dlk-1 activation, and allow increased preadipocyte differentiation. These apparently divergent roles for TIMP-3 in adipogenesis may explain the opposing set of results summarized above. In view

of these interesting results, the roles of TIMP-3 in preadipocyte differentiation and adipose tissue remodelling were investigated further in our primary human cell culture model.

Chapter 5:

Tissue inhibitor of metalloproteinases-3 in human adipose tissue remodelling

5.1: Introduction

Tissue inhibitor of metalloproteinases (TIMP)-3 is an important regulator of metalloproteinase function, with ubiquitous expression and a broad spectrum of activity [177]. It has been implicated in the remodelling events that occur in the vascular wall and myocardium in hypertension and heart failure [220-222], and in the ovary during the menstrual cycle [223-226], as well as in the growth of various cancers [227-229]. As outlined in Chapter 1, previous investigations of TIMP-3 expression in adipocyte-like cell lines, murine adipose tissue and human subjects with type 2 diabetes (T2DM) have shown that TIMP-3 is expressed by adipose tissue, where it is downregulated in rodent genetic and nutritional models of obesity (see Chapter 1 for references). There is reduced skeletal muscle TIMP-3 expression in diabetic *Insr+/-* mice and in human T2DM subjects, and *Timp3*-null mice become insulin resistant when fed a high-fat diet.

My investigations have shown that there are high steady-state *Timp3* mRNA levels in human primary *in vitro*-differentiated adipocytes, and that these levels are decreased by an inflammatory stimulus or during differentiation (Chapter 3, Figures 3.7 and 3.9). Furthermore, in human whole adipose tissue, *Timp3* mRNA levels in subcutaneous adipose tissue are positively correlated with subcutaneous mean cross-sectional adipocyte area (Spearman $\rho = 0.429$, $p = 0.041$), a correlation that becomes stronger and more statistically significant when the data are controlled for total adipose tissue volume (Spearman $\rho = 0.700$, $p < 0.0001$). When the data are controlled for subcutaneous adipocyte area, *Timp3* expression is negatively correlated with HOMA-IR (Spearman $\rho = -0.505$, $p = 0.017$) and with visceral adipose tissue volume (Spearman $\rho = -0.445$, $p = 0.038$). Moreover, controlling the data for *Timp3* expression results in the expected correlation between subcutaneous adipocyte area and HOMA-IR being identified (Spearman $\rho = 0.502$, $p = 0.017$) – this correlation is not apparent in the uncontrolled data (see Chapter 4, Table 4.5)

The data summarized above therefore suggest roles for TIMP-3 in adipose tissue growth in obesity. These roles may be subdivided into two major areas – inflammation and adipogenesis. TNF-α mediated adipose tissue inflammation is a well-documented feature of obesity (see Chapter 1, section 1.1.2). TIMP-3 is the main inhibitor for ADAM-17/TNF-α converting enzyme (TACE), which activates TNF-α by cleaving the soluble active form from the membrane-bound form, suggesting a potential link between TIMP-3 activity and adipose tissue inflammation in obesity

(see Chapter 1). Furthermore, ADAM-17/TACE is thought to be the sheddase responsible for cleaving murine Pref-1 (see Chapter 1, section 1.3.3.3), allowing it to exert its anti-adipogenic activity. By virtue of its ability to inhibit (i) ADAM-17 and (ii) various metalloproteinases implicated in the extracellular matrix turnover that occurs in preadipocyte differentiation, I hypothesized that TIMP-3 may play a role in adipogenic differentiation of preadipocytes.

My investigations of TIMP-3 function in human adipose tissue remodelling therefore focused on its roles in adipose tissue inflammation and in preadipocyte differentiation.

5.2: Roles of TIMP-3 in adipose tissue inflammation

In order to investigate the role of TIMP-3 in human adipose tissue inflammation, an adenoviral vector was used to overexpress human TIMP-3 in cultured primary human adipose-derived mesenchymal stromal cells (hereafter referred to as preadipocytes) (see Chapter 2 for description of viral transduction protocol), which were subsequently stimulated with TNF-α. Briefly, cells from three independent donors were incubated in serum-free media containing no adenovirus, control adenovirus (LacZ-expressing RAd35, designated Ad0 hereafter) or TIMP-3 overexpressing adenovirus (RAdTIMP3, designated AdT3 hereafter) at a multiplicity of infection (MOI) of 500 for 48 hours. Media were then removed and cells were incubated in control, serum-free medium containing 100μg/ml heparin, serum-free medium containing 50ng/ml TNF-α, or serum-free medium containing both heparin and TNF-α, for a further 48 hours. Media were then collected and an ELISA was performed for IL-8. This readout was chosen as it has been previously shown that human preadipocytes and *in vitro*-differentiated adipocytes express interleukin (IL)-8 in response to TNF-α ([162], see Chapter 3, Figure 3.1). Heparin was included in the experimental condition as it has been shown to block re-uptake of TIMP-3 by cells, increasing pericellular levels (see Chapter 2, section 2.6.1).

As can be seen in Figure 5.1, the use of a control virus does not significantly change IL-8 concentration in conditioned media from human preadipocytes following TNF-α stimulation (mean ± SD, no virus vs. Ad0: 11685.4 pg/ml ± 9371.4 vs. 9340.3 pg/ml ± 3354.1, $p > 0.05$). However, following treatment with TNF-α, cells transduced with AdT3 express more IL-8 as compared to cells transduced with control Ad0 (mean ±

SD, Ad0 vs. AdT3: 9340.3 pg/ml ± 3354.1 vs. 30945.5 pg/ml ± 3536.1, p < 0.0001). Furthermore, inhibition of TIMP-3 reuptake by heparin appears to further increase IL-8 expression by human preadipocytes overexpressing TIMP-3 (mean ± SD, AdT3-TNF-α vs. AdT3-TNF-α+heparin: 30945.5 pg/ml ± 3536.1 vs 43879.8 pg/ml ± 8508.9). In fact, both the use of virus to overexpress TIMP-3 and the presence or absence of TNF-α and heparin significantly regulate the secretion of IL-8 by primary human cultured preadipocytes (Two-way ANOVA, virus: p < 0.0001; TNF-α/heparin p < 0.0001; Figure 5.1).

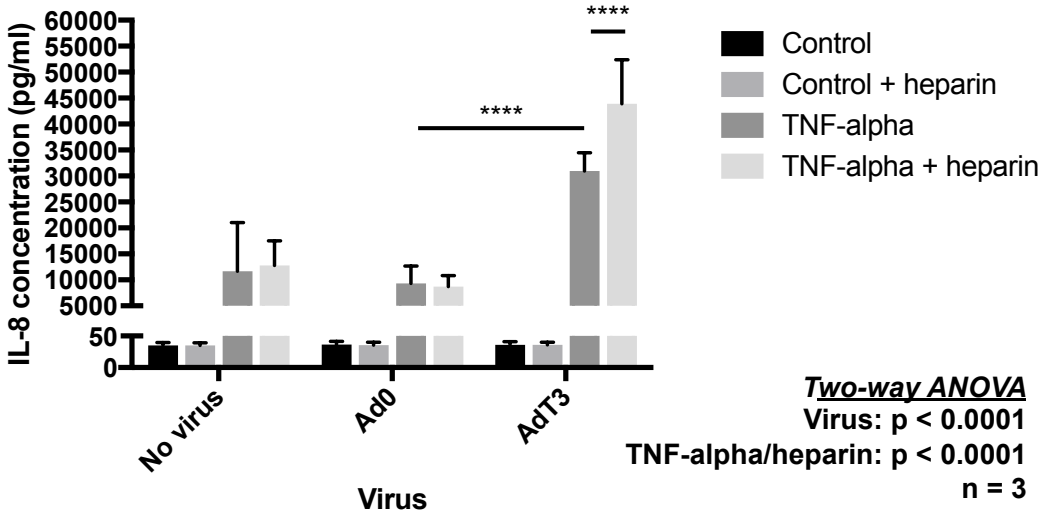

Figure 5.1: Overexpression of TIMP-3 using a viral transduction system increases IL-8 secretion by primary cultured human preadipocytes. Cells were transduced with control virus (Ad0) or human TIMP-3-overexpressing adenovirus (AdT3). IL-8 concentration in cell culture supernatants following 48 hours of treatment in serum free media ± TNF-alpha ± heparin was quantified using ELISA. Data is from 3 biological replicates from each of 3 different donors (each bar represents the mean + SD for these 9 samples). For all viral conditions, IL-8 secretion was significantly increased by TNF-alpha ± heparin as compared to untreated control using an unpaired Student's *t* test (p < 0.0001).

Given that TIMP-3 plays a role in the regulation of TNF receptor-I shedding from cell membranes and hence, activity [230], I proceeded to investigate the effect of TIMP-3 overexpression on soluble TNFR levels in cell culture media. Primary human preadipocyte cultures established from four independent donors were transduced with control (Ad0) adenovirus and TIMP-3 overexpressing (AdT3) adenovirus, and subsequently stimulated with TNF-α for 48 hours as described earlier. Cell culture media were collected and soluble TNF receptor-I (sTNFR-I) concentrations were assayed using ELISA (see Chapter 2) (Figure 5.2).

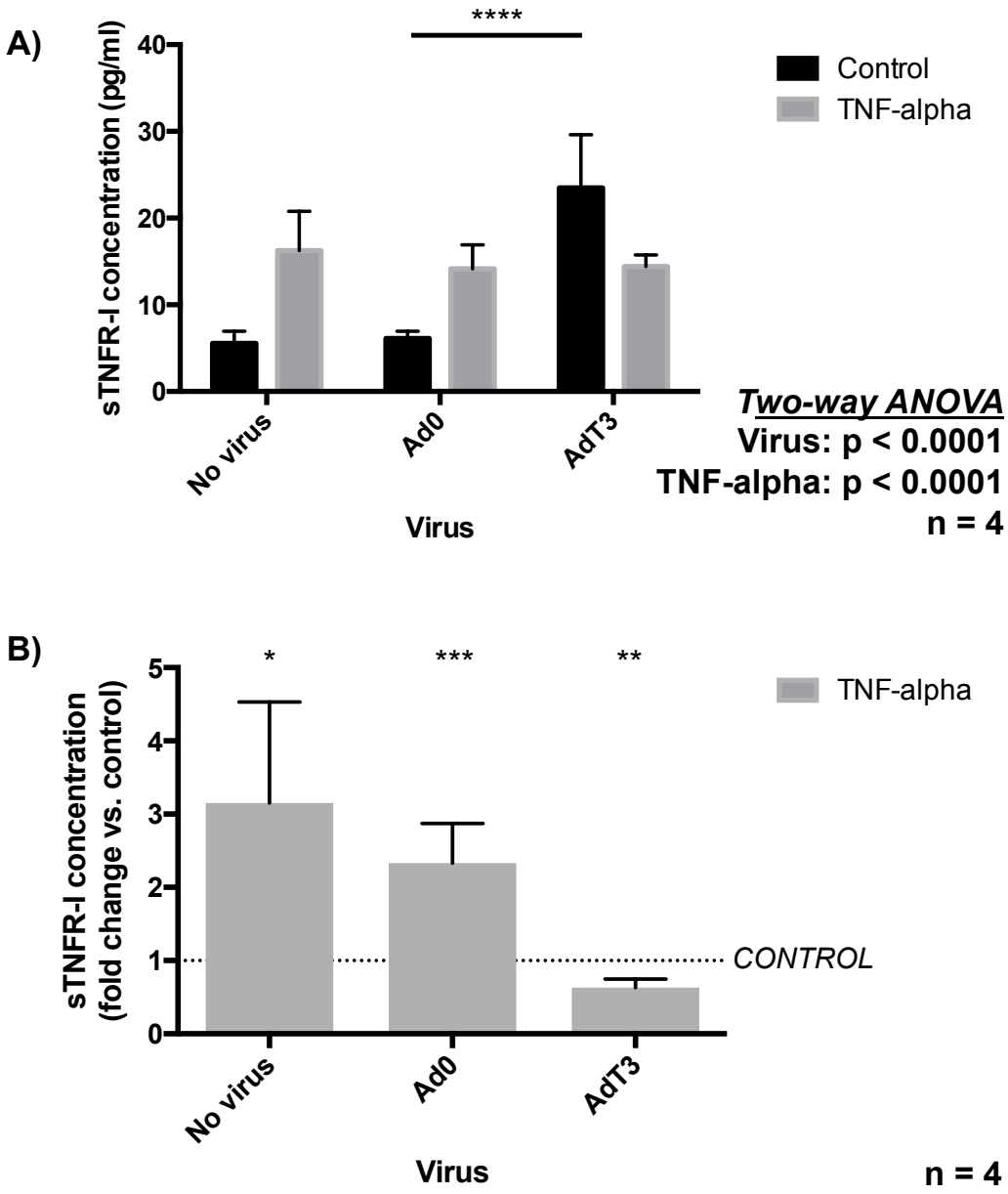

Figure 5.2: A) Basal shedding of soluble TNF receptor (sTNFR)-I is increased by TIMP-3 overexpression. Cells were transduced with control virus (Ad0) or human TIMP-3-overexpressing adenovirus (AdT3). Soluble TNFR-I concentration in cell culture supernatants following 48 hours of treatment in serum free media ± TNF-alpha was quantified using ELISA. B) Induced shedding of sTNFR-I is inhibited by TIMP-3 overexpression. Bars show mean fold change + SD in sTNFR-I concentration for TNF-alpha condition vs. control (cells not exposed to TNF-alpha; set at 1), for each viral condition. Data are from 3 biological replicates from each of 4 different donors (each bar represents the mean + SD for these 12 samples). (*, $p < 0.05$; **, $p < 0.01$; ***, $p < 0.001$; ****, $p < 0.0001$).

As shown in Figure 5.2A, there was no statistically significant difference between basal sTNFR-I shedding in cells not transduced with virus and those transduced with Ad0 control virus (sTNFR-I concentration, mean ± SD: 5.54 pg/ml ± 1.41 vs. 6.12 pg/ml ± 0.81). Basal sTNFR-I shedding was increased almost fourfold, however, by TIMP-3 overexpression (mean ± SD, Ad0 vs. AdT3: 6.12 pg/ml ± 0.81 vs. 23.5 pg/ml ± 6.13, $p < 0.0001$). Exposure to TNF-α induces shedding of TNFR-I by control cultured primary human preadipocytes (mean fold change ± SD: 3.23 ± 1.45, $p < 0.05$) or those transduced with control adenovirus (2.35 ± 0.58, $p < 0.001$). An increase in shedding of cell-surface receptors, cell adhesion proteins and other membrane proteins is a well-recognised feature of inflammation [231, 232] so human preadipocytes are behaving like many other cells of mesenchymal lineage in this regard. TIMP-3 overexpression, on the other hand, inhibits TNF-α-induced shedding of sTNFR-1 (mean fold change ± SD, no TNF-α control vs. TNF-α in AdT3 condition: 0.67 ± 0.14, $p < 0.01$) (Figure 5.2B).

As the level of shed, soluble TNFR-I in conditioned culture medium was increased when cells were transduced with AdT3, I sought to investigate the effect of TIMP-3 overexpression on total TNFR-I protein expression. Western blotting of cell lysates prepared from cells from two independent donors treated as described earlier revealed an increased expression of total TNFR-I by cells overexpressing TIMP-3 as compared to preadipocytes exposed to control Ad0 virus (Figure 5.3). This is in keeping with findings in human DLD colon carcinoma cells, in which constitutive expression of human TIMP-3 leads to increased surface expression of TNF-alpha receptor [230].

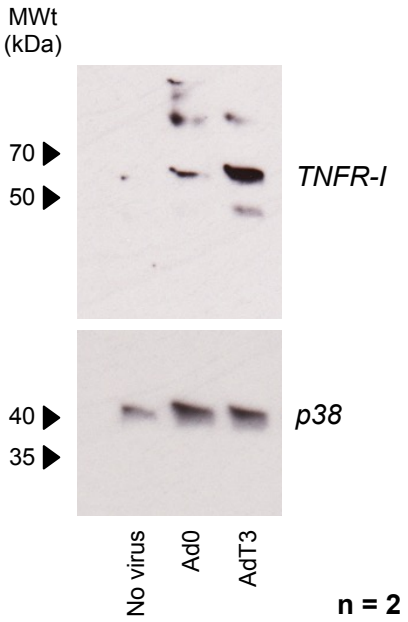

Figure 5.3: TIMP-3 overexpression increases total TNFR-I expression by human preadipocytes. Cells were transduced with control virus (Ad0) or human TIMP-3-overexpressing adenovirus (AdT3); a 'no virus' control was also used. Cell lysates were collected after 48 hours of transduction and subjected to immunoblotting. Following probing for TNFR-I, membranes were stripped and reprobed for p38 as a loading control. Lysates from two independent donors were analysed; representative blot shown.

5.3: Roles of TIMP-3 in adipogenic differentiation

As shown in Chapter 4, human subcutaneous adipose *Timp3* expression is positively correlated with adipocyte size, and negatively partially correlated with visceral adipose tissue (VAT) volume & HOMA-IR when controlling by mean subcutaneous adipocyte area. These data are suggestive of a role for TIMP-3 in the regulation of adipogenesis.

I focused on two pathways by which TIMP-3 may play a role in the regulation of adipogenic differentiation. TIMP-3 is the primary inhibitor for ADAM-17, which is thought to be the primary sheddase responsible for shedding and activation of Dlk-1, the negative regulator of adipogenesis. Increased TIMP-3 expression may therefore be expected to inhibit ADAM-17 activity, reduce Dlk-1 activation, and allow increased preadipocyte differentiation. However, as outlined above in the case of TNFR-I, TIMP-3 overexpression increased basal sTNFR-I shedding (Figure 5.2A) and total

TNFR-I expression (Figure 5.3), suggesting a potentially complex role for TIMP-3 in the regulation of Dlk-1 activity.

Moreover, TIMP-3 also inhibits MMPs, and is therefore expected to inhibit extracellular matrix turnover via its inhibition of collagenases such as MMP-14 [177]. Increased TIMP-3 expression may therefore result in reduced collagenolysis required for adipogenesis, leading to reduced preadipocyte differentiation and adipocyte hypertrophy.

Given these potentially conflicting roles for TIMP-3 in the regulation of adipogenesis, I investigated (1) the effect of variable TIMP-3 expression on regulation of Dlk-1, and (2) the effect of TIMP-3 overexpression on collagenolysis by differentiating preadipocytes.

5.3.1 Dlk-1 expression and shedding

The expression, at mRNA level, of Dlk-1 in whole-tissue samples of subcutaneous adipose tissue (SAT) and VAT was shown in Chapter 4, where Dlk-1 expression was shown to vary with metabolic, histological and anthropometric parameters. Given that Dlk-1 regulation is thought to have similarities to TNFR-I in terms of shedding from the cell membrane, I adopted the same approach to investigation of the roles of inflammation and TIMP-3 overexpression in Dlk-1 metabolism. Primary preadipocyte cultures from two independent donors were stimulated with TNF-α at a concentration of 50 ng/ml for 48 hours. Media were collected, TCA precipitated as described in the Chapter 2, and subjected to immunoblot using a primary antibody targeted against an epitope found in the extracellular region of Dlk-1, N-terminal to its cleavage site. Similarly, cell lysates were recovered and used to assess the expression of full-length Dlk-1 by immunoblot using a primary antibody targeted against an intracellular epitope found C-terminal to the cleavage site. As shown in Figure 3.4A, inflammatory stimulation with TNF-α increases soluble (s)Dlk-1 shedding into culture medium, without regulating total Dlk-1 expression. This is in keeping with the effect of TNF stimulation on TNFR-I shedding (Figure 5.2).

I then proceeded to treat preadipocytes from three independent donors with control and TIMP-3-overexpressing adenovirus as described in section 5.2 and in the Chapter 2. Media and lysates were collected after 48 hours and immunoblotting was performed using the anti-Dlk-1 primary antibodies outlined above. As with TNFR-I, basal shedding of sDlk-1 is increased in cells overexpressing TIMP-3, but in contrast

to the situation with TNFR-I, total Dlk-1 appears unaffected by TIMP-3 overexpression (Figure 5.4B).

To investigate the effect of *Timp3* gene silencing on Dlk-1 shedding, cells were transfected with *Timp3*-targeting small interfering (si)RNA, as described in Chapter 2. Briefly, preadipocytes isolated from a unique donor were cultured to ~50% confluence, and transfected with with targeting siRNA using the siIMPORTER™ siRNA transfection reagent. Following 24 hours of exposure to targeting siRNA, media were changed and cells were incubated in serum-free medium for 48 hours. Media were then collected, TCA precipitated, and immunoblotting was performed, probing for sDlk-1. As shown in Figure 5.4C, *Timp3* knockdown results in reduced sDlk-1 shedding into the medium by preadipocytes. These results therefore suggest that TIMP-3 overexpression results in increased sDlk-1 shedding, and reduced expression of TIMP-3 protein leads to reduced sDlk-1 shedding.

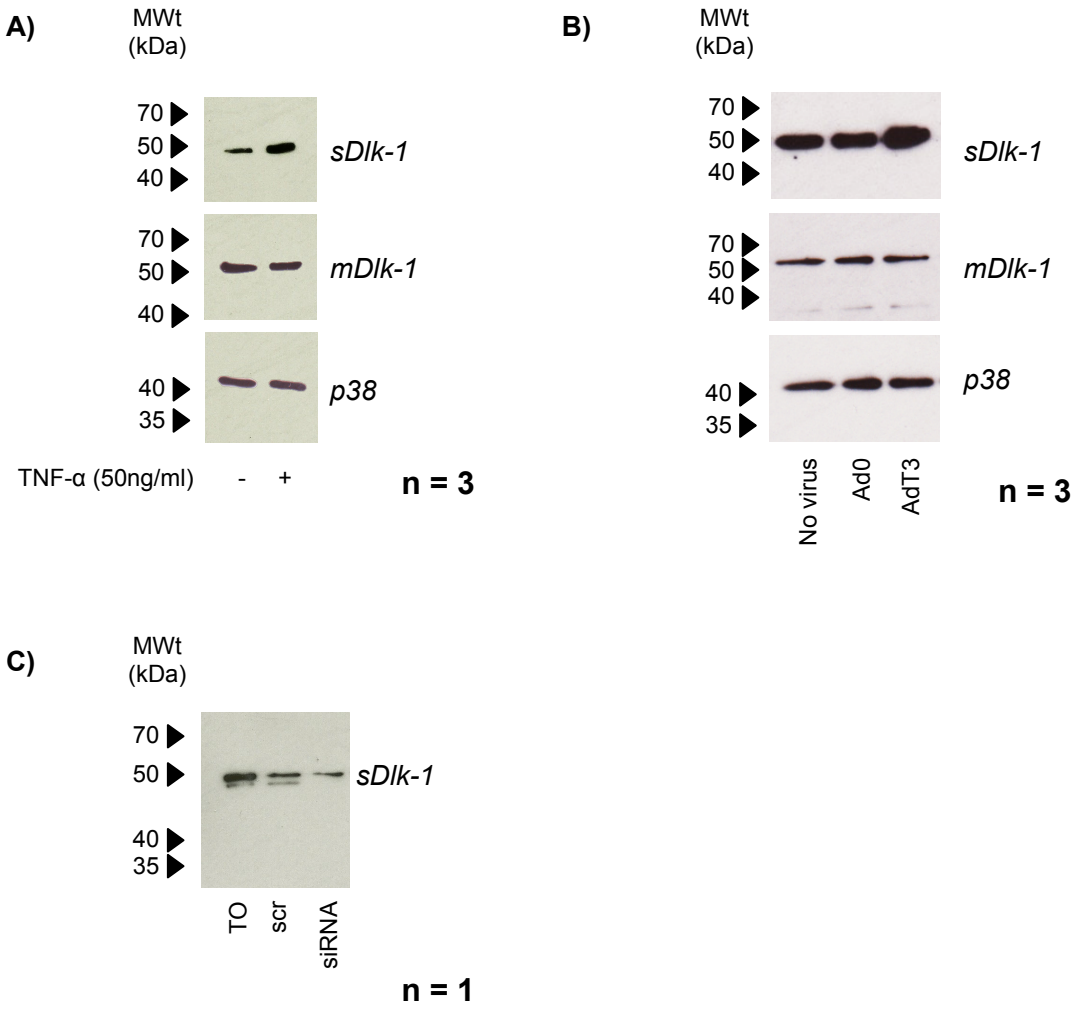

Figure 5.4: Soluble (s)Dlk-1 shedding is regulated by inflammatory stimuli and TIMP-3 expression. A) Stimulation of cultured primary preadipocytes with TNF-alpha increases sDlk-1 shedding, but total Dlk-1 protein expression is unaffected. B) TIMP-3 overexpression following transduction with AdT3 adenovirus increases sDlk-1 shedding, but does not regulate total Dlk-1 expression, in contrast to the effect on total TNFR-I. C) *Timp3* silencing using siRNA results in reduced sDlk-1 shedding. The number of cultures from independent donors used for each experiment is given (n); representative blots are shown. (TO: transfection agent only; scr: scrambled oligonucleotide [negative control]; siRNA: *Timp3*-targeting small inhibitory RNA; mDlk-1: total Dlk-1 protein).

5.3.2 Regulation of extracellular matrix turnover

In order to assess the effects of TIMP-3 overexpression on regulation of extracellular matrix turnover in adipogenic differentiation, I adapted an extracellular matrix model used for other mesenchymal cell types, namely plating preadipocytes on collagen I films. Collagen I was chosen as it is the main constituent of the extracellular matrix surrounding murine preadipocytes *in vivo* [41, 42, 53]. The protocol is described in detail in Chapter 2, but briefly, plates were coated with 100µg/cm^2 acid-extracted rat-tail collagen I (Corning, Wiesbaden, Germany). Preadipocytes were seeded at a

density of 20,000 cells/cm^2, and allowed to habituate on the collagen film (or no collagen control, designated 'plastic' hereafter) for 24 hours. As outlined in Chapter 3, human primary *in vitro*-differentiated adipocytes express MPs and TIMPs when grown in normal culture multi-well plates. To ensure that differentiating human preadipocytes express collagenases, gelatinases and TIMPs when cultured on collagen I films, I subjected cultures of primary preadipocytes from two independent donors to proadipogenic conditions over an eight-day period. Cultures were arrested at day 0 (set as 24 hours after seeding), days 1, 2, 4, 6 and 8. RNA was extracted from cell lysates and qRT-PCR was performed to determine expression of adiponectin (*Adipoq*, a marker of differentiation), *Mmp1, Mmp2, Mmp14, Timp1, Timp2, Timp3* and *Timp4*, with *Rplp0* used as the comparator gene. Collagen I films inhibit preadipocyte differentiation in culture, as assessed by *Adipoq* expression (Figure 5.5).

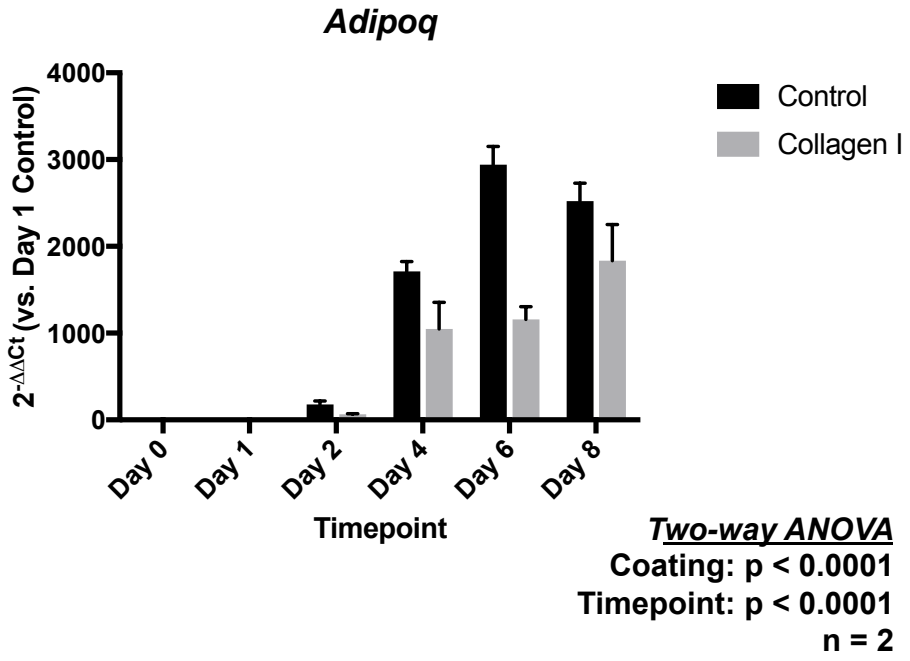

Figure 5.5: Adipogenic differentiation of human adipose-derived mesenchymal stem cells is reduced on collagen I coating, as assessed by adiponectin (*Adipoq*) expression. qRT-PCR analysis of RNA extracted from preadipocytes from two independent donors was performed over the course of the first eight days of differentiation, with day 0 being the day that cells were exposed to proadipogenic medium. Bars show mean $2^{-\Delta\Delta Ct}$ + SD of four replicates from each of two donors, with *Rplp0* expression and *Adipoq* expression on plastic control at day 1 being used as comparators. Day 0 plastic control could not be used as there is no detectable adiponectin expression prior to adipogenic stimulation. Data were analysed using a two-way ANOVA, with coating (that is – plastic control vs. collagen I) and timepoint entered as factors.

With respect to *Mmp1*, *Mmp2* and *Mmp14*, steady-state levels of mRNA are significantly higher for all three genes at all timepoints when cells are grown on collagen I as opposed to plastic control (one-way ANOVA for coating, $p < 0.01$ for *Mmp1*, $p < 0.0001$ for *Mmp2* and *Mmp14*), as has been demonstrated in various other mesenchymal cell types [233, 234]. The expression timecourse for *Mmp1* is characterised by sharp downregulation at the onset of differentiation, which is particularly profound when cells are seeded on plastic control –expression on day 8 is 0.8 ± 0.1% (mean±SD) that at day 0 (Figure 5.6). In the case of both *Mmp2* and *Mmp14*, expression is upregulated by differentiation, reaching a peak by day 2 to 4 (one-way ANOVA for timepoint, $p < 0.0001$ for *Mmp2* and *Mmp14*).

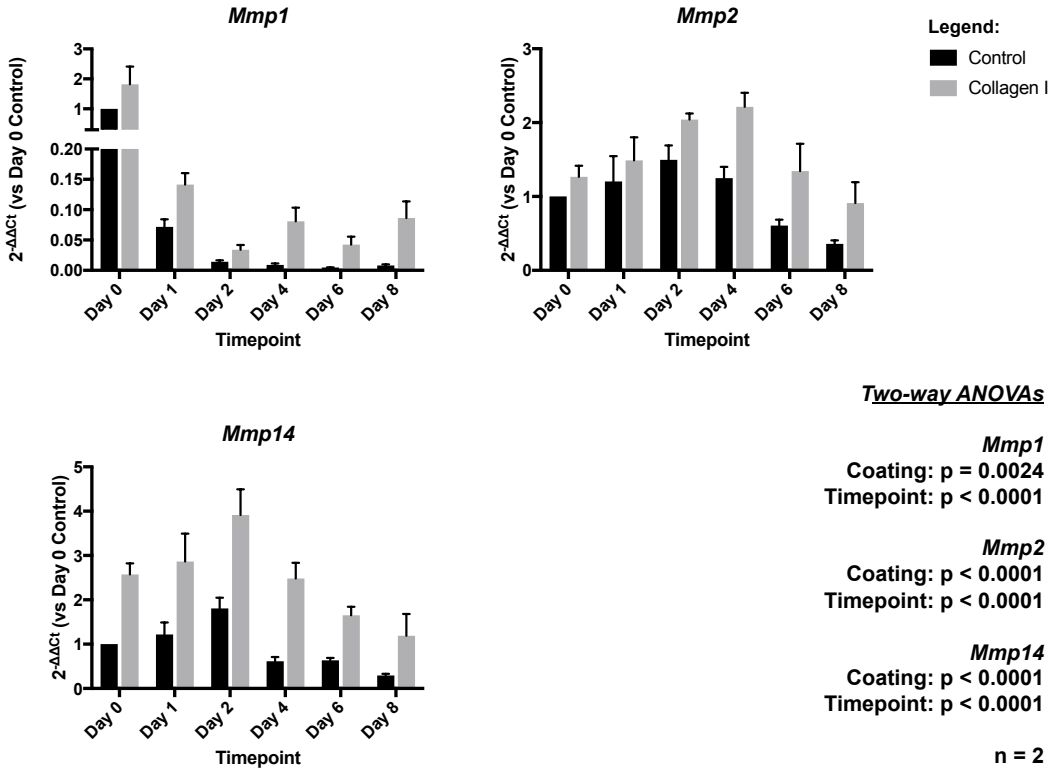

Figure 5.6: Expression of key matrix metalloproteinases in preadipocytes is regulated by matrix and adipogenesis. qRT-PCR analysis of RNA extracted from preadipocytes from two independent donors was performed over the course of the first eight days of differentiation, with day 0 being the day that cells were exposed to proadipogenic medium. Bars show mean $2^{-\Delta\Delta Ct}$ + SD of four replicates from each of two donors, with *Rplp0* expression and GOI expression on plastic control at day 0 being used as comparators. Data were analysed using a two-way ANOVA, with coating and timepoint entered as factors.

Timp1 to *Timp3* are all downregulated by proadipogenic medium. As discussed in Chapter 3 (Figure 3.9B), the decrease in mRNA steady-state level for *Timp3* is particularly profound. By day 8, there is a 97.6 ± 0.4% reduction in expression on plastic control and 97.2 ± 0.7% reduction on collagen I (mean±SD) as compared to day 0. This expression pattern has also been previously demonstrated in 3T3-L1 preadipocyte-like cells [96], and appears to be independent of coating. *Timp4*, on the other hand, appears upregulated during adipogenic differentiation, with a peak at day 4 for both plastic control (fold increase 8.0 ± 0.8 [mean±SD]) and collagen I (fold increase 9.7 ± 2.1) (Figure 5.7).

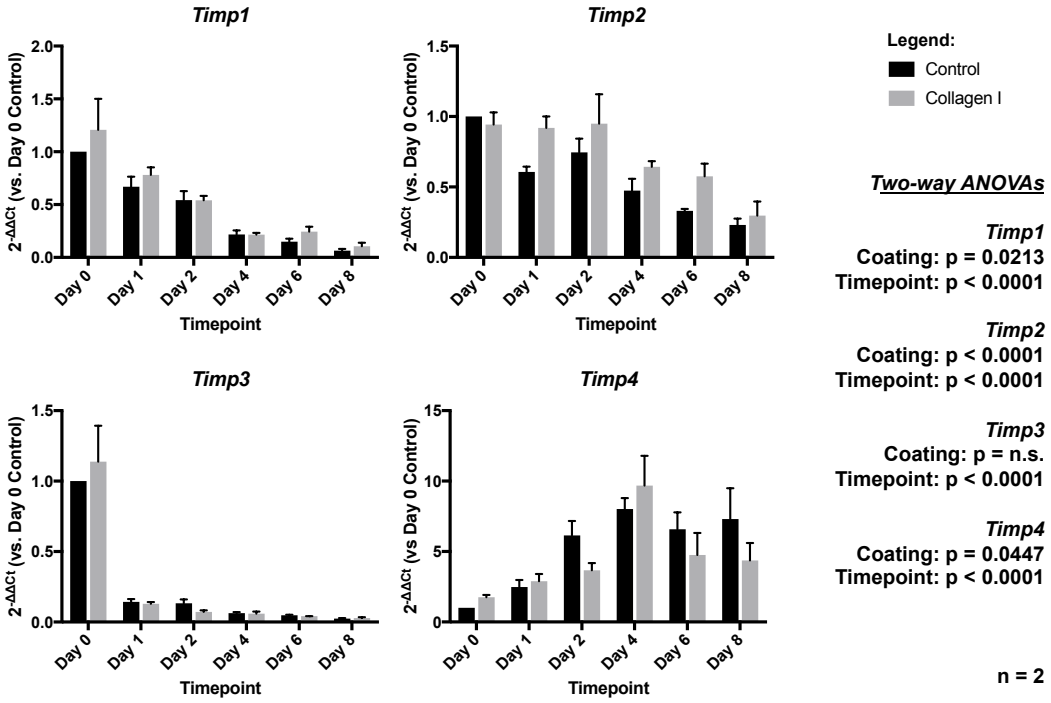

Figure 5.7: Expression of four TIMPs by preadipocytes is regulated by adipogenesis, and less statistically significantly by matrix. qRT-PCR analysis of RNA extracted from preadipocytes from two independent donors was performed over the course of the first eight days of differentiation, with day 0 being the day that cells were exposed to proadipogenic medium. Bars show mean $2^{-\Delta\Delta Ct}$ + SD of four replicates from each of two donors (8 samples in total), with *Rplp0* expression and GOI expression on plastic control at day 0 being used as comparators. Data were analysed using a two-way ANOVA, with coating and timepoint entered as factors.

I proceeded to assess the effect of adipogenic differentiation and inflammatory stimulation on collagen I turnover. Preadipocytes were seeded on collagen I films as described previously, and allowed to habituate for 24 hours. Cells were then stimulated with proadipogenic media, TNF-α at 50 ng/ml, or both for 48 hours. Media were collected, and a hydroxyproline assay (see Chapter 2) was performed to provide a quantitative assessment of the degree of collagen I turnover in the differing experimental conditions. To my knowledge, this is the first use of the hydroxyproline assay to assess matrix remodeling by human preadipocytes.

As seen in Figure 5.8, inflammatory stimulation increases hydroxyproline release into culture media by preadipocytes (control vs. TNF-α [mean±SD]: 2.82 μg/ml ± 1.40 vs. 5.30 μg/ml ± 1.27, $p = 0.0006$). Similarly, proadipogenic conditions lead to greater hydroxyproline release, (control vs. differentiation medium [mean±SD]: 2.82 μg/ml ± 1.40 vs. 5.31 μg/ml ± 1.86, $p = 0.0023$), suggesting increased collagen I turnover. Adding TNF-α to differentiation medium marginally reduces hydroxyproline release as opposed to the case with differentiation medium (differentiation medium vs. differentiation medium+TNF-α [mean±SD]: 5.31 μg/ml ± 1.86 vs. 4.30 μg/ml ± 1.12), but this difference is not statistically significant.

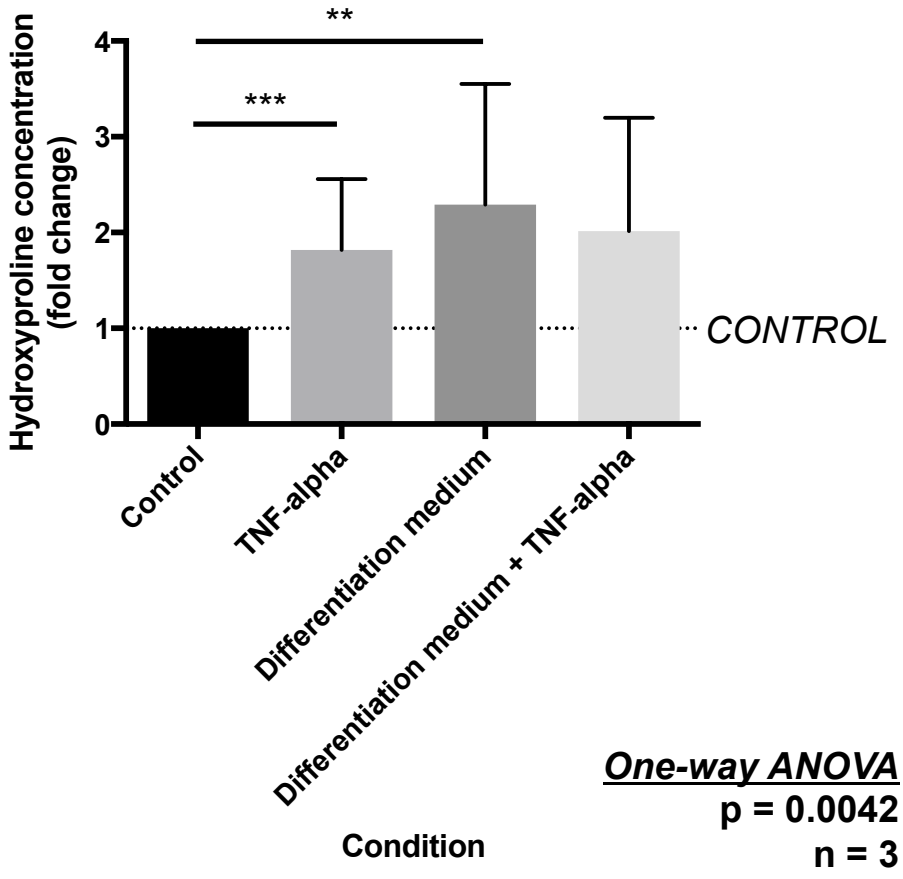

Figure 5.8: Inflammatory stimulation and proadipogenic conditions increase collagen I turnover. Hydroxyproline assay was performed to quantify hydroxyproline concentration (a measure of collagen breakdown) in media conditioned for 48 hours by preadipocytes stimulated with TNF-alpha, differentiation medium, or both. Data shown is mean fold change + SD as compared to control (set at 1) for 3 replicates from each of three independent donors. Statistical analysis was performed by one-way ANOVA with *post hoc* Dunnett's multiple comparisons test (**: $p < 0.01$; ***: $p < 0.001$).

For experiments assessing the effect of TIMP-3 overexpression on collagen turnover, preadipocytes were transduced with Ad0 or AdT3 adenovirus for 48 hours (or placed in serum-free medium without adenovirus) prior to seeding on collagen. Briefly, cells from four independent donors were exposed to control or TIMP-3-overexpressing adenovirus for 48 hours as described previously, trypsinised and seeded on collagen I films at a density of 2×10^4 cells/cm^2. Cells were then allowed to habituate on collagen I for 24 hours, before being subjected to proadipogenic conditions for 48 hours. Media were collected and hydroxyproline assay was performed to assess collagen I turnover.

As shown previously, differentiation medium significantly increases collagen I turnover as gauged by hydroxyproline release (Figure 5.9). There was no significant difference between hydroxyproline release by 'no virus' cells and those treated with Ad0 control adenovirus when these were stimulated with proadipogenic media (mean hydroxyproline concentration ± SD, no virus vs. Ad0 control in differentiation condition: 8.76 µg/ml ± 1.47 vs. 7.83 µg/ml ± 1.49). However, cells transduced with AdT3 adenovirus released approximately 40% less hydroxyproline in proadipogenic conditions when compared to cells transduced with control adenovirus, indicating that TIMP-3 overexpression reduces collagen I turnover (mean ± SD, Ad0 control vs. AdT3 in differentiation condition: 7.83 µg/ml ± 1.49 vs. 4.88 µg/ml ± 1.46) (Figure 5.9).

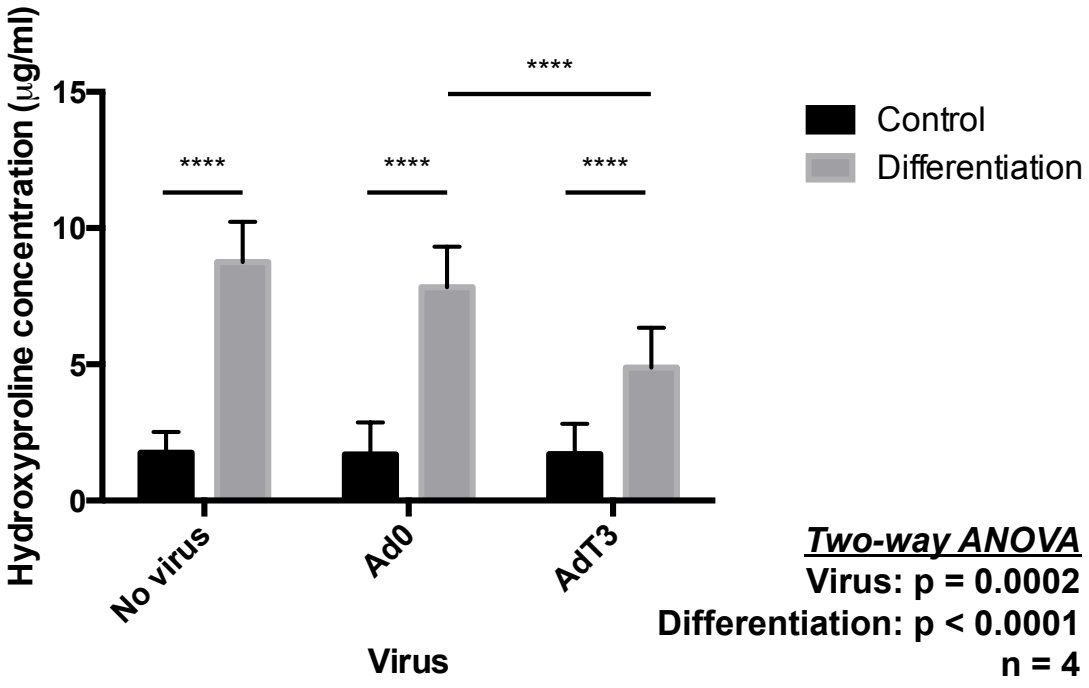

Figure 5.9: TIMP-3 overexpression reduces collagen I turnover by human preadipocytes. Hydroxyproline assay was performed to quantify hydroxyproline concentration (a measure of collagen breakdown) in media conditioned for 48 hours by preadipocytes stimulated with differentiation medium, following transduction with control adenovirus (Ad0) or TIMP-3-overexpressing adenovirus (AdT3). Data shown is mean + SD for 3 replicates from each of four independent donors. Statistical analysis was performed by two-way ANOVA with *post hoc* Dunnett's multiple comparisons test (****: $p < 0.0001$).

5.3.3 Functional effects of TIMP-3 overexpression and sDlk-1 treatment on differentiation

In order to assess the direct effect on TIMP-3 overexpression on adipogenic differentiation, human preadipocytes transduced with AdT3 adenovirus, control Ad0 adenovirus or not exposed to adenovirus were differentiated according to standard protocols, and differentiation efficiency was assessed using quantitative Oil Red O staining or fluorescent lipophilic dye uptake (see Chapter 2). These experiments did not yield conclusive results as prolonged differentiation courses led to suspected increased cell death in the TIMP-3-overexpressing cells. Promotion of apoptosis by TIMP-3 overexpression has been described previously [235-238]. The results obtained from these experiments, along with a discussion on potential further experiments, are found in Appendix B.

Similarly, differentiating preadipocytes were exposed to different concentrations of recombinant human soluble (rhs)Dlk-1 (R&D Systems, Abingdon, UK), in an attempt to investigate the effect of direct treatment of preadipocytes with Dlk-1. As outlined in Appendix B, results from these experiments were similarly inconclusive.

5.4: Discussion

Given the statistically significant correlations found between *Timp3* expression and various adipose measures of metabolically unhealthy obesity (MUO), I sought to investigate the role of TIMP-3 in human adipose inflammation and expansion. As a result of the experiments described in this Chapter, I have shown that TIMP-3 overexpression significantly increases the effect of TNF-α stimulation on IL-8 secretion by human preadipocytes. Furthermore, TIMP-3 overexpression increases TNFR-I expression by human preadipocytes, and increases the concentration of soluble TNFR-I shed into the culture medium. Conversely, TIMP-3 overexpression increases soluble Dlk-1 shedding into the culture medium without affecting membrane-bound Dlk-1 expression by preadipocytes. In parallel, *Timp3* gene silencing reduces sDlk-1 shedding. Another mechanism by which TIMP-3 can regulate adipogenic differentiation is suggested by the fact that overexpression of this TIMP reduces collagen I turnover by differentiating preadipocytes, as quantified by hydroxyproline release into culture media.

As discussed in Chapter 1, 'healthy' SAT expansion in overnutrition may underpin the existence of metabolically healthy obesity (MHO), which constitutes ~10% of obesity, and is thought to occur via a balanced combination of hyperplasia (that is, adipogenic differentiation of adipose mesenchymal stromal cells [preadipocytes] and hypertrophy of existing mature adipocytes [156, 171]. In MUO, hypertrophy is thought to constitute the main mode of adipose expansion [156]. Hypertrophied adipocytes are implicated in metabolic dysfunction (that is, insulin resistance, diabetes) in obesity as these adipocytes release more free fatty acids into the circulation than smaller adipocytes, leading to more ectopic lipids [239] – the presence of lipids in sites other than SAT, such as VAT, the liver and pancreas is independently associated with insulin resistance and eventual diabetes [240-242]. Hyperplastic expansion relies on the existence of a persistent, self-perpetuating pool of preadipocytes, to be called on to undergo adipogenic differentiation when required. Extreme examples demonstrating the effect of inhibited/absent preadipocyte differentiation include patients with the various types of lipodystrophy, who have little/no subcutaneous adipose tissue but large ectopic lipid reserves in visceral adipose, liver and other sites [33, 243].

In turn, adipogenesis requires tightly regulated turnover of surrounding extracellular matrix by preadipocytes. Various families of proteases are thought to be involved, amongst them metalloproteinases and their inhibitors. For example, MMP-14 remodels collagen I surrounding mouse preadipocytes, and is required for their differentiation in 3D culture [109]. It is well-established that TIMP-3 is a major inhibitor of a broad range of metalloproteinases, including MMP-14. TIMP-3 knockout mice demonstrate an interesting phenotype when challenged with a high-fat diet (HFD), including higher circulating insulin demonstrating insulin resistance and MUO [136]. Conversely, in mice where macrophages overexpress TIMP-3, HFD feeding results in improved metabolic and lipid overspill parameters as compared to wild-type counterparts [244]. TIMP-3 also appears to regulate sheddases in a complex manner, with increased basal shedding of certain shed receptors (e.g. LRP [207], VCAM-1 [210]) but decreased induced shedding (e.g. VCAM-1 [210]). Pref-1 is shed by ADAM-17 to allow activation of its antiadipogenic activity [119], and it is hypothesized that its human ortholog, Dlk-1, undergoes similar post-translational regulation.

My data appear to be consistent with these previously elucidated functions of TIMP-3. I found that TIMP-3 overexpression increases sDlk-1 and TNFR-I shedding into

the culture medium (Figures 5.2 and 5.4). With respect to the latter, it is unclear whether this is independent of or as a consequence of increased TNFR-I expression (Figure 5.3). An investigation of the timecourses of TNFR-I mRNA expression, TNFR-I protein expression, and sTNFR-I shedding into the culture medium, and how these relate to each other, would help address this question.

Certainly, increased expression of TNFR-I as a result of TIMP-3 overexpression may explain the augmented effect of TNF-α stimulation in terms of IL-8 expression (Figure 5.1). TNFR-I upregulation would lead to increased TNF receptors on the cell surface in the 48 hours prior to TNF-α treatment.

To my knowledge, this is the first time that the well-established and widely-used hydroxyproline release assay has been employed to provide a quantitative measure of the degree of collagen I turnover by human preadipocytes. This assay is relatively simple to perform and having a quantitative measure of preadipocyte extracellular matrix turnover in differentiation will be an extremely useful tool in future investigation of adipose tissue expansion, including whether this can be modified by pharmaceutically-interesting targets.

Using this assay, I have found that TIMP-3 overexpression reduces hydroxyproline release in adipogenic differentiation. This may occur through the inhibition of collagenolytic activity of MMP-14 and other metalloproteinases by TIMP-3. Given that TIMP-3 has also been implicated in the regulation of Dlk-1 shedding, this TIMP emerges as a novel node integrating inflammatory signals with networks controlling adipose remodelling. Dynamic modulation of TIMP-3 expression may be essential for healthy adipose tissue growth in nutrient excess, regulating the balance between hypertrophic and hyperplasic modes of expansion. In MUO, however, excess TIMP-3 may increase basal Dlk-1 shedding and reduce matrix turnover in adipogenesis, restricting preadipocyte differentiation and shifting AT growth towards adipocyte hypertrophy (Figure 5.10).

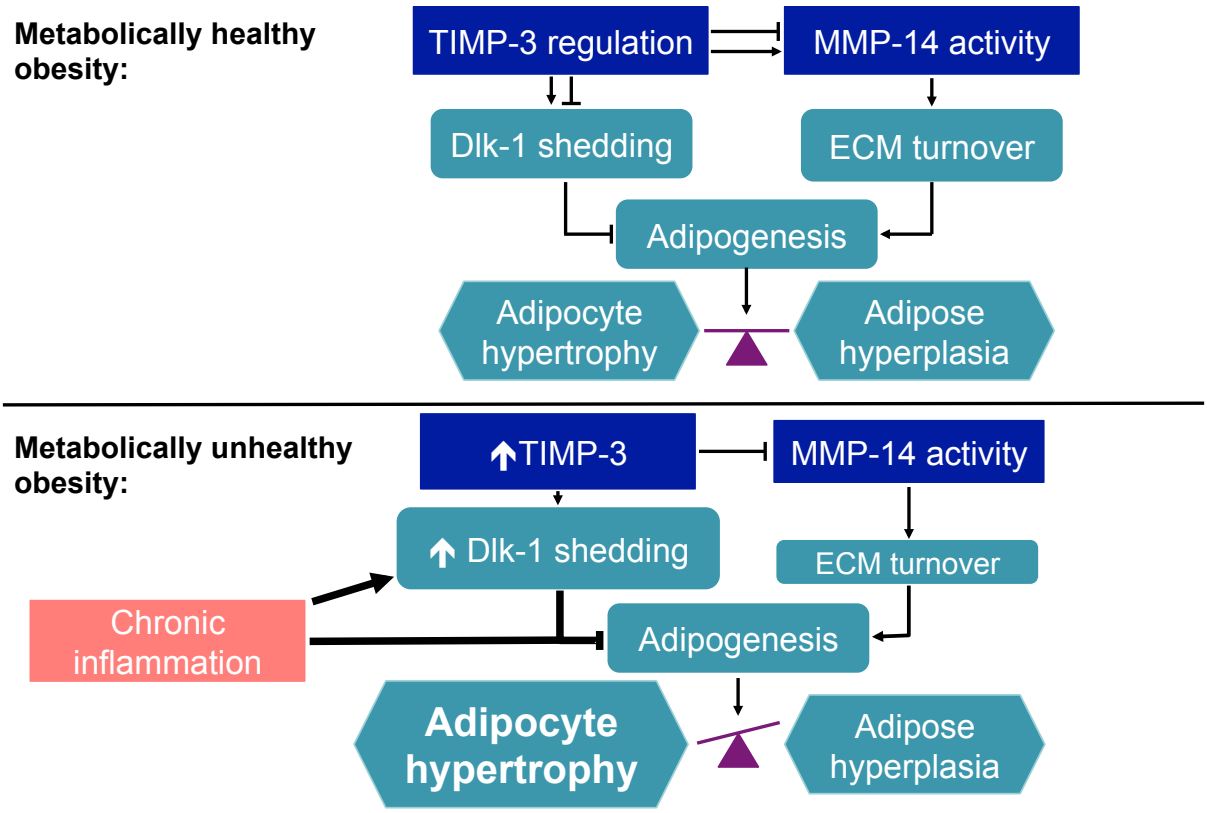

Figure 5.10: TIMP-3 may help regulate the balance between hypertrophy and hyperplasia in adipose tissue expansion. In metabolically healthy obesity, TIMP-3 expression may be dynamically regulated, variously inhibiting and allowing MMP-14 activity, and modulating Dlk-1 shedding via its complex role in affecting basal and stimulated shedding of this anti-adipogenic mediator. In metabolically unhealthy obesity, excess TIMP-3 expression (as seen in my clinical study (see Chapter 4) may inhibit ECM turnover and lead to increased Dlk-1 shedding, reducing hyperplasia and tipping the balance towards metabolically-disadvantageous adipocyte hypertrophy. The chronic inflammation typical of metabolically unhealthy obesity may exacerbate matters by inhibiting adipogenesis further, through increased Dlk-1 shedding and other pathways (ECM: extracellular matrix).

Further experiments are suggested by the results of this study. A timecourse of mRNA expression (using quantitative RT-PCR) of *Tnfrl* and *Dlk1*, over the first 48 hours following transduction with TIMP-3-overexpressing adenovirus, would help determine whether TIMP-3 overexpression results in any early changes in TNFR-I and Dlk-1 expression. Moreover, given the conflicting evidence regarding whether expression of TNF-α by human preadipocytes and adipocytes is of functional significance in human adipose tissue [245-247], expression analysis of TNF-α mRNA and protein by human primary *in vitro*-differentiated adipocytes and adipose-derived mesenchymal stem cells (that is, our preferred culture model) would be useful to unpick the effects of exogenously applied TNF-α in my experiments versus that which is endogenously expressed.

Little is known about the downstream signalling pathways triggered by Dlk-1 (indeed, its 'receptor' is a matter of contention, as outlined in Chapter 1). However, it is thought that MAPK/ERK signalling is central to Dlk-1's antiadipogenic effect (see Chapter 1, section 1.3.3.3). Analysis of MAPK/ERK phosphorylation, for example, as well as activation of other members of the Ras-Raf-MEK-ERK pathway would be helpful to elucidate whether exogenously-added recombinant human soluble Dlk-1 is having any effect in human preadipocyte cultures.

TIMP-3 overexpression is known to trigger apoptosis in certain cell types [235-238]. It has not been described in human adipocytes or preadipocytes, but attempting to track differentiation over a prolonged timecourse was unsuccessful, largely due to cell death. The use of cell viability assays (such as propidium iodide staining and quantification by flow cytometry) and apoptosis assays (such as fluorescent anti-annexin V antibodies) would help determine whether TIMP-3 overexpression does indeed trigger apoptosis in human preadipocytes and in *in vitro*-differentiated adipocytes, and if so, the timecourse over which this happens.

Chapter 6: Discussion

6.1: Introduction

Human beings in developed economies, and increasingly in the developing world, largely live in an energy-rich environment, with progressively easier access to cheap, high-energy foods. Indeed, there is evidence that the major global nutrition issue has shifted from undernutrition to overnutrition – the World Health Organisation (WHO) now speaks of a 'double burden' of nutrition, and its own 2015 figures indicated that more than 1.9 billion adults worldwide were overweight while 462 million were underweight [248]. Given its role in the 'safe' storage of excess ingested energy in the form of triglycerides, overnutrition constitutes a major 'stressor' on white adipose tissue (WAT) and the associated metabolic pathways that allow it to perform this function. Greater understanding of the metabolic stress placed on WAT by overnutrition allows us distinguish 'healthy' from 'unhealthy' subcutaneous adipose tissue (SAT) expansion. The former, which may underpin the existence of metabolically healthy obesity (MHO) estimated to constitute between 10% and 34% of all obesity depending on the criteria used [249], is thought to occur via a balanced combination of hyperplasia (that is, adipogenic differentiation of adipocyte precursors or preadipocytes) and hypertrophy of existing mature adipocytes [171]. In metabolically unhealthy obesity (MUO), on the other hand, hypertrophy is thought to constitute the main mode of unhealthy adipose expansion [156, 171, 250]. Hypertrophied adipocytes are implicated in metabolic dysfunction leading to insulin resistance, type 2 diabetes and increased cardiovascular risk, as these adipocytes release more free fatty acids (FFAs) into the circulation than smaller adipocytes, leading to more 'ectopic' lipids [129, 216, 251]. The presence of lipids in sites other than SAT, such as visceral adipose tissue (VAT), the liver and pancreas is independently associated with insulin resistance [240, 242, 252]. Furthermore, WAT characterized by a high proportion of hypertrophied adipocytes demonstrates greater markers of tissue inflammation, such as crown-like structures and inflammatory cytokine expression [251].

Whether the main mode of WAT expansion is hypertrophy or hyperplasia, both processes require extracellular matrix (ECM) remodelling in order to occur. It is important to acknowledge the central role that the ECM plays in all tissue function, and WAT is no exception. Indeed, given its remarkable capacity to change volume markedly in times of nutrient excess or deficiency, WAT perhaps has more in common with other tissues that are mainly composed of ECM, such as bone or cartilage. In these tissues, dysfunctional remodelling is implicated in well-recognised

clinical outcomes, such as osteoporosis in the case of bone [253, 254] or osteoarthritis in the case of cartilage [255, 256]. Similarly, I hypothesise that regulated, physiologically-appropriate ECM remodelling is crucial for normal WAT function, and that adipocyte-expressed metalloproteinases (MPs) and their tissue inhibitors (TIMPs), are important effectors of this metabolically-important WAT ECM turnover.

Figure 6.1 summarises the main points made in Chapter 1 (Introduction). Briefly, adipocytes and preadipocytes express MPs and TIMPs, and expression levels are related to body mass index (BMI), diet and WAT inflammatory status. Manipulation of MP/TIMP expression can have metabolic sequelae in rodent models. Metalloproteinases such as MMPs-2 and -14, and ADAM-12 may all be involved in remodeling of pericellular matrix during changes in adipocyte size and in adipogenic differentiation. Therefore, chronic low-grade maladaptive inflammation, MP/TIMPs expression, ECM turnover, adipogenic differentiation and metabolic sequelae may all be interrelated in obesity.

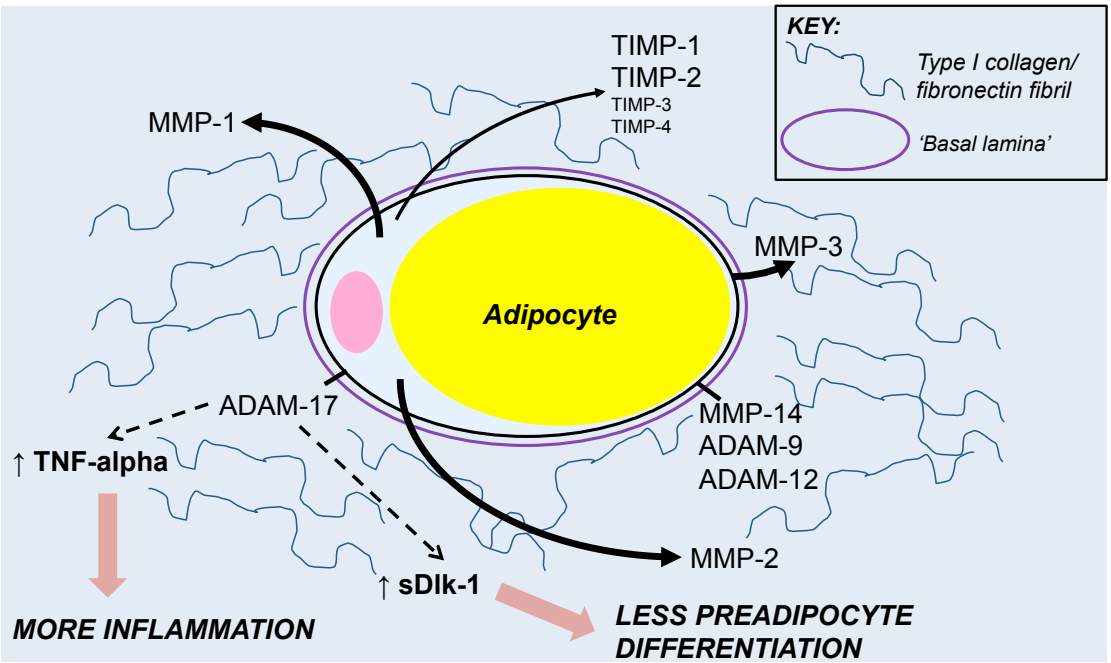

Figure 6.1: Human and murine adipocytes (and preadipocytes) express (solid arrows) a range of MPs and TIMPs that have important roles in WAT inflammation and ECM turnover. As outlined in Chapters 1 and 3, MMPs-1, -2, -3 and -14 are constitutively or inducibly expressed by these cells, with inflammation being a major positive regulator. TIMPs-1 to -4 are also expressed at high levels, with TIMP-3 and TIMP-4 being downregulated in chronically 'inflamed' WAT. TIMP-3 downregulation may have a 'disinhibitory' effect on ADAM-17 activity (dashed arrows), leading to increased TNF-α and Dlk-1 shedding, with consequences that include increased WAT inflammation and reduced adipogenic differentiation.

The research questions laid out in Chapter 1, section 1.5 (page 29) map to the Results chapters. I discuss how these studies have addressed these questions below.

6.2: Which are the key MPs and TIMPs expressed by human adipocytes and preadipocytes, and how is this expression modulated by inflammatory or pro-adipogenic stimuli? (addressed in experiments detailed in **Chapter 3**)

The results laid out in Chapter 3 are consistent with the majority of the literature on adipose MP and TIMP expression in cell culture. 3T3-L1 and 3T3-F442A preadipocytes have long been known to express MMP-2 and MMP-14 mRNA and protein [80, 81] – these were amongst the highest expressed transcripts in my Taqman Low-Density Array (TLDA). Interestingly, although MMP-9 has also been extensively studied in these murine adipocyte models (3T3-L1 and 3T3-F442A cells), it was not one of the most highly expressed MMPs in my TLDA. In keeping with experiments in SGBS adipocytes, human primary preadipocytes and primary adipocytes [84, 88], *Mmp1* and *Mmp3* were upregulated with inflammatory stimuli (TNF-α and LPS) in my study. Likewise, in keeping with experiments in 3T3-L1 preadipocytes and human primary preadipocytes, *Timp3* was downregulated by adipogenic differentiation in my experiments [96].

The expression pattern of metalloproteinases and their inhibitors in murine models of obesity is summarized in Chapter 1, Table 1.1 (page 14). The mRNA and protein expression of certain metalloproteinases and TIMPs is consistently upregulated across several mouse models. For example, MMP-2, MMP-14 and TIMP-1 were expressed at higher levels in obese models as compared to lean controls. In my expression analysis, MMP-2, MMP-14 and TIMP-1 were amongst the highest expressed metalloproteinases and TIMPs. Other MMPs with consistent upregulation in various mouse models of obesity include MMPs-3, -12 and -19. In my TLDA-based expression analysis, MMP-3 was not highly expressed by primary human *in vitro*-differentiated adipocytes, but its mRNA expression was upregulated approximately threefold by stimulation with lipopolysaccharide (LPS) (Figure 3.2, page 65). Both MMP-12 and MMP-19 were poorly expressed by cells in my culture model, and this expression was not regulated to any significant degree by inflammatory stimulation (Figure 3.2, page 65).

mRNA expression of MMP-7 and TIMP-3 appear consistently downregulated in various murine models of obesity. In my TLDA-based expression analysis, MMP-7 is not significantly expressed by cells in my culture model, and its expression is not regulated to any significant degree by inflammatory stimulation. On the other hand, TIMP-3 is one of the most highly expressed transcripts assayed, and downregulation of mRNA and protein expression in inflammatory conditions forms the basis of subsequent experiments looking at its role in human adipose biology (Chapter 5). Therefore, the results from my expression analysis show some important similarities with the expression of metalloproteinases and their inhibitors in murine models, as well as some differences.

What my study adds is that it is, to my knowledge, the first description of the mRNA expression of all 66 human MPs and TIMPs in primary human *in vitro*-differentiated adipocytes. Thus, it provides a resource for other researchers in the field of human adipose tissue remodelling. However, there are some limitations to my approach that can be addressed in future studies.

Firstly, these experiments were carried out in human *in vitro*-differentiated primary adipocyte culture. As outlined in Chapter 2, this culture model is well-described and has been used extensively in our group. However, cultures are established by isolating the stromo-vascular fraction of human abdominal adipose tissue by collagenase digestion and centrifugal separation. The population of cells that is initially plated (passage 0) contains various cell types, including true preadipocytes, mesenchymal stem cells, fibroblasts, endothelial cells, macrophages, monocytes, lymphocytes and others. Previous work in our lab has shown that subcutaneous adipose tissue-derived primary human preadipocyte cultures are CD45-negative after one passage, suggesting that the cells in this cell culture model are not contaminated by hematopoietic cells [257]. However, this remains far from a homogeneous population of cells. There is an advantage in continuing to use this cell culture model in spite of this limitation in that it can be said to reflect the mix of cell types found in adipose tissue more accurately than using, for example, preadipocyte models. Given the intercellular communication that occurs between different cell types in all tissues, having a number of different cells *in vitro* may be deemed to more accurately reflect the situation *in vivo*. Nevertheless, it is desirable for the purposes of *in vitro* experimentation to have a clearer understanding of the exact cell composition of the cultures being used, in order to be able to attribute results, including changes in expression of genes or proteins of interest, to one cell type or another. In turn, this

improved understanding will translate into more targeted approaches – that focus on the correct cell type – when designing and conducting investigational studies including clinical trials of novel pharmacological agents. Future studies may benefit from a better characterization of the cellular composition of human *in vitro*-differentiated adipocyte cultures, through the use of techniques such as flow cytometry and immunohistochemical staining. Attempts to isolate 'true' preadipocytes – that is, cells that are committed to differentiate into adipocytes – are currently limited by the lack of good preadipocyte markers, surface or otherwise. Further research that identifies such markers should be rapidly applied to studies of this nature in order to better characterize and validate the cell culture model currently being used in the majority of human adipose research.

Secondly, these cultures were grown on tissue culture flasks, plates and dishes, and represent 'two dimensional' (2D) culture models. It is well known that culture in three dimensions (3D), or indeed in contact with extracellular matrix constituents such as collagen or fibrinogen, significantly changes the behaviour of cultured cells, including expression of genes/proteins of interest, differentiation, and viability, and preadipocytes/adipocytes are no exception [109, 189, 233, 258-260]. The seminal studies by Chun *et al* bear highlighting, as they showed that murine preadipocytes lacking MMP-14 differentiated normally in 2D but failed to differentiate in 3D [109, 110]. Thus, my studies should be repeated in a three-dimensional culture model, in which mesenchymal stromal cells are grown and differentiated in collagen gels, in order to assess the expression of the genes and proteins of interest I have identified in this more physiologically-representative model.

6.3: In human adipose tissue, what role does TIMP-3 play in regulating i) ECM turnover and ii) expression and shedding of the anti-adipogenic mediator Dlk-1, and ultimately adipogenic differentiation and hyperplastic adipose expansion? (addressed in experiments detailed in **Chapter 5**)

As a broad-spectrum inhibitor of many metalloproteinases including collagenases and sheddases, TIMP-3 emerges as a potentially key node in the remodelling protein interaction network (Figure 6.2).

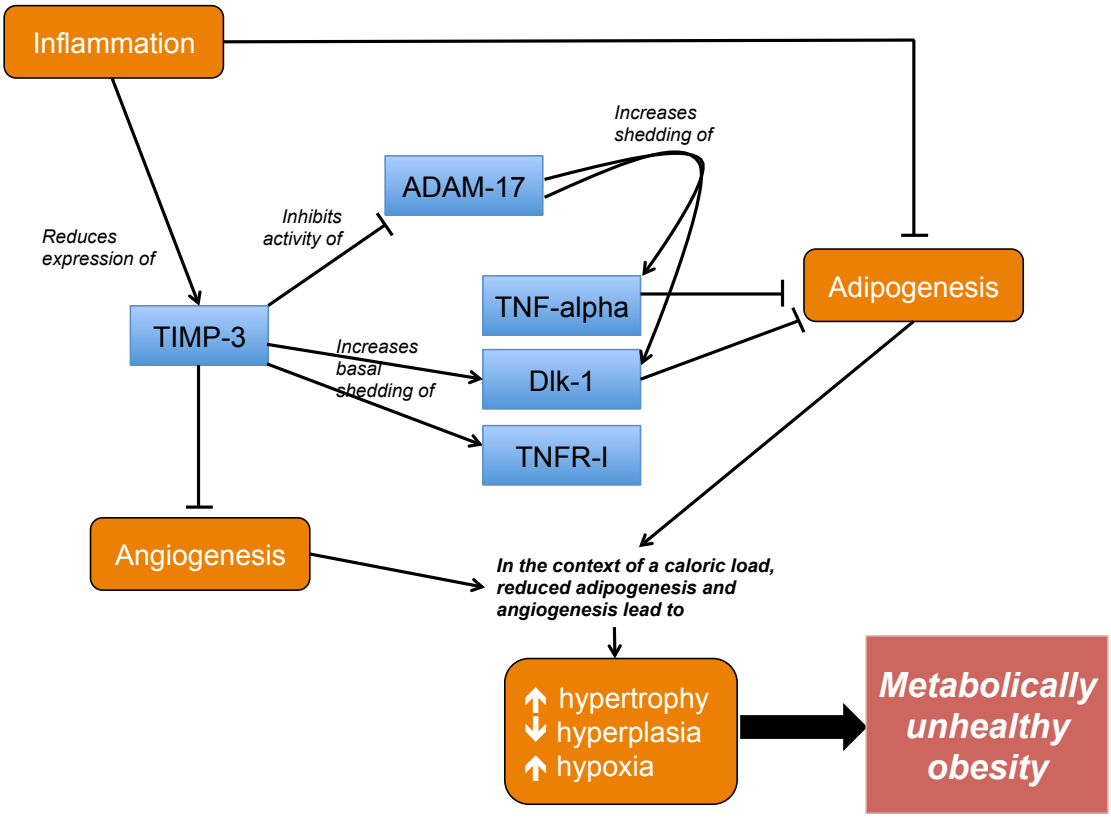

Figure 6.2: TIMP-3 is implicated in many processes that are involved in dysfunctional adipose remodelling leading to metabolically unhealthy obesity. In this figure, processes are in orange boxes, and proteins of interest are in blue boxes. Inflammation has been shown to directly inhibit adipogenesis, and my and others' work has shown that TIMP-3 expression is modulated by inflammatory stimuli. TIMP-3, in turn, has direct and indirect (via inhibition of ADAM-17 activity) effects on TNF-alpha, Dlk-1 and TNFR-I solubilisation and therefore activity. TIMP-3 has been shown by others to reduce angiogenesis. When adipose tissue expands as a result of a positive energy balance, the combination of reduced adipogenesis and reduced angiogenesis leads to increased hypertrophy, reduced hyperplasia and increased hypoxia, all of which are features of dysfunctional adipose tissue in metabolically unhealthy obesity.

TIMP-3 knockout mice demonstrate an interesting phenotype when challenged with a high-fat diet (HFD), including higher circulating insulin (denoting insulin resistance) and MUO [136]. Conversely, in mice where macrophages overexpress TIMP-3, HFD feeding results in improved metabolic and lipid overspill parameters as compared to wild-type counterparts [244]. TIMP-3 also appears to regulate sheddases in a complex manner, with increased basal shedding and decreased induced shedding of shed receptors (e.g. VCAM-1 [210]). The ADAM-17/TIMP-3 axis has been found to have a metabolic role in human skeletal muscle [152], but remains poorly understood in human adipose tissue.

In Chapter 5, my data on the effects of manipulation of TIMP-3 expression are presented. TIMP-3 overexpression significantly enhances the effect of TNF-α on IL-8

expression by human preadipocytes, This may be because, under non-inflammatory conditions, TIMP-3 overexpression increases TNFR-I expression by these cells, and increases the concentration of soluble TNFR-I shed into the culture medium. Therefore, in conditions of high TIMP-3 expression, more TNFR-I on the cell surface may lead to increased TNF-α-stimulated signalling.

TIMP-3 overexpression in non-inflammatory conditions increases soluble Dlk-1 shedding into the culture medium. I did not observe a corresponding increase in membrane-bound Dlk-1 expression by preadipocytes, which is in contrast to the situation with TNFR-I. However, *Timp3* gene silencing reduces sDlk-1 shedding, providing further evidence that TIMP-3 does indeed regulate constitutive Dlk-1 shedding.

When incubated with an inflammatory mediator (TNF-α), adipocyte and preadipocyte expression of TIMP-3 is repressed, which would be expected to lead to increased Dlk-1 shedding. This is indeed what I observed when sDlk-1 shedding was assessed following TNF-α stimulation of preadipocytes (Figure 5.4A).

Figure 6.3 demonstrates how TIMP-3 regulation may be central to the switch between hyperplastic and hypertrophic modes of WAT expansion. Hyperplastic expansion relies on the existence of a persistent, self-perpetuating pool of preadipocytes, to be called on to undergo adipogenic differentiation when required. Extreme examples of the effect of inhibited or absent preadipocyte differentiation include patients with the various types of lipodystrophy, who have little/no subcutaneous adipose tissue but large ectopic lipid reserves in visceral adipose, liver and other sites [33, 243]. The *Pref1*-null mouse phenotype is reminiscent of this, with adipocyte hypertrophy, increased hepatic fat, and increased circulating free fatty acids [125]. By allowing unrestricted adipogenic differentiation, the absence of Pref-1 in development may conceivably lead to the consumption of preadipocytes earlier on in life, with a switch to predominantly hypertrophic adipose expansion occurring sooner and thus the development of adverse metabolic outcomes. Similarly, young adults who have undergone total body irradiation (TBI) in the treatment of cancer as children represent a less extreme phenotype. This cohort exhibits a characteristic metabolic phenotype, consisting of metabolic dysfunction and central obesity [261-263]. It is thought that spinal and truncal irradiation may have affected preadipocyte reserves, leaving them with a smaller functional preadipocyte pool in adulthood [264, 265].

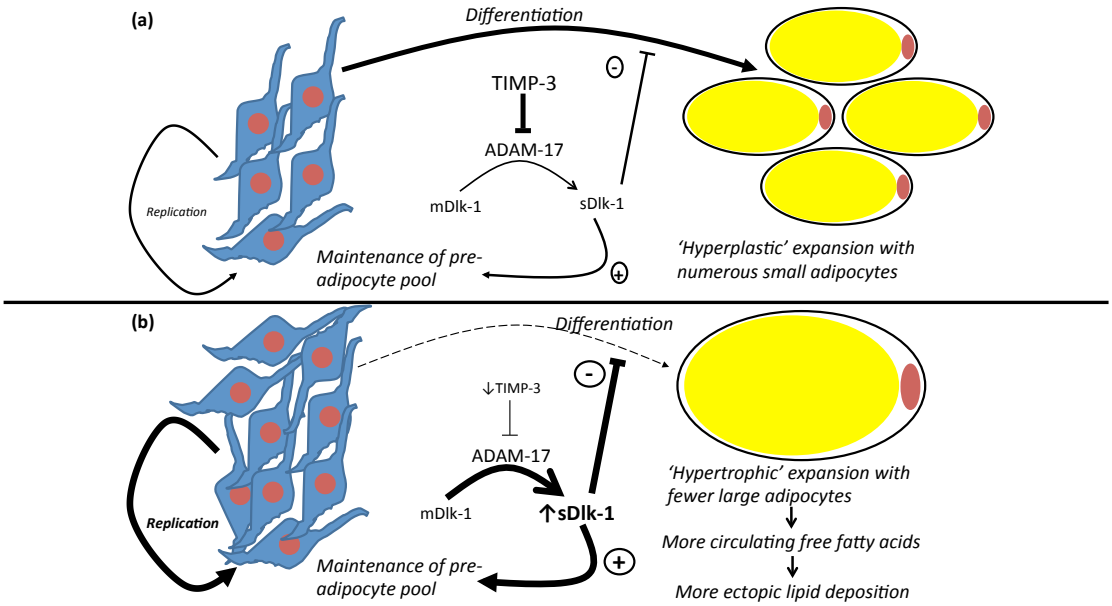

Figure 6.3: TIMP-3 may be a crucial regulator of the balance between hyperplastic and hypertrophic modes of adipose tissue expansion. (a) In metabolically healthy adipose, TIMP-3 expression exerts a tonic inhibitory effect on Dlk-1 shedding, allowing maintenance of the preadipocyte pool and some recruitment into adipogenic differentiation. (b) In inflamed adipose TIMP-3 downregulation leads to adipocyte hypertrophy via inhibition of differentiation.

However, modulation of Dlk-1 shedding is one mechanism by which TIMP-3 can regulate adipogenesis. I also found that TIMP-3 overexpression reduces collagen I turnover by differentiating preadipocytes, as quantified by hydroxyproline release into culture media. This suggests that the effect of TIMP-3 on adipogenesis is complex, and indeed, I was unable to determine the overall effect of TIMP-3 overexpression on preadipocyte differentiation (Appendix B).

The discussion section of Chapter 5 (Section 5.4, page 111) outlines the major strengths and limitations of the experiments contained within this chapter. It is worth highlighting that my study represents the first attempt, to my knowledge, to develop a method for quantifying the degree of collagen turnover by human primary preadipocytes in culture, which in turn can be used as a model for extracellular matrix turnover. Such a tool may be used by other researchers in the field of adipose tissue remodelling to better understand the factors that contribute to increased or decreased extracellular matrix turnover by adipose-resident cells, and potentially to test pharmacological agents that could modulate this process.

6.4: In human adipose tissue, does altered MP/TIMP expression contribute to maladaptive adipose tissue remodelling, whole-body lipid maldistribution and metabolic dysfunction? (addressed in experiments detailed in **Chapter 4**)

This study is, to my knowledge, the first of its kind in attempting to study the relationship between human adipose MP and TIMP expression and human adipose tissue remodelling, human whole-body lipid distribution, and markers of human metabolic dysfunction. I identified *Timp3*, *Dlk1*, *Mmp2*, *Mmp14*, and *Mmp1* as genes of interest whose mRNA expression in whole subcutaneous and visceral adipose tissue samples varied with measures of adipose tissue dysfunction and metabolic dysfunction, such as mean adipocyte cross-sectional area, subcutaneous and visceral adipose tissue volume, fasting glucose and fasting triglycerides.

The major results regarding *Timp3* are summarised in Table 4.5. Briefly, SAT *Timp3* expression is positively correlated with mean subcutaneous adipocyte area – a correlation that becomes significantly stronger when controlling for total adipose tissue volume. This implies that in subjects with the same total adipose tissue volume (a proxy for adiposity), higher TIMP-3 levels are associated with larger adipocytes, in keeping with the in vitro results that high TIMP-3 levels increase basal Dlk-1 shedding and inhibit collagenolysis, potentially reducing hyperplastic expansion and increasing the degree of hypertrophy in the tissue. On the other hand, SAT *Timp3* steady-state mRNA levels are negatively correlated with both HOMA-IR and VAT volume, implying that high levels of TIMP-3 are metabolically advantageous. This apparent paradox may be resolved if high TIMP-3 levels are hypothesised to limit uncontrolled adipogenesis when faced with the adipose stressor of overnutrition, TIMP-3 excess is beneficial as it moderates preadipocyte recruitment, allowing sufficient undifferentiated preadipocytes to persist in a self-sustaining pool. However, when faced with persistent energy excess, this preadipocyte pool is exhausted, leading to adipocyte hypertrophy and metabolic dysfunction.

This hypothesis for TIMP-3's role in adipose biology appears to be at least in part supported by the phenotype of the *Timp3*-/- (knockout) mouse [136, 138, 266]. As outlined in Chapter 1 (section 1.3.4.3) and in Appendix A, Table A.2, the offspring of *Timp3* null mice crossed with insulin receptor haploinsufficient (*Insr*+/-) mice fed a HFD demonstrate a metabolically unfavourable phenotype (which is consistent with my result that lower SAT *Timp3* levels are associated with higher HOMA-IR, implying insulin resistance). In spite of the fact that they gain less weight than controls, they

have hypertrophied white adipocytes, suggesting that a lack of TIMP-3 leads to rapid preadipocyte pool depletion when faced with caloric excess (in the form of a HFD), leading to metabolically unfavourable adipose expansion by hypertrophy. It is worth noting, however, that given TIMP-3's myriad roles in normal tissue function, adipose tissue dysfunction in *Timp3* knockout mice is almost certainly due to further mechanisms other than modulation of adipogenesis. For example, *Timp3*-/- mice have higher circulating TNF-alpha levels [266], and increased tissue inflammation in organs other than adipose tissue, such as the liver; the latter is associated with hepatic steatosis and liver failure [267, 268]. Both adipose tissue inflammation and hepatic steatosis have been independently associated with the development of insulin resistance [269] [8, 9], meaning that the adverse metabolic phenotype in TIMP-3 deficient mice has a complex aetiology.

An analysis of how *Dlk1* mRNA expression in subcutaneous and visceral adipose tissue relates to various measures of adipose tissue remodeling and whole-body lipid distribution is found in section 4.3.2 (page 88). Briefly, donors with no SAT mRNA expression of *Dlk1* had higher VAT volumes (as a proportion of total adipose tissue volume). In donors where SAT *Dlk1* mRNA expression was detectable, this correlated negatively with mean subcutaneous adipocyte cross-sectional area. These results can be explained if *Dlk1* mRNA expression is taken to be a surrogate marker for the number of preadipocytes in the tissue sample. In individuals with few subcutaneous preadipocytes (perhaps as a result of depletion of the preadipocyte pool), there is low *Dlk1* mRNA expression, and a relative inability of the SAT to expand by hyperplasia. Thus, the SAT is characterised by larger, hypertrophied adipocytes, and diversion of lipids to the visceral compartment, resulting in a relatively larger visceral adipose depot.

The expression of *Dlk1* mRNA by whole VAT samples (and thus, using the previous assumption, the presence of visceral preadipocytes) is negatively correlated with percentage VAT volume, and is associated with higher fasting triglycerides. These results do not fit neatly in with the previous hypothesis, indicating that the function of Dlk-1 in adipose tissue is likely to be complex. Indeed, the phenotypes of mutant rodent strains where the *Pref1* gene (the mouse ortholog of *Dlk1*) is manipulated are complex, with both *Pref1* overexpression and knockout resulting in adverse metabolic phenotypes (Table 1.4, page 20). The decreased adipose tissue mass, hyperlipidaemia and insulin resistance described in *Pref1*-overexpressing mice is reminiscent of human lipodystrophy, and may result from excessive Pref-1 inhibiting

adipogenesis and thus adipose expansion by hyperplasia. On the other hand, *Pref1* knockout results in larger fat depots, hypertrophied adipocytes and hyperlipidaemia, suggesting that the lack of an inhibitor of adipogenesis results in relative depletion of preadipocytes, and once again a metabolically-adverse phenotype [123, 125, 270].

MMP-14 has been previously described as a regulator of adipogenesis in murine preadipocytes, with preadipocytes lacking MMP-14 failing to differentiate in three-dimensional culture [109]. In humans, a single-nucleotide polymorphism close to the catalytic domain of MMP-14 was found to be associated with higher body mass index and waist-to-hip ratio in a Japanese cohort consisting of 3,647 subjects [110]. In my study, *Mmp14* mRNA expression by VAT samples is positively correlated with abdominal subcutaneous adipose tissue volume (section 4.3.3, page 91). This may reflect increased adipogenesis in visceral adipose tissue in subjects with increased abdominal subcutaneous adipose tissue, perhaps as a result of the abdominal SAT compartment approaching its expansion limit and more lipids being diverted to the VAT compartment. I also observed a negative correlation between subcutaneous *Mmp14* mRNA expression and VAT volume in the subset of subjects who were postmenopausal. This finding was unexpected, and to my knowledge has not been described elsewhere, and certainly deserves further investigation given the fact that postmenopausal women have increased cardiometabolic risk and demonstrate a shift towards visceral fat distribution [271, 272].

As stated earlier, my study differs from other human work in that, to my knowledge, it is the first one that focused on adipose tissue-specific expression of metalloproteinases and their tissue inhibitors, and the association between this expression and markers of dysregulated adipose tissue remodelling, whole-body lipid distribution, and metabolic dysfunction. Other human studies have largely focused on circulating MMP levels, such as MMP-2 and MMP-9 [143, 145, 146], or when they have focused on adipose expression of these metalloproteinases, have not investigated whole-body adipose distribution, for example by assessing the relative sizes of adipose depots [142, 143]. Another subset of human studies investigating the role of metalloproteinases and their inhibitors in obesity and type 2 diabetes has focused on single nucleotide polymorphisms and other sequence variants in genes of interest, including *Mmp3* [150], *Mmp14* [110], and *Adamts9* [155]. In the case of investigations in humans on the role of ADAM-17/TACE and TIMP-3 in obesity and metabolic dysfunction, these have focused on their role in skeletal muscle, rather than in adipose tissue [152, 153]. The closest study to mine is that by O'Connell *et al*

[154], which found that visceral *Dlk1* mRNA expression is significantly correlated with visceral adipocyte hypertrophy, hepatic steatosis, and increased fasting glucose and triglycerides. However, this study did not look at the role of MPs and TIMPs such as ADAM-17 and TIMP-3 in regulating Dlk-1 function.

A number of limitations and plans for future work are described in the Discussion section of Chapter 4 (Section 4.4, page 92). Briefly, future work will focus on using adipose tissue from male subjects, as tissue from female subjects only was used in view of the use of adipose tissue from female donors to establish primary human cultures in the initial phases of this research (see Chapters 2 and 3). Interesting work that can then be carried out is a comparison between the results from males and from females.

Expression analysis of MP/TIMP targets of interest was limited to mRNA expression as detected by qRT-PCR. Increased expression of this type does not necessarily mean increased MP/TIMP activity, and thus increased contribution to adipose tissue function. In order to determine MP and TIMP protein levels in donated tissue biopsies, future studies will need to use techniques such as immunohistochemistry for proteins of interest.

A significant limitation of the analyses of adipocyte cross-sectional area in relation to MP/TIMP expression and other metabolic markers was the use of only two non-consecutive slides for each depot. As outlined previously, a further section of each adipose sample has already been prepared and stained, and the fixed/embedded samples are stored in the Norfolk and Norwich University Hospital Tissue Bank, meaning that further sections can be cut, mounted and stained. Thus, it should be relatively straightforward for researchers interested in pursuing this line of investigation further to obtain more photomicrographs of these samples, thus increasing the number of unique slides tested per donor.

Lastly, it is important to note that expression was assessed in whole adipose tissue biopsies, meaning that it is impossible to attribute any changes in expression of a target MP/TIMP to any one particular cell type. It is well-known that the stromo-vascular fraction of adipose tissue contains multiple cells types that are highly active in adipose tissue remodelling, such as adipose tissue macrophages and fibroblasts [47, 273, 274]. Future work could use immunohistochemistry or whole mount in situ hybridisation to associate increases or decreases in expression or particular

MPs/TIMPs of interest with particular cell types, thus better understanding the contribution that these cells make to the adipose tissue remodeling process.

Clearly, there are many outstanding questions that are raised by these studies. Firstly, why should a hypothesized shift towards adipocyte hypertrophy in high *Timp3*-expressing subjects lead to reduced insulin resistance? It is known that adipocyte hypertrophy does not necessarily lead to adverse metabolic parameters, such as in the collagen VI/leptin-deficient mouse which has larger adipocyte than ob/ob and wild-type controls, but improved metabolic status [45]. That said, TIMP-3 excess likely inhibits remodelling required for adipocyte hypertrophy by inhibiting metalloproteases responsible for basal lamina (that is, its collagen IV, collagen VI and laminin) turnover.

It also remains to be established how the adipocyte-preadipocyte ratio varies with *Timp3* expression. If the above reasoning is applied, *Timp3* expression would be expected to be negatively correlated with this ratio – that is, high *Timp3* would lead to more preadipocytes being maintained in the undifferentiated state. Sections of adipose tissue in our study could be stained for, for example, Dlk-1 to count the number of preadipocytes, and the adipocyte/preadipocyte ratio could be assessed in terms of its value as a marker of adipose tissue expansibility.

Work in mouse models may also contribute to these investigations. It would be interesting to study what happens to the adipocyte/preadipocyte ratio in *Timp3*-null mice fed a HFD over time, as compared to wild-type/haploinsufficient littermates. I would hypothesise that *Timp3* knockout mice would have a higher adipocyte-preadipocyte ratio due to preadipocyte pool exhaustion.

To further understand the role of TIMP-3 in human adipose function, a longitudinal cohort study could be designed to classify, at recruitment, study subjects into high *Timp3*-expressing or low *Timp3*-expressing groups. Subjects could then be followed up over a long period of time to track adipose distribution, development of adverse metabolic parameters and possibly adipocyte size. Obesity and T2DM are ideal diseases to be studied in this way, as the outcome rate is very high. Similarly, a case-control design could be used wherein high and low *Timp3*-expressing subject groups could undergo a period of overfeeding, and the effects on WAT remodelling, lipid distribution, and metabolic parameters could be compared.

Such studies will allow a better understanding, and rejection or refinement of the model outlined at the end of Chapter 5 (Figure 5.10). In this model, TIMP-3 acts as a central node that integrates adipogenesis and adipose inflammation by virtue of its roles in regulating collagenolysis and sDlk-1 shedding. If TIMP-3 proves to be such an important mediator of adipose dysfunction in nutrient excess, it may yet turn out to be an attractive therapeutic target. Given that it is ubiquitously expressed in various human tissues, ways of targeting adipose-specific TIMP-3 would need to be identified. Ultimately, however, the general, population-focused advice to limit overnutrition and undertake activities that tip energy balance towards increased expenditure remain the best methods to reduce WAT stressors and maintain metabolic health.

Appendix A:
Additional Tables

	Increase adipogenesis				Decrease adipogenesis			
	Inhibitor	*Cell type or organism*	*Dose and spectrum of inhibition (if applicable)*	*Ref.*	*Inhibitor*	*Cell type or organism*	*Dose and spectrum of inhibition (if applicable)*	*Ref.*
1. Pharmacological inhibitor	1. GM6001/ Ilomastat/ Galardin	3T3-L1	10μM, Inhibits MMPs-1, -2, -3, -7, -8, -9, -12, -14, and -26	[98]	1. GM6001/ Ilomastat /Galardin	3T3-L1	25 μM, Inhibits MMPs-1, -2, -3, -7, -8, -9, -12, -14, and -26	[80]
	2. MMP-3 Inhibitor II/CAS 161314-17-6 (Merck)	3T3-L1	20 μM, MMP-3	[99]	2. MMP-2 Inhibitor I/CAS 10335-69-0 (Merck)	3T3-L1	20 μM, MMP-2	[80]
	3. Tolylsam	3T3-F442A	25-100 μM, inhibits MMPs-2, -9 and -12	[275]	3. CT1746	3T3-F442A	10 μM, Hydroxamic acid MMP inhibitor with specificity for gelatinases	[92]
					4. Batimastat/BB-94	3T3-L1	10 μM, Broad-spectrum MMP inhibitor	[7]
					5. Batimastat/BB-94	3T3-F442A	10 μM, Broad-spectrum MMP inhibitor	[81]
					6. Captopril	3T3-F442A	1mM, gelatinase inhibitor	[81]
					7. Tolylsam	Male WT mice (C57Bl/6)	100mg/kg/day, inhibits MMPs-2, -9 and -12	[130]

					8. Tolylsam	Male *ob/ob* mice	100mg/kg/day, inhibits MMPs-2, -9 and -12	[276]
					9. GM6001/ Ilomastat /Galardin	Male WT mice (mixed 75% C57/Bl6 and 25% 129SVj)	100mg/kg/day, Inhibits MMPs-1, -2, -3, -7, -8, -9, -12, -14, and -26	[277]
					10. Bay 12-9566 (Bayer)	Male ob/ob mice	100mg/kg/day, Inhibits MMPs-2, -3, -9 and -13, but not MMP-1	[278]
					11. Ro 28-2653	Male WT mice (C57Bl/6) fed a HFD	30mg/kg/day, Inhibits MMPs-2, -9 and -14	[279]
					12. Tolylsam	Male WT (C57Bl/6) or *Mmp2-/-* mice fed a HFD	100mg/kd/day, inhibits MMPs-2, -9 and -12	[275]
B. TIMP	1. rhTIMP-1	3T3-L1	250μM, Most MMPs and ADAM-10, but weak for MMPs-14, -16, -19 and -24	11266461	1. hTIMP-3 (transfection with expression vector)	3T3-L1	All MMPs, ADAMs-10, -12, -17, -28 and -33; ADAMTSs-1, -4, and -5, ADAMTS-2 (weak)	[96]

				2. rmTIMP-1	3T3-L1	25-100µg/ml, Most MMPs and ADAM-10, but weak for MMPs-14, -16, -19 and -24	[93]
C. Antibody				1. Anti-MMP-2 & anti-MMP-9	3T3-F442A	10-100ng/ml	[81]
				2. Anti-MMP-2 & anti-MMP-9	3T3-L1	1ug/ml	[80]
D. Gene knockdown	1. MMP-3	3T3-L1	[99]				

(Ref.: reference; rh: recombinant human; rm: recombinant murine)

Table A.1: The effects of manipulation of metalloproteinase function, using different strategies, on adipogenesis.

Gene	Manipulation/experiment	Phenotype vs. control	References
Mmp2	Knockout (*Mmp2*-/-) fed HFD for 15 weeks	1. Gain less weight 2. Smaller adipose depots 3. Larger adipocytes	[130]
Mmp3	Knockout (*Mmp3*-/-) fed HFD for 15 weeks	1. Hyperphagic 2. Larger adipose depots 3. Perigonadal adipose tissue has larger adipocytes 4. Mammary adipose has larger adipocytes	[98]
Mmp9	Knockout (*Mmp9*-/-) fed HFD	No difference	[131]
Mmp11	Knockout (*Mmp11*-/-) fed HFD	1. Gain more weight 2. Larger adipose depots 3. Larger adipocytes 4. Fasting glucose/triglyceride/total cholesterol levels – no difference	[132]
Mmp11	Transgenic mice overexpressing MMP-11 (*Mmp11*-Tg) fed HFD	1. Gain less weight 2. Lower glucose on glucose tolerance test 3. Lower glucose on insulin tolerance test 4. Smaller adipocytes	[280]
Mmp14	Knockout (*Mmp14*-/-)	1. Preadipocytes do not differentiate in 3D collagen gel 2. Mice have undetectable serum leptin and increased hepatic triglyceride	[109]
Mmp14	Haploinsufficient (*Mmp14*+/-) fed HFD	1. Gain less weight 2. Smaller inguinal and perigonadal adipose depots 3. No differences in food intake or metabolic rates	[110]
Mmp12	Knockout (*Mmp12*-/-) fed HFD	1. Gain weight at same rate 2. Smaller subcutaneous adipocytes 3. Higher plasma glucose 4. Lower number of crown-like structures in adipose tissue	[134]
Mmp19	Knockout (*Mmp19*-/-) fed HFD	1. Gain more weight 2. Larger adipocytes in inguinal and perigonadal adipose depots	[133]
Adam12	Knockout (*Adam12*-/-) fed HFD	1. Gain less weight 2. Smaller adipose depots with fewer adipocytes of same size as controls 3. Smaller brown adipose tissue depots 4. Smaller liver	[135]
Adam12	Knockout (*Adam12*-/-) fed SFD	1. More insulin sensitive on insulin tolerance test 2. Lower circulating triglycerides 3. Lower circulating non-esterified fatty acids	[135]
Adam12	Transgenic mice overexpressing the soluble form of ADAM-12 under a muscle creatinine kinase promoter	1. Larger adipose depots 2. Greater number of similarly sized adipocytes in all depots 3. Large numbers of adipocytes in skeletal muscle	[107]
Adam17	Knockout (*Adam17*-/-)	Lethal in perinatal period	[139]
Adam17	Haploinsufficient (*Adam17*+/-) crossed	Do not become hyperinsulinaemic	[136]

	with insulin receptor haploinsufficient strain (*Insr*+/-), offspring fed HFD		
Adam17	Haploinsufficient (*Adam17*+/-) fed HFD	1. Gain less weight 2. Lower fed glucose 3. Lower fasting and fed insulin 4. Lower fasting and fed non-esterified fatty acid levels	[122]
Timp1	*Timp1*-overexpressing transgenic mouse strain	Accelerated mammary gland involution and replacement by adipose tissue	[98]
Timp1	Knockout (*Timp1*-/-) fed HFD	1. Gain less weight 2. Lower fasting glucose 3. Lower total cholesterol	[141]
Timp3	Knockout (*Timp3*-/-) crossed with insulin receptor haploinsufficient strain (*Insr*+/-), offspring fed HFD	1. Gain less weight 2. Larger adipocytes 3. Hyperglycaemic 4. Hyperinsulinaemic 5. Increased mRNA expression of inflammatory mediators (CCL2, MCP-1, IL-6) by adipose tissue 6. Increased hepatic fat, with increased liver transaminases	[136, 266]

Table A.2: Phenotypes of mutant rodent strain where MP/TIMP genes are manipulated. (HFD: high-fat diet; SFD: standard fat diet; 3D: three-dimensional)

MP or TIMP	Alternative name	Involvement in obesity and metabolism	Evidence	Reference(s)
MMP-1	Collagenase 1	1. mRNA/protein expressed by adipocyte models and primary adipocytes 2. mRNA/protein expression increased by exposure to inflammatory conditions	• Microarray study in SBGS pre/adipocytes, with ELISA confirmation • mRNA (qRT-PCR) and protein (ELISA) expression in human primary pre/adipocytes	[84], [88]
MMP-2	Gelatinase A	1. mRNA expressed by murine epididymal adipose tissue 2. mRNA expression increased in rodent genetic and nutritional models of obesity 3. Protein expression increased in subcutaneous adipose tissue of human patients with T2DM 4. Larger subcutaneous adipocytes in T2DM patients with increased MMP-2 expression 5. Protein expression and activity increased during preadipocyte differentiation	• mRNA expression analysis in mouse epididymal WAT • mRNA expression and histological analysis of human adipose tissue and primary human adipocyte cultures • mRNA and protein expression analysis, and gelatin zymography analysis, in murine 3T3F442A preadipocyte cell line • Plasma protein levels increased in obese patients	[7, 81, 143]
MMP-3	Stromelysin 1	1. mRNA expressed by murine epididymal/subcutaneous adipose tissue 2. mRNA and protein expression increased by	• Microarray study in adipocyte model (SBGS adipocytes), with ELISA confirmation • mRNA expression analysis in mouse epididymal and	[7, 84, 92, 150]

		exposure to inflammatory conditions 3. mRNA expression increased in rodent genetic and nutritional models of obesity 4. Reduced mRNA expression with increasing BMI in humans 5. Sequence variants associated with obesity and T2DM	subcutaneous WAT • Genome analysis in human subjects	
MMP-7	Matrilysin	1. mRNA expressed by murine epididymal and subcutaneous adipose tissue 2. mRNA expression decreased in rodent genetic and nutritional models of obesity	mRNA expression analysis in mouse epididymal and subcutaneous WAT	[7, 92]
MMP-9	Gelatinase B	1. mRNA expressed by murine epididymal and subcutaneous adipose tissue 2. mRNA and protein expression increased by exposure to inflammatory conditions 3. mRNA and protein expression decreased in rodent nutritional model of obesity 4. Protein expression and	• Microarray study in adipocyte model (SBGS adipocytes) • mRNA expression analysis in mouse epididymal and subcutaneous WAT • mRNA expression analysis of human adipose tissue and primary human adipocyte cultures • mRNA and protein expression analysis, and gelatin zymography analysis, in murine	[81, 84, 92]

		activity increased during preadipocyte differentiation	3T3F442A preadipocyte cell line	
MMP-10	Stromelysin 2	1. mRNA expressed by adipocyte model 2. mRNA expression increased by exposure to inflammatory conditions	Microarray study in adipocyte model (SBGS adipocytes)	[84]
MMP-11	Stromelysin 3	1. mRNA expressed by murine epididymal and subcutaneous adipose tissue 2. mRNA expression increased in rodent nutritional model of obesity	mRNA expression analysis in mouse epididymal and subcutaneous WAT	[92, 280]
MMP-12	Macrophage elastase	1. mRNA expressed by murine epididymal and subcutaneous adipose tissue 2. mRNA expression increased by exposure to inflammatory conditions 3. mRNA expression increased in rodent genetic and nutritional models of obesity	• Microarray study in adipocyte model (SBGS adipocytes) • mRNA expression analysis in mouse epididymal and subcutaneous WAT	[7, 84, 92]
MMP-13	Collagenase 3	1. mRNA expressed by murine epididymal and subcutaneous adipose tissue 2. mRNA expression increased in rodent nutritional model of obesity	mRNA expression analysis in mouse epididymal and subcutaneous WAT	[92]

MMP-14	MT1-MMP	1. mRNA expressed by murine epididymal and subcutaneous adipose tissue 2. mRNA expression increased in rodent genetic and nutritional models of obesity 3. *Mmp14* null mice have smaller adipocytes than wild-type mice 4. Preadipocytes from *Mmp14* null mice do not differentiate normally in 3D culture media	• mRNA expression analysis in mouse epididymal and subcutaneous WAT • Metabolic studies of mutant rodent models • Analysis of primary rodent adipocyte cultures	[7, 92, 109]
MMP-16	MT3-MMP	1. mRNA expressed by epididymal and subcutaneous adipose tissue 2. mRNA expression decreased in rodent nutritional model of obesity	mRNA expression analysis in mouse epididymal and subcutaneous WAT	[92]
MMP-19		1. mRNA expressed by epididymal adipose tissue 2. mRNA expression increased by exposure to inflammatory conditions 3. mRNA expression increased in rodent genetic and nutritional models of obesity	• Microarray study in adipocyte model (SBGS adipocytes) • mRNA expression analysis in mouse epididymal WAT	[7, 84]
MMP-24	MT5-MMP	1. mRNA expressed by epididymal and subcutaneous adipose tissue	mRNA expression analysis in mouse epididymal and subcutaneous WAT	[281]

		2. mRNA expression decreased in rodent nutritional model of obesity		
ADAM-12	Meltrin-α	1. *Adam12* null mice have fewer adipocytes than wild-type mice when fed a HFD 2. Overexpression of *Adam12* results in increased adipogenesis	Metabolic studies of mutant rodent models	[61]
ADAM-17	TACE	1. *Tace*+/- mice are protected from the metabolic effects of *Insr* haploinsufficiency 2. TAPI-1 (a TACE inhibitor) administration reverses the hyperglycaemia seen in diabetic *Insr*+/- mice 3. *Tace*+/- mice gain less weight and are less insulin resistant than wild-type mice when fed a HFD 4. $Tace^{\Delta Zn/\Delta Zn}$ mice display better glucose tolerance than wild-type mice 5. WAT from *Tace*+/- and $Tace^{\Delta Zn/\Delta Zn}$ mice has smaller adipocytes 6. Modulation of TACE expression affects preadipocyte differentiation	• Metabolic studies of mutant rodent models • Studies using 3T3-L1 preadipocyte models (reduced TACE expression using siRNA, reduced TACE activity using GM6001, increased TACE expression using Lenti-TACE virus transfection) • mRNA and protein expression analysis in human skeletal muscle	[119, 122, 124, 136, 138, 152]

	7. *Tace*+/- mice have reduced sPref-1 levels when fed a HFD as compared to wild-type mice 8. T2DM patients have increased TACE activity in their skeletal muscle		
ADAMTS9	Cluster of SNPs upstream to ADAMTS9 gene is human T2DM susceptibility locus	Meta-analysis of 3 genome-wide association studies	[155]
TIMP-1	1. mRNA expressed by murine epididymal and subcutaneous adipose tissue 2. mRNA expression increased in rodent genetic and nutritional models of obesity	mRNA expression analysis in mouse epididymal and subcutaneous WAT	[7, 281]
TIMP-3	1. mRNA expressed by murine epididymal adipose tissue 2. mRNA expression decreased in rodent genetic and nutritional models of obesity 3. *Timp3* null mice become insulin resistant when fed HFD or crossed with *Insr*+/- mice 4. Reduced skeletal muscle mRNA and protein expression and activity in diabetic *Insr*+/- mice	• mRNA expression analysis in mouse epididymal WAT • Metabolic studies of mutant rodent models • mRNA and protein expression analysis in human skeletal muscle	[7, 136, 138, 152]

	5. T2DM patients have reduced TIMP-3 mRNA and protein levels in their skeletal muscle		
TIMP-4	1. mRNA expressed by murine epididymal and subcutaneous adipose tissue 2. mRNA expression decreased in rodent nutritional model of obesity	mRNA expression analysis in mouse epididymal and subcutaneous WAT	[92]

Table A.3: Summary of the roles metalloproteinases and their tissue inhibitors may play in obesity and metabolic disease, with sources of evidence.

Gene	Mean C_T	SD
Mmp2	21.85	0.55
Timp2	22.93	0.31
Timp1	23.38	0.43
Mmp14	24.59	0.57
Timp3	24.71	0.32
Adam9	25.03	0.38
Adam12	25.55	0.56
Adamts2	26.12	0.65
Timp4	26.44	0.58
Adam10	26.81	0.41
Adam15	27.23	0.43
Adamts1	27.30	0.56
Mmp19	28.09	0.33
Adamts5	28.16	0.63
Mmp3	28.20	0.84
Adamts4	28.60	0.26

Table A.4: mRNA expression of most highly expressed genes in control medium. The top quartile of MP and TIMP genes expressed by primary human adipocytes in low glucose culture medium is shown, ranked by cycling threshold (C_T) values. Mean C_T values from 3 biological replicates of each of 3 independent donors are shown. Standard deviations (SD) for C_T values demonstrate consistent expression levels across replicates and donors (n = 3).

Appendix B:
Functional effects of sDlk-1 and TIMP-3

B.1: Role of Dlk-1 in human adipogenesis

As outlined in Chapter 1, Pref-1 and its human ortholog Dlk-1 are thought to act as antiadipogenic mediators that are activated as a result of the sheddase activity of ADAM-17 (see Chapter 1, section 1.3.3.3). In Chapter 5, TIMP-3 was found to positively regulate basal Dlk-1 shedding (see Chapter 5, section 5.3.1). I therefore proceeded to investigate whether Dlk-1 added to differentiating preadipocyte cultures inhibited adipogenesis in a dose-dependent manner. Primary preadipocytes from one donor were cultured as per standard protocols (see Chapter 2, section 2.2). At the initiation of differentiation and in all following media changes over the course of differentiation, recombinant human soluble (rhs)Dlk-1 (R&D Systems, Minneapolis, MN, USA) was added to proadipogenic medium in a series of concentrations (control [0nM], 5nM, 50nM and 500nM). This concentration curve was chosen following review of the existing literature on the use of soluble (s)Pref-1 in the inhibition of adipogenesis and the product's datasheet. In the only similar study identified, Smas and colleagues added an *E. coli*-expressed sPref-1/glutathione S-transferase (GST) fusion protein to 3T3-L1 culture media at a concentration of 50nM [117]. The datasheet supplied by R&D Systems advises use of rhsDlk-1 at a concentration of 3.3µg/ml – or, given a molecular weight of 50kDa, ~66nM. Therefore, a logarithmic concentration curve was constructed around 50nM.

At the end of differentiation, brightfield light micrographs were obtained (Figure B.1), and the cells were lysed, RNA extracted, reverse transcribed and used in qRT-PCR for adiponectin (*Adipoq*, a marker of adipogenesis [282]) (Figure B.2). Although microscopic examination suggested that rhsDlk-1 had an inhibitory effect on preadipocyte differentiation, this was not clearly seen in expression analysis of *Adipoq*.

Potential further experiments and further analysis that can be performed to better understand the role, if any, of Dlk-1 in human adipogenesis are described in Chapter 6.

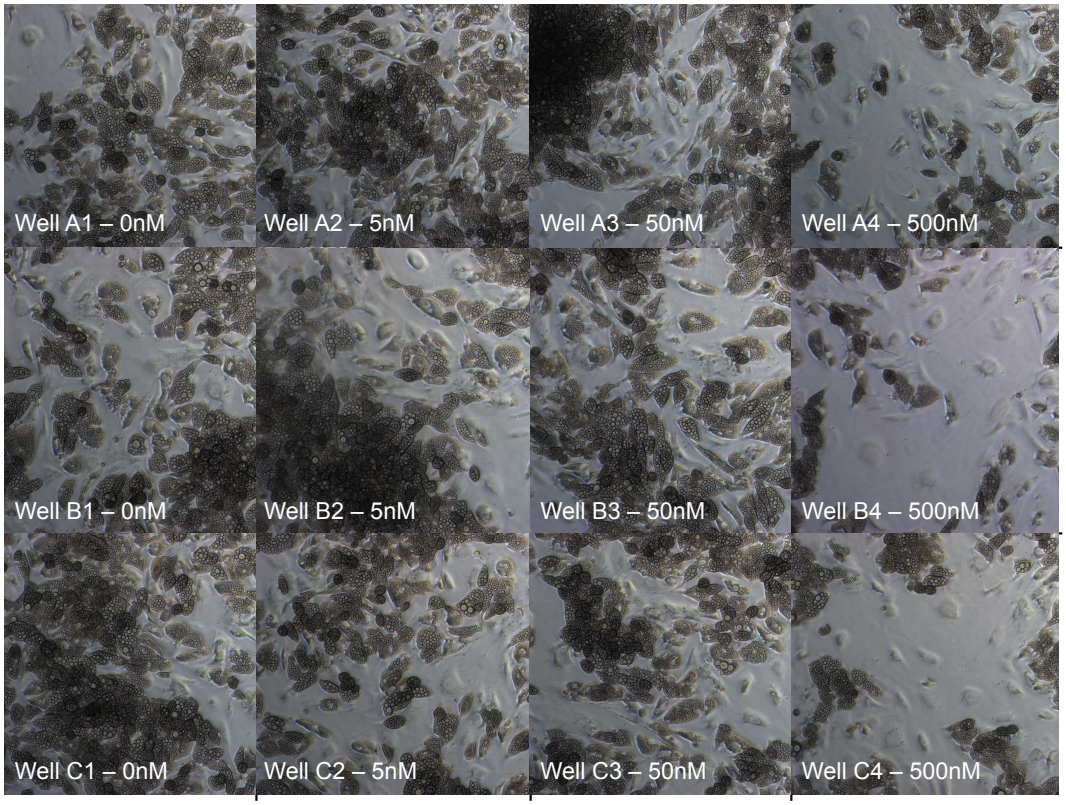

Figure B.1: Representative view, at 10x magnification, of the centre of each well in which cells exposed to different concentrations of rhsDlk-1 were cultured. Image acquired using the Zeiss Axiovert 40 CFL inverted microscope using the AxioVision LE software V4.8 (Carl Zeiss Microscopy, Cambridge, UK).

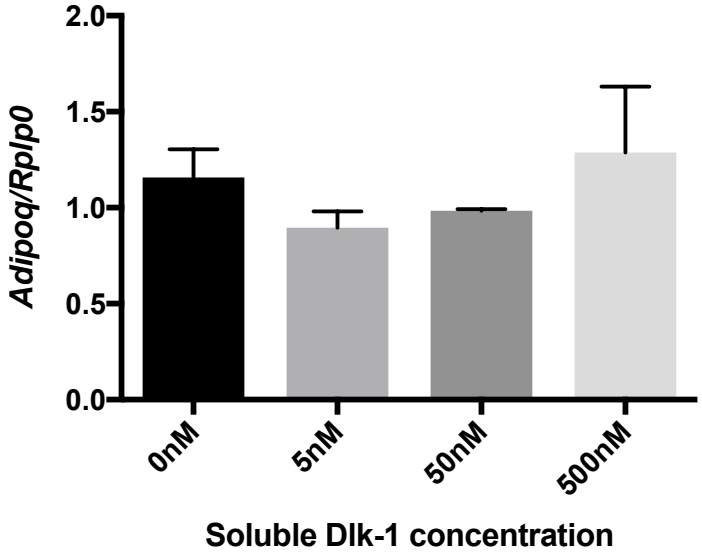

Figure B.2: qRT-PCR for adiponectin (*Adipoq*) expression in adipocytes following addition of rhsDlk-1 does not suggest any antiadipogenic activity. No statistically significant differences were found between the conditions were different concentrations of rhsDlk-1 were added.

B.2: TIMP-3 overexpression in human adipogenesis

Given the hypothesis outlined in Chapter 5 (section 5.4) and Chapter 6, I sought to understand the direct role that TIMP-3 overexpression has in the differentiation of human primary preadipocytes. Cells isolated from three unique donors were transduced with Ad0 and AdT3 adenovirus as described in Chapters 2 and 5, and stimulated with proadipogenic medium. Differentiation was carried out as per standard protocols. After 8 days, differentiation was quantified using the QBT® Fatty Acid Uptake Assay Kit (section 2.3.3) (Figure B.3). Although significant differences were noted in both qualitative (Figure B.3A) and quantitative (Figure B.3B) analysis, a high degree of cell death was noted in the AdT3 condition. Therefore, it remains uncertain whether the smaller number of differentiated cells in this condition reflects decreased adipogenesis or fewer viable cells overall. As discussed in Chapter 6, viability and apoptosis assays may help distinguish between these two situations.

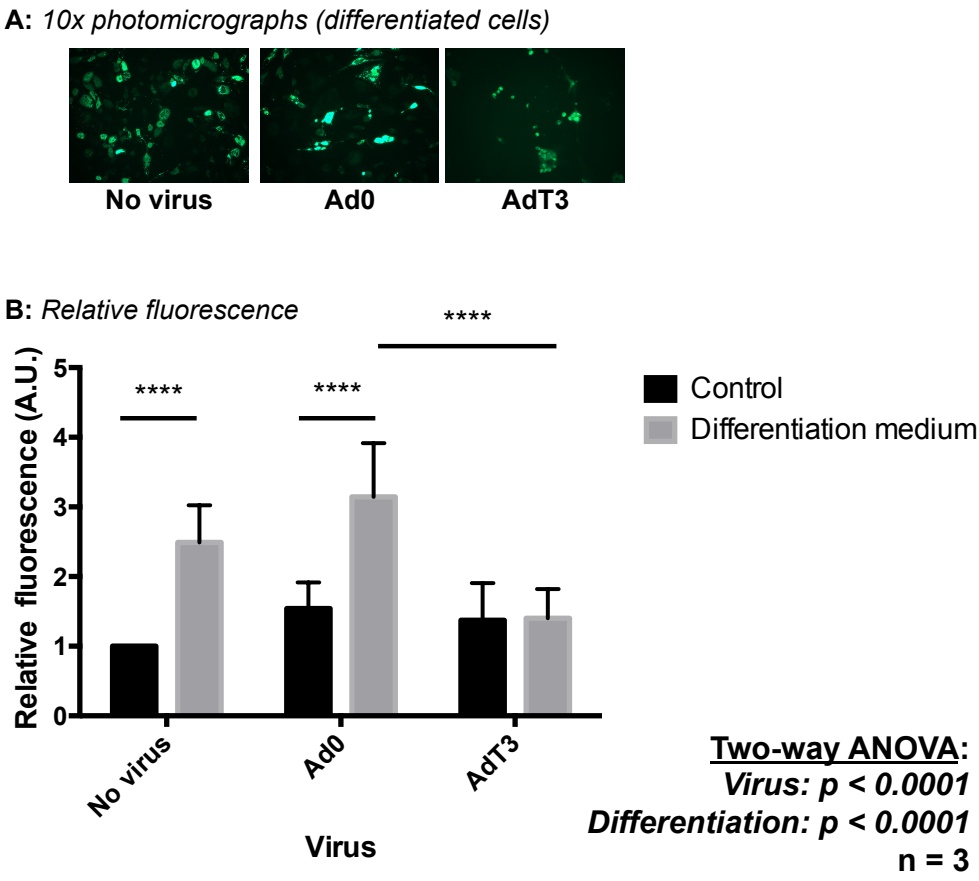

Figure B.3: A) 10x photomicrographs of differentiating preadipocytes following treatment with QBT® lipiphilic fluorescent dye. Image acquired using the Zeiss Axioplan 2ie widefield upright microscope using the AxioVision LE software V4.8 (Carl Zeiss Microscopy, Cambridge, UK). B) Cells treated with QBT® dye were subjected to spectrophotometry to quantify the degree of fluorescent dye uptake. Results are taken from three biological replicates from three unique donors for each condition (mean + SD of thee nine conditions), and normalised to the 'no virus, no differentiation' control (set at 1). Cells appear to have been inhibited from differentiating in the AdT3 condition, but no normalisation for cell viability was performed. (****, $p < 0.0001$)

Bibliography

1. WHO. *Obesity and Overweight Factsheet No. 311*. 2016; Available from: http://www.who.int/mediacentre/factsheets/fs311/en/.
2. Shaw, J.E., R.A. Sicree, and P.Z. Zimmet, *Global estimates of the prevalence of diabetes for 2010 and 2030.* Diabetes Res Clin Pract, 2010. **87**(1): p. 4-14.
3. Xu, X.J., W.J. Pories, L.G. Dohm, and N.B. Ruderman, *What distinguishes adipose tissue of severely obese humans who are insulin sensitive and resistant?* Curr Opin Lipidol, 2013. **24**(1): p. 49-56.
4. J.M., B., T. J.L., and S. L., *Biochemistry*. 5th edition ed. 2002, New York: W. H. Freeman.
5. Rosen, E.D. and B.M. Spiegelman, *Adipocytes as regulators of energy balance and glucose homeostasis.* Nature, 2006. **444**(7121): p. 847-53.
6. van Harmelen, V., T. Skurk, K. Rohrig, Y.M. Lee, M. Halbleib, I. Aprath-Husmann, and H. Hauner, *Effect of BMI and age on adipose tissue cellularity and differentiation capacity in women.* Int J Obes Relat Metab Disord, 2003. **27**(8): p. 889-95.
7. Chavey, C., B. Mari, M.N. Monthouel, S. Bonnafous, P. Anglard, E. Van Obberghen, and S. Tartare-Deckert, *Matrix metalloproteinases are differentially expressed in adipose tissue during obesity and modulate adipocyte differentiation.* J Biol Chem, 2003. **278**(14): p. 11888-96.
8. Hotamisligil, G.S., *Inflammation and metabolic disorders.* Nature, 2006. **444**(7121): p. 860-7.
9. Kahn, S.E., R.L. Hull, and K.M. Utzschneider, *Mechanisms linking obesity to insulin resistance and type 2 diabetes.* Nature, 2006. **444**(7121): p. 840-6.
10. Despres, J.P. and I. Lemieux, *Abdominal obesity and metabolic syndrome.* Nature, 2006. **444**(7121): p. 881-7.
11. Schneider, H.J., H. Glaesmer, J. Klotsche, S. Bohler, H. Lehnert, A.M. Zeiher, W. Marz, D. Pittrow, G.K. Stalla, H.U. Wittchen, and D.S. Group, *Accuracy of anthropometric indicators of obesity to predict cardiovascular risk.* J Clin Endocrinol Metab, 2007. **92**(2): p. 589-94.
12. Garg, A., *Regional adiposity and insulin resistance.* J Clin Endocrinol Metab, 2004. **89**(9): p. 4206-10.
13. Fox, C.S., J.M. Massaro, U. Hoffmann, K.M. Pou, P. Maurovich-Horvat, C.Y. Liu, R.S. Vasan, J.M. Murabito, J.B. Meigs, L.A. Cupples, R.B. D'Agostino, Sr., and C.J. O'Donnell, *Abdominal visceral and subcutaneous adipose tissue compartments: association with metabolic risk factors in the Framingham Heart Study.* Circulation, 2007. **116**(1): p. 39-48.
14. Zhang, M., T. Hu, S. Zhang, and L. Zhou, *Associations of Different Adipose Tissue Depots with Insulin Resistance: A Systematic Review and Meta-analysis of Observational Studies.* Sci Rep, 2015. **5**: p. 18495.
15. Yaskolka Meir, A., L. Tene, N. Cohen, I. Shelef, D. Schwarzfuchs, Y. Gepner, H. Zelicha, M. Rein, N. Bril, D. Serfaty, S. Kenigsbuch, Y. Chassidim, B. Sarusy, D. Dicker, J. Thiery, U. Ceglarek, M. Stumvoll, M. Bluher, M.J. Stampfer, A. Rudich, and I. Shai, *Intrahepatic fat, abdominal adipose tissues, and metabolic state: magnetic resonance imaging study.* Diabetes Metab Res Rev, 2017.
16. Shoelson, S.E., J. Lee, and A.B. Goldfine, *Inflammation and insulin resistance.* J Clin Invest, 2006. **116**(7): p. 1793-801.
17. Xu, H., G.T. Barnes, Q. Yang, G. Tan, D. Yang, C.J. Chou, J. Sole, A. Nichols, J.S. Ross, L.A. Tartaglia, and H. Chen, *Chronic inflammation in fat plays a crucial role in the development of obesity-related insulin resistance.* J Clin Invest, 2003. **112**(12): p. 1821-30.
18. Dandona, P., A. Aljada, and A. Bandyopadhyay, *Inflammation: the link between insulin resistance, obesity and diabetes.* Trends Immunol, 2004. **25**(1): p. 4-7.
19. Saltiel, A.R. and J.M. Olefsky, *Inflammatory mechanisms linking obesity and metabolic disease.* J Clin Invest, 2017. **127**(1): p. 1-4.

20. McLaughlin, T., S.E. Ackerman, L. Shen, and E. Engleman, *Role of innate and adaptive immunity in obesity-associated metabolic disease.* J Clin Invest, 2017. **127**(1): p. 5-13.
21. Festa, A., R. D'Agostino, Jr., R.P. Tracy, and S.M. Haffner, *Elevated levels of acute-phase proteins and plasminogen activator inhibitor-1 predict the development of type 2 diabetes: the insulin resistance atherosclerosis study.* Diabetes, 2002. **51**(4): p. 1131-7.
22. Yudkin, J.S., C.D. Stehouwer, J.J. Emeis, and S.W. Coppack, *C-reactive protein in healthy subjects: associations with obesity, insulin resistance, and endothelial dysfunction: a potential role for cytokines originating from adipose tissue?* Arterioscler Thromb Vasc Biol, 1999. **19**(4): p. 972-8.
23. Crewe, C., Y.A. An, and P.E. Scherer, *The ominous triad of adipose tissue dysfunction: inflammation, fibrosis, and impaired angiogenesis.* J Clin Invest, 2017. **127**(1): p. 74-82.
24. Weisberg, S.P., D. McCann, M. Desai, M. Rosenbaum, R.L. Leibel, and A.W. Ferrante, Jr., *Obesity is associated with macrophage accumulation in adipose tissue.* J Clin Invest, 2003. **112**(12): p. 1796-808.
25. Wentworth, J.M., G. Naselli, W.A. Brown, L. Doyle, B. Phipson, G.K. Smyth, M. Wabitsch, P.E. O'Brien, and L.C. Harrison, *Pro-inflammatory CD11c+CD206+ adipose tissue macrophages are associated with insulin resistance in human obesity.* Diabetes, 2010. **59**(7): p. 1648-56.
26. Wu, H., S. Ghosh, X.D. Perrard, L. Feng, G.E. Garcia, J.L. Perrard, J.F. Sweeney, L.E. Peterson, L. Chan, C.W. Smith, and C.M. Ballantyne, *T-cell accumulation and regulated on activation, normal T cell expressed and secreted upregulation in adipose tissue in obesity.* Circulation, 2007. **115**(8): p. 1029-38.
27. Christiansen, T., B. Richelsen, and J.M. Bruun, *Monocyte chemoattractant protein-1 is produced in isolated adipocytes, associated with adiposity and reduced after weight loss in morbid obese subjects.* Int J Obes (Lond), 2005. **29**(1): p. 146-50.
28. Yudkin, J.S., M. Kumari, S.E. Humphries, and V. Mohamed-Ali, *Inflammation, obesity, stress and coronary heart disease: is interleukin-6 the link?* Atherosclerosis, 2000. **148**(2): p. 209-14.
29. Feinstein, R., H. Kanety, M.Z. Papa, B. Lunenfeld, and A. Karasik, *Tumor necrosis factor-alpha suppresses insulin-induced tyrosine phosphorylation of insulin receptor and its substrates.* J Biol Chem, 1993. **268**(35): p. 26055-8.
30. Hofmann, C., K. Lorenz, S.S. Braithwaite, J.R. Colca, B.J. Palazuk, G.S. Hotamisligil, and B.M. Spiegelman, *Altered gene expression for tumor necrosis factor-alpha and its receptors during drug and dietary modulation of insulin resistance.* Endocrinology, 1994. **134**(1): p. 264-70.
31. Hotamisligil, G.S., N.S. Shargill, and B.M. Spiegelman, *Adipose expression of tumor necrosis factor-alpha: direct role in obesity-linked insulin resistance.* Science, 1993. **259**(5091): p. 87-91.
32. Slawik, M. and A.J. Vidal-Puig, *Adipose tissue expandability and the metabolic syndrome.* Genes Nutr, 2007. **2**(1): p. 41-5.
33. Bindlish, S., L.S. Presswala, and F. Schwartz, *Lipodystrophy: Syndrome of severe insulin resistance.* Postgrad Med, 2015. **127**(5): p. 511-6.
34. Russell, A.P., *Lipotoxicity: the obese and endurance-trained paradox.* Int J Obes Relat Metab Disord, 2004. **28 Suppl 4**: p. S66-71.
35. Slawik, M. and A.J. Vidal-Puig, *Lipotoxicity, overnutrition and energy metabolism in aging.* Ageing Res Rev, 2006. **5**(2): p. 144-64.
36. Eldor, R. and I. Raz, *Lipotoxicity versus adipotoxicity—The deleterious effects of adipose tissue on beta cells in the pathogenesis of type 2 diabetes* Diabetes Res Clin Pract, 2006. **74S**(2): p. S3-S8.
37. Calzadilla Bertot, L. and L.A. Adams, *The Natural Course of Non-Alcoholic Fatty Liver Disease.* Int J Mol Sci, 2016. **17**(5).

38. Lilla, J., D. Stickens, and Z. Werb, *Metalloproteases and adipogenesis: a weighty subject.* Am J Pathol, 2002. **160**(5): p. 1551-4.
39. Mariman, E.C. and P. Wang, *Adipocyte extracellular matrix composition, dynamics and role in obesity.* Cell Mol Life Sci, 2010. **67**(8): p. 1277-92.
40. Sun, K., C.M. Kusminski, and P.E. Scherer, *Adipose tissue remodeling and obesity.* J Clin Invest, 2011. **121**(6): p. 2094-101.
41. Smas, C.M. and H.S. Sul, *Control of adipocyte differentiation.* Biochem J, 1995. **309 (Pt 3)**: p. 697-710.
42. Divoux, A. and K. Clement, *Architecture and the extracellular matrix: the still unappreciated components of the adipose tissue.* Obes Rev, 2011. **12**(5): p. e494-503.
43. Napolitano, L., *The Differentiation of White Adipose Cells. An Electron Microscope Study.* J Cell Biol, 1963. **18**: p. 663-79.
44. Aikio, M., H. Elamaa, D. Vicente, V. Izzi, I. Kaur, L. Seppinen, H.E. Speedy, D. Kaminska, S. Kuusisto, R. Sormunen, R. Heljasvaara, E.L. Jones, M. Muilu, M. Jauhiainen, J. Pihlajamaki, M.J. Savolainen, C.C. Shoulders, and T. Pihlajaniemi, *Specific collagen XVIII isoforms promote adipose tissue accrual via mechanisms determining adipocyte number and affect fat deposition.* Proc Natl Acad Sci U S A, 2014.
45. Khan, T., E.S. Muise, P. Iyengar, Z.V. Wang, M. Chandalia, N. Abate, B.B. Zhang, P. Bonaldo, S. Chua, and P.E. Scherer, *Metabolic dysregulation and adipose tissue fibrosis: role of collagen VI.* Mol Cell Biol, 2009. **29**(6): p. 1575-91.
46. DeFronzo, R.A., *Dysfunctional fat cells, lipotoxicity and type 2 diabetes.* Int J Clin Pract Suppl, 2004(143): p. 9-21.
47. Lin, T.H. Chun, and L. Kang, *Adipose extracellular matrix remodelling in obesity and insulin resistance.* Biochem Pharmacol, 2016. **119**: p. 8-16.
48. Birbrair, A., T. Zhang, D.C. Files, S. Mannava, T. Smith, Z.M. Wang, M.L. Messi, A. Mintz, and O. Delbono, *Type-1 pericytes accumulate after tissue injury and produce collagen in an organ-dependent manner.* Stem Cell Res Ther, 2014. **5**(6): p. 122.
49. Pellicoro, A., P. Ramachandran, J.P. Iredale, and J.A. Fallowfield, *Liver fibrosis and repair: immune regulation of wound healing in a solid organ.* Nat Rev Immunol, 2014. **14**(3): p. 181-94.
50. Sgalla, G., A. Biffi, and L. Richeldi, *Idiopathic pulmonary fibrosis: Diagnosis, epidemiology and natural history.* Respirology, 2016. **21**(3): p. 427-37.
51. Kadler, K.E., D.F. Holmes, J.A. Trotter, and J.A. Chapman, *Collagen fibril formation.* Biochem J, 1996. **316 (Pt 1)**: p. 1-11.
52. Alkhouli, N., J. Mansfield, E. Green, J. Bell, B. Knight, N. Liversedge, J.C. Tham, R. Welbourn, A.C. Shore, K. Kos, and C.P. Winlove, *The mechanical properties of human adipose tissues and their relationships to the structure and composition of the extracellular matrix.* Am J Physiol Endocrinol Metab, 2013. **305**(12): p. E1427-35.
53. Divoux, A., J. Tordjman, D. Lacasa, N. Veyrie, D. Hugol, A. Aissat, A. Basdevant, M. Guerre-Millo, C. Poitou, J.D. Zucker, P. Bedossa, and K. Clement, *Fibrosis in human adipose tissue: composition, distribution, and link with lipid metabolism and fat mass loss.* Diabetes, 2010. **59**(11): p. 2817-25.
54. Tam, C.S., J.D. Covington, S. Bajpeyi, Y. Tchoukalova, D. Burk, D.L. Johannsen, C.M. Zingaretti, S. Cinti, and E. Ravussin, *Weight gain reveals dramatic increases in skeletal muscle extracellular matrix remodeling.* J Clin Endocrinol Metab, 2014. **99**(5): p. 1749-57.
55. Bradshaw, A.D., D.C. Graves, K. Motamed, and E.H. Sage, *SPARC-null mice exhibit increased adiposity without significant differences in overall body weight.* Proc Natl Acad Sci U S A, 2003. **100**(10): p. 6045-50.
56. Kos, K. and J.P. Wilding, *SPARC: a key player in the pathologies associated with obesity and diabetes.* Nat Rev Endocrinol, 2010. **6**(4): p. 225-35.
57. Marcelin, G., A. Ferreira, Y. Liu, M. Atlan, J. Aron-Wisnewsky, V. Pelloux, Y. Botbol, M. Ambrosini, M. Fradet, C. Rouault, C. Henegar, J.S. Hulot, C. Poitou, A. Torcivia,

R. Nail-Barthelemy, J.C. Bichet, E.L. Gautier, and K. Clement, *A PDGFRalpha-Mediated Switch toward CD9high Adipocyte Progenitors Controls Obesity-Induced Adipose Tissue Fibrosis.* Cell Metab, 2017. **25**(3): p. 673-685.
58. Parks, W.C., C.L. Wilson, and Y.S. Lopez-Boado, *Matrix metalloproteinases as modulators of inflammation and innate immunity.* Nat Rev Immunol, 2004. **4**(8): p. 617-29.
59. Stocker, W., F. Grams, U. Baumann, P. Reinemer, F.X. Gomis-Ruth, D.B. McKay, and W. Bode, *The metzincins--topological and sequential relations between the astacins, adamalysins, serralysins, and matrixins (collagenases) define a superfamily of zinc-peptidases.* Protein Sci, 1995. **4**(5): p. 823-40.
60. Kessenbrock, K., V. Plaks, and Z. Werb, *Matrix metalloproteinases: regulators of the tumor microenvironment.* Cell, 2010. **141**(1): p. 52-67.
61. Edwards, D.R., M.M. Handsley, and C.J. Pennington, *The ADAM metalloproteinases.* Mol Aspects Med, 2008. **29**(5): p. 258-89.
62. Murphy, G., *The ADAMs: signalling scissors in the tumour microenvironment.* Nat Rev Cancer, 2008. **8**(12): p. 929-41.
63. Hooper, N.M., *Families of zinc metalloproteases.* FEBS Lett, 1994. **354**(1): p. 1-6.
64. Gomis-Ruth, F.X., *Structural aspects of the metzincin clan of metalloendopeptidases.* Mol Biotechnol, 2003. **24**(2): p. 157-202.
65. Bertini, I., V. Calderone, M. Fragai, C. Luchinat, S. Mangani, and B. Terni, *Crystal structure of the catalytic domain of human matrix metalloproteinase 10.* J Mol Biol, 2004. **336**(3): p. 707-16.
66. Ouellette, A.J. and M.E. Selsted, *Paneth cell defensins: endogenous peptide components of intestinal host defense.* Faseb J, 1996. **10**(11): p. 1280-9.
67. Pilcher, B.K., J.A. Dumin, B.D. Sudbeck, S.M. Krane, H.G. Welgus, and W.C. Parks, *The activity of collagenase-1 is required for keratinocyte migration on a type I collagen matrix.* J Cell Biol, 1997. **137**(6): p. 1445-57.
68. Corry, D.B., A. Kiss, L.Z. Song, L. Song, J. Xu, S.H. Lee, Z. Werb, and F. Kheradmand, *Overlapping and independent contributions of MMP2 and MMP9 to lung allergic inflammatory cell egression through decreased CC chemokines.* Faseb J, 2004. **18**(9): p. 995-7.
69. McQuibban, G.A., J.H. Gong, J.P. Wong, J.L. Wallace, I. Clark-Lewis, and C.M. Overall, *Matrix metalloproteinase processing of monocyte chemoattractant proteins generates CC chemokine receptor antagonists with anti-inflammatory properties in vivo.* Blood, 2002. **100**(4): p. 1160-7.
70. Salter, R.C., T.G. Ashlin, A.P. Kwan, and D.P. Ramji, *ADAMTS proteases: key roles in atherosclerosis?* J Mol Med (Berl), 2010. **88**(12): p. 1203-11.
71. Yan, C. and D.D. Boyd, *Regulation of matrix metalloproteinase gene expression.* J Cell Physiol, 2007. **211**(1): p. 19-26.
72. Van den Steen, P.E., B. Dubois, I. Nelissen, P.M. Rudd, R.A. Dwek, and G. Opdenakker, *Biochemistry and molecular biology of gelatinase B or matrix metalloproteinase-9 (MMP-9).* Crit Rev Biochem Mol Biol, 2002. **37**(6): p. 375-536.
73. Dranse, H.J., S. Muruganandan, J.P. Fawcett, and C.J. Sinal, *Adipocyte-secreted chemerin is processed to a variety of isoforms and influences MMP3 and chemokine secretion through an NFkB-dependent mechanism.* Mol Cell Endocrinol, 2016. **436**: p. 114-29.
74. Eck, S.M., J.S. Blackburn, A.C. Schmucker, P.S. Burrage, and C.E. Brinckerhoff, *Matrix metalloproteinase and G protein coupled receptors: co-conspirators in the pathogenesis of autoimmune disease and cancer.* J Autoimmun, 2009. **33**(3-4): p. 214-21.
75. Blobel, C.P., *ADAMs: key components in EGFR signalling and development.* Nat Rev Mol Cell Biol, 2005. **6**(1): p. 32-43.
76. Murphy, G., H. Stanton, S. Cowell, G. Butler, V. Knauper, S. Atkinson, and J. Gavrilovic, *Mechanisms for pro matrix metalloproteinase activation.* APMIS, 1999. **107**(1): p. 38-44.

77. Toth, M., M.M. Bernardo, D.C. Gervasi, P.D. Soloway, Z. Wang, H.F. Bigg, C.M. Overall, Y.A. DeClerck, H. Tschesche, M.L. Cher, S. Brown, S. Mobashery, and R. Fridman, *Tissue inhibitor of metalloproteinase (TIMP)-2 acts synergistically with synthetic matrix metalloproteinase (MMP) inhibitors but not with TIMP-4 to enhance the (Membrane type 1)-MMP-dependent activation of pro-MMP-2.* J Biol Chem, 2000. **275**(52): p. 41415-23.
78. Murphy, G., *Tissue inhibitors of metalloproteinases.* Genome Biol, 2011. **12**(11): p. 233.
79. Green, H. and O. Kehinde, *Sublines of mouse 3T3 cells that accumulate lipid.* Cell, 1974. **1**(3): p. 113-116.
80. Croissandeau, G., M. Chretien, and M. Mbikay, *Involvement of matrix metalloproteinases in the adipose conversion of 3T3-L1 preadipocytes.* Biochem J, 2002. **364**(Pt 3): p. 739-46.
81. Bouloumie, A., C. Sengenes, G. Portolan, J. Galitzky, and M. Lafontan, *Adipocyte produces matrix metalloproteinases 2 and 9: involvement in adipose differentiation.* Diabetes, 2001. **50**(9): p. 2080-6.
82. Kralisch, S., U. Lossner, M. Bluher, R. Paschke, M. Stumvoll, and M. Fasshauer, *Tissue inhibitor of metalloproteinase 1 expression and secretion are induced by beta-adrenergic stimulation in 3T3-L1 adipocytes.* J Endocrinol, 2006. **189**(3): p. 665-70.
83. Wabitsch, M., R.E. Brenner, I. Melzner, M. Braun, P. Moller, E. Heinze, K.M. Debatin, and H. Hauner, *Characterization of a human preadipocyte cell strain with high capacity for adipose differentiation.* Int J Obes Relat Metab Disord, 2001. **25**(1): p. 8-15.
84. O'Hara, A., F.L. Lim, D.J. Mazzatti, and P. Trayhurn, *Microarray analysis identifies matrix metalloproteinases (MMPs) as key genes whose expression is up-regulated in human adipocytes by macrophage-conditioned medium.* Pflugers Arch, 2009. **458**(6): p. 1103-14.
85. O'Hara, A., F.L. Lim, D.J. Mazzatti, and P. Trayhurn, *Stimulation of inflammatory gene expression in human preadipocytes by macrophage-conditioned medium: upregulation of IL-6 production by macrophage-derived IL-1beta.* Mol Cell Endocrinol, 2012. **349**(2): p. 239-47.
86. Brown, L.M., H.L. Fox, S.A. Hazen, K.F. LaNoue, S.R. Rannels, and C.J. Lynch, *Role of the matrixin MMP-2 in multicellular organization of adipocytes cultured in basement membrane components.* Am J Physiol, 1997. **272**(3 Pt 1): p. C937-49.
87. Fenech, M., T.E. Swingler, J. Gavrilovic, M. Sampson, and J.J. Turner, *The role of metalloproteinases and their inhibitors in adipose tissue inflammation and the development of type 2 diabetes.* Endocrine Abstracts, 2012. **28**: p. P164.
88. Gao, D. and C. Bing, *Macrophage-induced expression and release of matrix metalloproteinase 1 and 3 by human preadipocytes is mediated by IL-1beta via activation of MAPK signaling.* J Cell Physiol, 2011. **226**(11): p. 2869-80.
89. Lijnen, H.R., E. Maquoi, P. Holvoet, A. Mertens, F. Lupu, P. Morange, M.C. Alessi, and I. Juhan-Vague, *Adipose tissue expression of gelatinases in mouse models of obesity.* Thromb Haemost, 2001. **85**(6): p. 1111-6.
90. Doering, C.H., J.G. Shire, S. Kessler, and R.B. Clayton, *Genetic and biochemical studies of the adrenal lipid depletion phenotype in mice.* Biochem Genet, 1973. **8**(1): p. 101-11.
91. Rossmeisl, M., J.S. Rim, R.A. Koza, and L.P. Kozak, *Variation in type 2 diabetes--related traits in mouse strains susceptible to diet-induced obesity.* Diabetes, 2003. **52**(8): p. 1958-66.
92. Maquoi, E., C. Munaut, A. Colige, D. Collen, and H.R. Lijnen, *Modulation of adipose tissue expression of murine matrix metalloproteinases and their tissue inhibitors with obesity.* Diabetes, 2002. **51**(4): p. 1093-101.
93. Meissburger, B., L. Stachorski, E. Roder, G. Rudofsky, and C. Wolfrum, *Tissue inhibitor of matrix metalloproteinase 1 (TIMP1) controls adipogenesis in obesity in mice and in humans.* Diabetologia, 2011. **54**(6): p. 1468-79.

94. Van Hul, M. and H.R. Lijnen, *Effect of weight loss on gelatinase levels in obese mice.* Clin Exp Pharmacol Physiol, 2011. **38**(9): p. 647-9.
95. Moreno-Navarrete, J.M. and J.M. Fernandez-Real, *Adipocyte Differentiation*, in *Adipose Tissue Biology*, M.E. Symonds, Editor. 2012, Springer. p. 17-38.
96. Bernot, D., E. Barruet, M. Poggi, B. Bonardo, M.C. Alessi, and F. Peiretti, *Down-regulation of tissue inhibitor of metalloproteinase-3 (TIMP-3) expression is necessary for adipocyte differentiation.* J Biol Chem, 2010. **285**(9): p. 6508-14.
97. Bauters, D., M. Van Hul, and H.R. Lijnen, *Gelatinase B (MMP-9) gene silencing does not affect murine preadipocyte differentiation.* Adipocyte, 2014. **3**(1): p. 50-3.
98. Alexander, C.M., S. Selvarajan, J. Mudgett, and Z. Werb, *Stromelysin-1 regulates adipogenesis during mammary gland involution.* J Cell Biol, 2001. **152**(4): p. 693-703.
99. Meissburger, B., J. Ukropec, E. Roeder, N. Beaton, M. Geiger, D. Teupser, B. Civan, W. Langhans, P.P. Nawroth, D. Gasperikova, G. Rudofsky, and C. Wolfrum, *Adipogenesis and insulin sensitivity in obesity are regulated by retinoid-related orphan receptor gamma.* EMBO Mol Med, 2011. **3**(11): p. 637-51.
100. Sadowski, T. and J. Steinmeyer, *Effects of non-steroidal antiinflammatory drugs and dexamethasone on the activity and expression of matrix metalloproteinase-1, matrix metalloproteinase-3 and tissue inhibitor of metalloproteinases-1 by bovine articular chondrocytes.* Osteoarthritis Cartilage, 2001. **9**(5): p. 407-15.
101. Richardson, D.W. and G.R. Dodge, *Dose-dependent effects of corticosteroids on the expression of matrix-related genes in normal and cytokine-treated articular chondrocytes.* Inflamm Res, 2003. **52**(1): p. 39-49.
102. Yamazaki, T., T. Yokoyama, H. Akatsu, T. Tukiyama, and T. Tokiwa, *Phenotypic characterization of a human synovial sarcoma cell line, SW982, and its response to dexamethasone.* In Vitro Cell Dev Biol Anim, 2003. **39**(8-9): p. 337-9.
103. Kylmaniemi, M., A. Oikarinen, K. Oikarinen, and T. Salo, *Effects of dexamethasone and cell proliferation on the expression of matrix metalloproteinases in human mucosal normal and malignant cells.* J Dent Res, 1996. **75**(3): p. 919-26.
104. Kawaguchi, N., C. Sundberg, M. Kveiborg, B. Moghadaszadeh, M. Asmar, N. Dietrich, C.K. Thodeti, F.C. Nielsen, P. Moller, A.M. Mercurio, R. Albrechtsen, and U.M. Wewer, *ADAM12 induces actin cytoskeleton and extracellular matrix reorganization during early adipocyte differentiation by regulating beta1 integrin function.* J Cell Sci, 2003. **116**(Pt 19): p. 3893-904.
105. Pierleoni, C., F. Verdenelli, M. Castellucci, and S. Cinti, *Fibronectins and basal lamina molecules expression in human subcutaneous white adipose tissue.* Eur J Histochem, 1998. **42**(3): p. 183-8.
106. Antras, J., F. Hilliou, G. Redziniak, and J. Pairault, *Decreased biosynthesis of actin and cellular fibronectin during adipose conversion of 3T3-F442A cells. Reorganization of the cytoarchitecture and extracellular matrix fibronectin.* Biol Cell, 1989. **66**(3): p. 247-54.
107. Kawaguchi, N., X. Xu, R. Tajima, P. Kronqvist, C. Sundberg, F. Loechel, R. Albrechtsen, and U.M. Wewer, *ADAM 12 protease induces adipogenesis in transgenic mice.* Am J Pathol, 2002. **160**(5): p. 1895-903.
108. Kurisaki, T., A. Masuda, K. Sudo, J. Sakagami, S. Higashiyama, Y. Matsuda, A. Nagabukuro, A. Tsuji, Y. Nabeshima, M. Asano, Y. Iwakura, and A. Sehara-Fujisawa, *Phenotypic analysis of Meltrin alpha (ADAM12)-deficient mice: involvement of Meltrin alpha in adipogenesis and myogenesis.* Mol Cell Biol, 2003. **23**(1): p. 55-61.
109. Chun, T.H., K.B. Hotary, F. Sabeh, A.R. Saltiel, E.D. Allen, and S.J. Weiss, *A pericellular collagenase directs the 3-dimensional development of white adipose tissue.* Cell, 2006. **125**(3): p. 577-91.
110. Chun, T.H., M. Inoue, H. Morisaki, I. Yamanaka, Y. Miyamoto, T. Okamura, K. Sato-Kusubata, and S.J. Weiss, *Genetic link between obesity and MMP14-dependent adipogenic collagen turnover.* Diabetes, 2010. **59**(10): p. 2484-94.

111. Tortorella, M.D., R.Q. Liu, T. Burn, R.C. Newton, and E. Arner, *Characterization of human aggrecanase 2 (ADAM-TS5): substrate specificity studies and comparison with aggrecanase 1 (ADAM-TS4).* Matrix Biol, 2002. **21**(6): p. 499-511.
112. Gorski, D.J., W. Xiao, J. Li, W. Luo, M. Lauer, J. Kisiday, A. Plaas, and J. Sandy, *Deletion of ADAMTS5 does not affect aggrecan or versican degradation but promotes glucose uptake and proteoglycan synthesis in murine adipose derived stromal cells.* Matrix Biol, 2015. **47**: p. 66-84.
113. Rose-John, S., *ADAM17, shedding, TACE as therapeutic targets.* Pharmacol Res, 2013. **71**: p. 19-22.
114. Horiuchi, K., *A brief history of tumor necrosis factor alpha--converting enzyme: an overview of ectodomain shedding.* Keio J Med, 2013. **62**(1): p. 29-36.
115. Jing, K., J.Y. Heo, K.S. Song, K.S. Seo, J.H. Park, J.S. Kim, Y.J. Jung, D.Y. Jo, G.R. Kweon, W.H. Yoon, B.D. Hwang, K. Lim, and J.I. Park, *Expression regulation and function of Pref-1 during adipogenesis of human mesenchymal stem cells (MSCs).* Biochim Biophys Acta, 2009. **1791**(8): p. 816-26.
116. Appelbe, O.K., A. Yevtodiyenko, H. Muniz-Talavera, and J.V. Schmidt, *Conditional deletions refine the embryonic requirement for Dlk1.* Mech Dev, 2013. **130**(2-3): p. 143-59.
117. Smas, C.M. and H.S. Sul, *Pref-1, a protein containing EGF-like repeats, inhibits adipocyte differentiation.* Cell, 1993. **73**(4): p. 725-34.
118. Wang, Y., C. Hudak, and H.S. Sul, *Role of preadipocyte factor 1 in adipocyte differentiation.* Clin Lipidol, 2010. **5**(1): p. 109-115.
119. Wang, Y. and H.S. Sul, *Ectodomain shedding of preadipocyte factor 1 (Pref-1) by tumor necrosis factor alpha converting enzyme (TACE) and inhibition of adipocyte differentiation.* Mol Cell Biol, 2006. **26**(14): p. 5421-35.
120. Mei, B., L. Zhao, L. Chen, and H.S. Sul, *Only the large soluble form of preadipocyte factor-1 (Pref-1), but not the small soluble and membrane forms, inhibits adipocyte differentiation: role of alternative splicing.* Biochem J, 2002. **364**(Pt 1): p. 137-44.
121. Mortensen, S.B., C.H. Jensen, M. Schneider, M. Thomassen, T.A. Kruse, J. Laborda, S.P. Sheikh, and D.C. Andersen, *Membrane-tethered delta-like 1 homolog (DLK1) restricts adipose tissue size by inhibiting preadipocyte proliferation.* Diabetes, 2012. **61**(11): p. 2814-22.
122. Serino, M., R. Menghini, L. Fiorentino, R. Amoruso, A. Mauriello, D. Lauro, P. Sbraccia, M.L. Hribal, R. Lauro, and M. Federici, *Mice heterozygous for tumor necrosis factor-alpha converting enzyme are protected from obesity-induced insulin resistance and diabetes.* Diabetes, 2007. **56**(10): p. 2541-6.
123. Lee, K., J.A. Villena, Y.S. Moon, K.H. Kim, S. Lee, C. Kang, and H.S. Sul, *Inhibition of adipogenesis and development of glucose intolerance by soluble preadipocyte factor-1 (Pref-1).* J Clin Invest, 2003. **111**(4): p. 453-61.
124. Gelling, R.W., W. Yan, S. Al-Noori, A. Pardini, G.J. Morton, K. Ogimoto, M.W. Schwartz, and P.J. Dempsey, *Deficiency of TNFalpha converting enzyme (TACE/ADAM17) causes a lean, hypermetabolic phenotype in mice.* Endocrinology, 2008. **149**(12): p. 6053-64.
125. Moon, Y.S., C.M. Smas, K. Lee, J.A. Villena, K.H. Kim, E.J. Yun, and H.S. Sul, *Mice lacking paternally expressed Pref-1/Dlk1 display growth retardation and accelerated adiposity.* Mol Cell Biol, 2002. **22**(15): p. 5585-92.
126. Wang, Y., L. Zhao, C. Smas, and H.S. Sul, *Pref-1 interacts with fibronectin to inhibit adipocyte differentiation.* Mol Cell Biol, 2010. **30**(14): p. 3480-92.
127. Kim, K.A., J.H. Kim, Y. Wang, and H.S. Sul, *Pref-1 (preadipocyte factor 1) activates the MEK/extracellular signal-regulated kinase pathway to inhibit adipocyte differentiation.* Mol Cell Biol, 2007. **27**(6): p. 2294-308.
128. Sul, H.S., *Minireview: Pref-1: role in adipogenesis and mesenchymal cell fate.* Mol Endocrinol, 2009. **23**(11): p. 1717-25.

129. Isakson, P., A. Hammarstedt, B. Gustafson, and U. Smith, *Impaired preadipocyte differentiation in human abdominal obesity: role of Wnt, tumor necrosis factor-alpha, and inflammation.* Diabetes, 2009. **58**(7): p. 1550-7.
130. Van Hul, M. and H.R. Lijnen, *A functional role of gelatinase A in the development of nutritionally induced obesity in mice.* J Thromb Haemost, 2008. **6**(7): p. 1198-206.
131. Van Hul, M., H. Piccard, and H.R. Lijnen, *Gelatinase B (MMP-9) deficiency does not affect murine adipose tissue development.* Thromb Haemost, 2010. **104**(1): p. 165-71.
132. Lijnen, H.R., H.B. Van, L. Frederix, M.C. Rio, and D. Collen, *Adipocyte hypertrophy in stromelysin-3 deficient mice with nutritionally induced obesity.* Thromb Haemost, 2002. **87**(3): p. 530-5.
133. Pendas, A.M., A.R. Folgueras, E. Llano, J. Caterina, F. Frerard, F. Rodriguez, A. Astudillo, A. Noel, H. Birkedal-Hansen, and C. Lopez-Otin, *Diet-induced obesity and reduced skin cancer susceptibility in matrix metalloproteinase 19-deficient mice.* Mol Cell Biol, 2004. **24**(12): p. 5304-13.
134. Bauters, D., M. Van Hul, and H.R. Lijnen, *Macrophage elastase (MMP-12) in expanding murine adipose tissue.* Biochim Biophys Acta, 2013. **1830**(4): p. 2954-9.
135. Masaki, M., T. Kurisaki, K. Shirakawa, and A. Sehara-Fujisawa, *Role of meltrin {alpha} (ADAM12) in obesity induced by high- fat diet.* Endocrinology, 2005. **146**(4): p. 1752-63.
136. Menghini, R., S. Menini, R. Amoruso, L. Fiorentino, V. Casagrande, V. Marzano, F. Tornei, P. Bertucci, C. Iacobini, M. Serino, O. Porzio, M.L. Hribal, F. Folli, R. Khokha, A. Urbani, R. Lauro, G. Pugliese, and M. Federici, *Tissue inhibitor of metalloproteinase 3 deficiency causes hepatic steatosis and adipose tissue inflammation in mice.* Gastroenterology, 2009. **136**(2): p. 663-72 e4.
137. Wree, A., A. Kahraman, G. Gerken, and A. Canbay, *Obesity affects the liver - the link between adipocytes and hepatocytes.* Digestion, 2011. **83**(1-2): p. 124-33.
138. Federici, M., M.L. Hribal, R. Menghini, H. Kanno, V. Marchetti, O. Porzio, S.W. Sunnarborg, S. Rizza, M. Serino, V. Cunsolo, D. Lauro, A. Mauriello, D.S. Smookler, P. Sbraccia, G. Sesti, D.C. Lee, R. Khokha, D. Accili, and R. Lauro, *Timp3 deficiency in insulin receptor-haploinsufficient mice promotes diabetes and vascular inflammation via increased TNF-alpha.* J Clin Invest, 2005. **115**(12): p. 3494-505.
139. Jackson, L.F., T.H. Qiu, S.W. Sunnarborg, A. Chang, C. Zhang, C. Patterson, and D.C. Lee, *Defective valvulogenesis in HB-EGF and TACE-null mice is associated with aberrant BMP signaling.* EMBO J, 2003. **22**(11): p. 2704-16.
140. Kaneko, H., T. Anzai, K. Horiuchi, K. Morimoto, A. Anzai, T. Nagai, Y. Sugano, Y. Maekawa, H. Itoh, T. Yoshikawa, Y. Okada, S. Ogawa, and K. Fukuda, *Tumor necrosis factor-alpha converting enzyme inactivation ameliorates high-fat diet-induced insulin resistance and altered energy homeostasis.* Circ J, 2011. **75**(10): p. 2482-90.
141. Lijnen, H.R., D. Demeulemeester, B. Van Hoef, D. Collen, and E. Maquoi, *Deficiency of tissue inhibitor of matrix metalloproteinase-1 (TIMP-1) impairs nutritionally induced obesity in mice.* Thromb Haemost, 2003. **89**(2): p. 249-55.
142. Dubois, S.G., Y.D. Tchoukalova, L.K. Heilbronn, J.B. Albu, D.E. Kelley, S.R. Smith, X. Fang, and E. Ravussin, *Potential role of increased matrix metalloproteinase-2 (MMP2) transcription in impaired adipogenesis in type 2 diabetes mellitus.* Biochem Biophys Res Commun, 2008. **367**(4): p. 725-8.
143. Derosa, G., I. Ferrari, A. D'Angelo, C. Tinelli, S.A. Salvadeo, L. Ciccarelli, M.N. Piccinni, A. Gravina, F. Ramondetti, P. Maffioli, and A.F. Cicero, *Matrix metalloproteinase-2 and -9 levels in obese patients.* Endothelium, 2008. **15**(4): p. 219-24.
144. Ghanim, H., A. Aljada, D. Hofmeyer, T. Syed, P. Mohanty, and P. Dandona, *Circulating mononuclear cells in the obese are in a proinflammatory state.* Circulation, 2004. **110**(12): p. 1564-71.

145. Glowinska-Olszewska, B. and M. Urban, *Elevated matrix metalloproteinase 9 and tissue inhibitor of metalloproteinase 1 in obese children and adolescents.* Metabolism, 2007. **56**(6): p. 799-805.
146. Glowinska-Olszewska, B., M. Urban, and B. Florys, *[Selected matrix metalloproteinases (MMP-2, MMP-9) in obese children and adolescents].* Endokrynol Diabetol Chor Przemiany Materii Wieku Rozw, 2006. **12**(3): p. 179-83.
147. Tinahones, F.J., L. Coin-Araguez, M.D. Mayas, E. Garcia-Fuentes, C.H. Del Pozo, J. Vendrell, F. Cardona, R.M. Calvo, M.J. Obregon, and R. El Bekay, *Obesity-associated insulin resistance is correlated to adipose tissue vascular endothelial growth factors and metalloproteinase levels.* BMC Physiol, 2012. **12**(1): p. 4.
148. Aljada, A., H. Ghanim, P. Mohanty, T. Syed, A. Bandyopadhyay, and P. Dandona, *Glucose intake induces an increase in activator protein 1 and early growth response 1 binding activities, in the expression of tissue factor and matrix metalloproteinase in mononuclear cells, and in plasma tissue factor and matrix metalloproteinase concentrations.* Am J Clin Nutr, 2004. **80**(1): p. 51-7.
149. Patel, C., H. Ghanim, S. Ravishankar, C.L. Sia, P. Viswanathan, P. Mohanty, and P. Dandona, *Prolonged reactive oxygen species generation and nuclear factor-kappaB activation after a high-fat, high-carbohydrate meal in the obese.* J Clin Endocrinol Metab, 2007. **92**(11): p. 4476-9.
150. Traurig, M.T., P.A. Permana, S. Nair, S. Kobes, C. Bogardus, and L.J. Baier, *Differential expression of matrix metalloproteinase 3 (MMP3) in preadipocytes/stromal vascular cells from nonobese nondiabetic versus obese nondiabetic Pima Indians.* Diabetes, 2006. **55**(11): p. 3160-5.
151. Cugino, D., F. Gianfagna, W. Ahrens, S. De Henauw, A.C. Koni, S. Marild, D. Molnar, L.A. Moreno, Y. Pitsiladis, P. Russo, A. Siani, M. Tornaritis, T. Veidebaum, and L. Iacoviello, *Polymorphisms of matrix metalloproteinase gene and adiposity indices in European children: results of the IDEFICS study.* Int J Obes (Lond), 2013. **37**(12): p. 1539-44.
152. Monroy, A., S. Kamath, A.O. Chavez, V.E. Centonze, M. Veerasamy, A. Barrentine, J.J. Wewer, D.K. Coletta, C. Jenkinson, R.M. Jhingan, D. Smokler, S. Reyna, N. Musi, R. Khokka, M. Federici, D. Tripathy, R.A. DeFronzo, and F. Folli, *Impaired regulation of the TNF-alpha converting enzyme/tissue inhibitor of metalloproteinase 3 proteolytic system in skeletal muscle of obese type 2 diabetic patients: a new mechanism of insulin resistance in humans.* Diabetologia, 2009. **52**(10): p. 2169-81.
153. Tripathy, D., G. Daniele, T.V. Fiorentino, Z. Perez-Cadena, A. Chavez-Velasquez, S. Kamath, P. Fanti, C. Jenkinson, F. Andreozzi, M. Federici, A. Gastaldelli, R.A. Defronzo, and F. Folli, *Pioglitazone improves glucose metabolism and modulates skeletal muscle TIMP-3-TACE dyad in type 2 diabetes mellitus: a randomised, double-blind, placebo-controlled, mechanistic study.* Diabetologia, 2013. **56**(10): p. 2153-63.
154. O'Connell, J., L. Lynch, A. Hogan, T.J. Cawood, and D. O'Shea, *Preadipocyte factor-1 is associated with metabolic profile in severe obesity.* J Clin Endocrinol Metab, 2011. **96**(4): p. E680-4.
155. Zeggini, E., L.J. Scott, R. Saxena, B.F. Voight, J.L. Marchini, T. Hu, P.I. de Bakker, G.R. Abecasis, P. Almgren, G. Andersen, K. Ardlie, K.B. Bostrom, R.N. Bergman, L.L. Bonnycastle, K. Borch-Johnsen, N.P. Burtt, H. Chen, P.S. Chines, M.J. Daly, P. Deodhar, C.J. Ding, A.S. Doney, W.L. Duren, K.S. Elliott, M.R. Erdos, T.M. Frayling, R.M. Freathy, L. Gianniny, H. Grallert, N. Grarup, C.J. Groves, C. Guiducci, T. Hansen, C. Herder, G.A. Hitman, T.E. Hughes, B. Isomaa, A.U. Jackson, T. Jorgensen, A. Kong, K. Kubalanza, F.G. Kuruvilla, J. Kuusisto, C. Langenberg, H. Lango, T. Lauritzen, Y. Li, C.M. Lindgren, V. Lyssenko, A.F. Marvelle, C. Meisinger, K. Midthjell, K.L. Mohlke, M.A. Morken, A.D. Morris, N. Narisu, P. Nilsson, K.R. Owen, C.N. Palmer, F. Payne, J.R. Perry, E. Pettersen, C. Platou, I. Prokopenko, L. Qi, L. Qin, N.W. Rayner, M. Rees, J.J. Roix, A. Sandbaek, B. Shields, M. Sjogren, V. Steinthorsdottir, H.M. Stringham, A.J. Swift, G. Thorleifsson, U. Thorsteinsdottir, N.J.

Timpson, T. Tuomi, J. Tuomilehto, M. Walker, R.M. Watanabe, M.N. Weedon, C.J. Willer, T. Illig, K. Hveem, F.B. Hu, M. Laakso, K. Stefansson, O. Pedersen, N.J. Wareham, I. Barroso, A.T. Hattersley, F.S. Collins, L. Groop, M.I. McCarthy, M. Boehnke, and D. Altshuler, *Meta-analysis of genome-wide association data and large-scale replication identifies additional susceptibility loci for type 2 diabetes.* Nat Genet, 2008. **40**(5): p. 638-45.
156. Bays, H.E., J.M. Gonzalez-Campoy, G.A. Bray, A.E. Kitabchi, D.A. Bergman, A.B. Schorr, H.W. Rodbard, and R.R. Henry, *Pathogenic potential of adipose tissue and metabolic consequences of adipocyte hypertrophy and increased visceral adiposity.* Expert Rev Cardiovasc Ther, 2008. **6**(3): p. 343-68.
157. Wallace, T.M. and D.R. Matthews, *The assessment of insulin resistance in man.* Diabet Med, 2002. **19**(7): p. 527-34.
158. Brenner, C., B. Foxwell, and J.J. Turner, *Toll Like Receptor Signalling in Human Adipocytes.* Immunology, 2008. **125**(S1): p. 84.
159. Brenner, C., R.E. Simmonds, S. Wood, V. Rose, M. Feldmann, and J. Turner, *TLR Signalling and Adapter Utilization in Primary Human In vitro Differentiated Adipocytes.* Scand J Immunol, 2012. **76**(4): p. 359-70.
160. Turner, J.J., K.M. Foxwell, R. Kanji, C. Brenner, S. Wood, B.M. Foxwell, and M. Feldmann, *Investigation of nuclear factor-kappaB inhibitors and interleukin-10 as regulators of inflammatory signalling in human adipocytes.* Clin Exp Immunol, 2010. **162**(3): p. 487-93.
161. Asada, S., M. Kuroda, Y. Aoyagi, Y. Fukaya, S. Tanaka, S. Konno, M. Tanio, M. Aso, K. Satoh, Y. Okamoto, T. Nakayama, Y. Saito, and H. Bujo, *Ceiling culture-derived proliferative adipocytes retain high adipogenic potential suitable for use as a vehicle for gene transduction therapy.* Am J Physiol Cell Physiol, 2011. **301**(1): p. C181-5.
162. Chung, S., K. Lapoint, K. Martinez, A. Kennedy, M. Boysen Sandberg, and M.K. McIntosh, *Preadipocytes mediate lipopolysaccharide-induced inflammation and insulin resistance in primary cultures of newly differentiated human adipocytes.* Endocrinology, 2006. **147**(11): p. 5340-51.
163. Tchkonia, T., N. Giorgadze, T. Pirtskhalava, Y. Tchoukalova, I. Karagiannides, R.A. Forse, M. DePonte, M. Stevenson, W. Guo, J. Han, G. Waloga, T.L. Lash, M.D. Jensen, and J.L. Kirkland, *Fat depot origin affects adipogenesis in primary cultured and cloned human preadipocytes.* Am J Physiol Regul Integr Comp Physiol, 2002. **282**(5): p. R1286-96.
164. Kuri-Harcuch, W. and H. Green, *Increasing activity of enzymes on pathway of triacylglycerol synthesis during adipose conversion of 3T3 cells.* J Biol Chem, 1977. **252**(6): p. 2158-60.
165. Minteer, D., K.G. Marra, and J.P. Rubin, *Adipose-derived mesenchymal stem cells: biology and potential applications.* Adv Biochem Eng Biotechnol, 2013. **129**: p. 59-71.
166. Gesta, S., Y.H. Tseng, and C.R. Kahn, *Developmental origin of fat: tracking obesity to its source.* Cell, 2007. **131**(2): p. 242-56.
167. Fonseca-Alaniz, M.H., J. Takada, M.I. Alonso-Vale, and F.B. Lima, *Adipose tissue as an endocrine organ: from theory to practice.* J Pediatr (Rio J), 2007. **83**(5 Suppl): p. S192-203.
168. Kwok, K.H., K.S. Lam, and A. Xu, *Heterogeneity of white adipose tissue: molecular basis and clinical implications.* Exp Mol Med, 2016. **48**: p. e215.
169. Teunis, T., M.R. Heerma van Voss, M. Kon, and J.F. van Maurik, *CT-angiography prior to DIEP flap breast reconstruction: a systematic review and meta-analysis.* Microsurgery, 2013. **33**(6): p. 496-502.
170. Xu, H., J.K. Sethi, and G.S. Hotamisligil, *Transmembrane tumor necrosis factor (TNF)-alpha inhibits adipocyte differentiation by selectively activating TNF receptor 1.* J Biol Chem, 1999. **274**(37): p. 26287-95.
171. Jo, J., O. Gavrilova, S. Pack, W. Jou, S. Mullen, A.E. Sumner, S.W. Cushman, and V. Periwal, *Hypertrophy and/or Hyperplasia: Dynamics of Adipose Tissue Growth.* PLoS Comput Biol, 2009. **5**(3): p. e1000324.

172. Negrel, R. and C. Dani, *Cultures of adipose precursor cells and cells of clonal lines from animal white adipose tissue.* Methods Mol Biol, 2001. **155**: p. 225-37.
173. Davidson, R.K., J.G. Waters, L. Kevorkian, C. Darrah, A. Cooper, S.T. Donell, and I.M. Clark, *Expression profiling of metalloproteinases and their inhibitors in synovium and cartilage.* Arthritis Res Ther, 2006. **8**(4): p. R124.
174. Swingler, T.E., J.G. Waters, R.K. Davidson, C.J. Pennington, X.S. Puente, C. Darrah, A. Cooper, S.T. Donell, G.R. Guile, W. Wang, and I.M. Clark, *Degradome expression profiling in human articular cartilage.* Arthritis Res Ther, 2009. **11**(3): p. R96.
175. Livak, K.J. and T.D. Schmittgen, *Analysis of relative gene expression data using real-time quantitative PCR and the 2(-Delta Delta C(T)) Method.* Methods, 2001. **25**(4): p. 402-8.
176. Holmes, J.L. and R.S. Pollenz, *Determination of aryl hydrocarbon receptor nuclear translocator protein concentration and subcellular localization in hepatic and nonhepatic cell culture lines: development of quantitative Western blotting protocols for calculation of aryl hydrocarbon receptor and aryl hydrocarbon receptor nuclear translocator protein in total cell lysates.* Mol Pharmacol, 1997. **52**(2): p. 202-11.
177. Brew, K. and H. Nagase, *The tissue inhibitors of metalloproteinases (TIMPs): an ancient family with structural and functional diversity.* Biochim Biophys Acta, 2010. **1803**(1): p. 55-71.
178. Amour, A., M. Hutton, V. Knauper, P.M. Slocombe, A. Webster, M. Butler, C.G. Knight, B.J. Smith, A.J. Docherty, and G. Murphy, *Inhibition of the metalloproteinase domain of mouse TACE.* Ann N Y Acad Sci, 1999. **878**: p. 728-31.
179. Apte, S.S., B.R. Olsen, and G. Murphy, *The gene structure of tissue inhibitor of metalloproteinases (TIMP)-3 and its inhibitory activities define the distinct TIMP gene family.* J Biol Chem, 1995. **270**(24): p. 14313-8.
180. Troeberg, L., K. Fushimi, R. Khokha, H. Emonard, P. Ghosh, and H. Nagase, *Calcium pentosan polysulfate is a multifaceted exosite inhibitor of aggrecanases.* Faseb J, 2008. **22**(10): p. 3515-24.
181. Toth, M., A. Sohail, and R. Fridman, *Assessment of gelatinases (MMP-2 and MMP-9) by gelatin zymography.* Methods Mol Biol, 2012. **878**: p. 121-35.
182. Snoek-van Beurden, P.A. and J.W. Von den Hoff, *Zymographic techniques for the analysis of matrix metalloproteinases and their inhibitors.* Biotechniques, 2005. **38**(1): p. 73-83.
183. Ramos-Kuri, M., K. Rapti, H. Mehel, S. Zhang, P.S. Dhandapany, L. Liang, A. Garcia-Carranca, R. Bobe, R. Fischmeister, S. Adnot, D. Lebeche, R.J. Hajjar, L. Lipskaia, and E.R. Chemaly, *Dominant negative Ras attenuates pathological ventricular remodeling in pressure overload cardiac hypertrophy.* Biochim Biophys Acta, 2015. **1853**(11 Pt A): p. 2870-84.
184. Wilkinson, G.W. and A. Akrigg, *Constitutive and enhanced expression from the CMV major IE promoter in a defective adenovirus vector.* Nucleic Acids Res, 1992. **20**(9): p. 2233-9.
185. Gritsiuk, A.I., M.B. Mamedov, and V.I. Shchigel'skii, *[Coagulologic characteristics of different stages of chronic circulatory insufficiency in atherosclerotic cardiosclerosis].* Kardiologiia, 1976. **16**(12): p. 25-32.
186. Bernstein, E., A.A. Caudy, S.M. Hammond, and G.J. Hannon, *Role for a bidentate ribonuclease in the initiation step of RNA interference.* Nature, 2001. **409**(6818): p. 363-6.
187. Rand, T.A., K. Ginalski, N.V. Grishin, and X. Wang, *Biochemical identification of Argonaute 2 as the sole protein required for RNA-induced silencing complex activity.* Proc Natl Acad Sci U S A, 2004. **101**(40): p. 14385-9.
188. Ameres, S.L., J. Martinez, and R. Schroeder, *Molecular basis for target RNA recognition and cleavage by human RISC.* Cell, 2007. **130**(1): p. 101-12.
189. Artym, V.V. and K. Matsumoto, *Imaging cells in three-dimensional collagen matrix.* Curr Protoc Cell Biol, 2010. **Chapter 10**: p. Unit 10 18 1-20.

190. Itoh, Y., N. Ito, H. Nagase, R.D. Evans, S.A. Bird, and M. Seiki, *Cell surface collagenolysis requires homodimerization of the membrane-bound collagenase MT1-MMP.* Mol Biol Cell, 2006. **17**(12): p. 5390-9.
191. Itoh, Y., N. Ito, H. Nagase, and M. Seiki, *The second dimer interface of MT1-MMP, the transmembrane domain, is essential for ProMMP-2 activation on the cell surface.* J Biol Chem, 2008. **283**(19): p. 13053-62.
192. Shoulders, M.D. and R.T. Raines, *Collagen structure and stability.* Annu Rev Biochem, 2009. **78**: p. 929-58.
193. Gorres, K.L. and R.T. Raines, *Prolyl 4-hydroxylase.* Crit Rev Biochem Mol Biol, 2010. **45**(2): p. 106-24.
194. Fan, M.H., Q. Zhu, H.H. Li, H.J. Ra, S. Majumdar, D.L. Gulick, J.A. Jerome, D.H. Madsen, M. Christofidou-Solomidou, D.W. Speicher, W.W. Bachovchin, C. Feghali-Bostwick, and E. Pure, *Fibroblast Activation Protein (FAP) Accelerates Collagen Degradation and Clearance from Lungs in Mice.* J Biol Chem, 2016. **291**(15): p. 8070-89.
195. Riley, G.P., R.L. Harrall, C.R. Constant, M.D. Chard, T.E. Cawston, and B.L. Hazleman, *Tendon degeneration and chronic shoulder pain: changes in the collagen composition of the human rotator cuff tendons in rotator cuff tendinitis.* Ann Rheum Dis, 1994. **53**(6): p. 359-66.
196. Giordano, A., A. Frontini, and S. Cinti, *Adipose organ nerves revealed by immunohistochemistry.* Methods Mol Biol, 2008. **456**: p. 83-95.
197. Schneider, C.A., W.S. Rasband, and K.W. Eliceiri, *NIH Image to ImageJ: 25 years of image analysis.* Nat Methods, 2012. **9**(7): p. 671-5.
198. Newman, D., C. Kelly-Morland, O.D. Leinhard, B. Kasmai, R. Greenwood, P.N. Malcolm, T. Romu, M. Borga, and A.P. Toms, *Test-retest reliability of rapid whole body and compartmental fat volume quantification on a widebore 3T MR system in normal-weight, overweight, and obese subjects.* J Magn Reson Imaging, 2016. **44**(6): p. 1464-1473.
199. Pippitt, K., M. Li, and H.E. Gurgle, *Diabetes Mellitus: Screening and Diagnosis.* Am Fam Physician, 2016. **93**(2): p. 103-9.
200. Turner, J.J., K.M. Foxwell, R. Kanji, C. Brenner, S. Wood, B.M. Foxwell, and M. Feldmann, *Investigation of NF-kB inhibitors and interleukin-10 as regulators of inflammatory signalling in human adipocytes.* Clin Exp Immunol, 2010. **162**(3): p. 487-93
201. Kim, F., M. Pham, I. Luttrell, D.D. Bannerman, J. Tupper, J. Thaler, T.R. Hawn, E.W. Raines, and M.W. Schwartz, *Toll-like receptor-4 mediates vascular inflammation and insulin resistance in diet-induced obesity.* Circ Res, 2007. **100**(11): p. 1589-96.
202. Conde, J., M. Scotece, R. Gomez, V. Lopez, J.J. Gomez-Reino, F. Lago, and O. Gualillo, *Adipokines: biofactors from white adipose tissue. A complex hub among inflammation, metabolism, and immunity.* Biofactors, 2011. **37**(6): p. 413-20.
203. Lehr, S., S. Hartwig, and H. Sell, *Adipokines: a treasure trove for the discovery of biomarkers for metabolic disorders.* Proteomics Clin Appl, 2012. **6**(1-2): p. 91-101.
204. Bruun, J.M., A.S. Lihn, A.K. Madan, S.B. Pedersen, K.M. Schiott, J.N. Fain, and B. Richelsen, *Higher production of IL-8 in visceral vs. subcutaneous adipose tissue. Implication of nonadipose cells in adipose tissue.* Am J Physiol Endocrinol Metab, 2004. **286**(1): p. E8-13.
205. Sharabiani, M.T., R. Vermeulen, C. Scoccianti, F.S. Hosnijeh, L. Minelli, C. Sacerdote, D. Palli, V. Krogh, R. Tumino, P. Chiodini, S. Panico, and P. Vineis, *Immunologic profile of excessive body weight.* Biomarkers, 2011. **16**(3): p. 243-51.
206. Hudak, C.S. and H.S. Sul, *Pref-1, a gatekeeper of adipogenesis.* Front Endocrinol (Lausanne), 2013. **4**: p. 79.
207. Scilabra, S.D., L. Troeberg, K. Yamamoto, H. Emonard, I. Thogersen, J.J. Enghild, D.K. Strickland, and H. Nagase, *Differential Regulation of Extracellular Tissue Inhibitor of Metalloproteinases-3 Levels by Cell Membrane-bound And Shed Low Density Lipoprotein Receptor-related Protein 1.* J Biol Chem, 2012.

208. Troeberg, L., C. Lazenbatt, E.K.M.F. Anower, C. Freeman, O. Federov, H. Habuchi, O. Habuchi, K. Kimata, and H. Nagase, *Sulfated glycosaminoglycans control the extracellular trafficking and the activity of the metalloprotease inhibitor TIMP-3.* Chem Biol, 2014. **21**(10): p. 1300-9.
209. Nagase, H., *Substrate Specificity of MMPs*, in *Matrix Metalloproteinase Inhibitors in Cancer Therapy*, N.J. Clendeninn and K. Appelt, Editors. 2001, Humana Press: New Jersey.
210. Singh, R.J., J.C. Mason, E.A. Lidington, D.R. Edwards, R.K. Nuttall, R. Khokha, V. Knauper, G. Murphy, and J. Gavrilovic, *Cytokine stimulated vascular cell adhesion molecule-1 (VCAM-1) ectodomain release is regulated by TIMP-3.* Cardiovasc Res, 2005. **67**(1): p. 39-49.
211. Madec, S., M. Chiarugi, E. Santini, C. Rossi, P. Miccoli, E. Ferrannini, and A. Solini, *Pattern of expression of inflammatory markers in adipose tissue of untreated hypertensive patients.* J Hypertens, 2010. **28**(7): p. 1459-65.
212. Unal, R., A. Yao-Borengasser, V. Varma, N. Rasouli, C. Labbate, P.A. Kern, and G. Ranganathan, *Matrix metalloproteinase-9 is increased in obese subjects and decreases in response to pioglitazone.* J Clin Endocrinol Metab, 2010. **95**(6): p. 2993-3001.
213. Mann, E., D. Singer, J. Pitkin, N. Panay, and M.S. Hunter, *Psychosocial adjustment in women with premature menopause: a cross-sectional survey.* Climacteric, 2012. **15**(5): p. 481-9.
214. Kahn, S.E., B. Zinman, S.M. Haffner, M.C. O'Neill, B.G. Kravitz, D. Yu, M.I. Freed, W.H. Herman, R.R. Holman, N.P. Jones, J.M. Lachin, and G.C. Viberti, *Obesity is a major determinant of the association of C-reactive protein levels and the metabolic syndrome in type 2 diabetes.* Diabetes, 2006. **55**(8): p. 2357-64.
215. Romu, T., N. Dahlstrom, O.D. Leinhard, and M. Borga, *Robust water fat separated dual-echo MRI by phase-sensitive reconstruction.* Magn Reson Med, 2016.
216. Tchoukalova, Y.D., C. Koutsari, M.V. Karpyak, S.B. Votruba, E. Wendland, and M.D. Jensen, *Subcutaneous adipocyte size and body fat distribution.* Am J Clin Nutr, 2008. **87**(1): p. 56-63.
217. Andersson, D.P., D. Eriksson Hogling, A. Thorell, E. Toft, V. Qvisth, E. Naslund, A. Thorne, M. Wiren, P. Lofgren, J. Hoffstedt, I. Dahlman, N. Mejhert, M. Ryden, E. Arner, and P. Arner, *Changes in subcutaneous fat cell volume and insulin sensitivity after weight loss.* Diabetes Care, 2014. **37**(7): p. 1831-6.
218. Wurst, U., T. Ebert, S. Kralisch, M. Stumvoll, and M. Fasshauer, *Serum levels of the adipokine Pref-1 in gestational diabetes mellitus.* Cytokine, 2015. **71**(2): p. 161-4.
219. Miksztowicz, V., N. Siseles, N. Fernandez Machulsky, L. Schreier, and G. Berg, *Increase in MMP-2 activity in overweight and obese women is associated with menopausal status.* Climacteric, 2012. **15**(6): p. 602-6.
220. Fedak, P.W., S. Verma, R.D. Weisel, and R.K. Li, *Cardiac remodeling and failure From molecules to man (Part II).* Cardiovasc Pathol, 2005. **14**(2): p. 49-60.
221. Raffetto, J.D. and R.A. Khalil, *Matrix metalloproteinases and their inhibitors in vascular remodeling and vascular disease.* Biochem Pharmacol, 2008. **75**(2): p. 346-59.
222. Schrimpf, C., T. Koppen, J.S. Duffield, U. Boer, S. David, W. Ziegler, A. Haverich, O.E. Teebken, and M. Wilhelmi, *TIMP3 is Regulated by Pericytes upon Shear Stress Detection Leading to a Modified Endothelial Cell Response.* Eur J Vasc Endovasc Surg, 2017. **54**(4): p. 524-533.
223. Goldman, S. and E. Shalev, *MMPS and TIMPS in ovarian physiology and pathophysiology.* Front Biosci, 2004. **9**: p. 2474-83.
224. Rosewell, K.L., F. Li, M. Puttabyatappa, J.W. Akin, M. Brannstrom, and T.E. Curry, Jr., *Ovarian expression, localization, and function of tissue inhibitor of metalloproteinase 3 (TIMP3) during the periovulatory period of the human menstrual cycle.* Biol Reprod, 2013. **89**(5): p. 121.

225. Selvais, C., H.P. Gaide Chevronnay, P. Lemoine, S. Dedieu, P. Henriet, P.J. Courtoy, E. Marbaix, and H. Emonard, *Metalloproteinase-dependent shedding of low-density lipoprotein receptor-related protein-1 ectodomain decreases endocytic clearance of endometrial matrix metalloproteinase-2 and -9 at menstruation.* Endocrinology, 2009. **150**(8): p. 3792-9.
226. Hickey, M., J. Crewe, L.A. Mahoney, D.A. Doherty, I.S. Fraser, and L.A. Salamonsen, *Mechanisms of irregular bleeding with hormone therapy: the role of matrix metalloproteinases and their tissue inhibitors.* J Clin Endocrinol Metab, 2006. **91**(8): p. 3189-98.
227. Anand-Apte, B., L. Bao, R. Smith, K. Iwata, B.R. Olsen, B. Zetter, and S.S. Apte, *A review of tissue inhibitor of metalloproteinases-3 (TIMP-3) and experimental analysis of its effect on primary tumor growth.* Biochem Cell Biol, 1996. **74**(6): p. 853-62.
228. Ripley, D., R. Tunuguntla, L. Susi, and N. Chegini, *Expression of matrix metalloproteinase-26 and tissue inhibitors of metalloproteinase-3 and -4 in normal ovary and ovarian carcinoma.* Int J Gynecol Cancer, 2006. **16**(5): p. 1794-800.
229. Petrovic, N., A. Sami, J. Martinovic, M. Zaric, I. Nakashidze, S. Lukic, and S. Jovanovic-Cupic, *TIMP-3 mRNA expression levels positively correlates with levels of miR-21 in in situ BC and negatively in PR positive invasive BC.* Pathol Res Pract, 2017. **213**(10): p. 1264-1270.
230. Smith, M.R., H. Kung, S.K. Durum, N.H. Colburn, and Y. Sun, *TIMP-3 induces cell death by stabilizing TNF-alpha receptors on the surface of human colon carcinoma cells.* Cytokine, 1997. **9**(10): p. 770-80.
231. Dreymueller, D., S. Uhlig, and A. Ludwig, *ADAM-family metalloproteinases in lung inflammation: potential therapeutic targets.* Am J Physiol Lung Cell Mol Physiol, 2015. **308**(4): p. L325-43.
232. Scheller, J., A. Chalaris, C. Garbers, and S. Rose-John, *ADAM17: a molecular switch to control inflammation and tissue regeneration.* Trends Immunol, 2011. **32**(8): p. 380-7.
233. Haas, T.L., S.J. Davis, and J.A. Madri, *Three-dimensional type I collagen lattices induce coordinate expression of matrix metalloproteinases MT1-MMP and MMP-2 in microvascular endothelial cells.* J Biol Chem, 1998. **273**(6): p. 3604-10.
234. Thompson, E.W., M. Yu, J. Bueno, L. Jin, S.N. Maiti, F.L. Palao-Marco, H. Pulyaeva, J.W. Tamborlane, R. Tirgari, I. Wapnir, and et al., *Collagen induced MMP-2 activation in human breast cancer.* Breast Cancer Res Treat, 1994. **31**(2-3): p. 357-70.
235. Finan, K.M., G. Hodge, A.M. Reynolds, S. Hodge, M.D. Holmes, A.H. Baker, and P.N. Reynolds, *In vitro susceptibility to the pro-apoptotic effects of TIMP-3 gene delivery translates to greater in vivo efficacy versus gene delivery for TIMPs-1 or -2.* Lung Cancer, 2006. **53**(3): p. 273-84.
236. Kallio, J.P., S. Hopkins-Donaldson, A.H. Baker, and V.M. Kahari, *TIMP-3 promotes apoptosis in nonadherent small cell lung carcinoma cells lacking functional death receptor pathway.* Int J Cancer, 2011. **128**(4): p. 991-6.
237. Edwards, D.R., *TIMP-3 and endocrine therapy of breast cancer: an apoptosis connection emerges.* J Pathol, 2004. **202**(4): p. 391-4.
238. Baker, A.H., A.B. Zaltsman, S.J. George, and A.C. Newby, *Divergent effects of tissue inhibitor of metalloproteinase-1, -2, or -3 overexpression on rat vascular smooth muscle cell invasion, proliferation, and death in vitro. TIMP-3 promotes apoptosis.* J Clin Invest, 1998. **101**(6): p. 1478-87.
239. Acosta, J.R., I. Douagi, D.P. Andersson, J. Backdahl, M. Ryden, P. Arner, and J. Laurencikiene, *Increased fat cell size: a major phenotype of subcutaneous white adipose tissue in non-obese individuals with type 2 diabetes.* Diabetologia, 2016. **59**(3): p. 560-70.
240. Singh, R.G., H.D. Yoon, L.M. Wu, J. Lu, L.D. Plank, and M.S. Petrov, *Ectopic fat accumulation in the pancreas and its clinical relevance: A systematic review, meta-analysis, and meta-regression.* Metabolism, 2017. **69**: p. 1-13.

241. Brons, C. and L.G. Grunnet, *MECHANISMS IN ENDOCRINOLOGY: Skeletal muscle lipotoxicity in insulin resistance and type 2 diabetes: a causal mechanism or an innocent bystander?* Eur J Endocrinol, 2017. **176**(2): p. R67-R78.
242. Byrne, C.D. and G. Targher, *Ectopic fat, insulin resistance, and nonalcoholic fatty liver disease: implications for cardiovascular disease.* Arterioscler Thromb Vasc Biol, 2014. **34**(6): p. 1155-61.
243. Huang-Doran, I., A. Sleigh, J.J. Rochford, S. O'Rahilly, and D.B. Savage, *Lipodystrophy: metabolic insights from a rare disorder.* J Endocrinol, 2010. **207**(3): p. 245-55.
244. Menghini, R., V. Casagrande, S. Menini, A. Marino, V. Marzano, M.L. Hribal, P. Gentileschi, D. Lauro, O. Schillaci, G. Pugliese, P. Sbraccia, A. Urbani, R. Lauro, and M. Federici, *TIMP3 overexpression in macrophages protects from insulin resistance, adipose inflammation, and nonalcoholic fatty liver disease in mice.* Diabetes, 2012. **61**(2): p. 454-62.
245. Montague, C.T., J.B. Prins, L. Sanders, J. Zhang, C.P. Sewter, J. Digby, C.D. Byrne, and S. O'Rahilly, *Depot-related gene expression in human subcutaneous and omental adipocytes.* Diabetes, 1998. **47**(9): p. 1384-91.
246. Skurk, T., M. Birgel, Y.M. Lee, and H. Hauner, *Effect of troglitazone on tumor necrosis factor alpha and transforming growth factor beta expression and action in human adipocyte precursor cells in primary culture.* Metabolism, 2006. **55**(3): p. 309-16.
247. Coppack, S.W., *Pro-inflammatory cytokines and adipose tissue.* Proc Nutr Soc, 2001. **60**(3): p. 349-56.
248. WHO. *Double burden of malnutrition*. 2015 [cited 2017 13th March 2017]; Available from: http://www.who.int/nutrition/double-burden-malnutrition/en/.
249. Munoz-Garach, A., I. Cornejo-Pareja, and F.J. Tinahones, *Does Metabolically Healthy Obesity Exist?* Nutrients, 2016. **8**(6).
250. Haller, H., W. Leonhardt, M. Hanefeld, and U. Julius, *Relationship between adipocyte hypertrophy and metabolic disturbances.* Endokrinologie, 1979. **74**(1): p. 63-72.
251. Gustafson, B., S. Gogg, S. Hedjazifar, L. Jenndahl, A. Hammarstedt, and U. Smith, *Inflammation and impaired adipogenesis in hypertrophic obesity in man.* Am J Physiol Endocrinol Metab, 2009. **297**(5): p. E999-E1003.
252. Montani, J.P., J.F. Carroll, T.M. Dwyer, V. Antic, Z. Yang, and A.G. Dulloo, *Ectopic fat storage in heart, blood vessels and kidneys in the pathogenesis of cardiovascular diseases.* Int J Obes Relat Metab Disord, 2004. **28 Suppl 4**: p. S58-65.
253. Komori, T., *Animal models for osteoporosis.* Eur J Pharmacol, 2015. **759**: p. 287-94.
254. Appelman-Dijkstra, N.M. and S.E. Papapoulos, *Modulating Bone Resorption and Bone Formation in Opposite Directions in the Treatment of Postmenopausal Osteoporosis.* Drugs, 2015. **75**(10): p. 1049-58.
255. Pap, T. and A. Korb-Pap, *Cartilage damage in osteoarthritis and rheumatoid arthritis--two unequal siblings.* Nat Rev Rheumatol, 2015. **11**(10): p. 606-15.
256. Adatia, A., K.D. Rainsford, and W.F. Kean, *Osteoarthritis of the knee and hip. Part I: aetiology and pathogenesis as a basis for pharmacotherapy.* J Pharm Pharmacol, 2012. **64**(5): p. 617-25.
257. Brenner, C., *Immune-Mediated Regulation of Glucose Uptake in Human Adipocytes*, in *Kennedy Institute of Rheumatology*2011, Imperial College London: London.
258. Atkinson, S.J., R.V. Ward, J.J. Reynolds, and G. Murphy, *Cell-mediated degradation of type IV collagen and gelatin films is dependent on the activation of matrix metalloproteinases.* Biochem J, 1992. **288 (Pt 2)**: p. 605-11.
259. Ibrahimi, A., F. Bonino, S. Bardon, G. Ailhaud, and C. Dani, *Essential role of collagens for terminal differentiation of preadipocytes.* Biochem Biophys Res Commun, 1992. **187**(3): p. 1314-22.
260. Pasarica, M., B. Gowronska-Kozak, D. Burk, I. Remedios, D. Hymel, J. Gimble, E. Ravussin, G.A. Bray, and S.R. Smith, *Adipose tissue collagen VI in obesity.* J Clin Endocrinol Metab, 2009. **94**(12): p. 5155-62.

261. Amin, P., S. Shah, D. Walker, and S.R. Page, *Adverse metabolic and cardiovascular risk following treatment of acute lymphoblastic leukaemia in childhood; two case reports and a literature review.* Diabet Med, 2001. **18**(10): p. 849-53.
262. Barnea, D., N. Raghunathan, D.N. Friedman, and E.S. Tonorezos, *Obesity and Metabolic Disease After Childhood Cancer.* Oncology (Williston Park), 2015. **29**(11): p. 849-55.
263. Mostoufi-Moab, S., J. Magland, E.J. Isaacoff, W. Sun, C.S. Rajapakse, B. Zemel, F. Wehrli, K. Shekdar, J. Baker, J. Long, and M.B. Leonard, *Adverse Fat Depots and Marrow Adiposity Are Associated With Skeletal Deficits and Insulin Resistance in Long-Term Survivors of Pediatric Hematopoietic Stem Cell Transplantation.* J Bone Miner Res, 2015. **30**(9): p. 1657-66.
264. Mayson, S.E., V.E. Parker, M.H. Schutta, R.K. Semple, and M.R. Rickels, *Severe insulin resistance and hypertriglyceridemia after childhood total body irradiation.* Endocr Pract, 2013. **19**(1): p. 51-8.
265. Nylander, V., L.R. Ingerslev, E. Andersen, O. Fabre, C. Garde, M. Rasmussen, K. Citirikkaya, J. Baek, G.L. Christensen, M. Aznar, L. Specht, D. Simar, and R. Barres, *Ionizing Radiation Potentiates High-Fat Diet-Induced Insulin Resistance and Reprograms Skeletal Muscle and Adipose Progenitor Cells.* Diabetes, 2016. **65**(12): p. 3573-3584.
266. Leco, K.J., P. Waterhouse, O.H. Sanchez, K.L. Gowing, A.R. Poole, A. Wakeham, T.W. Mak, and R. Khokha, *Spontaneous air space enlargement in the lungs of mice lacking tissue inhibitor of metalloproteinases-3 (TIMP-3).* J Clin Invest, 2001. **108**(6): p. 817-29.
267. Mohammed, F.F., D.S. Smookler, S.E. Taylor, B. Fingleton, Z. Kassiri, O.H. Sanchez, J.L. English, L.M. Matrisian, B. Au, W.C. Yeh, and R. Khokha, *Abnormal TNF activity in Timp3-/- mice leads to chronic hepatic inflammation and failure of liver regeneration.* Nat Genet, 2004. **36**(9): p. 969-77.
268. Black, R.A., *TIMP3 checks inflammation.* Nat Genet, 2004. **36**(9): p. 934-5.
269. Petersen, M.C., D.F. Vatner, and G.I. Shulman, *Regulation of hepatic glucose metabolism in health and disease.* Nat Rev Endocrinol, 2017. **13**(10): p. 572-587.
270. Villena, J.A., C.S. Choi, Y. Wang, S. Kim, Y.J. Hwang, Y.B. Kim, G. Cline, G.I. Shulman, and H.S. Sul, *Resistance to high-fat diet-induced obesity but exacerbated insulin resistance in mice overexpressing preadipocyte factor-1 (Pref-1): a new model of partial lipodystrophy.* Diabetes, 2008. **57**(12): p. 3258-66.
271. Milewicz, A., U. Tworowska, and M. Demissie, *Menopausal obesity--myth or fact?* Climacteric, 2001. **4**(4): p. 273-83.
272. Palmer, B.F. and D.J. Clegg, *The sexual dimorphism of obesity.* Mol Cell Endocrinol, 2015. **402**: p. 113-9.
273. Catalan, V., J. Gomez-Ambrosi, A. Rodriguez, and G. Fruhbeck, *Role of extracellular matrix remodelling in adipose tissue pathophysiology: relevance in the development of obesity.* Histol Histopathol, 2012. **27**(12): p. 1515-28.
274. Page-McCaw, A., A.J. Ewald, and Z. Werb, *Matrix metalloproteinases and the regulation of tissue remodelling.* Nat Rev Mol Cell Biol, 2007. **8**(3): p. 221-33.
275. Van Hul, M., D. Bauters, and R.H. Lijnen, *Differential effects of a gelatinase inhibitor on adipocyte differentiation and adipose tissue development.* Clin Exp Pharmacol Physiol, 2013. **40**(10): p. 689-97.
276. Van Hul, M. and H.R. Lijnen, *Matrix metalloproteinase inhibition impairs murine adipose tissue development independently of leptin.* Endocr J, 2011. **58**(2): p. 101-7.
277. Lijnen, H.R., E. Maquoi, L.B. Hansen, B. Van Hoef, L. Frederix, and D. Collen, *Matrix metalloproteinase inhibition impairs adipose tissue development in mice.* Arterioscler Thromb Vasc Biol, 2002. **22**(3): p. 374-9.
278. Rupnick, M.A., D. Panigrahy, C.Y. Zhang, S.M. Dallabrida, B.B. Lowell, R. Langer, and M.J. Folkman, *Adipose tissue mass can be regulated through the vasculature.* Proc Natl Acad Sci U S A, 2002. **99**(16): p. 10730-5.

279. Demeulemeester, D., D. Collen, and H.R. Lijnen, *Effect of matrix metalloproteinase inhibition on adipose tissue development.* Biochem Biophys Res Commun, 2005. **329**(1): p. 105-10.
280. Dali-Youcef, N., K. Hnia, S. Blaise, N. Messaddeq, S. Blanc, C. Postic, P. Valet, C. Tomasetto, and M.C. Rio, *Matrix metalloproteinase 11 protects from diabesity and promotes metabolic switch.* Sci Rep, 2016. **6**: p. 25140.
281. Maquoi, E., D. Demeulemeester, G. Voros, D. Collen, and H.R. Lijnen, *Enhanced nutritionally induced adipose tissue development in mice with stromelysin-1 gene inactivation.* Thromb Haemost, 2003. **89**(4): p. 696-704.
282. Martella, E., C. Bellotti, B. Dozza, S. Perrone, D. Donati, and E. Lucarelli, *Secreted adiponectin as a marker to evaluate in vitro the adipogenic differentiation of human mesenchymal stromal cells.* Cytotherapy, 2014. **16**(11): p. 1476-85.